Universidad Autónoma de Madrid
Facultad de Ciencias
Departamento de Biología Molecular

Control transcripcional de las redes neuronales en la corteza somatosensorial

Tesis Doctoral

Carlos García Briz
Madrid, 2017

Universidad Autónoma de Madrid
Facultad de Ciencias
Departamento de Biología Molecular

Control transcripcional de las redes neuronales en la corteza somatosensorial

Memoria de Investigación presentada por **Carlos García Briz,**
Licenciado en Biotecnología, para optar al grado
de **Doctor por la Universidad Autónoma de Madrid**

Trabajo dirigido por la Doctora Marta Nieto López
Madrid, 2017

Este trabajo ha sido realizado en el laboratorio de la Dra. Marta Nieto en el Departamento de Biología Molecular y Celular del Centro Nacional de Biotecnología. Carlos García Briz ha sido financiado por una beca "Formación de Personal Investigador" desde Diciembre de 2012 hasta Noviembre de 2016.

Facultad de Ciencias
Departamento de Biología Molecular

La Dra. Dª Marta Nieto López

CERTIFICA:

Que D. Carlos García Briz ha realizado bajo su dirección el presente trabajo titulado "Control transcripcional de las redes neuronales en la corteza somatosensorial" con el objeto de obtener el Grado de Doctor.

Y para que conste a todos los efectos, firma el presente certificado.

Fdo.: Dra. Dª Marta Nieto López

Madrid, año 2017.

A mis padres

RESUMEN

La corteza cerebral es la responsable de las funciones cognitivas superiores, la integración de la percepción sensorial y la consciencia. Para poder llevar a cabo estas funciones tan complejas, es necesario que las neuronas corticales se especifiquen y conecten correctamente durante el desarrollo. Los factores de transcripción (FT) específicos de subtipo instruyen programas moleculares que determinan las características fundamentales de la función y conectividad neuronal mediante mecanismos sólo entendidos parcialmente. En concreto, se sabe muy poco de la forma en que estos FT se relacionan y coordinan con los mecanismos dependientes de actividad durante el ensamblaje de los circuitos. En esta tesis, investigamos el papel de los diferentes FT y su relación con la actividad en la formación de los circuitos de las láminas superiores de la corteza somatosensorial.

Hemos caracterizado la función de Cux1 y Cux2, dos FT homedominio expresados selectivamente en las láminas II-III y IV, en el desarrollo de los compartimentos dendríticos y axonales de las neuronas de la lámina II-III. Mediante el análisis de pérdida y ganancia de función in vivo demostramos que, aunque el nivel de expresión de tanto Cux1 como de Cux2 influye en ambos compartimentos dendríticos, estos FT tienen efectos diferentes. Los cambios en Cux1 producen un efecto más marcado en el desarrollo del compartimento basal, mientras que la modulación de Cux2 tiene una influencia más fuerte en el compartimento apical. Respecto al papel de estos FT en la formación de los axones de la lámina II-III, los resultados demuestran que Cux1, pero no Cux2, es necesario para la formación de las proyecciones del cuerpo calloso (CC) de la corteza somatosensorial debido a su regulación transcripcional de los canales de potasio dependientes de voltaje Kv1. Esta regulación transcripcional de la excitabilidad contribuye a un cambio a un modo de disparo dependiente de Kv1 durante el desarrollo postnatal que es necesario para una inervación contralateral correcta. Estos efectos distintos de los genes Cux podrían ser importantes para la diversificación funcional de las neuronas de la lámina II-III en diferentes subpoblaciones con distintos patrones de conectividad, integración en el circuito y modos de respuesta neuronal.

También hemos examinado un mecanismo dependiente de Lhx2 que inicia la formación del circuito neuronal en la corteza de barriles del área somatonsensorial, un circuito que comprende los axones talamocorticales y las neuronas de la lámina IV. En un trabajo en colaboración, contribuimos a demostrar que Lhx2 regula vías genéticas que son cruciales para permitir la formación de barriles en las neuronas postmitóticas de la lámina IV. Cuando eliminamos este FT selectivamente en esta población utilizando un ratón KO condicional, las neuronas de la lámina IV muestran una plasticidad incorrecta debido a la falta de expresión de los genes encargados de la respuesta a la actividad. Estos fallos en la plasticidad incluyen la incapacidad de polarizar las dendritas, causada por la falta de Btbd3. Además, en estos mutantes, los axones talamocorticales alcanzan la corteza de barriles pero fallan en la remodelación de sus ramificaciones, no restringiéndolas al barril.

En conjunto, esta tesis contribuye a arrojar luz acerca de las funciones de diversos FT y la actividad neuronal en la conectividad de la corteza cerebral. Nuestros resultados indican que el funcionamiento defectuoso de los mecanismos regulados por FT podría explicar la etiología y patología de muchos de los trastornos mentales con origen en el desarrollo. Por tanto, la comprensión de los mecanismos descritos en esta tesis pueden contribuir a encontrar nuevos enfoques terapéuticos para el tratamiento de aquéllos trastornos en los que haya una conectividad aberrante.

ABSTRACT

The cerebral cortex is the responsible of the higher cognitive functions, the integration of the sensory perception and the consciousness. In order to perform such complex functions, cortical neurons must be correctly specified at a molecular level and connected during development. Neuronal subtype-specific transcription factors (FT) instruct molecular programs that determine the key features of neuronal function and connectivity by mechanisms only partially understood. In particular, little is known about how these FT are related and coordinate the activity-dependent mechanisms during circuit assembly. In this thesis we investigate the role of different FT, and their relationship with the activity in the formation of the circuits involving the upper layers of the somatosensory cortex.

We characterize the function of Cux1 and Cux2, two homeodomain FT selectively expressed in layer II-III and IV neurons, in the development of dendritic compartments and axons of layer II-III neurons. By in vivo loss and gain of function analysis we show that, while the expression level of either Cux1 or Cux2 influences both dendritic compartments, these FT have distinct effects. Changes in Cux1 result in a more marked effect on the development of the basal compartment, whereas modulation of Cux2 has a stronger influence on the apical compartment. Regarding the role of these FT in the axonal formation of layer II-III neurons, the results demonstrate that Cux1, but not Cux2, is necessary for the formation of the corpus callosum (CC) projections of the somatosensory cortex due to its developmental transcriptional regulation of Kv1 voltage-dependent potassium channels. This transcriptional regulation of excitability contributes to a postnatal switch to a Kv1-dependent firing mode that we show is required for successful contralateral innervation. These distinct effects of Cux genes might account for the functional diversification of layer II-III neurons into different subpopulations, with distinct connectivity patterns, integration in the circuit, and modes of neuronal response.

We also examined a Lhx2-dependent mechanism initiating the neuronal circuit formation in the barrel cortex of the somatosensory area, a circuit comprising thalamocortical axons and layer IV neurons. In collaboration, we contribute to show that Lhx2 regulates crucial genetic pathways in layer IV postmitotic neurons to enable barrel formation. When this FT is selectively deleted in this population using conditional knockout mice, layer IV neurons show an aberrant plasticity due to the lack of expression of the genes involved in the response to activity. These failures in plasticity include the inability to develop polarized dendrites due to the lack of Btbd3. Also, in these mutants, thalamocortical axons reach the barrel cortex but fail to remodel their arbors in a manner restricted to the barrel.

Altogether this thesis contributes to shed light on the role of several FT and neuronal activity in the connectivity of the cerebral cortex. Our results indicate that malfunctions in the mechanisms regulated by FT could explain the etiology and pathology of many mental disorders of developmental origin. Therefore, these mechanisms described in this thesis can contribute to find novel therapeutic approaches for the treatment of those diseases showing aberrant connectivity.

ÍNDICE

ÍNDICE DE FIGURAS

Cux1 and Cux2 Selectively Target Basal and Apical dendritic Compartments of Layer II-III Cortical Neurons

Cux1 Enables Interhemispheric Connections of Layer II/III by Regulating Kv1-Dependent Firing

ÍNDICE DE TABLAS

CLASE DE ABREVIATURAS

4-OHT: 4-hydroxytamoxifeno.
5HT: Serotonina (de su composición química 5-hidroxitriptamina).
A1: Área Auditoria Primaria.
ACSF: Artificial Cerebrospinal Fluid (Fluido cerebroespinal artificial).
AC1: Adenilil ciclasa tipo 1 (Del inglés, adenylyl cyclase type 1).
ADN: Ácido Desoxirribonucleico (en inglés, DNA).
AP: Action Potential (Potencial de acción).
ARN: Ácido Ribonucleico (en inglés, RNA).
BDNF: Proteína de secreción de nombre completo Brain derived neurotrophic factor.
Brn1: Factor de transcripción de nombre completo POU-homeodomain transcription factor Pou3f3.
Brn2: Factor de transcripción de nombre completo POU-homeodomain transcription factor Pou3f2.
Ca2+: Catión calcio.
cAMP: Adenosín monofosfato cíclico (del inglés, cyclic adenosine monophosphate).
CC: Cuerpo Calloso.
CGR: Células de Glía Radiales.
cKO: Ratón knock-out condicional.
Cl-: Anión cloro.
CR: Célula Cajal-Retzius.
CTB: Cholera toxin subunit B (Subunidad B de la toxina colérica).
Ctip2: Factor de transcripción de nombre completo COUP-TF interacting protein 2.
Cux1: Factor de transcripción de nombre completo Cut-like1.
Cux2: Factor de transcripción de nombre completo Cut-like2.
DAPI: Marcador nuclear diclorhidrato de 4',6-diamidino-2-fenilindol.
Dcc: Receptor transmembrana de nombre completo Deleted in colorectal cancer.
E(nº): Día Embrionario.
Emx1: Factor de transcripción de nombre completo Empty spiracles homologue 1.
Emx2: Factor de transcripción de nombre completo Empty spiracles homologue 2.
Epac2: Factor de intercambio de guanina de nombre completo Exchange protein directly activated by cAMP 2.

FBS: Suero bovino fetal (en inglés, fetal bovine serum).
Fezf2: Factor de transcripción de nombre completo Fez family zinc finger 2.
Foxg1: Factor de transcripción de nombre completo Forkhead box G1.
FoxP2: Factor de transcripción de nombre completo Forkhead box P2.
FT: Factores de Transcripción.
GFP: Proteína verde fluorescente (en inglés, green fluorescent protein).
GT: Ganglio Trigémino.
HARS: Regiones humanas aceleradas (Del inglés, Human Accelerated Regions).
ISI: Interspike Interval (Intervalo entre disparos).
IUE: Electroporación in utero (in utero electroporation).
K+: Catión potasio.
KO: Modificación genética para la inactivación de un gen (en inglés, Knockout).
Kv: Canal de potasio dependiente de voltaje.
Lhx2: Factor de transcripción de nombre completo LIM homeobox 2.
L(nº): Cortical layer (Lámina de la corteza).
Lmo4: Lim sólo-dominio 4 (del inglés, Lim domain-only 4).
LV: Local Variation of ISIs (Variación local de los intervalos entre disparos).
M1: Área Motora Primaria.
MAPK: MAP Kinasas (del inglés, Mitogen-Activated Protein Kinases).
MB: Materia Blanca.
mGluR5: Receptor de glutamato (del inglés, Metabotropic glutamate receptor 5).
N LIV: Neurona de la lámina IV.
Na+: Catión sodio.
Nav: Canal de sodio dependiente de voltaje.
NE: Neuroepitelio.
Netrin: Netrina.
NMDA: Receptores de glutamato N-metil-D-aspartato.
NMDAR2B: Subunidad 2B del receptor de NMDA.
NIO: Nervio Infraorbital.
NP: Neuronas de Proyección.
NPCT: Neurona de proyección corticotalámica.
NPLP: Neurona de proyección de las láminas profundas.
NPLS: Neurona de proyección de las láminas superficiales.
NPSC: Neurona de proyección subcortical.
Nrp1 : Receptor de membrana Neuropilina 1.
NT3: Neurotrofina 3.
P(nº): Día Postnatal.
PA: Potenciales de Acción.
Pax 6: Factor de transcripción de nombre completo Paired box 6.
PBS: Tampón fosfato salino (en inglés, Phosphate buffered saline).

PBST: Tritón X-100 diluido en PBS.
PCR: Reacción en cadena de la polimerasa (en inglés, Polymerase Chain Reaction).
PFA: Paraformaldehyde.
PI: Progenitores Intermedios.
PLC1: Fosfatidilinositol fosfolipasa C (del inglés, phosphatidylinositol phospholipase C).
PMBSF: Posterior medial barrel subfield (zona de barriles posteromedial)
PP: Preplaca.
PSD95: Proteína sináptica (del inglés, postsynaptic density protein 95).
Q-PCR: Reacción en cadena de la polimerasa cuantitativa o en tiempo real.
Robo: Receptor de membrana de nombre completo Roundabout homolog.
Rorβ/Rorb: Factor de transcripción de nombre completo RAR-related orphan receptor.
S1: Área Somatonsensorial Primaria.
S2: Área Somatonsensorial Secundaria.
Satb2: Factor de transcripción de nombre completo Special AT-rich sequence binding protein 2.
Sema: Molécula de secreción o presente en la superficie celular Semaforina.
shRNA: Ácido ribonucleico de horquillado corto (del inglés, short hairpin RNA).
Slit: Molécula soluble de nombre Slit homolog 2.
Sox5: Factor de transcripción de nombre completo SRY-box containing gene 5.
SP: Subplaca.
SS: área somatosensorial de la corteza cerebral.
TAOK2: Kinasa de nombre completo Thousand-and-one-amino acid 2 kinasa.
Tbr1: Factor de transcripción de nombre completo T-box brain gene 1.
TCAs: Thalamocortical axons (Axones talamocorticales)
TF: Transcription Factor (Factor de Transcripción).
TRANSFAC: Base de datos biológica (BIOBASE: Transcription factor binding sites).
TTX: Tetrodotoxina.
Ube3a: Ubiquitina ligasa E3A.
Unc5c: Receptor Unc5 homólogo C.
V1: Área Visual Primaria.
Wnt: Proteína soluble cuyo nombre proviene de la fusión de wingless + int (integración de MMTV=virus de tumor mamario de ratón).
WM: Whitte Matter (Materia Blanca).
WT: Fenotipo silvestre (en inglés, Wild Type).
Xlr3b: Proteína remodeladora de la cromatina (del inglés, X-linked lymphocyte-regulated 3B).
Xlr4b: Proteína remodeladora de la cromatina (del inglés, X-linked lymphocyte-regulated 4B).
Zic2: Factor de transcripción con dominios de unión a ADN tipo dedos de Zinc (en inglés, Zinc Finger Transcription Factor).
ZM: Zona Medial.
ZSV: Zona Subventricular.
ZV: Zona Ventricular.

INTRODUCCIÓN

"Si quieres construir un barco, no empieces por buscar madera, cortar tablas o distribuir el trabajo. Evoca primero en los hombres y mujeres el anhelo del vasto e inmenso mar."

(Antoine de Saint-Exupéry, "Ciudadela")

INTRODUCCIÓN

La neurociencia -la rama de la ciencia que estudia el sistema nervioso- comenzó a finales del siglo XIX cuando Camillo Golgi desarrolló la tinción argéntica. Esta tinción permitía marcar aleatoriamente las neuronas, revelando la morfología de las células nerviosas de distintas regiones. Gracias a esta técnica, Ramón y Cajal llevó a cabo el primer gran estudio de la anatomía neuronal, publicado en el libro "Textura del sistema nervioso del hombre y los vertebrados" (Ramon y Cajal 1899). El científico español fue el primero en identificar las sinapsis y en proponer que el sistema nervioso no era continuo, sino que estaba formado por redes de neuronas cuyos impulsos eran enviados en una sola dirección. Esta transmisión de la información se haría a través del axón de una neurona hacia la siguiente célula de la red, que la recibiría a través de las dendritas y el cuerpo celular. Además, Cajal enunció su "doctrina de la neurona", vigente hoy en día, según la cual las neuronas son las estructuras básicas y funcionales del sistema nervioso, además de ser únicas anatómica, embriológica y funcionalmente.

El sistema nervioso es, con diferencia, el órgano más complejo de los mamíferos. Tiene casi cien mil millones de neuronas de diferentes tipos (Herculano-Houzel 2009) conectadas entre sí a través de miles de contactos que dan lugar a circuitos que nos permiten llevar a cabo funciones muy diversas. Algunos de estos circuitos, necesarios para los procesos más fundamentales, han sido conservados entre especies a lo largo de la evolución. Otros circuitos más complejos han surgido en los animales más evolucionados para llevar a cabo funciones mucho más avanzadas como almacenar recuerdos o aprender. El cerebro, la región más evolucionada del sistema nervioso, es en los seres humanos el responsable del razonamiento y la consciencia, dos de las características que nos definen como especie (Innocenti 2011; Molnar 2011).

DESARROLLO TEMPRANO DEL SISTEMA NERVIOSO CENTRAL

La gastrulación supone la formación de las tres capas germinales embrionarias (endodermo, mesodermo y ectodermo) que después formarán todos los tejidos embrionarios y órganos. El ectodermo es la capa externa que dará lugar al sistema nervioso. Para ello forma la placa neural que, al doblarse, da lugar al tubo neural a través de un proceso llamado neurulación. La parte caudal del tubo neural va a formar la espina

dorsal, mientras que la parte rostral formará el encéfalo, constituido inicialmente por tres vésiculas cerebrales: El prosencéfalo, el mesencéfalo y el romboencéfalo (Kandel et al. 2000).

En el estadío de tres vesículas el cerebro se dobla dos veces, dando lugar a la flexura cervical en la unión de la espina dorsal y el romboencéfalo y a la flexura cefálica en la unión del romboencéfalo y el mesencéfalo. La flexura cefálica se mantiene prominente a lo largo del desarrollo, estableciendo una clara diferenciación entre el eje longitudinal del prosencéfalo con el tronco del encéfalo y la espina dorsal. Dos de las tres vesículas embrionarias se van a subdividir a lo largo del desarrollo. La del prosencéfalo da lugar al telencéfalo (su parte dorsal generará la corteza cerebral y el hipocampo, y el territorio ventral originará los ganglios basales, núcleo amigdalino y al bulbo olfatorio) y al diencéfalo (que generará el tálamo, el hipotálamo, subtálamo, epitálamo y la retina) y la del romboencéfalo da lugar al metaencéfalo (al final del desarrollo dará lugar al cerebelo) y al mielencéfalo (bulbo raquídeo) (**Figura 1**). Estas subdivisiones, junto con el mesencéfalo y la espina dorsal, suponen las seis regiones principales del sistema nervioso maduro (Kandel et al. 2000).

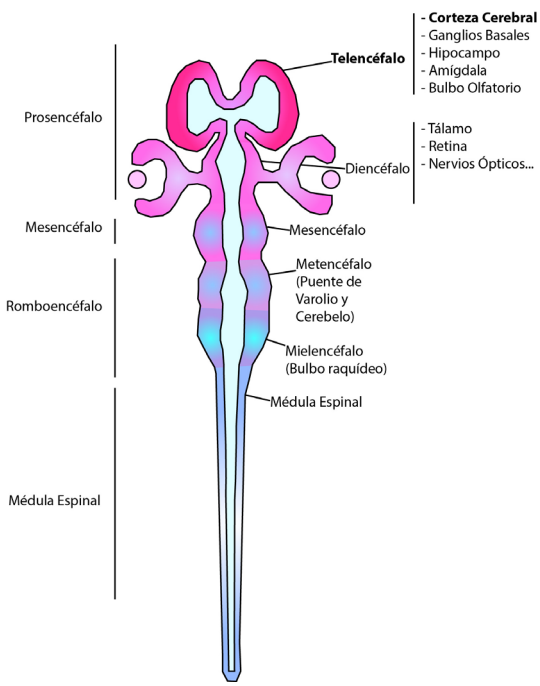

Figura 1. Estadío de 5 vesículas. En los primeros estadíos del desarrollo sólo existen tres vesículas cerebrales. Después, el prosencéfalo da lugar al telencéfalo (objeto de estudio de esta tesis) y al diencéfalo; el romboencéfalo al metencéfalo y al mielencéfalo. Adaptado de KANDEL.

LA CORTEZA CEREBRAL

La corteza cerebral es la responsable de las funciones cognitivas superiores y participa de manera clave en la consciencia y en la integración de la percepción sensorial y elaboración de las respuestas. Por tanto, no es extraño que sea la estructura cerebral que más se ha expandido a lo largo de la evolución representando el 85% del volumen cerebral total (DeFelipe and Ramon y Cajal 1988; Douglas and Martin 2007). Está formada por dos hemisferios que contienen la materia gris (cuerpos celulares) y blanca (fibras con mielina) y dividida en diferentes regiones: la neocorteza (el objeto de estudio de esta tesis, también conocida como isocorteza) y la allocorteza, que se subdivide en arquicorteza y paleocorteza (Kaas 2009). Presenta una elevada conectividad tanto dentro de ella misma como con regiones extracorticales y se encarga de procesar las señales que el organismo recibe del exterior y de generar una respuesta a las mismas.

La neocorteza es la parte más grande y evolucionada de la corteza. Es una estructura compleja compuesta por cientos de tipos neuronales y varios tipos de células gliales (Guillemot 2007; Molyneaux et al. 2007; Tasic et al. 2016; Zeisel et al. 2015). Además, es una estructura altamente organizada en diversos niveles superpuestos, lo cual es esencial para su funcionamiento normal según se infiere de las patologías humanas en las que aparecen defectos en la laminación (Kato 2015). En primer lugar, la corteza está compuesta por seis láminas paralelas a las meninges (el límite externo de la corteza) que agrupan neuronas con morfologías, patrones de conec-

tividad específica del circuito (DeFelipe and Ramon y Cajal 1988; Lefort et al. 2009) e identidad molecular (Molyneaux et al. 2007) similares. En segundo lugar, se divide a nivel tangencial en áreas anatómicas diferentes que están especializadas funcionalmente (Alfano and Studer 2013). Estas áreas, que también están definidas por su estructura celular, bioquímica, conectividad y sus patrones de expresión génica, se generan durante el desarrollo embrionario y podrán ser modificadas en etapas más tardías del desarrollo mediante la entrada de información sensorial (Alfano and Studer 2013; O'Leary and Sahara 2008; Sur and Rubenstein 2005). Hay cuatro áreas primarias corticales: el área somatosensorial primaria (S1) que procesa información sensorial del cuerpo, el área visual primaria (V1) que procesa información visual originada en los ojos, el área auditoria primaria (A1) que procesa información del oído interno/cóclea y el área motora primaria (M1) que controla el movimiento voluntario del cuerpo. Sobre las áreas se hablará en más detalle más adelante en esta introducción.

FORMACIÓN DE LAS LÁMINAS CORTICALES

Los dos tipos principales de neuronas de la corteza son las neuronas de proyección (NP) y las interneuronas. Las NP nacen en la pared dorsal del ventrículo del telencéfalo, son neuronas glutamatérgicas (excitatorias) y en su mayoría de morfología piramidal cuyos axones inervan regiones intracorticales (dentro de la propia corteza), subcorticales (otras estructuras cerebrales) o subcerebrales (fuera del cerebro, constituido fudnamentalmente por corteza, hipocampo y ganglios basales). Las interneuronas, en cambio, liberan neurotransmisores inhibitorios y sus conexiones son locales. Las interneuronas tienen su origen fuera de la corteza, en las eminencias gangliónicas y el área preóptica, y migran tangencialmente a través de la zona marginal y zona intermedia para poblar la placa cortical (Anderson et al. 2001; Anderson et al. 2002; Gelman et al. 2009). Debido a que el objeto de estudio de esta tesis doctoral son principalmente las neuronas excitatorias, no se profundizará en la descripción del desarrollo de las interneuronas.

La neocorteza surge del prosencéfalo cuando las células neuroepiteliales comienzan a diferenciarse en células de glía radiales (CGR) (Smart 1973) alrededor del día embrionario (E) 10 (en ratones) y de la quinta semana gestacional en humanos (Muller and O'Rahilly 1988). Las CGR son progenitores corticales con morfología bipolar que residen en la zona ventricular (ZV) del cerebro en desarrollo; tienen una unión apical a la superficie ventricular y una unión basal a la superficie de la pía. Las CGR dan lugar otro tipo de progenitores, los progenitores intermedios (PI) (Noctor et al. 2004), que residen en la zona subventricular (ZSV) y que se caracterizan por perder una o ambas uniones radiales. Típicamente, las CGR se dividen simétricamente para autorrenovarse y asimétricamente para generar una nueva CGR y una neurona o un PI que migrará a la ZSV. Además, los PI van a generar la mayoría de las neuronas de todas las capas; normalmente se dividen una vez de manera simétrica expandiendo la cantidad de neuronas postmitóticas (**Figura 2**) (De Juan Romero and Borrell 2015). Las CGR y los PI presentan diferencias a nivel morfológico y molecular, contribuyen diferencialmente a las distintas capas de las corteza, y pueden subdivirse en distintas clases (De Juan Romero and Borrell 2015; Englund et al. 2005; Molyneaux et al. 2005; Nieto et al. 2004; Tarabykin et al. 2001). Conforme proliferan, las sucesivas generaciones de precursores restringen su potencial de forma que las CGR pueden generar tanto las neuronas de las láminas inferiores como, a través de los PI, las de las láminas superiores (Malatesta et al. 2000; Noctor et al. 2001). Aunque tradicionalmente se ha pensado que los PI únicamente podían dar lugar a las neuronas de las láminas superiores, en el último año se ha demostrado que también pueden originar neuronas de las láminas inferiores (Mihalas et al. 2016).

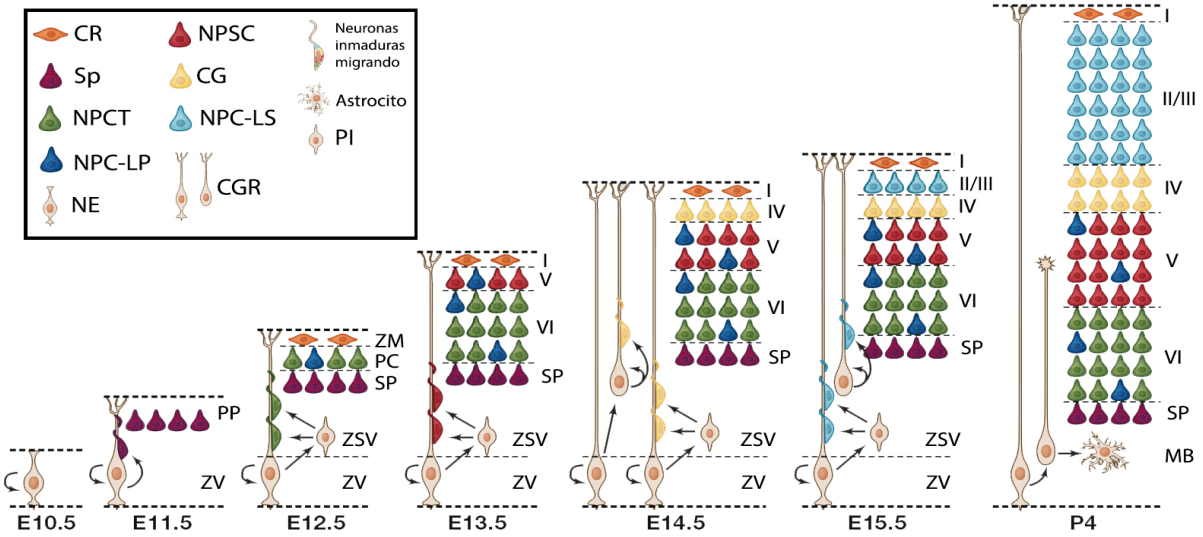

Figura 2. Las distintas poblaciones de progenitores generan neuronas de proyección "de dentro a fuera". Las neuronas son generadas en la ZV y ZSV y migran radialmente, gracias a la glía radial, a la capa que les corresponde. CR: Célula Cajal-Retzius; SP: Subplaca; NPCT: Neurona de proyección corticotalámica; NPLP: Neurona de proyección de las láminas profundas; NE: Neuroepitelio; NPSC: Neurona de proyección subcortical; N LIV: Neurona de la lámina IV; NPLS: Neurona de proyección de las láminas superficiales; CGR: Célula de glía radial; PI: Progenitor intermedio; PP: Preplaca; ZV: Zona Ventricular; ZSV: Zona subventricular; ZM: Zona Medial; MB: Materia Blanca E: Día embrionario; P: Día postnatal. Adaptado de Woodworth et al.

Las neuronas no van a residir en el lugar en el que nacen. Los progenitores se dividen originando las neuronas post-mitóticas, que se posicionan en la neocorteza migrando radial y tangencialmente adheridas a las proyecciones de las CGR de la que se separan al contactar con estructuras de la pía (Rakic 1988). Por tanto, la formación de la corteza se desarrolla secuencialmente en una forma que se describe como "desde el interior hacia el exterior" en la que las neuronas que nacen después migran sobre las nacidas antes para llegar a su posición final. Debido a esto, las neuronas que nacen más temprano están situadas en las láminas más internas y viceversa. A E10.5 las primeras neuronas postmitóticas en la ZV migran para formar la preplaca. La neurogénesis continúa y a E12.5 nuevas neuronas postmitóticas dividen la preplaca en zona marginal y subplaca, formando entre medias la placa cortical que después dará lugar a la lámina VI (Allendoerfer and Shatz 1994; Marin-Padilla 1998). Las neuronas generadas a E13.5 migran sobre las de la lámina VI y forman la V (Angevine and Sidman 1961; Caviness 1982). De E14.5 en adelante, las neuronas de las láminas superficiales proceden de divisiones simétricas de los PI de la ZSV (Haubensak et al. 2004; Miyata et al. 2004; Nieto et al. 2004; Noctor et al. 2004; Rash and Grove 2006). Primero a las de la IV (E14.5) y después las de las láminas II-III (E15.5-E16.5) (Caviness 1982; Molyneaux et al. 2007; Noctor et al. 2004; Rakic 1974; Tissir and Goffinet 2003). Finalmente, a partir de E18.5, las CGR dan lugar a astrocitos y oligodendrocitos; las células de glía (**Figura 2**) (Luskin et al. 1988; Malatesta et al. 2003).

A lo largo de la evolución se observa un aumento en la complejidad de las láminas corticales en cuanto a subclases de neuronas piramidales que ha contribuido a la suma de nuevos circuitos y funciones de la corteza. Las teorías actuales sugieren que el desarrollo neuronal en dos fases (a partir de la ZV y de la ZSV) habría permitido la expansión de las láminas corticales de forma coordinada con la aparición de nuevos tipos neuronales (De Juan Romero and Borrell 2015).

LOS FACTORES DE TRANSCRIPCIÓN COMO CÓDIGOS MOLECULARES QUE DETERMINAN LA DIFERENCIACIÓN E IDENTIDAD NEURONAL

Tanto las funciones de las neuronas piramidales de cada lámina como su morfología, procedencia y patrones de conectividad son similares, sin embargo, no son poblaciones totalmente homogéneas y existen subpoblaciones con diferentes funciones y expresión molecular dentro de cada lámina. La diferenciación de las neuronas en estos subtipos diferentes se produce gracias a programas de factores de transcripción (FT) que se inician en los progenitores o en neuronas inmaduras y que por ende son fundamentales para establecer el patrón correcto de conectividad de la corteza (Fame et al. 2011; Leone et al. 2008; Molyneaux et al. 2007). Aunque la determinación del destino laminar tiene una parte mediada por señales extrínsecas, la progresión para generar un subtipo de neurona específico y la coordinación temporal es, al menos parcialmente, intrínseca a los progenitores (Guillemot 2007; Shen et al. 2006). Los FT determinan la identidad molecular de los distintos tipos de NP. Desde la neurogénesis temprana se expresan FT que van a determinar las subsiguientes cascadas de activación de otros FT activados en su progenie, el tipo neuronal que van a generar los progenitores, la posición que estas neuronas adoptarán dentro de la corteza y hasta su integración selectiva en los distintos circuitos. Así pues, también podemos encontrar FT específicos de tipo neuronal o regional expresados en todos o sólo en parte de los tipos celulares que constituyen un linaje o linajes neuronales (es decir, en los precursores), en las neuronas indiferenciadas migrando o en las neuronas posicionadas en sus láminas definitivas. Además, dentro de los FT expresados en neuronas, la expresión puede tener lugar en todas o sólo en alguna de las distintas etapas de su vida (**Figura 3**).

Emx2, Foxg1, Lhx2, y Pax6 constituyen un primer grupo de FT que determinan la dorsalización y arealización de los progenitores corticales gracias a la represión de otros FT determinantes de destinos distintos al cortical (Mallamaci and Stoykova 2006; Muzio and Mallamaci 2003; Quinn et al. 2007). Un segundo grupo de genes relacionados con el proceso de diferenciación actúa en progenitores y neuronas postmitóticas recién divididas. Estos FT se expresan de forma específica en cada tipo neuronal (en las distintas láminas y áreas corticales, así como en sus subpoblaciones). Este tipo de FT incluyen a Cux1 y Cux2, objeto de esta tesis. Cux1 se expresa desde el estadío de progenitor hasta la madurez y durante toda la vida de la neurona, de manera que está presente tanto en los precursores de la ZSV como en las neuronas post-mitóticas de las láminas superiores. Cux2 por su parte, se expresa en los PI y actualmente existe controversia sobre si es selectivo o no de las láminas superiores (Eckler et al. 2015; Franco et al. 2012; Gil-Sanz et al. 2015; Guo et al. 2013). Otros FT únicamente se van a expresar en ciertos momentos del desarrollo, pero su contribución será igualmente fundamental para la determinación de la identidad neuronal (**Figura 3**) (McConnell 1990; Merot et al. 2009). Es necesario remarcar que un mismo FT puede tener funciones diferentes en función del momento o tipo neural en el que se exprese. Por ejemplo, Lhx2, está presente tanto en las ZV y ZSV durante la generación de las neuronas de las láminas superiores como en las neuronas post-mitóticas en un momento posterior del desarrollo (**Figura 3**). En este sentido, si bien se ha descrito que en un primer momento es esencial

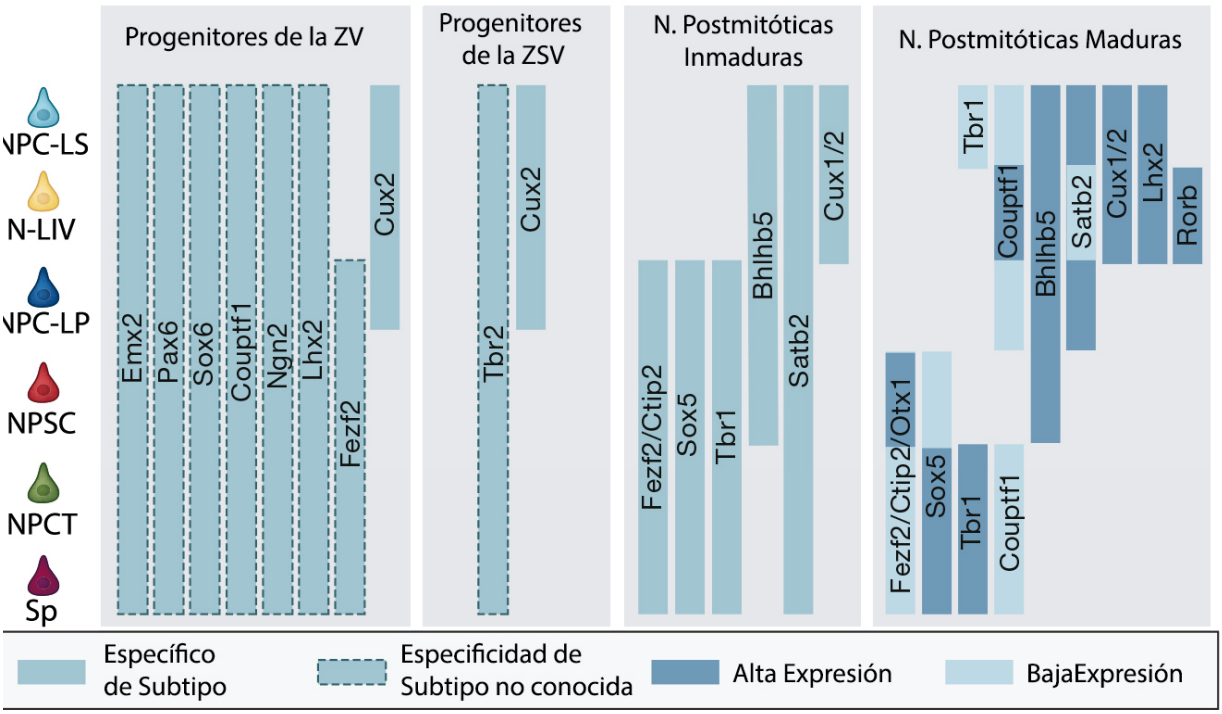

Figura 3. La combinación progresiva de diferentes FT determina la identidad de las neuronas de proyección. NPLS: Neurona de proyección de las láminas superficiales; N LIV: Neurona de la lámina IV; NPLP: Neurona de proyección de las láminas profundas; NPSC: Neurona de proyección subcortical; NPCT: Neurona de proyección corticotalámica; SP: Subplaca. Adaptado de Woodworth et al.

para el establecimiento de la identidad neocortical de los progenitores corticales (Chou et al. 2009; Hsu et al. 2015; Monuki et al. 2001), su papel en las neuronas de las láminas superiores aún no ha sido determinado claramente.

Las diferentes láminas corticales se caracterizan, entre otras cosas, por expresar uno o varios FT específicos. La expresión espacio-temporal de estos FT va a variar en cada caso; mientras que algunos están presentes en toda la lámina, otros van a estarlo únicamente en subpoblaciones específicas dentro de ellas. A modo de ejemplo, Cux1, Cux2 y Lhx2 son marcadores de las láminas II-III y IV (Bulchand et al. 2003; Nieto et al. 2004); Brn1, Brn2 de las II-III y V (Magdaleno et al. 2006; Sugitani et al. 2002); Rorβ de la IV (Moreno-Juan et al. 2017; Schaeren-Wiemers et al. 1997); Foxp2 de la lámina VI (Ferland et al. 2003) y Ctip2 y Fezf2 la V y la VI (Arlotta et al. 2005; De la Rossa et al. 2013; Inoue et al. 2004; Leid et al. 2004; Molyneaux et al. 2005; Rouaux and Arlotta 2013). Además, Ctip2, Sox5 y Tbr1 marcan, en función de sus niveles relativos de expresión, los diferentes subtipos de neuronas corticofugales (Figura 3) (Arlotta et al. 2005). A pesar de los grandes avances de la última década en cuanto a la descripción de los códigos moleculares que codifican las diferentes subpoblaciones neuronales (AllenDevelopingMouseBrainAtlas 2008), el papel concreto de estos FT en la adquisición

de las características neuronales maduras y en la formación de conexiones funcionales selectivas para dar lugar a los complejos circuitos del cerebro continúa siendo, en términos relativos, una gran incógnita.

LOS FACTORES DE TRANSCRIPCIÓN CUX1 Y CUX2

En esta tesis doctoral tienen especial relevancia los FT Cux1 y Cux2 que, a pesar de ser ambos homólogos en vertebrados del gen *Cut* de Drosophila y compartir muchas similitudes, presentan diferencias en cuanto a estructura y función. Los genes *Cux* dan lugar a un grupo de homeo-proteínas conservado entre los eucariotas superiores que consta de varios dominios de unión al ADN: un homeodominio y una, dos o tres repeticiones Cut. En ratón, la expresión de ambos es diferente: Cux1 se expresa en múltiples tejidos y presenta varias isoformas originadas por corte y empalme (splicing) alternativo y proteólisis de la proteína (Hulea and Nepveu 2012; Sansregret and Nepveu 2008); Cux2 -del que sólo se conoce una isoforma- se restringe mayoritariamente al sistema nervioso, sistema urogenital y páncreas en el desarrollo (Gingras et al. 2005; Iulianella et al. 2003; Iulianella et al. 2009; Nieto et al. 2004; Pal et al. 2015; Zimmer et al. 2004). Ambos genes parecen estar regulados directa o indirectamente por Pax6, ya que dejan de expresarse en ratones KO para ese gen (Georgala et al. 2011; Gray et al. 2017; Nieto et al. 2004; Zimmer et al. 2004). Respecto a la corteza, Cux1 y Cux2 marcan selectivamente las neuronas piramidales de láminas superiores (II-III y IV) y no se expresan en las inferiores, a excepción de una población muy minoritaria en la lámina V. Su expresión mayoritaria se da inicialmente en los PI en el caso de Cux2, mientras que Cux1 presenta niveles muy bajos en el precursor a nivel de ARN y proteína, y no es hasta que la neurona comienza su migración cuando su presencia es claramente detectable. La expresión de ambas proteínas se mantiene después durante toda la vida de las láminas II-III y IV (Franco et al. 2012; Nieto et al. 2004). En cuanto a áreas, ambos genes abarcan las láminas superiores o tardías de todas ellas, pero sus patrones de expresión divergen ligeramente. Mientras que Cux1 presenta niveles más altos en la corteza somatosensorial que en la cingulada, visual y motora, la expresión de Cux2 está enriquecida en las áreas frontal e insular (Nieto et al. 2004; Rowell et al. 2010). Cux2 también se expresa en niveles altos en una población de interneuronas que nace en el subpalio y migra a la neocorteza (Cobos et al. 2006), aunque no es necesario para que estas se desarrollen correctamente. En humanos, mientras que CUX2 también define las láminas superiores de la corteza cerebral (Arion et al. 2007), la expresión de CUX1 es ubicua (Ramdzan and Nepveu 2014).

Cux1 y Cux2 se unen a las mismas secuencias de ADN (hay múltiples secuencias consenso diferentes), aunque Cux1 las une con mayor afinidad. Pueden actuar como activadores o represores de la expresión génica, y se han descrito funciones que pueden ser exclusivas de uno de los dos (Cux1 o Cux2) (Cubelos et al. 2008; Hulea and Nepveu 2012) o comunes y aditivas (Cubelos et al. 2010). Cux1, por ejemplo, es conocido por su implicación tanto en la supresión tumoral como en su progresión (Ramdzan and Nepveu 2014). Su función en progenitores neurales aún no está clara, sin embargo, se sabe que Cux2 controla la decisión de salida del ciclo celular en los PI, de forma que si no está presente, se expanden los precursores (Cubelos et al. 2008; Ferrere et al. 2006; Nieto et al. 2004). Los ratones KO de *Cux2* muestran una expansión de la ZSV, un aumento en los niveles de ciclina D2 (no publicado), así como un número excesivo de neuronas de las láminas superiores, lo que sugiere una posible relación de este FT con la expansión de la corteza cerebral ocurrida a lo largo de la evolución (Cubelos et al. 2008). A nivel post-mitótico, ambas proteínas regulan de forma complementaria, aditiva y no redundante la ramificación de las dendritas, la morfología de las espinas y la sinaptogénesis en las

neuronas corticales de las láminas superiores (Cubelos et al. 2010). Aunque sabemos muy poco de cómo llevan a cabo estas funciones, sí que se conoce que los genes *Cux* promueven la estabilidad sináptica y la maduración gracias a mecanismos que implican la regulación de las proteínas NMDAR2B, PSD95 y la regulación de directa de los genes Xlr4b y Xlr3b (Cubelos et al. 2010). Sin embargo, el papel diferencial de estos FT en la compartimentalización de las dendritas y en otros procesos de conectividad tales como la ramificación y refinamiento axonal o la formación de mapas corticales no había sido abordado con anterioridad a esta tesis doctoral.

LA INTEGRACIÓN FUNCIONAL DE LA INFORMACIÓN SENSORIAL TIENE SU BASE EN LA FORMACIÓN CORRECTA DEL CIRCUITO DURANTE EL DESARROLLO

El circuito intracortical más básico es el que determinan las columnas corticales, definido por la conectividad entre las neuronas de las diferentes láminas. Este circuito se describió originalmente en la corteza somatosensorial (Mountcastle et al. 1957) al observar que las neuronas de una misma columna respondían con una actividad similar en respuesta a un estímulo. Años más tarde, Hubel y Wiesel demostraron que este tipo de circuitos no son exclusivos de las áreas corticales somatosensoriales. Gracias a sus estudios en la corteza visual, sabemos que su inervación también se organiza en columnas (dominancia ocular) y que existen otro tipo de columnas denominadas de orientación (Hubel and Wiesel 1962, 1963). Sobre estos fundamentos, la descripción detallada de la conectividad columnar de la corteza es aún objeto de estudio dado su elevado nivel de complejidad (Jiang et al. 2015; Lefort et al. 2009).

Para que la integración de la información sensorial sea funcional, es necesario que exista también una conectividad horizontal entre áreas. Por eso, las diferentes columnas se conectan entre ellas a nivel tangencial. La mayor parte de la información sensorial llega a estas columnas inicialmente desde las neuronas talamocorticales (Feldmeyer 2012) y esta actividad va a influir en el desarrollo de las distintas áreas corticales modulando la expresión génica, la citoarquitectura y la morfología celular (Li et al. 2013). Así, la información sensorial es fundamental para el desarrollo del circuito y las modificaciones que se produzcan en ésta (por ejemplo, por medio de experimentos de privación sensorial) van a afectar tanto al tamaño como a la funcionalidad de las áreas afectadas y de las adyacentes (Dehay et al. 1991; Frost 1982; Roe et al. 1990; Roe et al. 1993; Sharma et al. 2000; Sur et al. 1988).

LA CORTEZA DE BARRILES

La corteza de barriles del S1 ha sido utilizada durante mucho tiempo como modelo de circuitos corticales, procesamiento de información sensorial (Lefort et al. 2009) y plasticidad neuronal (De la Rossa et al. 2013). En ratones, uno de los principales órganos de percepción son sus bigotes, que transmiten los estímulos externos al S1 a través del tálamo. Estos estímulos provocan que las neuronas postmitóticas de S1 se agrupen de forma topográficamente ordenada, produciendo unas estructuras formadas por diferentes grupos de neuronas que recuerdan a barriles y que reciben los estímulos, representando a un bigote cada una (**Figura 6A**) (Woolsey and Van der Loos 1970). Para que la corteza de barriles se forme adecuadamente es necesaria la correcta transmisión de la información talámica durante un periodo crítico o de oportunidad comprendido entre el día postnatal (P) 0 y el P3 para la plasticidad estructural (Erzurumlu and Gaspar 2012; Van der Loos and Woolsey 1973) y hasta P14 en el caso de la plasticidad sináptica (Lendvai et al. 2000; Maravall et al. 2004a; Maravall et al. 2004b; Shoykhet et al. 2005; Stern et al. 2001). Una gran ventaja del estudio de esta estructura es que su conectividad circuital se conoce bien: la información sensorial externa producida por el movimiento

de los bigotes se transmite inicialmente al ganglio trigémino a través del nervio infraorbital y después al tallo encefálico y al tálamo. Como para el resto de modalidades sensoriales, la información se procesa en primer lugar en un núcleo talámico de primer orden desde el que va a un área primaria de la corteza (S1). Este área proyecta a otro núcleo talámico de mayor orden que, a su vez, inerva el área secundaria correspondiente (S2) (Frangeul et al. 2016). En el caso de S1, las neuronas del núcleo talámico ventroposterior son las responsables de enviar la información sensorial principalmente a la lámina IV (Pouchelon et al. 2014). Después, la información se transmite a lo largo de las columnas corticales: de la lámina IV a la II/III, de la II-III a la V y a la misma II-III, y de la V a la VI. Estas dos últimas láminas V y VI contienen NP corticofugales que van a enviar la respuesta cortical a dianas extra-corticales, incluyendo el núcleo talámico posteromedial que será el que inerve al S2 (Gilbert 1993; Porter et al. 2001). Esta organización se repite, en líneas generales, en el resto de áreas sensoriales. Los cuatro núcleos talámicos que proyectan a las áreas primarias corticales son el ventroposterior, el ventrolateral, el dorsal lateral geniculado y la parte ventral del núcleo geniculado medial que, respectivamente, van a enviar información a S1, M1, V1 y A1(Lopez-Bendito and Molnar 2003). Cabe destacar que en estos circuitos la mayoría de conexiones son intracorticales por lo que, a nivel funcional, una parte muy relevante tanto del procesamiento de la información como de su integración tienen lugar en la corteza cerebral (Conel 1953).

LA ESTRUCTURA DE LA DENDRITA COMO PUNTO DE REGULACIÓN PARA LA INTEGRACIÓN DE LA NEURONA EN CIRCUITOS ESPECÍFICOS DURANTE EL DESARROLLO

Las dendritas son procesos proximales al soma y relativamente cortos y gruesos en comparación con el axón. En la corteza la trayectoria de la dendrita principal es radial (Cline 2001; Kollins and Davenport 2013). A nivel funcional, las dendritas reciben principalmente información de los axones, la integran y la transmiten hacia el soma neuronal (Chilton and Gordon-Weeks 2007; Gulledge et al. 2005). La dendrita se forma tras la migración y a partir de extensiones de neuritas. Después tiene lugar una fase de formación de filopodios muy dinámicos cuyo resultado será la acumulación gradual de nuevas ramas (Libersat and Duch 2004; Urbanska et al. 2008). El árbol dendrítico va a madurar a la vez que surge la actividad sináptica. Esta maduración también comprende una etapa de prunning o poda de ramas dependiente de actividad (Kwon et al. 2006), de forma que se estabiliza volviéndose menos plástico (Cline 2001). La topología final de la dendrita influye de manera crítica en el procesamiento de la información sináptica entrante (Urbanska et al. 2008), ya que determina el número y el patrón de las sinapsis recibidas por cada neurona (McAllister 2000; Urbanska et al. 2008). Está regulada tanto por diversos factores extracelulares como por un programa genético intrínseco, mediado por FT (Y. N. Jan and Jan 2010; Urbanska et al. 2008). Entre los factores extracelulares destacan las interacciones entre células y con la matriz extracelular, diversas moléculas secretadas (quimiotrópicas, neurotransmisores, hormonas, factores de crecimiento y factores neurotróficos) y la actividad neuronal (Kollins and Davenport 2013; Urbanska et al. 2008). La regulación intrínseca mediada por FT es muy importante en el desarrollo dendrítico. Sirve para determinar el ritmo de crecimiento, la dirección o la extensión de las ramas y también para transducir las señales extracelulares antes mencionadas de manera específica de tipo celular (de la Torre-Ubieta and Bonni 2011; Polleux et al. 2016). Además de los genes *Cux*, otro ejemplo de un FT importante en la integración de la neurona en el circuito cortical es *Fezf2* (Fez family zinc finger 2). Este gen, que se expresa en las NP subcorticales de las láminas V y VI, regula su arquitectura dendrítica. Reduciendo los niveles de expresión de Fezf2 se

impide el crecimiento de las dendritas basales y se altera la orientación de las apicales, además de eliminarse las proyecciones axonales subcorticales de estas neuronas (B. Chen et al. 2005a; J. G. Chen et al. 2005b).

CONECTIVIDAD INTERHEMISFÉRICA

Los circuitos corticales tienen un nivel añadido de complejidad debido a que las conexiones pueden tener lugar en el mismo hemisferio cerebral (intrahemisféricas) o en el contrario (interhemisféricas). Las conexiones interhemisféricas son fundamentales para integrar la información entre ambos hemisferios cerebrales y entre áreas funcionales y tienen lugar gracias a que las NP de largo alcance forman comisuras a lo largo de la línea media, de forma que alcanzan tanto áreas homotópicas como heterotópicas del lado contralateral (Boyd et al. 1971; Hedreen and Yin 1981; Segraves and Rosenquist 1982; Yorke and Caviness 1975). En mamíferos, las principales comisuras que conectan ambos hemisferios son el cuerpo calloso (CC), la comisura hipocampal, y la comisura anterior. En esta tesis tiene especial importancia el CC, que es el mayor tracto nervioso de materia blanca de los mamíferos. Se encarga de la integración de la información de ambos hemisferios corticales para poder realizar funciones tan complejas como la cognición o el movimiento voluntario y coordinado. El CC es crítico no sólo para integrar adecuadamente la información percibida a través de los sentidos, sino también para responder de forma apropiada ante ésta y elaborar pensamientos complejos (Morcom et al. 2016). Por tanto, no es sorprendente que su ausencia congénita (agénesis o disgénesis) esté asociada con un gran número de enfermedades del cerebro con origen en el desarrollo (Edwards et al. 2014; Hetts et al. 2006) y de déficits neurológicos (Paul et al. 2007).

El CC del ratón está formado principalmente por axones de las neuronas piramidales de las láminas II-III (80%), V (20%) y algunos de la lámina VI (**Figura 2**) (Kier and Truwit 1996; Richards et al. 2004). No obstante, los estudios hechos con marcadores retrógrados en el cerebro adulto demostraron que no todas las neuronas de las láminas II-III y V van a formar el CC, sino que únicamente ciertas subpoblaciones de estas láminas emiten axones al hemisferio contralateral permitiendo la conexión de las diferentes áreas corticales (Fame et al. 2011; Mitchell and Macklis 2005). Las neuronas callosas emiten sus axones hacia la línea media, desde donde serán guiados hacia sus dianas por medio de factores intrínsecos (principalmente FT) y extrínsecos (moléculas guía) y de la actividad neuronal. En este proceso, los estudios iniciales describieron las neuronas pioneras, cuyos axones podrían navegar sin necesidad de otras pre-existentes y que servirán de guía para otros axones seguidores (Koester and O'Leary 1994), como de especial importancia. Más recientemente, se ha demostrado un papel fundamental de las estructuras de la línea media formadas por poblaciones gliales y moléculas solubles en la señalización del camino a seguir (Lindwall et al. 2007; Niquille et al. 2009; Nishikimi et al. 2013; Smith et al. 2006). Los programas moleculares responsables de la especificación de la subpoblación de las neuronas callosas no se conocen en detalle, aunque se sabe que hay algunos FT importantes. Este es el caso de Satb2 (Special AT-rich sequence binding protein 2), cuya expresión temprana en las láminas superiores es necesaria para la formación de la proyección callosa (Leone et al. 2015). En ratones en los que la expresión de Satb2 ha sido eliminada selectivamente en la corteza, los axones de las neuronas de las láminas II-III conectan sólo intrahemisféricamente y de forma aberrante (Leone et al. 2015). Es importante recalcar que al menos hay un grupo de neuronas callosas que no requiere Satb2 para proyectar al hemisferio contralateral (Alcamo et al. 2008; Leone et al. 2015; Lickiss et al. 2012).

La técnica de la electroporación in utero ha permitido conocer con gran detalle la dinámica de formación del

CC del ratón en el área S1 (Wang et al. 2007). Alrededor de P2 los axones callosos cruzan la línea media para llegar tres días más tarde a la región contralateral a inervar. A P8 los axones comienzan a invadir la placa cortical contralateral y en torno a P10, aquéllos que han alcanzado la zona homotópica en el hemisferio contrario, comienzan a ramificarse de forma exuberante. Finalmente se refinarán esas conexiones, principalmente gracias a procesos mediados por la actividad neuronal, de manera que solo se van a mantener las necesarias para circuito final. Después de P16, el patrón de conectividad va a sufrir únicamente pequeños cambios por lo que se considera que es bastante similar al que se mantendrá a lo largo de la vida adulta (**Figura 4**) (Wang et al. 2007).

A nivel molecular, lo primero que ocurre es la guía del axón a la zona intermedia. Una vez que las neuronas callosas han migrado a su lámina correspondiente, proyectan sus axones hacia debajo de la neocorteza para después girar hacia a la línea media. Este proceso está mediado por distintos receptores de la guía axonal regulados por FT como Satb2, que regula Unc5c (Receptor Unc5 homólogo C) y Dcc (Deleted in colorectal cáncer), dos receptores de Netrin1 que actúan haciendo que los axones del CC giren hacia la zona intermedia (Finger et al. 2002; Hong et al. 1999; Keino-Masu et al. 1996; Serafini et al. 1996; Srivatsa et al. 2014; Zhao et al. 2011).

El siguiente paso es la atracción hacia el otro hemisferio y en él van a ser fundamentales las estructuras de la línea media: poblaciones de neuronas o de glía que influyen en la formación del CC gracias a la secreción de moléculas guía y al contacto celular con los axones callosos y que, en ratones, están ya presentes a E15. Las estructuras formadas por poblaciones gliales son cuatro: la cremallera glial de la línea media, la cuña glial, la circunvolución supracallosa y el cabestrillo glial (Nishikimi et al. 2013; T. Shu and Richards 2001; Silver et al. 1982; Silver et al. 1993). Además de éstas, están

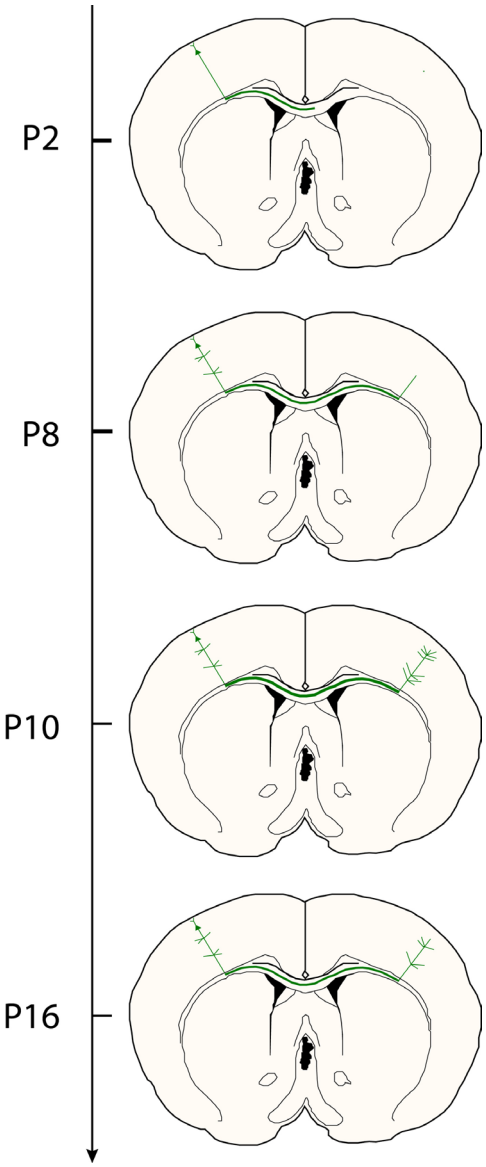

Figura 4. Desarrollo axonal del CC en el área somatosensorial. El cruce de la línea media tiene lugar a P2. A P8 los axones están comenzando a invadir el hemisferio contralateral. Alrededor de P10 los axones ramifican de forma exuberante, para refinarse unos días después. A P16, el patrón de inervación en el hemisferio contralateral es muy similar al del circuito maduro.

implicadas otras poblaciones no gliales como las neuronas GABAérgicas y glutamatérgicas que existen transitoriamente en la línea media y pueden atraer a los axones callosos (Niquille et al. 2009). Una de las moléculas que señalizan a los receptores de superficie axonales importante en la formación del CC es la Neuropilina 1 (Nrp1), el receptor de clase 3 de semaforinas (Sema3). Nrp1 se expresa en los axones de las neuronas pioneras de la corteza cingulada (Piper et al. 2009), que son la primeras en cruzar la línea media. Sema3C atrae esos axones hacia la línea media y Sema3A –expresada en el cabestrillo glial - los va a repeler del septo (bajo la materia blanca), impidiendo que se desvíen de su camino (Niquille et al. 2009; Piper et al. 2009). Para cruzar la línea media son importantes las efrinas, las Slits y sus receptores respectivos gracias a su expresión en las estructuras gliales de la línea media o en los axones del CC (Hu et al. 2003; Mendes et al. 2006). Por ejemplo, en ausencia de SLIT2 los axones callosos se dirigen al septo (Bagri et al. 2002; T. Shu et al. 2003; Unni et al. 2012).

Finalmente tiene lugar un viaje similar a través de la zona intermedia del hemisferio contralateral, en el que el tracto calloso se dirige hacia las dianas contralaterales y establece las conexiones en la placa cortical. En cepas de ratón como C57BL6, se ha descrito cómo la inervación sigue un orden topográfico y los axones callosos derivados de las neuronas de S1, M1 y V1 inervan densamente sólo el borde entre las áreas primarias y secundarias, pero no los territorios adyacentes(Fenlon and Richards 2015). Hay dos factores que se propone que influyen especialmente en este proceso: la posición de los axones en el tracto calloso durante el cruce de la línea media, mediada por la señalización Sema3A/Nrp1 (Piper et al. 2009; Zhou et al. 2013), y la relación entre la actividad de ambos hemisferios (Huang et al. 2013; Suarez et al. 2014). La importancia de la actividad se discutirá en detalle en el próximo apartado de esta tesis. No obstante, respecto a su papel en la formación del CC, multitud de estudios llevados a cabo en las últimas décadas han demostrado claramente que la inervación contralateral es muy sensible a las manipulaciones de la actividad tanto en el sistema visual como en el somatosensorial (Huang et al. 2013; Mizuno et al. 2007; Olavarria and Van Sluyters 1995; Suarez et al. 2014; Wang et al. 2007). De entre estos, los estudios más recientes son los que han permitido diseccionar que lo relevante para conectar con la diana no es la presencia o ausencia de actividad, sino el balance entre la actividad intrínseca y extrínseca. Al alterar la actividad intrínseca o extrínseca de sólo uno de los lados, la inervación contralateral se ve muy reducida, pero al alterar la actividad de ambos hemisferios por igual se rescata esa inervación (Huang et al. 2013; Mizuno et al. 2007; Suarez et al. 2014; Wang et al. 2007). Sin embargo, aún no se conocen los mecanismos moleculares dependientes de actividad que regulan este tipo de inervación.

LA ACTIVIDAD NEURONAL

Por actividad neuronal nos referimos a los cambios eléctricos que ocurren en las neuronas debido al movimiento de iones a través de su membrana plasmática. Esta dinámica iónica va a generar respuestas de diversa naturaleza relacionadas con el comportamiento y la comunicación neuronales. A pesar de que ya en tiempos de Cajal se intuía que la transmisión del impulso eléctrico entre neuronas era la base del funcionamiento del sistema nervioso, a día de hoy seguimos sin comprender todos los mecanismos que subyacen a la generación, transmisión y efectos de estos impulsos.

Aunque durante mucho tiempo se pensó que el establecimiento inicial de los circuitos estaba determinado únicamente por factores independientes de actividad, cada vez está más claro que los patrones de actividad previos a la recepción de estímulos externos y la actividad temprana posterior derivada de la experiencia son fundamentales para el desarrollo neuronal

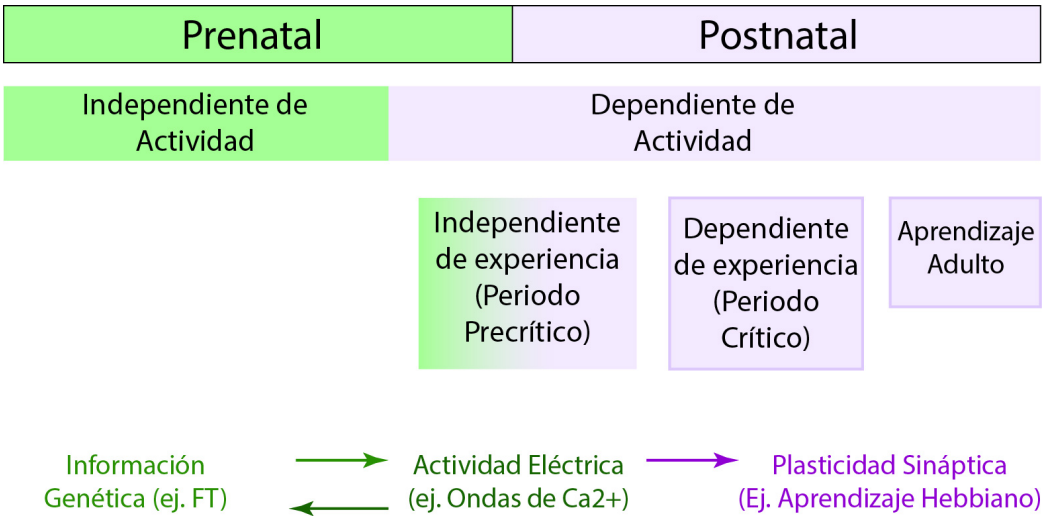

Figura 5. La formación de los circuitos neuronales tiene lugar gracias a la información genética de las neuronas y a la actividad eléctrica. Durante el desarrollo embrionario, los circuitos neuronales inmaduros y la conexiones topográficas iniciales se establecen gracias a la información genética. Con la emergencia de los diferentes canales, la actividad espontánea cobra importancia en la formación de la red. Adaptado de Khazipov et al, 2006.

normal (Blankenship and Feller 2010; Yamamoto and Lopez-Bendito 2012). La actividad espontánea es independiente de los estímulos externos y controla diversos procesos durante el desarrollo temprano, incluyendo la migración, la diferenciación neuronal y la guía axonal, aunque participa también en el refinamiento (Feller and Scanziani 2005; Kirkby et al. 2013; Penn et al. 1998; Rakic and Komuro 1995; Shatz and Stryker 1988). Las formas más tempranas de actividad espontánea dependen del intercambio directo de señales químicas o eléctricas a través de las uniones gap entre neuronas excitatorias. Estas uniones gap disminuyen en número a lo largo del tiempo (Peinado et al. 1993), a la vez que aumenta la importancia de las sinapsis químicas en la señalización neuronal (Leighton and Lohmann 2016). Por otro lado, la actividad inducida por estímulos externos determina de la conectividad final en las redes neuronales, por lo que va tener un papel destacado en el refinamiento del circuito (Degano et al. 2014; Jiao et al. 2011). En función del momento y de la subpoblación neuronal, tendrá más importancia un tipo de actividad u otro (**Figura 5**).

Como ya se ha adelantado en el apartado que concierne a la formación del CC, en los últimos cinco años se ha publicado una parte relativamente importante de los estudios que inciden sobre la función de la actividad en el desarrollo de esta comisura. Sin embargo, el papel de la actividad neuronal en otros sistemas se conoce desde hace tiempo. En el sistema visual fue donde primero se identificaron estos mecanismos al observar que la actividad espontánea, previa a la apertura del ojo, define las conexiones talamocorticales iniciales y la derivada de la experiencia es esencial para el refinamiento (Catalano and Shatz 1998; Katz and Shatz 1996). Estos trabajos iniciales en fetos de gato demostraron que la introducción del bloqueante de canales de sodio tetrodotoxina (TTX) en el momento en el que los primeros axones

procedentes del tálamo llegaban a las neuronas de la subplaca reducía la inervación cortical y la dispersaba hacia otras áreas de la corteza (Catalano and Shatz 1998). Esto contribuyó a demostrar definitivamente la importancia de la actividad espontánea en la topografía de la entrada de las conexiones talamocorticales y a proponer que la actividad temprana es importante para la formación del primer mapa (Sur and Leamey 2001), como luego se ha corroborado por ejemplo en el sistema olfatorio (Yu et al. 2004) o en las conexiones cortico-corticales. Respecto a estas últimas, la alteración de la actividad neuronal en las etapas iniciales del desarrollo de la corteza visual provoca que los axones ipsilaterales y contralaterales se vean afectados negativamente tanto a nivel de crecimiento como de generación de colaterales (Butler et al. 2001; Dantzker and Callaway 1998; Mizuno et al. 2007).

Durante el desarrollo cortical podemos observar diferentes patrones endógenos de actividad neuronal que pueden estar sincronizados entre varias neuronas (generando olas de actividad) o no estarlo (asíncronos) (Adelsberger et al. 2005; Khazipov and Luhmann 2006). Gracias a estudios hechos en ratas, sabemos que durante el desarrollo de la corteza hay tres patrones de actividad circuital: las ráfagas fusiformes, las oscilaciones gamma y las largas (Yang et al. 2009). Las ráfagas fusiformes están a menudo sincronizadas entre ambos hemisferios, incluso antes de la formación del CC. Marcano-Reik y colaboradores demostraron que la transección de esta comisura altera las ráfagas fusiformes, lo que deja una puerta abierta a una posible relación entre la sincronización de la actividad neuronal entre ambos hemisferios cerebrales mediante estos tipos de actividad y la formación correcta del CC (Marcano-Reik and Blumberg 2008; Marcano-Reik et al. 2010; Yang et al. 2016).

Las ondas de calcio que se generan de forma espontánea en las neuronas a lo largo del desarrollo reflejan cambios eléctricos. Estas ondas también van a ser importantes en diversos procesos y sus efectos variarán en función del tipo neuronal. Por ejemplo, en cuanto al crecimiento axonal, las ondas de Ca2+ van a correlacionar positivamente en algunas poblaciones y negativamente en otras (Gomez and Spitzer 1999; Mattson et al. 1988; Ming et al. 2001; Tang et al. 2003). En el contexto del área S1, cabe destacar un estudio reciente que demuestra que la alteración en las ondas de calcio del núcleo talámico geniculado ventromedial produce cambios en la expresión genética del resto de núcleos, así como un aumento de tamaño de la corteza de barriles (Moreno-Juan et al. 2017). Por tanto, la regulación transcripcional dependiente de este tipo de actividad parece representar un mecanismo importante en procesos relacionados con el desarrollo neocortical.

Una vez establecido el mapa inicial, las actividades espontánea y derivada de la experiencia van a definir la dinámica de elongación y eliminación de ramificaciones axonales. Gracias a ellas se modula la exuberancia inicial de ramificaciones formadas durante el desarrollo, de manera que únicamente se van a mantener aquellas conexiones que sean correctas para que el circuito pueda funcionar adecuadamente (Holtmaat et al. 2013; Maor-Nof et al. 2013; Marik et al. 2013). Estos procesos de refinamiento pueden estar mediados por mecanismos Hebbianos, si requieren la participación común de la neurona pre-sináptica y de la post-sináptica, o no-Hebbianos, cuando esa estabilización depende únicamente de la actividad pre o post-sináptica (Kirkby et al. 2013; Piochon et al. 2012). En este sentido, gracias a experimentos realizados en el sistema visual, sabemos que la maduración de sinapsis puede regular la ramificación axonal. La estabilización de los axones se favorece por la presencia de sinapsis maduras y cuando los axones no poseen sinapsis, o sólo tienen sinapsis inmaduras, se retraen (Antonini and Stryker 1993; Gibson and Ma 2011; Meyer and Smith 2006; Ruthazer et al. 2006). No obstante, también existen situaciones y tipos neuronales en los que se ha observado que el bloqueo de la

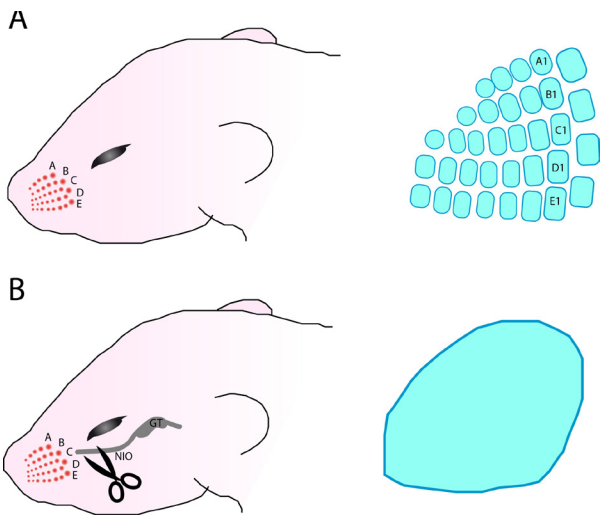

Figura 6. Diagrama esquemático de la plasticidad estructural de la corteza de barriles. A. El patrón inicial de los axones talamocorticales depende de la actividad derivada de la experiencia (Van der Loos & Woosley, 1970). **B.** Si se corta el nervio infraorbital (NIO), responsable de transmitir la información de los bigotes, los axones talamocorticales se distribuyen de forma aberrante y no se forman barriles en la corteza. GT: Ganglio trigémino. Adaptado de Erzumulu & Gaspar.

sinapsis no conlleva la retracción de sus axones (Koch et al. 2011). Respecto a los circuitos corticales del área somatosensorial, la actividad neuronal juega un papel fundamental en la formación de los patrones característicos de la corteza de barriles. La comunicación entre los axones talamocorticales y sus dianas postsinápticas, tiene lugar gracias a la transmisión glutamatérgica (Li et al. 2013). Los experimentos llevados a cabo en roedores han demostrado que la perturbación física de los folículos de los bigotes o del nervio infraorbital durante una ventana de tiempo que finaliza a P4 provoca alteraciones estructurales irreversibles en el mapa de barriles (**Figura 6B**) (Belford and Killackey 1980; Durham and Woolsey 1984; Erzurumlu and Gaspar 2012; Van der Loos and Woolsey 1973), mientras que eliminaciones del bigote entre P4 y P12 interrumpen la remodelación sináptica intracortical entre la lámina IV y la II-III dentro del barril (Allen et al. 2003; Erzurumlu and Gaspar 2012; Lendvai et al. 2000).

Por último, es importante mencionar que dentro de estos procesos de eliminación y extensión tiene especial relevancia el fenómeno de la competición axonal, también mediado por actividad. En la competición, las ramas de los axones vecinos emitidos por distintas neuronas van a pugnar por inervar una misma diana. La competición axonal ha sido muy estudiada en retina, donde se ha visto que la inhibición de la actividad de células ganglionares individuales afectaba negativamente tanto a su crecimiento axonal como a la formación de ramas colaterales. Sin embargo, este efecto se revertía al suprimir la actividad de las células ganglionares de retina vecinas (Hua et al. 2005; Shatz and Stryker 1978). Por consiguiente, la competición puede jugar un papel fundamental en la generación de mapas topográficos (Wiesel and Hubel 1963), incluyendo los de la corteza de barriles (Shepherd et al. 2003).

A pesar de que se conoce la importancia de la actividad en la expresión génica (West and Greenberg 2011), y de que se han descrito numerosos FT que regulan aspectos de la conectividad (Alcamo et al. 2008; Marcos-Mondejar et al. 2012; Shoemaker and Arlotta 2010), la influencia directa de determinados FT sobre la actividad eléctrica para modificar la conectividad no había sido muy explorada al inicio de esta tesis (Garcia-Frigola and Herrera 2010; Wolfram et al. 2012). La existencia de esta relación es de gran interés, ya que implica una coordinación entre los programas moleculares intrínsecos que especifican la diferenciación eléctrica de la neurona y el circuito, y los que regulan los circuitos neuronales a través de la identidad neuronal.

CANALES IÓNICOS

Los canales iónicos son proteínas transmembrana responsables tanto del potencial de la neurona en reposo como de los cambios de voltaje que se producen en esta. Se caracterizan por su selectividad restringida a determinados iones y, en muchos casos, por acti-

varse selectivamente gracias a un mecanismo concreto como voltaje, ligando, etc. (Catterall et al. 2012; Unwin 1989). Tras la activación, el canal se abre permitiendo que los iones fluyan a favor del gradiente electroquímico – hacia el interior o el exterior - hasta llegar a su potencial de equilibrio. Como resultado de este flujo de iones, cambia la diferencia de voltaje de la neurona con el exterior, lo que ocasionará efectos a distintos niveles. Estos cambios provocan el disparo de trenes de potenciales de acción (PA) (Catterall et al. 2012), pero también otros efectos como la activación de programas genéticos a través de cascadas de segundos mensajeros (West and Greenberg 2011), o la exocitosis de neurotransmisores en la hendidura sináptica y la activación e inactivación de otros canales dependientes de voltaje. La importancia de los canales iónicos en el correcto funcionamiento del sistema nervioso está totalmente aceptada y se ha descrito su implicación en múltiples enfermedades mentales (Brager and Johnston 2014; Schmunk and Gargus 2013).

Las características eléctricas de las neuronas están definidas, mayoritariamente, por los iones sodio, potasio, calcio y cloro (Na+, K+, Ca2+ y Cl-). Los principales responsables de producir los PA que van a caracterizar el disparo de las neuronas son el sodio y el potasio gracias a su respectivo paso a través de los canales dependientes de voltaje Nav y Kv. Las propiedades de apertura y cierre de estos canales van a marcar la dinámica de entrada y salida de estos cationes en la neurona, que va a ser lo que determine principalmente las características de los PA y de los trenes que estos forman.

En esta tesis doctoral tienen especial importancia los canales de potasio, y por eso los describiré en más detalle. Esta familia de canales iónicos es la más grande y diversa, con canales dependientes de voltaje (Kv), rectificadores hacia el interior (Kir) y activados por Ca2+, Na+ y ATP. Los Kv constan de cuatro subunidades con seis dominios transmembrana que pueden estar asociadas a subunidades auxiliares. La diferencia entre distintos tipos de Kv va a residir en su cinética de apertura y cierre, localización primaria y susceptibilidad ante agentes bloqueantes (Gutman et al. 2005; Krishnan et al. 2009). Existe una gran diversidad de canales Kv localizados en diferentes poblaciones neuronales y, dentro de estas, en distintos compartimentos. Gracias a sus características, van a determinar las corrientes de K+ que van a definir y a diferenciar los diferentes compartimentos y poblaciones en cuanto a la forma en que la actividad les influye (Heusser and Schwappach 2005; L. Y. Jan and Jan 2012; Robertson 1997). Los canales Kv1 se abren a voltajes cercanos al umbral del PA y su función más conocida es la de repolarizar la membrana plasmática tras éste, pero también son esenciales en la definición de distintas características del disparo (Johnston et al. 2010). Por ejemplo, los canales Kv1 situados en el segmento inicial del axón controlan la amplitud del potencial de acción en el axón y la eficacia sináptica en neuronas piramidales de la lámina V (Kole et al. 2007) y contribuyen a la formación de diferentes modo de disparo (Goldberg et al. 2008; Kole and Stuart 2012; Locke and Nerbonne 1997; Y. Shu et al. 2007).

Al igual que el resto de proteínas celulares, la expresión de canales iónicos depende de los FT activos en un momento determinado. Gracias a la expresión dinámica de un amplio repertorio de canales iónicos, se va a producir la adquisición de modos específicos de disparo (Bender and Trussell 2012). La relevancia de estos modos de disparo es clara en cuanto a la integración y procesamiento de la información en el circuito, pero su importancia para el establecimiento y mantenimiento de los circuitos neuronales durante el desarrollo no ha sido patente hasta estos últimos años (Dehorter et al. 2015; Rodriguez-Moreno et al. 2013). El modo de disparo va a definir, además, las diferentes poblaciones y subpoblaciones neuronales (De la Rossa et al. 2013; Doron et al. 2014; Maravall et al. 2004a; Otsuka and Kawaguchi 2011; Stanley 2013; Suter et

al. 2013). Por ejemplo, las neuronas piramidales suelen presentar patrones regulares de disparo -asociados a una alta capacidad de adaptación ante una estímulo-, mientras que las interneuronas GABAérgicas disparan siguiendo patrones de alta frecuencia de disparo –con poca capacidad de adaptación- (Connors and Gutnick 1990). Por otro lado, los distintos modos de disparo también están relacionados con la conectividad de esa neurona en el circuito. En el caso de las NP callosas de la lámina V, Otsuka y Kawaguchi demostraron que la diversidad fisiológica de esa población estaba vinculada a los distintos patrones de conectividad que presentaba (Otsuka and Kawaguchi 2011). Sin embargo, y a pesar de todos estos avances, aún estamos lejos de entender cuáles son los parámetros más adecuados para estudiar las diferentes consecuencias funcionales que los modos de disparo tienen sobre el comportamiento de la neurona (Doron et al. 2014).

RELEVANCIA CLÍNICA DE LA CORRECTA FORMACIÓN DE CIRCUITOS CORTICALES

Como he intentado reflejar en esta introducción, la formación de circuitos corticales es un proceso muy complejo en el que están involucrados multitud de elementos. Por tanto, la disfunción de cualquiera de ellos (o de otros aún por descubrir) podría ser una causa potencial de trastornos con origen en el desarrollo y, a su vez, una posible diana terapéutica. Dentro de estos elementos, encontramos algunos bien descritos en la literatura como ciertas moléculas solubles y sus receptores (Slit y Robo, Netrin y Dcc) o factores de transcripción como Satb2 (Morcom et al. 2016). Sin embargo, aún ignoramos muchos de los mecanismos implicados en la formación de estos circuitos y en el establecimiento y refinamiento de las conexiones axonales. En el caso del CC, por ejemplo, cada vez existen más evidencias de la importancia de la actividad neuronal en la formación de esta estructura (Huang et al. 2013; Mizuno et al. 2007; Suarez et al. 2014; Wang et al. 2007), por lo que el estudio de los canales iónicos en enfermedades en las que la conectividad interhemisférica está afectada parece una vía prometedora. De hecho, la alteración de la expresión de ciertos canales iónicos ya se ha relacionado con numerosos trastornos neurológicos como algunos tipos de epilepsia, esclerosis lateral amiotrófica, trastornos del espectro autista y otras neuropatías (Schmunk and Gargus 2013; Splawski et al. 2004; Vucic and Kiernan 2006). A la vista de todos estos antecedentes, parece claro que aumentar nuestro conocimiento sobre los mecanismos implicados en la formación de circuitos corticales nos va a permitir encontrar nuevas dianas terapéuticas para el tratamiento de numerosas enfermedades causadas por una conectividad aberrante.

OBJETIVOS

"Hazlo, o no lo hagas. Pero no lo intentes."
(Yoda, "El Imperio Contraataca").

OBJETIVOS

A lo largo de esta tesis doctoral me he centrado en el en el estudio de las funciones celulares y moleculares ejercidas por FT que determinan la identidad molecular de las neuronas de las láminas superiores durante la formación de los circuitos corticales del área somatosensorial. Los objetivos fundamentales de la tesis se plantearon en base a las funciones importantes de Cux1 y Cux2 en cuanto a la regulación de las estructuras dendríticas descritas anteriormente (Cubelos et al. 2010), y en base al hecho de que el CC en ratón se compone principalmente por axones emitidos por neuronas localizadas en la lámina II-III. Las investigaciones derivaron casi necesariamente en el desarrollo de otros objetivos relacionados con la formación de mapas y con el desarrollo de nuevos diseños experimentales. Así, las investigaciones presentadas responden a los siguientes objetivos:

1. Determinar el papel diferencial de Cux1 y Cux2 en los distintos compartimentos dendríticos.

2. Estudiar el papel de Cux1 y Cux2 en el desarrollo de las proyecciones axonales intra e interhemisféricas de las neuronas de las láminas II-III.

3. Determinar los mecanismos moleculares implicados en el control de la excitabilidad y conectividad mediados por Cux1.

4. Desarrollar un diseño experimental que facilite la caracterización de la conectividad cortical a nivel de estructura y función.

5. Estudiar la implicación de Lhx2 en la plasticidad inducida por la entrada talámica en las neuronas corticales durante la formación del mapa de barriles del área somatosensorial primaria.

MATERIALES Y MÉTODOS Y RESULTADOS

"Little darling, it's been a long cold lonely winter
Little darling, it feels like years since it's been here
Here comes the sun
Here comes the sun, and I say
It's all right."
(The Beatles, "Here Comes The Sun")

IN UTERO ELECTROPORATION APPROACHES TO STUDY THE EXCITABILITY OF NEURONAL SUBPOPULATIONS AND SINGLE-CELL CONNECTIVITY

Como se ha mencionado a lo largo de la introducción, hay diversos factores clave para el funcionamiento correcto de los circuitos corticales. Uno es la conectividad estructural per se, por lo que entender los mecanismos moleculares que influyen en el desarrollo de las dendritas y el axón es fundamental. El otro es relativo a cómo va a utilizarse esa conectividad, es decir, a la relación entre función y estructura que se refleja, entre otros aspectos, en las respuestas electrofisiológicas. Sin embargo, aún estamos lejos de comprender todos los mecanismos moleculares que subyacen a estos factores clave.

Para responder a esos problemas biológicos, es importante utilizar herramientas que nos permitan definir de forma precisa la conectividad y las características electrofisiológicas de las neuronas. La electroporación in utero (IUE) es una técnica muy potente que se ha desarrollado en los últimos 15 años y utilizado muy frecuentemente en corteza en la última década. El diseño habitual de la experimentación mediante IUE implica la modificación de la expresión génica en una población de un número de neuronas elevado. Sin embargo, para diseccionar mejor los mecanismos corticales es preferible una estrategia que permita marcar las neuronas modificadas genéticamente de forma individual. En este artículo describimos un protocolo que permite hacer esto mismo gracias a una combinación de la IUE con un sistema basado en la recombinasa CRE a diluciones límite. Por otro lado, en el manuscrito explicamos también un modo para analizar las propiedades eléctricas de las neuronas modificadas en la IUE. Ambas estrategias pueden ser utilizadas juntas o por separado y tanto en experimentos de ganancia como de pérdida de función. Por tanto, la utilización de este tipo de diseño experimental ha sido muy útil en esta tesis doctoral para diseccionar diversos mecanismos relacionados con el desarrollo de la corteza cerebral.

Mi contribución en este artículo ha sido mejorar e implementar la estrategia de dilución Cre y diseñar la metodología para el análisis de la estructura del axón de manera sistemática y en cortes seriados usando Fiji. Además del diseño de la técnica, he realizado todo el trabajo experimental relacionado con el análisis morfológico (cirugías, inmunohistoquímica, imagen), todas las figuras y la gran parte de la escritura del manuscrito. Por último, es necesario destacar que el protocolo descrito en este artículo comprende buena parte de la metodología empleada para llevar a cabo gran parte de los experimentos de esta tesis doctoral.

Video Article

In Utero Electroporation Approaches to Study the Excitability of Neuronal Subpopulations and Single-cell Connectivity

Carlos G. Briz[1], Marta Navarrete[2], José A. Esteban[2], Marta Nieto[1]

[1]Department for Molecular and Cellular Biology, Centro Nacional de Biotecnología (CNB-CSIC)

[2]Molecular Neurobiology Department, Centro de Biología Molecular "Severo Ochoa", Consejo Superior de Investigaciones Científicas (CSIC-UAM)

Correspondence to: Marta Nieto at mnlopez@cnb.csic.es

URL: https://www.jove.com/video/55139
DOI: doi:10.3791/55139

Keywords: Neuroscience, Issue 120, brain, development, cortex, electrophysiology, corpus callosum, electroporation

Date Published: 2/15/2017

Citation: Briz, C.G., Navarrete, M., Esteban, J.A., Nieto, M. *In Utero* Electroporation Approaches to Study the Excitability of Neuronal Subpopulations and Single-cell Connectivity. *J. Vis. Exp.* (120), e55139, doi:10.3791/55139 (2017).

Abstract

The nervous system is composed of an enormous range of distinct neuronal types. These neuronal subpopulations are characterized by, among other features, their distinct dendritic morphologies, their specific patterns of axonal connectivity, and their selective firing responses. The molecular and cellular mechanisms responsible for these aspects of differentiation during development are still poorly understood.

Here, we describe combined protocols for labeling and characterizing the structural connectivity and excitability of cortical neurons. Modification of the *in utero* electroporation (IUE) protocol allows the labeling of a sparse population of neurons. This, in turn, enables the identification and tracking of the dendrites and axons of individual neurons, the precise characterization of the laminar location of axonal projections, and morphometric analysis. IUE can also be used to investigate changes in the excitability of wild-type (WT) or genetically modified neurons by combining it with whole-cell recording from acute slices of electroporated brains. These two techniques contribute to a better understanding of the coupling of structural and functional connectivity and of the molecular mechanisms controlling neuronal diversity during development. These developmental processes have important implications on axonal wiring, the functional diversity of neurons, and the biology of cognitive disorders.

Video Link

The video component of this article can be found at https://www.jove.com/video/55139/

Introduction

The development of dendritic and axonal structures is an important facet of circuit regulation in the nervous system, including in the cerebral cortex. It plays a critical role during the selective wiring of the diverse neuronal subpopulations. A number of recent reports have shown that, in addition to connectivity, the molecular diversity of neurons is reflected by the acquisition of highly specific modes of firing. However, the mechanisms determining the excitability and connectivity of the distinct neuronal subtypes during development, as well as their degree of coordination, are still poorly understood[1,2].

In vivo loss- and gain-of-function analyses allow for the study of the relationship between the expression level of specific genes and their influence in the development of the circuit. *In utero* electroporation (IUE) is a technique widely used to study the function of a gene of interest in specific neuronal populations and to study the overall patterns of their connectivity. However, to determine the morphological characteristics of axons and dendrites in cortical layers in living mice, it is essential to label neurons sparsely. A Cre recombination system combined with IUE can be used to mark a sparse population of neurons at a sufficiently low density to resolve the projections emitted by individual cells of the identified cortical laminas. This method labels a sufficient number of neurons per cortex to obtain quantitative data after the analysis of reasonable numbers of electroporated brains (**Figure 1**). This manuscript presents a method for such fine analysis of connectivity. It also presents a similar strategy to analyze, in separate experiments, the electrical properties of neurons by performing current-clamp recordings on green fluorescence protein (GFP)-electroporated cells from acute cortical slices. These protocols are versatile and can be applied to the study of the excitability and connectivity of neurons of WT and transgenic animals, and also of neurons in which losses and gains of function are introduced by additional plasmids during IUE.

Although this protocol describes the electroporation of mice at embryonic day (E)15.5, this technique can be performed at any age between E9.5[3] and postnatal day (P)2[4]. While electroporation at early stages targets neurons and precursors of the thalamus and deep layers of the cortex, later-stage electroporation marks more superficial layers (*e.g.,* E15.5 IUE targets layer II-III neurons). In summary, the combination of IUE with single-cell morphological analysis and electrophysiology is a useful tool to elucidate the molecular mechanisms underlying the enormous structural and functional diversity of neurons in the nervous system.

Protocol

All animal procedures were approved by the Community of Madrid Animal Care and Use Committee, in compliance with national and European legislation (PROEX 118/14; PROEX 331/15). Maintain sterile conditions during the procedure.

1. *In Utero* Electroporation

NOTE: This protocol for IUE is adapted from others that have been previously published[5,6,7]. This manuscript describes a protocol for the IUE of E15.5 embryos, with modifications in the reporter strategy that allow for the study of the morphology of single neurons[8] and their electrophysiological properties in a separate experiment using standard GFP reporter plasmids.

1. Preparing the DNA
    1. Prepare DNA plasmids using an endotoxin-free isolation kit as per the manufacturer's instructions and dilute them in 1x phosphate-buffered saline (PBS).
        1. For single-cell labeling, prepare 10 µL of DNA mixture per surgery (1 µL per embryo) using the following constructs and final concentrations: plasmid encoding a fluorescent protein reporter (*e.g.,* CAG-DsRed2[9]), 1 µg/µL as a control for electroporation efficiency; experimental plasmid to be tested, typically at 1 µg/µL; LoxP-stop-LoxP-fluorescent protein plasmid (CALNL-GFP[10]), 1 µg/µL; and construct-encoding Cre[10], 1 - 4 ng/µL. Add 1 µL of 0.1% Fast Green in water (weight/volume) to visualize the injected DNA.
        NOTE: Cre recombination of the GFP construct occurs only in a few neurons, which allows the visualization and reconstruction of individual axonal projections (**Figure 1A**).
        2. For standard patch-clamp studies, prepare 10 µL of DNA mixture per surgery (1 µL per embryo) of the following plasmid encoding a fluorescent protein (*e.g.,* CAG-GFP[11]), 1 µg/µL as a reporter control; experimental plasmid, generally 1 µg/µL; and 1 µL of 0.1% Fast Green in water (weight/volume).
        NOTE: These are the standard electroporation conditions that analyze acute slices containing a large number of labeled excitatory neurons within the desired lamina. To perform patch-clamp studies in single cells, prepare the DNA as described in step 1.1.1.1.

2. Preparation for Surgery

1. Perform a survival surgery by using aseptic procedures. Ensure sterile conditions, including masks, gloves, instruments, and surgical field. Sterilize surgical instruments (scalpel, Adson forceps, hardened fine scissors, curved scissors, Dumont forceps, and needle holder).
2. Select borosilicate glass capillaries of 1/0.58-mm outer/inner diameter. Pull capillaries[3]. Target for an optimal tip length of 1 cm after pulling. Cut the needle tip at approximately a 30° angle using fine forceps (**Figure 1B**).
3. Prepare 500 mL of sterile isotonic solution (1x PBS or Hank´s Balanced Salt Solution (HBSS)). Add penicillin-streptomycin 1:100 and warm this solution to 37 °C. It can be stored at 4 °C after the surgery.
4. Subcutaneously inject a preoperative dose of analgesics (*e.g.,* carprofen, 5 mg/kg bodyweight).
5. Keep the animals warm for surgery by placing them on a heating pad. Warm a clean cage to 37 °C for postoperative recovery.

3. Surgery

1. Anesthetize a C57BL/6 E15.5 pregnant mouse with isoflurane. First, infuse a closed chamber with 3% isoflurane at 0.8 L/min oxygen and leave the mouse inside until it is asleep. Transfer the mouse to a heating pad and place the nose and mouth within a mask for delivery of isoflurane. Gradually decrease the anesthesia over the course of the surgery to 1.5% isoflurane via mask. Confirm proper anesthetization by observing a loss of the pedal reflex (toe pinch). The optimal procedure takes approximately 20 min and not more than 45 min.
2. Apply eye ointment to prevent the eyes from drying during the procedure.
3. Remove the hair from a ~ 3-cm region of the abdomen (using either an electric razor or depilatory cream). Wash the surgical area with cotton swabs infused with 70% ethanol, followed by an iodine-infused cotton swab. Repeat three times.
4. Cover the surgical area with sterile gauze to prevent infections.
5. Use the scalpel to make a vertical opening through the skin 2 cm long and parallel to the midline. Separate the skin and muscle of the abdomen using blunt curved scissors. Hold the muscle with the forceps and cut it through the linea alba to expose the abdominal cavity.
6. Locate the embryos with the help of the forceps. Moisten two wet cotton swabs with the sterile saline solution prepared in step 2.3 and use them to manipulate an accessible embryo out of the opening. Place the cotton swabs around the embryo and gently extract both uterine horns from the abdominal cavity. Keep the embryos and the opened abdominal cavity hydrated with warm saline solution throughout the procedure to prevent them from drying out.

4. Injection of DNA and Electroporation

1. Manipulate the embryos gently with fingers to locate the telencephalon (can be clearly visualized by the eye as the two more anterior vesicles of the brain). Place a prepared borosilicate capillary in a mouth pipette. Pass the tip of the needle through the uterus, avoiding blood vessels, until it reaches one lateral ventricle. Slowly inject approximately 1 µL of Fast Green-colored DNA solution until a large blue spot is observed.
2. Place the 7-mm platinum electrodes laterally on the head of the embryo (**Figure 1C**).
NOTE: DNA is negatively charged; therefore, it moves toward the positive electrode when voltage is applied between the platinum electrodes. By varying the location of the electrodes, different areas of the brain can be targeted.

3. Apply voltage via the platinum electrodes (for E15.5 embryos: 5 pulses, 38 V, 50-ms interval cycle length, 950-ms interval pause. These conditions vary depending on the developmental stage)[12].
   NOTE: See **Table 1** for voltage conditions and electrodes for different embryo stages.
4. Repeat steps 4.1 - 4.3 for each embryo.

5. End of the Surgery and Postoperation

1. Use cotton swabs to manipulate the uterus back into the mother. Fill the abdominal cavity with the warmed saline solution (add about 2 mL).
2. Suture the muscle with simple interrupted stitches or a continuous stitch. Use #6-0 sutures.
3. Use staples to close the external wound. Be careful to separate the skin from the muscle before stapling. Remove the nose mask.
4. Allow the mouse to recover for 30 min in the heated, clean cage before placing it in the animal facility room. Do not leave an animal unattended until it has regained sufficient consciousness to maintain sternal recumbency. Do not place an animal that has undergone surgery in the company of other animals until fully recovered.
5. Supervise the animal during the days following the surgery. Apply analgesics subcutaneously (carprofen, 5 mg/kg bodyweight) every 12 h for 2 days or according to animal legislation. No additional postoperative care is required for the pups.

6. Preparation and Analysis of the Samples

1. Optional: On P2, check for the expression of fluorescence in the electroporated pups using a fluorescent microscope; when the IUE is successful, fluorescence can clearly be seen in the head[13]. Mark or separate the mice that are positively electroporated for use in the following steps. Keep the dam and pups in standard animal facility conditions.
2. At the desired stage of study, perfuse the mice transcardially. Typically, the most active phase of dendritic and axonal growth corresponds to the first three postnatal weeks[2,14,15].
   1. Prepare 30 mL of 4% paraformaldehyde (PFA) in 1x PBS per mouse and chill it on ice.
      CAUTION: PFA is a known allergen and carcinogen. It is toxic. Wear appropriate personal protective equipment.
      NOTE: The amount of PFA needed depends on the age of the mouse (*e.g.*, for P16, 20 mL for the perfusion and 10 mL for the postfixation are needed).
   2. Prepare a ketamine-xylazine mix to anesthetize the animal with a 1:1:8 volumetric ratio of 100 µg/mL ketamine:100 µg/mL xylazine:PBS (prepare around 0.2 mL per mouse).
   3. Anesthetize the mouse by intraperitoneally injecting 0.2 mL of the mix prepared in step 6.2.2.
   4. Place the anesthetized mouse on its back. Make a horizontal incision above the thorax using a scalpel. Cut the muscle and the diaphragm with fine scissors until the heart can be observed.
      1. Make an incision in the right atrium with the fine scissors. Slowly inject 20 mL of PBS in the left ventricle with a 25-gauge needle in order to remove the blood. Inject 20 mL PFA (step 6.2.1) until the mouse is rigid and the organs become white.
      2. Immediately remove the head and make a midline incision in the skin from the neck to the skull. Gently peel away the skull using curved forceps and extract the brain. Take special care not to puncture or damage the brain during the removal of the skull. Put the brain in 10 mL of 4% PFA at 4 °C overnight to postfix it.

3. Cryoprotect fixed brains in 10 mL of 30% sucrose in PBS at 4 °C for 1 - 2 days, until they sink. Prepare 1-cm^3 aluminum foil cubes. Fill the cubes 2/3 of the way with OCT. Put the brains inside and freeze them by putting the cubes on dry ice. Store the frozen brains at -80 °C.
4. Place drop of OCT on the surface of the specimen disc, peel the aluminum foil from the histology cube, and position the cube at the desired orientation to the specimen disk on top of the liquid OCT. Apply firm pressure until it is fixed. Insert the specimen disc into the specimen head of the cryostat. Orient the specimen (move it into a favorable position relative to the knife/blade).
   1. Section the brains on the cryostat. Select 50 - 100 µm-thick floating cryosections[16] using a fine brush and place them in PBS.

5. Stain if desired.
   NOTE: For the study of axonal morphology, staining with a GFP antibody is strongly recommended[2].
   1. Block the sections for 1 h at room temperature with 5% fetal bovine serum in PBS containing 0.5% Triton-X 100 (blocking solution). Incubate overnight at 4 °C with 1:500 primary antibody (*e.g.,* rabbit anti-GFP) diluted in blocking solution.
   2. Wash the sections three times in PBS. Add 1:500 secondary antibody (*e.g.,* goat anti-rabbit Alexa Fluor 488) diluted in blocking solution and incubate for 1 h at room temperature. Wash the sections three times in PBS.
   3. Counterstain with DAPI (1:10,000) in PBS containing 0.5% Triton-X 100 for 10 min. Rinse the sections with PBS. Mount the sections in an aqueous mounting medium[16].

7. Imaging and Analysis

1. Fluorescence or confocal microscopy
   1. To reconstruct complete neurons, acquire the images with a high magnification (at least 40X) and high resolution (minimum 1,024 x 1,024). Select the "Tile scan" or equivalent option in the acquisition software to cover the area of interest, spanning all dendrites and axonal processes. Acquire a sufficient number of stacks on the z-axis to avoid a loss of information.
      NOTE: Generally, the microscope's software has an "Optimized stack" option, but if this is not the case, test manually to determine how many steps are necessary for the images to overlap in order to correctly define individual projections. Two crucial parameters are the pinhole and the objective; take into account "higher magnification, more resolution, and more necessary z-steps."

2. Analysis
   NOTE: Although several parameters can be analyzed, step 7.2.1 focuses on two: dendrite morphology and axon branching. Download Fiji (http://fiji.sc/).

1. Open the image, select the "Segmented line" option from the menu. Draw a line (moving up and down along the z-axis by scrolling the mouse) following the structure of the neuron. Go to "Analyze, Tools, ROI Manager, Add" (alternatively, press "t") to save the line. Repeat this process for every axon or dendrite of the analyzed neuron[2].
2. In the ROI Manager Menu press the "Measure" button to get the length (or additional parameters). Export the measurements to a text file or spreadsheet to analyze them.

8. Electrophysiology

NOTE: The goal of this protocol is to obtain whole-cell current-clamp recordings from layer II/III pyramidal cell neurons identified visually by GFP expression in GFP-electroporated mouse brains (or any other fluorescent protein previously electroporated). It is an adaptation of previously published methods[17,18]. Using this protocol it is possible to study the effect of a genetic modification introduced by IUE on the electric properties of the neuron. The acquisition of specific firing modes is a gradual process of differentiation that involves the dynamic expression of a wide repertoire of ion channels and that results in the expression of transient firing modes before late postnatal stages. For example, mature electrical responses are not observed in layer II/III of the somatosensory mouse cortex before P16[2,19].

1. Prerequisites for the acute slices
    1. Prepare sterile surgery tools to remove the brains from the mice: a guillotine, to remove the head; small scissors, to cut through the skull; forceps, to separate the skull from tissue; a spatula, to delicately remove brain tissue from its casing; a metallic slicer, to dissect the cortex into two equal halves; and a Pasteur pipette, to move slices from the vibratome (place them into a solution containing artificial cerebrospinal fluid (ACSF) for inspection, and then transfer the slices from ACSF to an incubation holding area).
    2. Prepare 1 L of ACSF using water of high purity (double-distilled water) containing 119 mM NaCl, 26 mM $NaHCO_3$, 11 mM glucose, 2.5 mM KCl, 1.2 mM $MgCl_2$, 2.5 mM $CaCl_2$, and 1 mM NaH_2PO_4. Titrate the pH to 7.3 - 7.4 with HCl or NaOH. Adjust the osmolarity to 290 mOsm.
    3. Bubble ACSF with carbogen (95% O_2/5% CO_2) for 15 - 20 min using Teflon tubes (~ 1 mm), to stabilize the pH to 7.3 - 7.4.
    4. Freeze 200 mL of ACSF solution saturated with carbogen at -80 °C for 10 - 15 min to generate a slushy dissection solution. Place a 100- x 20-mm tissue culture dish on ice for slicing the brain.
    5. Prepare 100 mL of 1% low-melting point agarose solution just before the start of the experiment. Cool the solution, cut out a square piece of agarose (dimensions: 1 x 1 x 0.5 mm), and superglue it to the back of the platform, right behind where the brain is sliced (agarose gel provides support for the brain during slicing). Make the front as flat as possible.

2. Obtaining acute slices
    1. Immobilize the mouse and anesthetize it with isoflurane 2%. Place the head into the guillotine opening and decapitate it swiftly. Remove its skull as fast as possible with the use of bone rangers or fine forceps. Put the brain into chilled ACSF.
    NOTE: It is important to perform this step quickly.
    2. Place the brain in the chilled culture dish. Cut off the cerebellum with small scissors.
    3. Pick up the brain with a spatula and blot it dry on a paper towel.
    4. Glue the ventrocaudal plane of the brain on a vibratome holder. Place the holder on a vibratome filled with ice-cold ACSF.
    5. Obtain acute slices by cutting 300-µm coronal sections (ensure continued carbogenation throughout the procedure, *e.g.,* place a bubbler (1-mm polytetrafluoroethylene tube) in the vibratome chamber) using the following vibratome settings: 0.06-mm amplitude and 0.08 - 0.10-mm/s speed. Set the advance to the slowest possible speed (~ 22 s per pass). Modify these optimal settings and obtain optimal conditions for each machine empirically if necessary.
    6. Incubate the acute slices for at least 60 min in ACSF supplemented with 3 mM *myo*-inositol, 0.4 mM ascorbic acid, and 2 mM sodium pyruvate while bubbling with 95% O_2/5% CO_2 gas. Maintain the temperature at 25 °C.
    7. Perform the slicing procedure in less than 15 min. If desired, the slices can be stored for 1 - 7 h before being transferred to the recording chamber for use.

3. Prerequisites for the whole-cell recording
    1. Make sure that the electrophysiology station is equipped with a recording chamber, a perfusion system, a microscope, electrodes (recording, stimulating, and ground), macro- and micromanipulators, a rigid vibration-resistant table-top and Faraday cage, a stimulator, an amplifier and analog-to-digital (A/D) converter, a computer with acquisition software, and a GFP (or any other fluorochrome) filter for analyzing genetically modified neurons[18] (**Figure 2A**).
    2. Prepare the intracellular solution, containing 115 mM potassium gluconate, 2 mM $MgCl_2$, 10 mM HEPES, 20 mM KCl, 4 mM Na_2ATP, and 0.3 mM Na_3GTP, adjusted to pH 7.2 by KOH and to 290 mOsm by KCl.
    3. Make patch pipettes by pulling borosilicate glass capillaries. Prepare patch electrodes using a micropipette puller. Use borosilicate capillaries (1.5-mm outer diameter, 0.86-mm inner diameter, 10-cm length). Make patch electrodes showing resistances of 3-10 MΩ when filled with intracellular solution.
    4. Perfuse the recording chamber with ACSF at a rate of 2 mL/min. Maintain the temperature of the chamber at approximately 33 °C.

4. Whole-cell recording
    1. Transfer the slices into the recording chamber using a Pasteur pipette (cut off the long tip) or a small brush. Hold down the slice with a harp. Perfuse the slices constantly with ACSF at a rate of 2 mL/min.
    2. Patch a GFP-positive neuron.
        1. Put the slice into the recording chamber and find the area of interest through the microscope at low magnification (10X). Then, find a GFP-positive cell to patch using the 60x objective.
        2. Fill the recording electrode with intracellular solution. Use the syringe linked to the filter (4-mm filter) and micro-loader tip to fill the recording electrode with intracellular solution.
        3. Place the glass pipette in the pipette holder. Place the pipette tip in the bath and focus on the tip. Once the pipette is in the bath, apply positive pressure through the back pressure control system.
        4. Patch a neuron that is fluorescent (**Figure 2B**).

1. Approach the cell of interest under visual guidance while maintaining back pressure in the pipette. Upon the appearance of a small dimple on the cell surface, release the pressure. At this point, a tight seal (resistance larger than 1 GΩ) may be formed. Otherwise, apply a light negative pressure (suction) to facilitate it.
2. While the seal is being formed, bring the holding voltage clamp to -60 mV. Once the GΩ seal is formed, apply a pulse of suction to rupture the cell membrane beneath the pipette and go into whole-cell mode. See reference[20] for more details.

5. Record the activity using current-clamp conditions[21]. Once in whole-cell mode, switch from voltage-clamp to current-clamp mode and start recording. For example, to record cell excitability, apply 500 ms-long depolarizing current injections (100 - 400 pA).
   1. Calculate the firing rates by plotting the number of action potentials along the train for increasing input currents.
      NOTE: Resting membrane potential, input resistance, and membrane capacitance may also be calculated from the recordings[21].

Representative Results

To characterize the morphological changes of neurons in detail and throughout development, it is essential to label neurons sparsely. A Cre-recombinase diluted system allows for the expression of a gene of interest in a sparse population of neurons, so that only those neurons that incorporate this enzyme express GFP (**Figure 1A**). Using this strategy, layer II-III is targeted and labeled by IUE at E15.5. CAG-DsRed2 at 1 µg/µL, is co-electroporated as a control and to identify positive electroporated brains in living animals. Importantly, after staining with anti-GFP antibody, the signal is strong enough to allow for the clear visualization of their dendritic morphologies and axons (**Figure 1D** and **E**).

After IUE and electrophysiology, the analysis of the parameters obtained from whole-cell recordings are used to compare the firing responses and excitability of electroporated cells under different conditions. Several parameters can be obtained. The parameters should be adapted to the particular study using specific patch-clamp analysis software. **Figure 2C** provides an example of the plot of the action potentials against the input current obtained from recordings of a WT layer II-III neuron that was electroporated at E15.5.

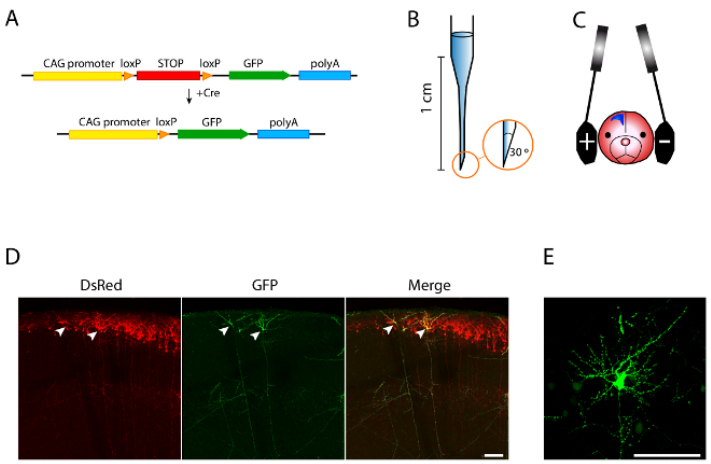

Figure 1. A Cre-recombinase Diluted Strategy Enables Sparse Labeling of Cortical Neurons. A. Schematic summary of the strategy. In neurons carrying both CALNL-GFP and CRE, the LoxP-STOP-LoxP cassette is excised out of CALNL-GFP, and GFP is expressed by the strong CAG promoter. **B.** Schematic drawing of a borosilicate capillary pulled using a micropipette puller. The tip is cut by forceps, creating a 30° angle. Measure 1 cm from the tip to the beginning of the narrower part of the capillary. **C.** Position of the electrodes to target the somatosensory cortex. The platinum electrodes are placed approximately over the ears of the embryo. Due to its negative charge, DNA goes toward the positive electrode when the voltage is applied. Variation in the position of the electrodes allows targeting different brain areas. **D.** Images obtained after vectors were delivered to layer II-III neurons by *in utero* electroporation at embryonic day 15.5; coronal sections were made at postnatal day 16. The CAG-DsRed2 vector was co-transfected as a control (left). GFP (middle) is expressed only in those neurons that also incorporated Cre, allowing the recombination of the LoxP sites in the CALNL-GFP vector. The sparse labeling allows individual neurons to be distinguished (arrowheads). **E.** High-magnification confocal image of the dendritic arbors of another sparsely labeled GFP neuron. Scale bars = 100 µm.
Please click here to view a larger version of this figure.

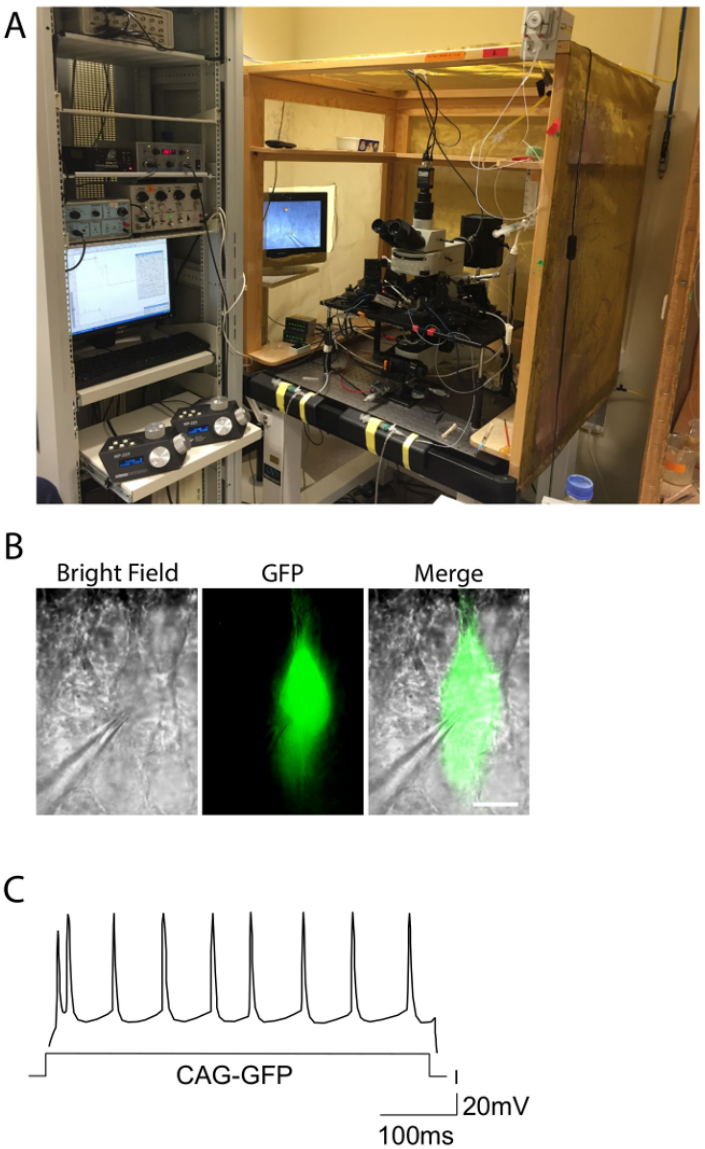

Figure 2. Electrophysiology Settings and Example of a Firing Response. A. Photograph shows the electrophysiology setup used for patch clamp experiments in acute slices. The setup is included in a Faraday cage to eliminate noise, and the equipment is on top of an anti-vibration table. Controllers of the motorized micromanipulators for the electrodes are observed on the left. **B.** Pyramidal neuron of a mouse electroporated with GFP, observed under bright field and green fluorescence conditions. The recording pipette attached to a GFP+ cell is noticeable. Scale bar= 10 µm. **C.** Firing patterns of a CAG-GFP electroporated control layer II-III neuron showing the typical regular-spiking response. The distribution of action potentials approximates to a regular distribution along the duration of input current (X-axis). Please click here to view a larger version of this figure.

Stage	Voltage	Electrodes	References
E9.5	7 V, 100 ms, 3 pulses	Stick platinum electrodes	Matsui *et al.*, 2011[3]
E12.5	30 V, 50 ms, 3 - 5 pulses	Forceps-type electrodes 3 mm	Saito, T., 2006[12]
E15.5	35-48 V, 50 ms, 5 pulses	Forceps-type electrodes 5-7 mm	Rodriguez-Tornos *et al.*, 2016[2], Saito, T., 2006[12]
P2	100 V, 50 ms, 5 pulses	Forceps-type electrodes 5-7 mm	Sonego *et al.*, 2013[4]

Table 1: Voltage Conditions and Electrodes for the Electroporation of Embryos.

Discussion

This protocol describes in detail how to label neurons of the somatosensory cortex of C75BL/6 mice in order to analyze their connectivity and their excitability. With respect to existing methods, it visualizes discriminating aspects of connectivity, such as the number of axonal branches per neuron, their precise topography, and their anatomical location. By altering the position of the electrodes, it is possible to target other neuron populations, such as the cingulate cortex (keep the same angle between the electrodes and the brain, but change the orientation of the poles) or the hippocampus[5], and perform similar experiments labeling individual neurons or broader populations, depending on the desired strategy. However, there are limitations to this, as not all populations are equally accessible or equally selectively labeled. For example, in the hippocampus, it is possible to selectively target late-born neurons of the CA1 region, but early electroporation marks heterogeneous populations of inner and outer pyramidal cells. In the cerebral cortex, neurons are born in a sequential manner, so the gestation day during the IUE determines which cortical layer is affected. Performing earlier IUE targets deeper neurons (*e.g.,* IUE at E14 labels layer IV neurons)[22].

For a successful IUE, it is recommended to take into account certain considerations. First, it is important to do the surgery in less than 30 min in order to reduce the stress on the mother and to increase the chances of survival of the pups. Second, the most difficult part of the procedure is the injection of the DNA—perform the injection via the borosilicate capillaries as gently as possible. If the embryos are pressed too hard, they can be harmed. In terms of troubleshooting the death of the embryos during DNA injections, beveling the tip with a 30° angle can increase the efficacy of this process. If a beveller is not available and the capillaries are cut solely with forceps, the correct angle can be confirmed in the dissecting microscope. Discard inadequate capillaries. Finally, adapting the electroporation conditions to the stage of the embryo is important in order to increase the survival rate (see **Table 1**).

Some considerations are necessary with regard to the reconstruction of axons and dendrites. To label individual neurons, the proper concentration of the Cre plasmid are essential to obtain a good, sparse expression and to avoid the confounding overlap of neuronal projections belonging to different neurons. Although this protocol proposes the use of 4 ng/µL, it may be necessary to adjust the plasmid concentration for each experiment, depending on the promoter used, the quality of the DNA preparation, and the method of DNA quantification (*e.g.,* reduce it to 2 ng/µL if labeling too many neurons). In addition, for axonal tracking, it is important to cut at an appropriate angle in order to have the whole neuron in the same plane.

Critical steps for successful patch-clamp recordings are the health of the tissue of the acute slices and the location and abundance of electroporated GFP-positive neurons. If patching steps fail or aberrant responses are found during the recordings, reduce the time for processing the acute slices. If GFP neurons are difficult to identify and locate due to their reduced numbers in the acute slice, ensure that sufficient CAG-GFP plasmid is included in the electroporation mix. With regard to the main limitations of the approaches described herein, the patch-clamp technique allows the recording of many different parameters describing the excitability of the neuron, but it does not evaluate aspects that depend on the whole circuit. Also, and as referred to above, not all neuronal subpopulations are accessible through IUE. In summary, in the future, these techniques can contribute to the further analysis of the structural and functional connectivity of different neuronal subpopulations in the brain.

Disclosures

The authors declare no conflicts of interest.

Acknowledgements

We are grateful to R. Gutiérrez and A. Morales for their excellent technical assistance and to L. A. Weiss for editing. C.G.B. is funded by the Spanish Ministerio de Ciencia e Innovación (MICINN), FPI-BES-2012-056011. This work was funded by a grant from BBVA Foundation and SAF2014-58598-JIN (MINECO) to M. Navarrete and by a grant from the Ramón Areces Foundation and grants SAF2014-52119-R and BFU2014-55738-REDT (from MINECO) to M. Nieto.

References

1. Dehorter, N. *et al.* Tuning of fast-spiking interneuron properties by an activity-dependent transcriptional switch. *Science.* **349** (6253), 1216-1220 (2015).
2. Rodriguez-Tornos, F. M. *et al.* Cux1 Enables Interhemispheric Connections of Layer II/III Neurons by Regulating Kv1-Dependent Firing. *Neuron.* **89** (3), 494-506 (2016).

3. Matsui, A., Yoshida, A. C., Kubota, M., Ogawa, M., & Shimogori, T. Mouse in utero electroporation: controlled spatiotemporal gene transfection. *J Vis Exp.* (54) (2011).
4. Sonego, M., Zhou, Y., Oudin, M. J., Doherty, P., & Lalli, G. In vivo postnatal electroporation and time-lapse imaging of neuroblast migration in mouse acute brain slices. *J Vis Exp.* (81) (2013).
5. Baumgart, J., & Baumgart, N. Cortex-, Hippocampus-, Thalamus-, Hypothalamus-, Lateral Septal Nucleus- and Striatum-specific In Utero Electroporation in the C57BL/6 Mouse. *J Vis Exp.* (107) (2016).
6. Petros, T. J., Rebsam, A., & Mason, C. A. In utero and ex vivo electroporation for gene expression in mouse retinal ganglion cells. *J Vis Exp.* (31) (2009).
7. Rice, H., Suth, S., Cavanaugh, W., Bai, J., & Young-Pearse, T. L. In utero electroporation followed by primary neuronal culture for studying gene function in subset of cortical neurons. *J Vis Exp.* (44) (2010).
8. Woodworth, M. B. *et al.* Ctip1 Regulates the Balance between Specification of Distinct Projection Neuron Subtypes in Deep Cortical Layers. *Cell Rep.* **15** (5), 999-1012 (2016).
9. Wickersham, I. R. *et al.* Monosynaptic restriction of transsynaptic tracing from single, genetically targeted neurons. *Neuron.* **53** (5), 639-647 (2007).
10. Matsuda, T., & Cepko, C. L. Controlled expression of transgenes introduced by in vivo electroporation. *Proc Natl Acad Sci U S A.* **104** (3), 1027-1032 (2007).
11. Matsuda, T., & Cepko, C. L. Electroporation and RNA interference in the rodent retina in vivo and in vitro. *Proc Natl Acad Sci U S A.* **101** (1), 16-22 (2004).
12. Saito, T. In vivo electroporation in the embryonic mouse central nervous system. *Nat Protoc.* **1** (3), 1552-1558 (2006).
13. Bullmann, T., Arendt, T., Frey, U., & Hanashima, C. A transportable, inexpensive electroporator for in utero electroporation. *Dev Growth Differ.* (2015).
14. Miller, M. Maturation of rat visual cortex. I. A quantitative study of Golgi-impregnated pyramidal neurons. *J Neurocytol.* **10** (5), 859-878 (1981).
15. Miller, M., & Peters, A. Maturation of rat visual cortex. II. A combined Golgi-electron microscope study of pyramidal neurons. *J Comp Neurol.* **203** (4), 555-573 (1981).
16. Cubelos, B. *et al.* Cux-2 controls the proliferation of neuronal intermediate precursors of the cortical subventricular zone. *Cereb Cortex.* **18** (8), 1758-1770 (2008).
17. Kang, J. Y., Kawaguchi, D., & Wang, L. Optical Control of a Neuronal Protein Using a Genetically Encoded Unnatural Amino Acid in Neurons. *J Vis Exp.* (109) (2016).
18. Mathis, D. M., Furman, J. L., & Norris, C. M. Preparation of acute hippocampal slices from rats and transgenic mice for the study of synaptic alterations during aging and amyloid pathology. *J Vis Exp.* (49) (2011).
19. Maravall, M., Stern, E. A., & Svoboda, K. Development of intrinsic properties and excitability of layer 2/3 pyramidal neurons during a critical period for sensory maps in rat barrel cortex. *J Neurophysiol.* **92** (1), 144-156 (2004).
20. Karadottir, R., & Attwell, D. Combining patch-clamping of cells in brain slices with immunocytochemical labeling to define cell type and developmental stage. *Nat Protoc.* **1** (4), 1977-1986 (2006).
21. Sakmann, B., & Neher, E. Patch clamp techniques for studying ionic channels in excitable membranes. *Annu Rev Physiol.* **46** 455-472 (1984).
22. Saito, T., & Nakatsuji, N. Efficient gene transfer into the embryonic mouse brain using in vivo electroporation. *Dev Biol.* **240** (1), 237-246 (2001).

Materials List for:

In Utero Electroporation Approaches to Study the Excitability of Neuronal Subpopulations and Single-cell Connectivity

Carlos G. Briz[1], Marta Navarrete[2], José A. Esteban[2], Marta Nieto[1]

[1]Department for Molecular and Cellular Biology, Centro Nacional de Biotecnología (CNB-CSIC)

[2]Molecular Neurobiology Department, Centro de Biología Molecular "Severo Ochoa", Consejo Superior de Investigaciones Científicas (CSIC-UAM)

Correspondence to: Marta Nieto at mnlopez@cnb.csic.es

URL: http://www.jove.com/video/55139
DOI: doi:10.3791/55139

Materials

Name	Company	Catalog Number	Comments
pCAG-Cre	Addgene	13775	
pCALNL-GFP	Addgene	13770	
pCAG-DsRed2	Addgene	15777	
pCAG-GFP	Addgene	11150	
Fast Green	Carl Roth	301.1	
EndoFree Plasmid Maxi Kit	QIAGEN	12362	
Carprofen (Rimadyl)	Pfizer GmbH	1615 ESP	
Isoflurane (IsoFlo)	Abbott (Esteve)	1385 ESP	
Ketamine (Imalgene)	Merial	2528-ESP	
Xylazine (Xilagesic)	Calier	0682-ESP	
Povidone Iodine	Meda	694109.6	
Eye Ointment (Lipolac)	Angelini	65.277	
Hanks' Balanced Salt Solution (HBSS)	Gibco by Life Technologies	24020-091	
Penicillin-Streptomycin	Sigma -Aldrich	P4333	
Scalpel Handle # 3 - 12 cm	Fine Science Tools	10003-12	
Scalpel Blades # 10	Fine Science Tools	10010-00	
Adson Forceps-Serrated - Straight 12 cm	Fine Science Tools	1106-12	
Hardened Fine Scissors - Straight 11 cm	Fine Science Tools	14090-11	
Scissors Mezenbaum-Nelson Curved L=14.5 cm	Teleflex	PO143281	
Thin curved tips - Style 7 Dumoxel	Dumont	0303-7-PO	
Dumont #5 Forceps-Inox	Fine Science Tools	11251-20	
Mathieu Needle Holder - Serrated	Fine Science Tools	12010-14	
AutoClip Applier	Braintree scientific, Inc	ACS APL	
9 mm AutoClips	MikRon Precision, Inc.	205016	
Sutures - Polysorb 6-0	Covidien	UL-101	
Electric Razor	Panasonic	ER 240	
Borosilicate glass capillaries (100 mm, 1.0/0.58 Outer/Inner diameter)	World Precision Instrument Inc.	1B100F-4	
Aspirator tube assemblies for calibrated microcapillary pipettes	Sigma -Aldrich	A5177-5EA	
Gauze (Aposan)	Laboratorios Indas, S.A.U.	C.N. 482232.8	

Cotton Swabs (Star Cott)	Albasa	-	
Needle 25 G (BD Microlance 3)	Becton, Dickinson and Company	300600	
Sucrose	Sigma -Aldrich	S0389	
Paraformaldehyde	Sigma -Aldrich	158127	
OCT Compound	Sakura	4583	
Tissue Culture Dish 100 x 20 mm	Falcon	353003	
GFP Tag Polyclonal Antibody	Thermo Fisher Scientific	A-11122	
Secondary Antibody, Alexa Fluor 488 conjugate	Thermo Fisher Scientific	A-11008	
DAPI	Sigma-Aldrich	D9542	
Fetal Bovine Serum	Thermo Fisher Scientific	10270106	
Triton X-100	Sigma-Aldrich	X100-500ML	
Electroporator ECM 830	BTX Harvard Apparatus	45-0002	
Platinum electrodes 650P 7 mm	Nepagene	CUY650P7	
Microscope for Fluorescent Imaging - MZ10F	Leica	-	
VIP 3000 Isofluorane Vaporizer	Matrx	-	
TCS-SP5 Laser Scanning System	Leica	-	
Axiovert 200 Microscope	Zeiss	-	
Cryostat - CM 1950	Leica	-	
P-97 Micropette Puller	Sutter Instrument Company	P-97	
Patch clamp analysis softwarw (p-Clamp Clampfit 10.3)	Molecular Devices	-	
Acquisition software (MultiClamp 700B Amplifier)	Molecular Devices	DD1440A	
Motorized Micromanipulator + Rotating Base	Sutter Instrument	MP-225	
Air Table	Newport	-	
Miniature Peristaltic Pumps	WPI	-	

CUX1 AND CUX2 SELECTIVELY TARGET BASAL AND APICAL DENDRITIC COMPARTMENTS OF LAYER II-III CORTICAL NEURONS

Como ya se ha mencionado en la introducción, las neuronas de las láminas II-III están caracterizadas por la expresión selectiva de Cux1 y Cux2 (Nieto et al. 2004). En un artículo publicado en mi laboratorio antes del comienzo de esta tesis doctoral, Cubelos y colaboradores demostraron que ambos FT eran necesarios y no redundantes para un desarrollo dendrítico normal. Únicamente al combinar la expresión de los dos se alcanzan los niveles de complejidad dendrítica característicos de las neuronas de las láminas II-III (Cubelos et al. 2010). Sin embargo, el papel concreto de cada uno de ellos en este proceso no se dilucidó en ese momento.

La importancia de las dendritas basales y apicales en la función de las neuronas sugiere que el control selectivo de estos compartimentos podría tener relación con las funciones no redundantes de Cux1 y Cux2. Las regiones apical y basal están especializadas funcionalmente, de manera que las modificaciones en el número de ramificaciones de uno de los compartimentos tiene consecuencias importantes para la neurona y el circuito del que ésta forma parte (de Anda et al. 2012; Miao et al. 2013; Niblock et al. 2000; Polleux et al. 2000; Srivastava et al. 2012; Tran et al. 2009).

En el artículo presentado en esta tesis doctoral, y ante la pregunta de si las funciones de Cux1 y Cux2 eran realmente equivalentes, analizamos los cambios específicos en los árboles dendríticos apical y basal de neuronas en las que la expresión de estos genes había sido alterada. Este estudio sirvió para confirmar que estos FT tienen efectos distintos en la topología de estas neuronas; aunque los dos afectan a ambos compartimentos dendríticos, el efecto de Cux1 es mucho más acusado en el basal y el de Cux2 en el apical. Los resultados presentados aquí confirman las funciones no redundantes de estos FT y aclaran sus funciones complementarias en la topología dendrítica de las neuronas de las láminas II-III. Además, describe un posible mecanismo que podría servir para definir diferentes subpoblaciones funcionales en estas láminas.

Mi contribución a este trabajo fue principalmente en la parte experimental (realización de las IUE, genotipado de las líneas transgénicas…), en el análisis estadístico de los resultados y en la elaboración de los experimentos destinados a dar respuesta a las críticas tras las revisiones para su publicación.

Cux1 and *Cux2* Selectively Target Basal and Apical Dendritic Compartments of Layer II-III Cortical Neurons

Beatriz Cubelos,[1] Carlos G. Briz,[2] Gemma María Esteban-Ortega,[2] Marta Nieto[2]

[1] Departamento de Biología Molecular, Centro de Biología Molecular 'Severo Ochoa', Universidad Autónoma de Madrid, UAM-CSIC, Nicolás Cabrera, 1, Madrid 28049, Spain

[2] Department of Molecular and Cellular Biology, Centro Nacional de Biotecnología, CNB-CSIC, Darwin 3, Campus de Cantoblanco, Madrid, 28049 Spain

Received 23 April 2014; revised 9 July 2014; accepted 21 July 2014

ABSTRACT: **A number of recent reports implicate the differential regulation of apical and basal dendrites in autism disorders and in the higher functions of the human brain. They show that apical and basal dendrites are functionally specialized and that mechanisms regulating their development have important consequences for neuron function. The molecular identity of layer II-III neurons of the cerebral cortex is determined by the overlapping expression of Cux1 and Cux2. We previously showed that both *Cux1* and *Cux2* are necessary and nonredundant for normal dendrite development of layer II-III neurons. Loss of function of either gene reduced dendrite arbors, while overexpression increased dendritic complexity and suggested additive functions. We herein characterize the function of *Cux1* and *Cux2* in the development of apical and basal dendrites. By *in vivo* loss and gain of function analysis, we show that while the expression level of either *Cux1* or *Cux2* influences both apical and basal dendrites, they have distinct effects. Changes in *Cux1* result in a marked effect on the development of the basal compartment whereas modulation of *Cux2* has a stronger influence on the apical compartment. These distinct effects of *Cux* genes might account for the functional diversification of layer II-III neurons into different subpopulations, possibly with distinct connectivity patterns and modes of neuron response. Our data suggest that by their differential effects on basal and apical dendrites, *Cux1* and *Cux2* can promote the integration of layer II-III neurons in the intracortical networks in highly specific ways.** Develop Neurobiol 75: 163–172, 2015

Keywords: **cortex; *cut*; *CDP*; dendrite; autism**

INTRODUCTION

Development of dendritic structures is an important facet of circuit regulation in the cerebral cortex. It is critical for the establishment of specific networks during differentiation and for decoding and transmitting electrical signals in mature circuit (Cline and Haas, 2008; Jan and Jan, 2010; Kulkarni and Firestein, 2012). Dendrites of pyramidal neurons are morphologically and functionally divided into basal and apical compartments (Barnes et al., 2008). Subcellular polarization is established early in migrating neurons, is maintained throughout the life of the cell, and is reflected in the asymmetric distribution of several cytoplasmic molecules and membrane receptors such as the alpha5 subunit of the integrin adhesion receptor VLA5 (Bi et al., 2001) and the neuropilin (Nrp) receptor 2 in the apical processes (Tran et al., 2009).

The apical and basal regions of the dendritic arbor are functionally specialized, and evidence shows that

Additional Supporting Information may be found in the online version of this article.

Correspondence to: B. Cubelos (bcubelos@cbm.csic.es) and M. Nieto (mnlopez@cnb.csic.es).

Contract grant sponsor: Ministerio de Ciencia e Innovación (MICINN); contract grant numbers: SAF2011-23735 (to M.N.), SAF2012-31279 (to B.C.), and RyC-2010-06251 (to B.C.).

Published online 24 July 2014 in Wiley Online Library (wileyonlinelibrary.com).
DOI 10.1002/dneu.22215

modifications in dendrite branch number or length in any of these compartments have important and selective consequences for neuron and circuit function (Niblock et al., 2000; Polleux et al., 2000; Tran et al., 2009; de Anda et al., 2012; Srivastava et al., 2012b; Miao et al., 2013). Basal and apical dendritic topology and length contribution to neurons' functions include facilitation of contact with potential axonal inputs, which are organized in layers in the cerebral cortex, as well as the restriction of the number of potential synapses (Tada and Sheng, 2006; Parrish et al., 2007; Shen and Scheiffele, 2010). Propagation of electrical signals also differs in distal apical and basal domains, and thus regulation of these compartments has selective consequences in input computation and in the amplification or silencing of presynaptic depolarization signals (Mainen and Sejnowski, 1996; Jia et al., 2010; Branco and Hausser, 2011; Feldman, 2012). A striking number of recent reports implicate mechanisms that regulate apical and basal development in autism disorders, highlighting not only the existence of these pathways but also their importance for higher functions of the human brain (de Anda et al., 2012; Srivastava et al., 2012b; Miao et al., 2013).

Layer II-III neurons characterize the mammalian cortex, show complex dendritic arbors, and participate in highly interconnected intracortical circuits involved in associative functions. At molecular level, their identity is determined by the selective expression of *Cux1* and *Cux2* (Nieto et al., 2004). These homeodomain proteins positively regulate dendritic growth and facilitate layer II-III neuron ability to integrate information from multiple axonal inputs, enabling their specialized tasks (Cubelos et al., 2010). *Cux1* and *Cux2* genes have very similar expression patterns, and both proteins are coexpressed in most superficial neurons, although not at equal levels (Nieto et al., 2004; Zimmer et al., 2004). Our earlier studies showed that, despite their similar expression and structure, both Cux proteins are necessary to sustain normal dendritic development of layer II-III neurons in a nonredundant manner; we demonstrated that their combinatorial expression is responsible for the distinctive complex dendritic arbor of these neurons (Cubelos and Nieto, 2010; Cubelos et al., 2010). The mechanisms responsible for these complementary functions remain unknown.

The relevance of apical and basal dendrites in neuron function suggests that the selective control of these compartments might account for the nonredundant functions of *Cux1* and *Cux2*. We, therefore, analyzed the specific changes in the apical and basal dendritic arbor that resulted from altering *Cux* expression. We found that *Cux1* and *Cux2* have distinct effects on the topology of superficial neurons. Modifying *Cux1* or *Cux2* expression affected both apical and basal branching, however, the effects of *Cux1* were stronger on basal dendrites, whereas modifying *Cux2* levels mainly altered apical dendrites. These results confirm the nonredundant functions of the two mammalian *Cux* paralogs and clarify their complementary functions on the dendritic topology of layer II-III neurons. It also defines a mechanism that might functionally diversify layer II-III neurons into different subpopulations, possibly with different connectivity patterns and modes of neuronal response.

METHODS

Animals

All animal procedures were approved by the Centro Nacional de Biotecnología Animal Care and Use Committee (N° 11001), in compliance with national and European Union legislation. *Cux2*$^{-/-}$ mice (C57BL6 background) have been described (Cubelos et al., 2008a). For overexpression, C57BL6 wild type (WT) mice (Harlan Laboratories) were used. The morning of the day of appearance of the vaginal plug was defined as embryonic day (E) 0.5.

In Utero Electroporation and GFP Immunohistochemistry

In utero electroporation was as described (Tabata and Nakajima, 2001). *shRNACux1, CAG-Cux1*, and *CAG-Cux2* (Cubelos et al., 2010) or empty p*CAG* used as control plasmids (1 μg/μL) were mixed with *pCAG-GFP* (1 μg/μL). Embryos were electroporated at E15.5. Electroporated mice were perfused at P21 with phosphate-buffered saline followed by a neutral-buffered 10% formalin solution (Sigma) (Cubelos et al., 2008a). Brains were postfixed overnight, embedded in sucrose and cryostat sectioned. Fifty micrometer sections with electroporated neurons were stained with anti-GFP (A-11122, Molecular Probes).

Confocal Microscopy and Morphological Analysis

Confocal microscopy was performed with a Bio-Rad Radiance 2100 laser scanning Zeiss axiovert 200 microscope (argon 488 nm laser line for excitation). After sectioning and staining, individual neurons of the somatosensory cortex were analyzed by obtaining 0.2 μm serial optical sections using confocal and Lasaf v1.8 software (Leica). Measurements were only made of neurons with the main apical process parallel to the plane of section that contacted layer I. Confocal sections were used to reconstruct neuron morphology using Lasaf v1.8 software. Dendritic processes were measured in the planar projection with LaserPix (Image-Pro Plus v.4.0, BioRad; see Supporting Information Fig. 1) and exported to excel file to process the data. The

cumulative dendritic length of total branches, and the number and cumulative length of primary, secondary, and tertiary branches was calculated.

Statistical Analysis

All results are expressed as the mean ± SEM. Experimental groups were compared with one-way ANOVA followed by Tukey's post hoc test. Test Student's two-sample *t* test. *p* values are indicated in figure legends.

RESULTS

Loss of Cux2 Function Mainly Affects Apical Dendrites

Our earlier studies demonstrated that overexpression of either *Cux1* or *Cux2* promote dendritogenesis, and *in vivo* knock-out and knock-down experiments showed that both genes have necessary functions for normal dendrite development (Cubelos et al., 2010). The nonredundant functions of Cux proteins suggest differential effects possibly on distinct neuronal compartments. To study this possibility, we analyzed the basal and apical dendrites of layer II-III neurons of the somatosensory cortex in WT and *Cux2*$^{-/-}$ mice; *CAG-GFP* (*CMV* immediate enhancer/*β-actin* promoter-green fluorescent protein) was electroporated *in utero* at embryonic day (E) 15.5 to label precursors that generate superficial neurons. Morphology of the targeted neurons was analyzed at postnatal day (P) 21, when dendrite development is complete. The total length of all dendrite processes was assessed as a measure of dendritic complexity, and the numbers and length of the primary, secondary, and tertiary branches were quantified. As previously reported, layer II-III neurons of the somatosensory cortex showed an elaborate dendritic morphology that was greatly decreased in *Cux2*$^{-/-}$ neurons [Fig. 1(a,b)]. Our measurements showed reduction in the total cumulative length of apical and basal dendrites in *Cux2*$^{-/-}$ compared to control mice; the apical compartment was more profoundly affected, with a >50% reduction [Fig. 1(c)]. This was due to a notable decrease in the number of secondary and tertiary apical branches [Fig. 1(d)], whose length did not change [Fig. 1(f)]. In contrast, in the basal compartment, only the number of *Cux2*$^{-/-}$ primary processes was slightly reduced compared to control neurons [Fig. 1(e)]. Morphology of shRNACux2 electroporated layer II-III neurons was undistinguishable from GFP neurons of the Cux2$^{-/-}$. This confirms previous results and validates the interchangeable use of these loss of function strategies (Supporting Information Fig. 2 and Cubelos et al., 2010).

Apical and basal dendrites of cortical neurons contact different axonal inputs, and presynaptic contacts influence dendrite development. Similarly, several secreted factors modulate dendrite development. To elucidate if the observed effects were a non-cell autonomous consequence of a possible undetected defect in *Cux2*$^{-/-}$ mice, we overexpressed *Cux2* into layer II-III neurons of the somatosensory cortex of *Cux2*$^{-/-}$ mice (*CAG-Cux2;Cux2*$^{-/-}$). The morphology of the targeted neurons was analyzed at P21. Our measurements showed an increase in the total cumulative dendritic length in *CAG-Cux2*; *Cux2*$^{-/-}$ compared to neurons in *Cux2*$^{-/-}$ mice [Fig. 2(a,b)]. This was due to a notable increase in the number of secondary and tertiary apical branches [Fig. 2(c,d)], whose length also slightly increased [Fig. 2(f)]. Compared to the WT, *CAG-Cux2*;*Cux2*$^{-/-}$ neurons showed a minor but significant increase in apical dendrites [Fig. 2(c,d)]. Compared to the *Cux2*$^{-/-}$, there was an increase in the basal compartment, but it was of lesser magnitude [Fig. 2(c,e)]. *CAG-Cux2*; *Cux2*$^{-/-}$ basal dendrites were undistinguishable of the WT control neurons [Fig. 2(c,e,g)]. These data suggests that overexpression using *CAG-Cux2* constructs results in higher levels of Cux2 protein that those found in WT neurons. Rescue and increase of the dendritic phenotypes of *Cux2*$^{-/-}$ by *Cux2* overexpression, and the stronger effect *CAG-Cux2* on the apical compartment, indicates cell autonomous effects independent of other possible defects in the *Cux2*$^{-/-}$ cortex. Taken together, data indicates a cell-autonomous preferential targeting of apical dendrites by *Cux2*.

Loss of Cux1 Function Affects both Apical and Basal Dendrites

Analysis of *Cux1*$^{-/-}$ mice was precluded because they die early after birth due to defects unrelated to the nervous system. Homozygous mutant mice have stunted growth and a high postnatal death rate (Luong et al., 2002; Cubelos et al., 2008b), and we do not recover any animals pasted P0 on our current colony. To obviate this prenatal lethality, we used *in utero* electroporation technique, similarly to our previous study (Cubelos et al., 2010). In addition *in utero* electroporation allows us to study *Cux* function in a WT context, with most axonal inputs unaffected, and to evaluate cell-autonomous mechanisms (Cubelos et al., 2008b). We electroporated previously characterized shRNA lentiviral constructs that specifically target *Cux1*, together with the CAG-GFP plasmid at E15.5 and analyzed layer II-III neurons of the P21 somatosensory cortex. *Cux1* down-modulated neurons showed a less elaborate dendritic morphology compared to WT

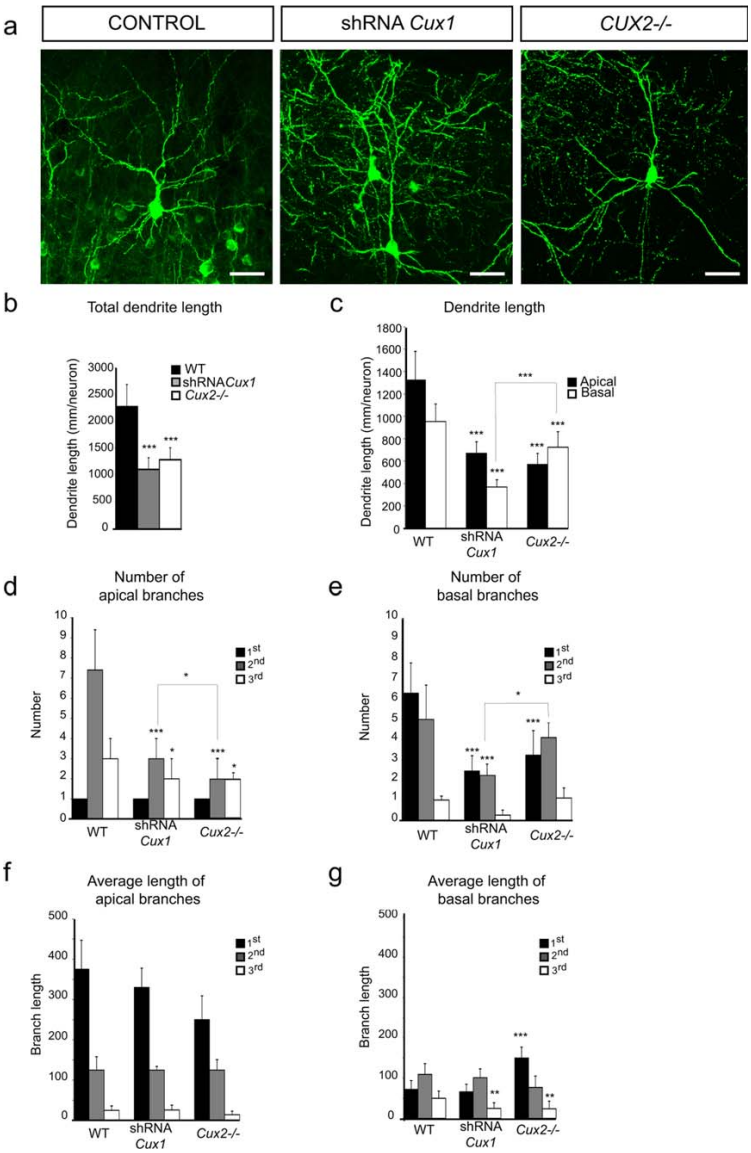

Figure 1 *Cux* deficient neurons show reduced dendritic tree in the somatosensory cortex. (a) Representative confocal micrographs showing GFP-expressing neurons in the P21 somatosensory cortex in control, shRNA*Cux1*, and *Cux2*$^{-/-}$ mice. Neuron morphology was analyzed after *in utero* electroporation of E15.5 cortical precursors. The morphology of pyramidal neurons in upper cortical layers is simpler, shorter, and with fewer dendritic branches in neurons targeted with shRNA*Cux1* and in upper layer neurons of *Cux2*$^{-/-}$ than in WT mice. Bar = 50 μm. (b) Cumulative total dendrite length per neuron in somatosensory cortex of WT, shRNA*Cux1*, and *Cux2*$^{-/-}$ mice. (c) Dendrite apical and basal length distribution shows differences between WT, shRNA*Cux1*, and *Cux2*$^{-/-}$ mice. (d) Primary, secondary, and tertiary dendrite branch numbers in the apical compartment. (e) Primary, secondary, and tertiary dendrite branch numbers in the basal compartment. (f) Length of primary, secondary, and tertiary dendrite branches in the apical compartment for WT, shRNA*Cux1*, and *Cux2*$^{-/-}$ mice. (g) Length of primary, secondary, and tertiary dendrite branches in the basal compartment for WT, shRNA*Cux1*, and *Cux2*$^{-/-}$ mice. Results represent mean ± SEM. Control, $n = 24$; *Cux2*$^{-/-}$, $n = 21$. One-way ANOVA followed by Tukey's post hoc test * $p < 0.05$, ** $p < 0.01$, *** $p < 0.001$ compared to controls.

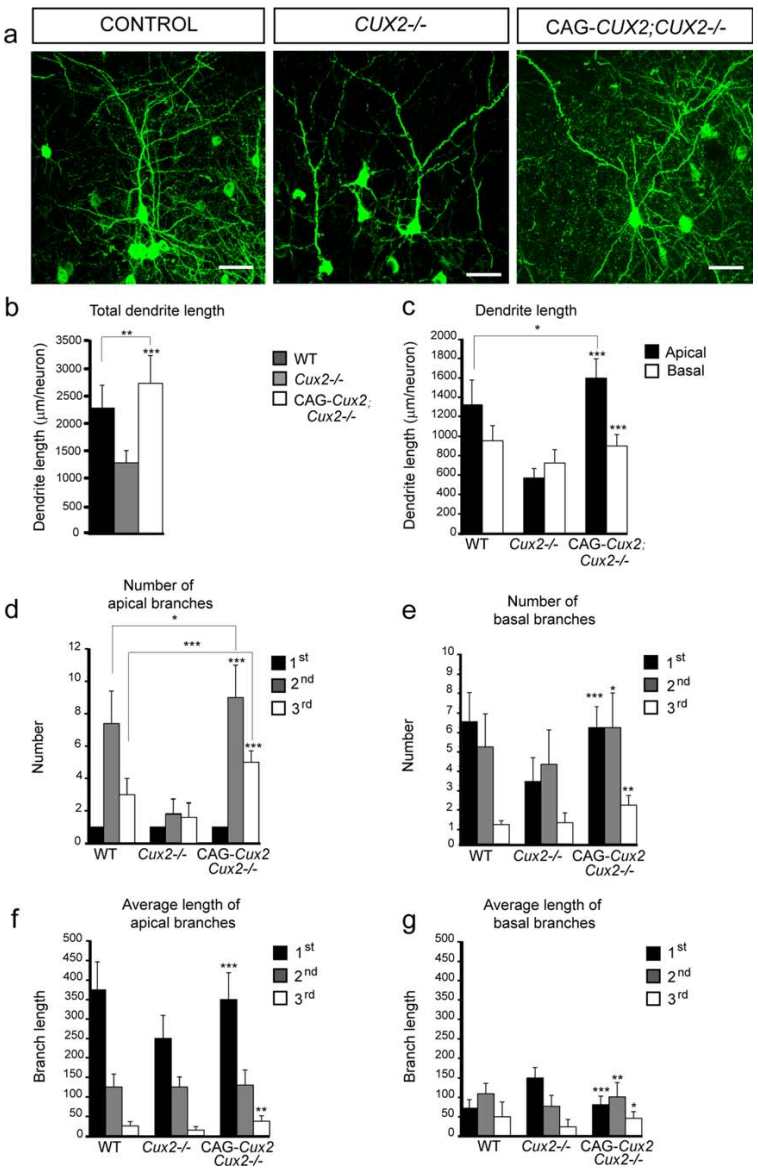

Figure 2 *Cux2* overexpression rescue apical dendrite length and branching of *Cux2*$^{-/-}$ upper layer neurons. *Cux2* overexpression in *Cux2*$^{-/-}$ animals increased apical dendrite complexity compared to *Cux2*$^{-/-}$ neurons electroporated with control vector. (a) Representative confocal micrographs showing GFP-expressing neurons of P21 somatosensory cortex. *CAG-Cux2* or *CAG* empty vectors were coelectroporated with the *CAG-GFP* construct in control WT or *Cux2*$^{-/-}$ animals. Bar = 50 µm. (b) Cumulative total dendrite length per neuron. (c) Total length of apical and basal branches. (d) Number of apical primary, secondary, and tertiary dendrites. (e) Number of basal primary, secondary, and tertiary dendrites. (f) Average length of primary, secondary, and tertiary apical dendrite branches (g) Average length of primary, secondary, and tertiary basal dendrite branches. Results represent mean ± SEM. Control *CAG-GFP*, $n = 24$; *Cux2*$^{-/-}$, $n = 21$; *CAG-Cux2*, $n = 17$. One-way ANOVA followed by Tukey's post hoc test * $p < 0.05$, ** $p < 0.01$, *** $p < 0.001$. *CAG-Cux2; Cux2*$^{-/-}$ is compared to *Cux2*$^{-/-}$ and WT-control. [Color figure can be viewed in the online issue, which is available at wileyonlinelibrary.com.]

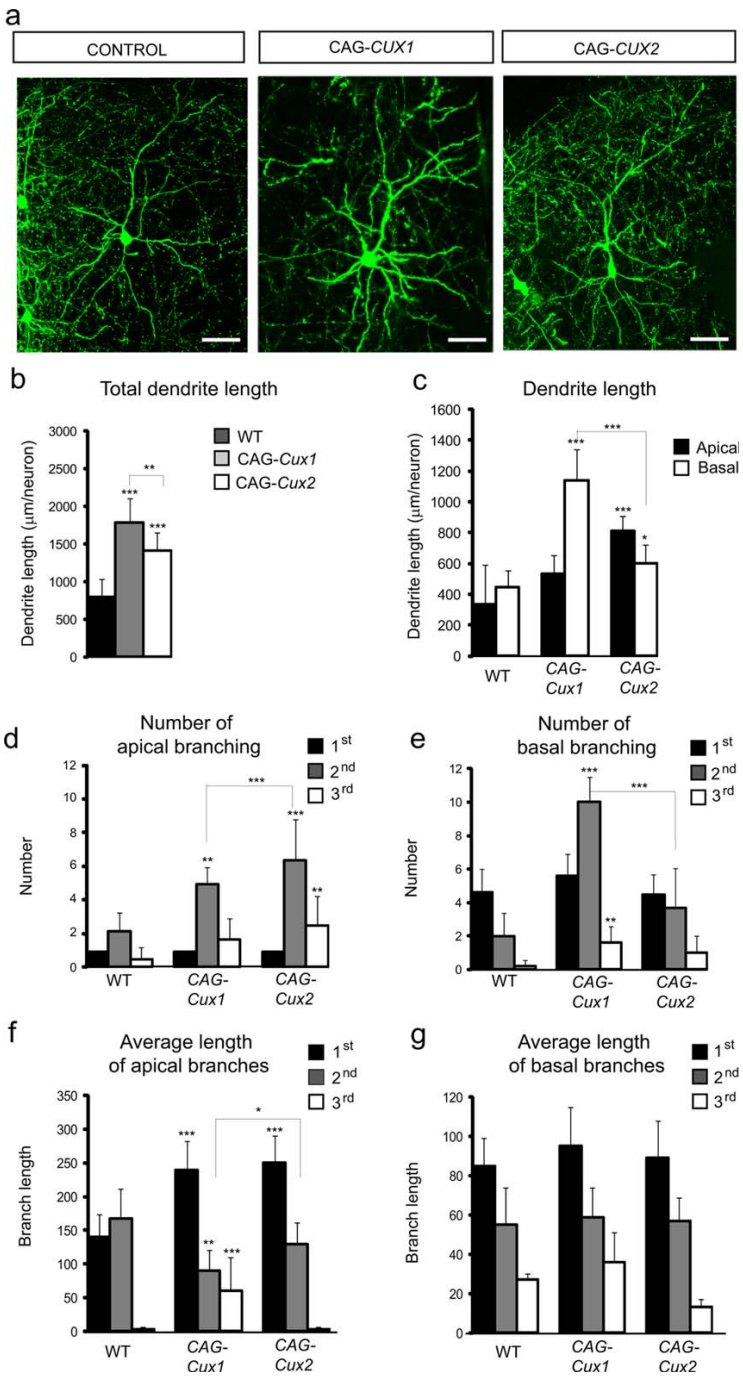
a
CONTROL
CAG-CUX1
CAG-CUX2
b
Total dendrite length
Dendrite length (µm/neuron)
WT
CAG-Cux1
CAG-Cux2
c
Dendrite length
Dendrite length (µm/neuron)
Apical
Basal
WT
CAG-Cux1
CAG-Cux2
d
Number of apical branching
Number
1st
2nd
3rd
e
Number of basal branching
f
Average length of apical branches
Branch length
g
Average length of basal branches

Figure 3.

neurons [Fig. 1(a,b)], as previously reported (Cubelos et al., 2010). Both apical and basal compartments were affected in *shRNACux1* targeted neurons compared to control. However, loss of *Cux1* function has a stronger effect on basal dendrites compared to loss of *Cux2* [Fig. 1(c)]. This was due to a profound decrease in the number of secondary and tertiary apical branches [Fig. 1(d)], whose length did not change [Fig. 1(f)].

Forced Cux1 and Cux2 Expression in Cingulate Neurons Promotes Selective Development of Basal and Apical Dendrites

To further assess the functions of *Cux* genes in the apical and basal compartments, we over-expressed *Cux1* and *Cux2* in the cingulated cortex of WT animals. Late-born neurons of the cingulate cortex have relatively simple dendritic morphologies (Cubelos et al., 2010) and are, therefore, an appropriate population in which to analyze possible selective effects of Cux proteins in stimulating dendritogenesis. These neurons express both *Cux1* and *Cux2*, with lower *Cux1* levels (Nieto et al., 2004; Ferrere et al., 2006). *CAG-Cux1* and *CAG-Cux2* constructs were electroporated *in utero* in the dorso-medial ventricle of E15.5 WT embryos, and mice were analyzed at P21. *Cux1* or *Cux2* overexpression did not affect the correct generation and migration of electroporated cells, as previously observed (Cubelos et al., 2010). Neurons electroporated with *CAG-GFP* alone served as controls; they had the characteristic morphology of superficial cingulate neurons, with a long apical dendrite that often branched into two before reaching the molecular layer (layer I), and with relatively few apical secondary branches [Fig. 3(a,d)]. The basal branches developed a more complex arbor, with a larger number of primary and secondary projections [Fig. 3(a)]. Nonetheless basal branches in the cingulate, presented less complexity than those of the somatosensory cortex [compare Figs. 1(c) and 3(c)]. Quantitative analysis of total dendritic length showed that both *Cux1* and *Cux2* overexpression induced a significant increase in neuron complexity [Fig. 3(a,b)]. Detailed examination of branching number and average length of specific dendrites showed that *Cux1* overexpression increased the number of secondary and tertiary branches in apical and basal compartments [Fig. 3(d,e)], indicating a general effect on stimulation of dendritogenesis. Nonetheless, the increase in basal dendrites was more marked [Fig. 3(e)]. Neurons with high *Cux2* levels behaved in a different manner, with a greater increase in the number of apical than of basal branches. Elevated expression of *Cux1* and *Cux2* affected the average length of apical branches but not of basal [Fig. 3(f,g)]. The results, thus, confirmed the stronger effects of *Cux2* in the apical branches observed in the $Cux2^{-/-}$ mice, and showed the distinct effects compared to *Cux1*, which also strongly stimulates basal dendrites. The results strongly suggest differential effects of *Cux1* and *Cux2*, which contributes to understand their complementary functions. They indicate that in WT cortex, the overlapping *Cux* expression patterns contributes to the generation of functionally diversified populations of layer II-III neurons.

DISCUSSION

We show that *Cux1* and *Cux2* have differential effects on dendrite development of cortical layer II-III neurons. While *Cux1* modulates more markedly the basal dendritic compartment, *Cux2* shows a more selective effect on apical dendrites. The distinct effects reported herein contribute to clarify the relevance of the coexpression and functions of *Cux1* and

Figure 3 *Cux1* and *Cux2* overexpression regulate dendrite length and branching in cingulate cortex. (a) Representative confocal micrographs showing GFP-expressing neurons. Neuron morphology was analyzed in the P21 cingulate cortex after in utero electroporation of E15.5 cortical precursors. *CAG-Cux1*, *CAGCux2*, or *CAG* empty vectors were coelectroporated with the *CAG-GFP* construct. *Cux1* or *Cux2* overexpression increased dendrite complexity of cingulate neurons compared with neurons electroporated with control vector. Bar = 50 μm. (b) Cumulative total dendrite length per neuron. (c) Total length of apical and basal branches differed when *Cux1* or *Cux2* was overexpressed. (d) Number of apical primary, secondary and tertiary dendrites. (e) Number of basal primary, secondary, and tertiary dendrites. (f) Length of primary, secondary, and tertiary dendrite branches in the apical compartment after *CAG-Cux1* or *CAG-Cux2* overexpression in neurons. (g) Length of primary, secondary, and tertiary dendrite branches in the basal compartment after *CAG-Cux1* or *CAG-Cux2* overexpression in neurons. Results represent mean ± SEM. Control *CAG-GFP*, $n = 14$; *CAG-Cux1*, $n = 12$; *CAG-Cux2*, $n = 17$. One-way ANOVA followed by Tukey's post hoc test * $p < 0.05$, ** $p < 0.01$, *** $p < 0.001$ compared to controls. [Color figure can be viewed in the online issue, which is available at wileyonlinelibrary.com.]

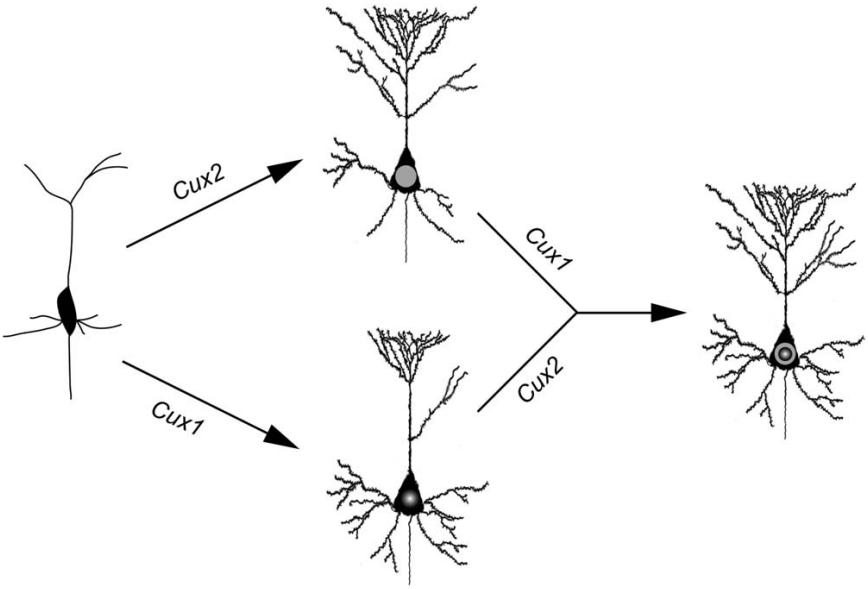

Figure 4 Cux proteins selectively target apical and basal dendritic domains of layer II-III cortical neurons. Scheme summarizing the additive and complementary functions of *Cux1* and *Cux2*. During brain development, *Cux1* expression has a stronger effect on the development of basal processes while *Cux2* preferentially contributes to apical dendrite differentiation. Coexpression of the two genes determines the final dendritic arbor of layer II-III neurons.

Cux2 in layer II-III neurons [Fig. 4], where they determine the final complexity of the dendritic arbor of these neurons (Cubelos et al., 2010).

Recent studies identified the importance of apical and basal dendrite regulation in the physiology and development of neuronal circuits; many of these reports established a link between these mechanisms and pathways implicated in human autism disorders. Several features of neuron function are related directly to dendrite polarity. Dendrite topography selects the number and type of presynaptic axons, which have a layered organization in the cortex, for the simple reason that it restricts accessibility to potential synapses. Axon contacts can even discriminate between basal and apical domains of the same neuron, probably by recognizing polarized signals (Mainen and Sejnowski, 1996; Petreanu et al., 2009; Jia et al., 2010). The modulation of apical and basal morphologies also influences input computation of the neuron and modulates neuron excitability and plasticity as propagation of electrical signals also differs in distal apical and basal domains (Jia et al., 2010; Branco and Hausser, 2011). The combination and modulation of *Cux1* and *Cux2* expression allows layer II-III neuron differentiation into further specialized subpopulations and might contribute to the formation and function of selected intracortical subnetworks (Yoshimura and Callaway, 2005; Yoshimura et al., 2005; Yassin et al., 2010). It might also explain the reported distinct complexity of basal dendrites of layer II-III neurons in the different areas of murine and human cortex (Elston, 2003; Ballesteros-Yanez et al., 2006).

The mechanisms that regulate dendrites downstream of *Cux*, or downstream of other transcription factors involved in the subclass specific dendrite determination are mostly unknown (Grueber et al., 2005; Parrish et al., 2007; Cline and Haas, 2008; Fame et al., 2011). They are likely linked to one or several cytoskeleton, membrane receptors, and signaling proteins reported to regulate dendritic differentiation (Kuijpers and Hoogenraad, 2011; Kulkarni and Firestein, 2012). Of particular interests are the selective effects of *Cux2* in apical dendrites. Some of above mentioned cellular mechanisms act selectively on apical or basal dendrites. Brain-derived neurotrophic factor and neurotrophin-3 (NT-3) for example, showed to enhance elongation of basal dendrites of layer II-III pyramidal neurons in the rat somatosensory cortex, but did not affected the apical processes (Baker et al., 1998; Niblock et al., 2000). Signaling of Sema3A through its receptor Nrp1/PlexA4 controls basal dendritic arborization

in layer V cortical neurons, providing another example of pathways stimulating polarized growth (Fenstermaker et al., 2004; Tran et al., 2009). The kinase TAOK2 mediates this effect through the interaction with Nrp1 molecules bound to Sema3A. TAOK2 is encoded by the autism spectrum disorder (ASD) susceptibility gene *TAOK2* (de Anda et al., 2012).

The study by de Anda et al. adds to previous work showing the importance of dendritic development in ASD and to recent work showing a link with developmental failures in apical and basal cell compartments. The Angelman syndrome protein ubiquitin-protein ligase E3A (*Ube3a*) promotes apical dendrite outgrowth by regulating the asymmetric distribution of the Golgi apparatus (Miao et al., 2013). *Epac2* rare coding variants are found in human subjects diagnosed with autism. Epac2 is a guanine nucleotide exchange factor (GEF) for the Ras-like small GTPase Rap necessary to maintain the basal compartment of layer II-III neurons of mice and humans (Srivastava et al., 2012b); and for learning and normal social interaction in mice (Yang et al., 2012; Srivastava et al., 2012a). These and other possible mechanisms mediating the selective targeting of apical domains by *Cux2*, or both apical and basal domains by *Cux1*, suggest a linkage of *Cux* genes with ASD. This requires further investigations also encouraged by studies showing that, in man, *CUX1* mediates abnormal transcriptional activation of two intronic single-nucleotide polymorphisms of *ENGRAILED2* linked to ASDs (Choi et al., 2012).

Our data demonstrates differential effects of *Cux1* and *Cux2* in dendritic development. These distinct functions might serve to specialize layer II-III neurons of the mammalian cortex as well as other neuronal subpopulations expressing *Cux1* or *Cux2*. The importance of apical and basal compartments for the high functions of the brain predicts that the molecular and cellular programs mediated by *Cux* genes contribute to the precise organization of cortical networks; it also suggests that mutations affecting *Cux* pathways might be implicated in autism disorders.

We thank R. Gutiérrez and A. Morales for excellent technical assistance and C. Mark for editorial assistance.CGB, GMEO BC performed the experiments. BC and MN designed, and analysed data. MN and BC obtained funding. All authors participated in the preparation of the manuscript. All authors approved the final manuscript.

Disclosure: The authors declare that they have no competing interests.

REFERENCES

Baker RE, Dijkhuizen PA, Van Pelt J, Verhaagen J. 1998. Growth of pyramidal, but not non-pyramidal, dendrites in long-term organotypic explants of neonatal rat neocortex chronically exposed to neurotrophin-3. Eur J Neurosci 10:1037–1044.

Ballesteros-Yanez I, Benavides-Piccione R, Elston GN, Yuste R, DeFelipe J. 2006. Density and morphology of dendritic spines in mouse neocortex. Neuroscience 138: 403–409.

Barnes AP, Solecki D, Polleux F. 2008. New insights into the molecular mechanisms specifying neuronal polarity in vivo. Curr Opin Neurobiol 18:44–52.

Bi X, Lynch G, Zhou J, Gall CM. 2001. Polarized distribution of alpha5 integrin in dendrites of hippocampal and cortical neurons. J Comp Neurol 435:184–193.

Branco T, Hausser M. 2011. Synaptic integration gradients in single cortical pyramidal cell dendrites. Neuron 69: 885–892.

Choi J, Ababon MR, Matteson PG, Millonig JH. 2012. Cut-like homeobox 1 and nuclear factor I/B mediate ENGRAILED2 autism spectrum disorder-associated haplotype function. Hum Mol Genet 21:1566–1580.

Cline H, Haas K. 2008. The regulation of dendritic arbor development and plasticity by glutamatergic synaptic input: A review of the synaptotrophic hypothesis. J Physiol 586:1509–1517.

Cubelos B, Nieto M. 2010. Intrinsic programs regulating dendrites and synapses in the upper layer neurons of the cortex. Commun Integr Biol 3:483–486.

Cubelos B, Sebastian-Serrano A, Beccari L, Calcagnotto ME, Cisneros E, Kim S, Dopazo A, et al. 2010. Cux1 and Cux2 regulate dendritic branching, spine morphology, and synapses of the upper layer neurons of the cortex. Neuron 66:523–535.

Cubelos B, Sebastian-Serrano A, Kim S, Moreno-Ortiz C, Redondo JM, Walsh CA, Nieto M. 2008a. Cux-2 controls the proliferation of neuronal intermediate precursors of the cortical subventricular zone. Cereb Cortex 18:1758–1770.

Cubelos B, Sebastian-Serrano A, Kim S, Redondo JM, Walsh C, Nieto M. 2008b. Cux-1 and Cux-2 control the development of Reelin expressing cortical interneurons. Dev Neurobiol 68:917–925.

de Anda FC, Rosario AL, Durak O, Tran T, Graff J, Meletis K, Rei D, et al. 2012. Autism spectrum disorder susceptibility gene TAOK2 affects basal dendrite formation in the neocortex. Nat Neurosci 15:1022–1031.

Elston GN. 2003. Cortex, cognition and the cell: New nsights into the pyramidal neuron and prefrontal function. Cereb Cortex 13:1124–1138.

Fame RM, MacDonald JL, Macklis JD. 2011. Development, specification, and diversity of callosal projection neurons. Trends Neurosci 34:41–50.

Feldman DE. 2012. The spike-timing dependence of plasticity. Neuron 75:556–571.

Fenstermaker V, Chen Y, Ghosh A, Yuste R. 2004. Regulation of dendritic length and branching by semaphorin 3A. J Neurobiol 58:403–412.

Ferrere A, Vitalis T, Gingras H, Gaspar P, Cases O. 2006. Expression of Cux-1 and Cux-2 in the developing somatosensory cortex of normal and barrel-defective mice. Anat Rec A Discov Mol Cell Evol Biol 288:158–165.

Grueber WB, Yang CH, Ye B, Jan YN. 2005. The development of neuronal morphology in insects. Curr Biol 15: R730–R738.

Jan YN, Jan LY. 2010. Branching out: Mechanisms of dendritic arborization. Nat Rev Neurosci 11:316–328.

Jia H, Rochefort NL, Chen X, Konnerth A. 2010. Dendritic organization of sensory input to cortical neurons in vivo. Nature 464:1307–1312.

Kuijpers M, Hoogenraad CC. 2011. Centrosomes, microtubules and neuronal development. Mol Cell Neurosci 48: 349–358.

Kulkarni VA, Firestein BL. 2012. The dendritic tree and brain disorders. Mol Cell Neurosci 50:10–20.

Luong MX, van der Meijden CM, Xing D, Hesselton R, Monuki ES, Jones SN, Lian JB, et al. 2002. Genetic ablation of the CDP/Cux protein C terminus results in hair cycle defects and reduced male fertility. Mol Cell Biol 22:1424–1437.

Mainen ZF, Sejnowski TJ. 1996. Influence of dendritic structure on firing pattern in model neocortical neurons. Nature 382:363–366.

Miao S, Chen R, Ye J, Tan GH, Li S, Zhang J, Jiang YH, et al. 2013. The Angelman syndrome protein Ube3a is required for polarized dendrite morphogenesis in pyramidal neurons. J Neurosci 33:327–333.

Niblock MM, Brunso-Bechtold JK, Riddle DR. 2000. Insulin-like growth factor I stimulates dendritic growth in primary somatosensory cortex. J Neurosci 20:4165–4176.

Nieto M, Monuki ES, Tang H, Imitola J, Haubst N, Khoury SJ, Cunningham J, Gotz M, Walsh CA. 2004. Expression of Cux-1 and Cux-2 in the subventricular zone and upper layers II-IV of the cerebral cortex. J Comp Neurol 479: 168–180.

Parrish JZ, Emoto K, Kim MD, Jan YN. 2007. Mechanisms that regulate establishment, maintenance, and remodeling of dendritic fields. Annu Rev Neurosci 30:399–423.

Petreanu L, Mao T, Sternson SM, Svoboda K. 2009. The subcellular organization of neocortical excitatory connections. Nature 457:1142–1145.

Polleux F, Morrow T, Ghosh A. 2000. Semaphorin 3A is a chemoattractant for cortical apical dendrites. Nature 404: 567–573.

Shen K, Scheiffele P. 2010. Genetics and cell biology of building specific synaptic connectivity. Annu Rev Neurosci 33:473–507.

Srivastava DP, Jones KA, Woolfrey KM, Burgdorf J, Russell TA, Kalmbach A, Lee H, et al. 2012a. Social, Communication, and Cortical Structural Impairments in Epac2-Deficient Mice. J Neurosci 32:11864–11878.

Srivastava DP, Woolfrey KM, Jones KA, Anderson CT, Smith KR, Russell TA, Lee H, et al. 2012b. An autism-associated variant of Epac2 reveals a role for Ras/Epac2 signaling in controlling basal dendrite maintenance in mice. PLoS Biol 10:e1001350.

Tabata H, Nakajima K. 2001. Efficient in utero gene transfer system to the developing mouse brain using electroporation: Visualization of neuronal migration in the developing cortex. Neuroscience 103:865–872.

Tada T, Sheng M. 2006. Molecular mechanisms of dendritic spine morphogenesis. Curr Opin Neurobiol 16:95–101.

Tran TS, Rubio ME, Clem RL, Johnson D, Case L, Tessier-Lavigne M, Huganir RL, et al. 2009. Secreted semaphorins control spine distribution and morphogenesis in the postnatal CNS. Nature 462:1065–1069.

Yang Y, Shu X, Liu D, Shang Y, Wu Y, Pei L, Xu X, et al. 2012. EPAC null mutation impairs learning and social interactions via aberrant regulation of miR-124 and Zif268 translation. Neuron 73:774–788.

Yassin L, Benedetti BL, Jouhanneau JS, Wen JA, Poulet JF, Barth AL. 2010. An embedded subnetwork of highly active neurons in the neocortex. Neuron 68: 1043–1050.

Yoshimura Y, Callaway EM. 2005. Fine-scale specificity of cortical networks depends on inhibitory cell type and connectivity. Nat Neurosci 8:1552–1559.

Yoshimura Y, Dantzker JL, Callaway EM. 2005. Excitatory cortical neurons form fine-scale functional networks. Nature 433:868–873.

Zimmer C, Tiveron MC, Bodmer R, Cremer H. 2004. Dynamics of Cux2 expression suggests that an early pool of SVZ precursors is fated to become upper cortical layer neurons. Cereb Cortex 14:1408–1420.

CUX1 ENABLES INTERHEMISPHERIC CONNECTIONS OF LAYER II/III NEURONS BY REGULATING KV1-DEPENDENT FIRING

Las neuronas de la lámina II-III incluyen subpoblaciones callosas y no callosas en proporciones no determinadas (Lefort et al. 2009; Petreanu et al. 2007). Como se ha adelantado en el apartado relativo a la formación del CC, en la última década diversos estudios (Mizuno et al. 2007; Suarez et al. 2014; Wang et al. 2007) han subrayado el papel de la excitabilidad intrínseca de estas neuronas como posible determinante del desarrollo del CC gracias a la regulación de la actividad cortical y de las formas de comunicación entre neuronas. Sin embargo aún queda mucho por saber acerca de cómo la actividad instruye la conectividad callosa.

A pesar de que hay numerosas evidencias de que los FT específicos de lámina como Cux1 están implicados en diversos aspectos de la identidad y conectividad neuronal (Cubelos et al. 2010; Fame et al. 2011; Lodato et al. 2015), apenas hay estudios que ahonden en la posible relación entre FT que determinan la identidad molecular de las diferentes poblaciones neuronales y la conectividad dependiente de actividad (Dehorter et al. 2015; Garcia-Frigola and Herrera 2010). En cuanto a las poblaciones de NP corticales, en los últimos años se han publicado diversos artículos que relacionan su identidad de lámina y su subgrupo dentro de ésta con diferentes formas de disparo (De la Rossa et al. 2013; Otsuka and Kawaguchi 2011). No obstante, la pregunta de hasta qué punto esta asociación se debe a su diferenciación intrínseca o si es consecuencia de la conectividad selectiva de estas neuronas sigue sin resolverse. El trabajo presentado en esta tesis demuestra la importancia de regular la actividad eléctrica durante la formación del circuito y cómo esto constituye un mecanismo del desarrollo sobre el que inciden los FT que determinan el tipo neuronal. Corroborando la idea de que la regulación de la excitabilidad de manera específica de tipo neuronal es muy relevante, y coincidiendo con los estudios de esta tesis, Dehorter y colegas demostraron que la actividad de la red modulaba dinámicamente las propiedades de una subpoblación de interneuronas a través de la regulación de la expresión del FT Er81 (Dehorter et al. 2015).

Los experimentos y conclusiones descritos en este artículo suponen el núcleo principal de esta tesis doctoral. En él mostramos que la regulación de los canales de la familia Kv1 por Cux1 es necesaria para que tenga lugar el cambio a un disparo más adaptable durante el desarrollo postnatal. La expresión regulada de los canales Kv1 permite que la neurona adquiera los parámetros del disparo que correlacionan con el éxito en la inervación. Esto sugiere fuertemente que la forma de disparo adaptativa es necesaria para la estabilización del axón calloso en el hemisferio contralateral.

Mi contribución en este artículo fue tanto la realización de trabajo experimental y análisis de los resultados (IUE, inmunohistoquímica, clonajes, genotipajes, análisis de imagen) como análisis estadístico y escritura del manuscrito. Los experimentos relativos a electrofisiología y sus análisis fueron realizados por Fernanda Rodríguez-Tornos, coautora principal del trabajo.

Article

Neuron

Cux1 Enables Interhemispheric Connections of Layer II/III Neurons by Regulating Kv1-Dependent Firing

Highlights

- *Cux1* couples neuronal identity and wiring through modulation of firing modes
- Cux1 transcription factor determines postnatal development of the corpus callosum
- *Cux1* determines *Kv1* expression levels and firing modes in layer II/III neurons
- Firing modes determine axonal connectivity during development

Authors

Fernanda M. Rodríguez-Tornos, Carlos G. Briz, Linnea A. Weiss, ..., Denis Jabaudon, José A. Esteban, Marta Nieto

Correspondence

mnlopez@cnb.csic.es

In Brief

Cux1 regulation of *Kv1* transcripts is necessary for a developmental postnatal switch to a strong-adapting firing response in layer II/III neurons. This firing mode is required for callosal innervation. Thus, *Cux1* couples the neurons' firing responses to their connectivity.

Rodríguez-Tornos et al., 2016, Neuron *89*, 494–506
February 3, 2016
http://dx.doi.org/10.1016/j.neuron.2015.12.020

CellPress

CellPress

Neuron
Article

Cux1 Enables Interhemispheric Connections of Layer II/III Neurons by Regulating Kv1-Dependent Firing

Fernanda M. Rodríguez-Tornos,[1,6] Carlos G. Briz,[1,6] Linnea A. Weiss,[1] Alvaro Sebastián-Serrano,[1,7] Saúl Ares,[1,2] Marta Navarrete,[3] Laura Frangeul,[4] Maria Galazo,[5] Denis Jabaudon,[4] José A. Esteban,[3] and Marta Nieto[1,*]

[1]Centro Nacional de Biotecnología (CNB-CSIC), Campus de Cantoblanco, Darwin 3, 28049 Madrid, Spain
[2]Departamento de Matemáticas Universidad Carlos III de Madrid, Grupo Interdisciplinar de Sistemas Complejos (GISC), 28911 Leganés, Madrid, Spain
[3]Centro de Biología Molecular "Severo Ochoa," Consejo Superior de Investigaciones Científicas (CSIC-UAM), 28049 Madrid, Spain
[4]Department of Basic Neurosciences, University of Geneva, 1211 Geneva 4, Switzerland
[5]HSCRB Harvard University, Cambridge, MA 02138, USA
[6]Co-first author
[7]Present address: Departamento de Bioquímica y Biología Molecular IV, Facultad de Veterinaria, Universidad Complutense de Madrid, 28040 Madrid, Spain
*Correspondence: mnlopez@cnb.csic.es
http://dx.doi.org/10.1016/j.neuron.2015.12.020

SUMMARY

Neuronal subtype-specific transcription factors (TFs) instruct key features of neuronal function and connectivity. Activity-dependent mechanisms also contribute to wiring and circuit assembly, but whether and how they relate to TF-directed neuronal differentiation is poorly investigated. Here we demonstrate that the TF Cux1 controls the formation of the layer II/III corpus callosum (CC) projections through the developmental transcriptional regulation of Kv1 voltage-dependent potassium channels and the resulting postnatal switch to a Kv1-dependent firing mode. Loss of *Cux1* function led to a decrease in the expression of *Kv1* transcripts, aberrant firing responses, and selective loss of CC contralateral innervation. Firing and innervation were rescued by re-expression of *Kv1* or postnatal reactivation of *Cux1*. Knocking down *Kv1* mimicked Cux1-mediated CC axonal loss. These findings reveal that activity-dependent processes are central bona fide components of neuronal TF-differentiation programs and establish the importance of intrinsic firing modes in circuit assembly within the neocortex.

INTRODUCTION

The corpus callosum (CC) connects the hemispheres of the cerebral cortex and allows the high associative functions of the mammalian brain. Partial or total CC agenesis is a feature of several developmental disorders (Fame et al., 2011). The CC is formed by myelinated axons that project from neurons in layers II/III (~80% in mouse) and V (~20%) and a very minor layer VI population (Fame et al., 2011). Cortical pyramidal layer II/III neurons are molecularly defined by the expression of the homeodomain transcription factor (TF) Cux1 (Britanova et al., 2008; Nieto et al., 2004). They include callosally and noncallosally projecting subpopulations in undetermined proportions (Lefort et al., 2009; Petreanu et al., 2007). Callosal neurons branch their axons at layers II/III and V, both contralaterally (interhemispheric) and ipsilaterally (intrahemispheric) (Fame et al., 2011; Lefort et al., 2009; Petreanu et al., 2007). Noncallosal layer II/III subpopulations project only ipsilaterally to layers II/III and V (Mitchell and Macklis, 2005).

Activity-dependent mechanisms are fundamental processes contributing to neuronal wiring and to the formation of functional circuits in the brain, but they are poorly understood (Ackman and Crair, 2014; Kano and Hashimoto, 2009; Kirkby et al., 2013; Stanley, 2013). In CC formation, studies have shown that diminishing layer II/III neurons' excitability by overexpressing the inward-rectifier potassium-ion channel Kir2.1 reduces axonal branching and changes the columnar patterns of callosal innervation in the contralateral hemisphere (Mizuno et al., 2010; Suárez et al., 2014; Wang et al., 2007). More recently, it was shown that altered innervation is not due to decreased firing rates per se, but because reducing excitability disrupts the balanced cortical activity of the hemispheres (Suárez et al., 2014). These studies pointed to the intrinsic excitability of neurons as possibly determining CC development by regulating the neurons' communication and/or forms of cortical activity. Yet much remains to be learned about how activity instructs callosal connectivity.

Cux1 and other layer-specific TFs have been shown to govern several aspects of neuronal identity and connectivity (Cubelos et al., 2010; Fame et al., 2011; Lodato et al., 2015). However, the possible links between TF determining the molecular identity of neuronal populations and activity-dependent wiring are only beginning to be investigated (García-Frigola and Herrera, 2010). A recent report demonstrated the coupling of Er81

expression and intrinsic excitability through the regulation of Kv1 channels in a subpopulation of interneurons. Importantly, it was shown that Er81 expression levels are dynamically modulated in an activity-dependent manner along the life of the neuron, providing a mechanistic explanation for the activity-dependent regulation of the excitability of these interneurons (Dehorter et al., 2015). In contrast, it is not known whether neuronal subtype-specific transcriptional programs instruct the specific firing responses of pyramidal neurons. Some reports have linked the identity of mature adult pyramidal neurons to their distinct firing responses (De la Rossa et al., 2013; Otsuka and Kawaguchi, 2011) but did not address to what extent this association is due to their intrinsic differentiation. Furthermore, it is unknown if and how TF-directed regulation of excitability might be related to selective wiring.

The acquisition of specific firing modes is a gradual process of differentiation that involves the dynamic expression of a wide repertoire of ion channels. Maturation of firing responses during the development of layer II/III neurons correlates with the onset of the critical period of maximal plasticity (Maravall et al., 2004). From postnatal day (P)10 to approximately P17 in rodent somatosensory (SS) cortex, spiking behavior of layer II/III neurons shifts from phasic (more spike-frequency adaptation) to regular (less spiking adaptation) over time, such that the number of action potentials (APs) elicited by a given stimulus increases (Locke and Nerbonne, 1997; Maravall et al., 2004). Concurrent with these electrical changes, the expression of voltage-gated potassium channels (Kv1) increases in cortical pyramidal neurons from P8 onward (Guan et al., 2011). Kv1 channels open at voltages close to AP threshold, limit excitability, and contribute to the emergence of distinct firing modes (Goldberg et al., 2008; Kole and Stuart, 2012; Locke and Nerbonne, 1997; Shu et al., 2007). These channels are key to the strong adapting behavior of P10–P12 layer II/III neurons: pharmacological blockade of Kv1 currents in these neurons decreased spiking adapting capacity and increased firing rates such that they resembled the firing responses of more mature P16 neurons (Locke and Nerbonne, 1997).

Here we investigate the role of the transcription factor Cux1 in callosal axon development. We find that downmodulation of *Cux1* expression results in complete impairment of callosal axonal innervation in the contralateral cortical plate and show that this is due to the inability to switch on Kv1-dependent firing responses. Our data indicate that transcriptional regulation of *Kv1.1* and *Kv1.3* genes by Cux1 contributes to the normal electrical differentiation and the developmental upregulation of Kv1 channels in layer II/III neurons. We also show that restoring Kv1 currents in Cux1-deficient neurons allows the acquisition of a strong-adapting firing mode and rescues contralateral CC innervation, while knocking down *Kv1* channels eliminates contralateral innervation. Restoring Cux1 expression after P8 is sufficient to rescue electrical and axonal defects of shRNA*Cux1* layer II/III neurons. Our data thus demonstrate that *Cux1*-mediated regulation of Kv1-dependent firing is a developmental mechanism that determines CC contralateral innervation of callosal layer II/III neurons. The results demonstrate the importance of electrical differentiation for the establishment of neuronal networks, which has implications for the treatment of neuronal disorders.

RESULTS

Cux1-Deficient Neurons Lose Callosal Contralateral Projections, but Not Ipsilateral Branches

To determine the role of *Cux1* in connectivity, we knocked down gene expression in layer II/III neurons of the SS cortex using a previously reported shRNA (shRNA*Cux1*) in conjunction with in utero electroporation (IUE) of wild-type (WT) embryonic day (E) 15 mouse cortices (Cubelos et al., 2010). This knockdown strategy circumvents the prenatal lethality of *Cux1* knockout mice (Cubelos et al., 2010) and allows the visualization of ipsilateral and contralateral axons of the targeted neurons via coelectroporation of a plasmid encoding the green fluorescent protein (CAG-GFP) (Cubelos et al., 2010; Figures 1A, 1B, and S1A, available online). Analysis of callosal contralateral axons appeared relevant because axonal retrotracing labeling of contralateral projections demonstrated that all labeled callosal layer II/III neurons expressed Cux1 (Figure S1B), as expected by the widespread expression of Cux1 in layer II/III (Britanova et al., 2008; Cubelos et al., 2010).

We first analyzed GFP-positive layer II/III axonal projections in control shRNA-electroporated mice at P16, an age at which the branching pattern reflects that of the mature circuit (Mizuno et al., 2010; Suárez et al., 2014). As shown in Figure 1C, in the electroporated ipsilateral side, GFP-positive dendritic and axonal processes intermingled with the somas of layer II/III targeted neurons, and axonal branches developed in layer V; in the contralateral hemisphere, callosal axons formed columns with profuse branching in layers II/III and V in the SS areas and a diffuse layer pattern in the insular cortex (Figures 1A and 1D). Upon shRNA-mediated *Cux1* knockdown, we did not detect any major defect in ipsilateral axonal projections in layers II/III and V (Figures 1E and 1G). In contrast, loss of *Cux1* function eliminated most of the GFP-positive axons in the contralateral hemisphere, both in the SS and the insular cortex, and greatly reduced those within the contralateral white matter (WM) (Figures 1F–1I). These defects were not due to delayed innervation, as they persisted at P28, nor could they be explained by alternative GFP axonal tracts toward ventral, frontal, or rostral areas (data not shown). They were also not due to neuronal death because, as we previously reported (Cubelos et al., 2010), shRNA*Cux1*-electroporated neurons did not show signs of degeneration or increased expression of the apoptotic marker Cleaved Caspase 3 (Figure S1C). The specificity of shRNA-*Cux1*-mediated defects in CC innervation was demonstrated by reversion of the innervation phenotype via coelectroporation of a shRNA*Cux1*-resistant *Cux1* construct (Supplemental Experimental Procedures and Figures S1D and S1E). As most layer II/III neurons also express the *Cux1* homolog *Cux2* (Cubelos et al., 2010), we also analyzed the effects of loss of function of *Cux2* on contralateral innervation using *Cux2* knockout mice or shRNA-*Cux2* in WT mice. These experiments did not reveal impaired CC contralateral connections (Figures S1D and S1E), which indicates that control of contralateral CC innervation is a *Cux1*-specific function. Overall, the results show that *Cux1* is essential for the establishment of CC contralateral axonal innervation.

We next analyzed earlier stages of CC axonal development to investigate the process leading to the absence of P16

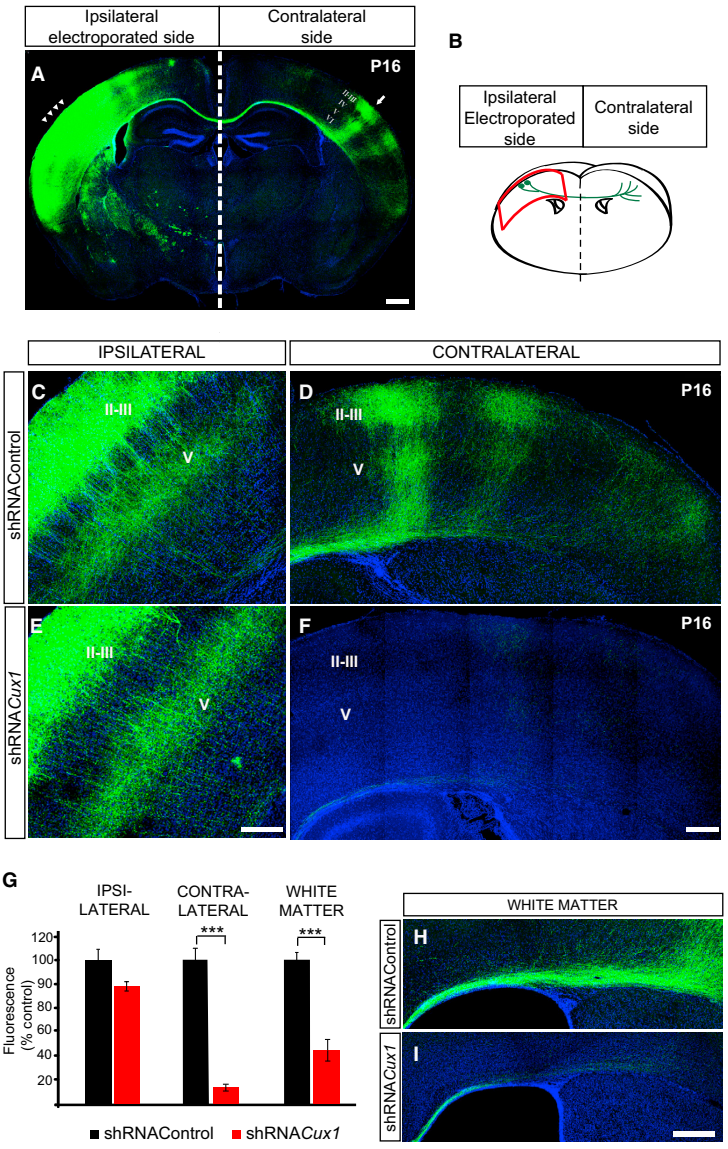

Figure 1. *Cux1* Is Essential for Contralateral CC Innervations at P16, but Not for Ipsilateral Branching

(A) Tile scan assembly of a coronal section of a P16 brain electroporated at E15.5 with CAG-GFP. The ipsilateral GFP signal (arrowheads) was saturated to visualize axons and the main contralateral column (arrow) in the contralateral side. Cortical layers are labeled on the contralateral side.

(B) Diagram showing axonal trajectories with the region of ipsilateral electroporated neurons outlined in red.

(C) GFP in the electroporated ipsilateral side marks layer II/III somas and branches in layers II/III and V.

(D) Contralateral innervation in control mice, including columns of axons branching in layers II/III and V in the SS cortex and an adjacent, more lateral, diffuse secondary column in the insular cortex.

(E) Ipsilateral projections of shRNA*Cux1* neurons.

(F) GFP signal is almost absent in the contralateral cortical plate of shRNA*Cux1*-electroporated brains. (Medial is right for C and E; left for D and F.)

(G) Quantification of GFP signal normalized to shRNAControl. Mean ± SEM. Student's t test p value *** ≤ 0.005.

(H and I) Contralateral WM at P16 shows decreased axonal density in shRNA*Cux1* (I) electroporated brains compared to control (H). Mean ± SEM.

Scale bars, 500 μm (A); 200 μm (C and E); 250 μm (D, F, H, and I).

contralateral CC axons induced by loss of *Cux1* function. At P2–P4, soon after axons cross the midline, no major differences were observed between control and *Cux1*-deficient axons (Figures S2Aand S2B). At P8, when axons branch in the WM and begin to invade the contralateral cortical plate, the only apparent difference was a slight increase in GFP signal in the WM of shRNA*Cux1*-electroporated brains as compared to controls (Figures 2A, 2B, and 2H). In contrast, by P10, the phenotype resulting from *Cux1* knockdown was striking and equivalent to that of P16 brains: while in control mice GFP-positive axons profusely invaded the contralateral territories in a still-unrefined columnar pattern (Figures 2C and 2E), only a few axons appeared in the cortical plate in shRNA*Cux1*-electroporated brains (Figures 2D, 2F, and 2G). There was also a significant decrease of GFP-positive axons in the WM at both P10 and P12 (Figures 2H and S2A), indicating a reduced number of WM branches compared to controls. At P28, the reduction in GFP signal in the contralateral WM of shRNA*Cux1*-targeted brains was as marked as, but not higher than, that observed at P16, indicating that not all WM axons are eventually eliminated (not shown). These data indicate that axons of *Cux1*-deficient neurons initiate invasion of the cortical plate normally but cannot sustain further development after P8. The reduction of GFP-positive axons in the cortical plate and WM observed between P8 and P10 suggests that *Cux1*-deficient axons retract.

The onset of axonal loss in *Cux1*-deficient conditions coincides with the earliest establishment of synapses, and it has been reported that CC axons that are unable to make synapses

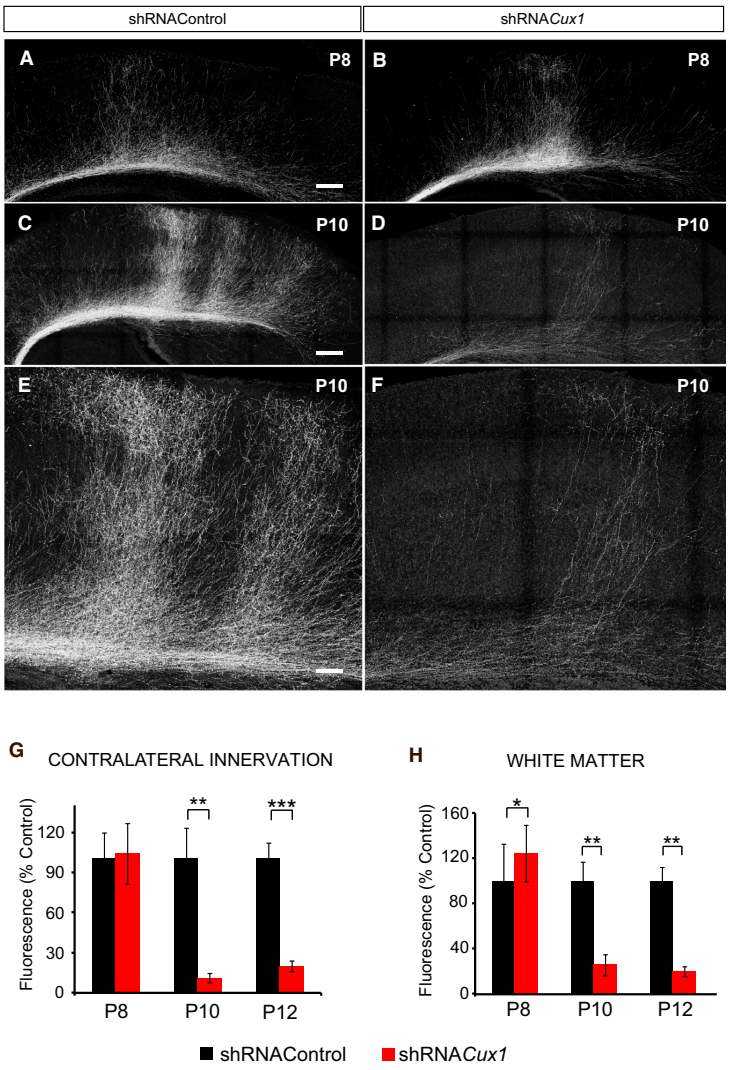

Figure 2. Defects in Contralateral CC Innervation of *Cux1*-Deficient Neurons during Postnatal Development

(A and B) At P8, no major differences were seen between control (A) and shRNA*Cux1* (B) neurons' contralateral axonal invasion of the cortical plate.

(C and D) At P10, control neurons exuberantly innervate the cortical plate (C), while shRNA*Cux1* electroporated neurons poorly innervate the cortical plate (D).

(E and F) Higher magnification of (C) and (D), respectively.

(G and H) Quantification of contralateral GFP signal (G) and axonal tract density (H) normalized to shRNAControl. Mean ± SEM. Student's t test p value * $\leq$ 0.05; ** $\leq$ 0.01. p value *** $\leq$ 0.001. Scale bars, 225 μm (A and C); 75 μm (E).

are eliminated (Wang et al., 2007). However, coelectroporation experiments with a construct encoding fluorescently tagged synaptophysin showed indistinguishable patterns of presynaptic clusters in the axons of control and *Cux1*-deficient neurons at P8 in both ipsilateral and contralateral territories (Figures S3A–S3C), indicating that the loss of shRNA*Cux1* CC axons is not due to a general inability to make synapses.

We next investigated whether a general deficit in branching mechanisms could explain the loss of CC innervation in *Cux1*-deficient neurons. To be able to reconstruct the branches of individual neurons, we activated GFP expression in a sparse population of control or shRNA*Cux1* cells by coelectroporating a GFP-floxed construct (pCALNL-GFP) and very low concentrations of a CRE plasmid (see Experimental Procedures). We then reconstructed individual axons at the contralateral cortical plate and analyzed the number of branches. This analysis showed no differences between P8 shRNA*Cux1* and control branches (Figures S3D and S3E). This indicated that *Cux1*-deficient callosal neurons can branch normally in contralateral territories until at least P8. At P10 there were very few axons in the cortical plate of shRNA*Cux1*-electroporated brains, but these few axons did not show defective branching compared to controls (Figures S3D and S3E). Thus, in *Cux*1-deficient contralateral axons, we did not observe any evidence to suggest a general branching deficit.

We further investigated potential branching deficits by analyzing the ipsilateral axons of *Cux1*-deficient layer II/III neurons projecting callosally. This also assessed whether axonal loss is specific to the contralateral axonal territory. As in P16 (Figure 1E), in IUE experiments targeting the majority of layer II/III neurons, no obvious differences were detected between ipsilateral axons of control and shRNA*Cux1*-targeted neurons at P4 (not shown) or P8 (Figure S2C). To distinguish possible differences with neurons projecting only ipsilaterally, the subpopulation of control and shRNA*Cux1*-targeted neurons with axons crossing to the contralateral hemisphere were retrograde labeled at P5 by fluorescently labeled cholera toxin subunit B (CTB) injections in the CC at the midline. Ipsilateral branches of individual CTB^+ neurons were analyzed at P11, when the major loss of contralateral axons has already occurred in shRNA*Cux1* brains, using the CRE-floxed-GFP dilution strategy. Reconstructions and quantifications of the number of

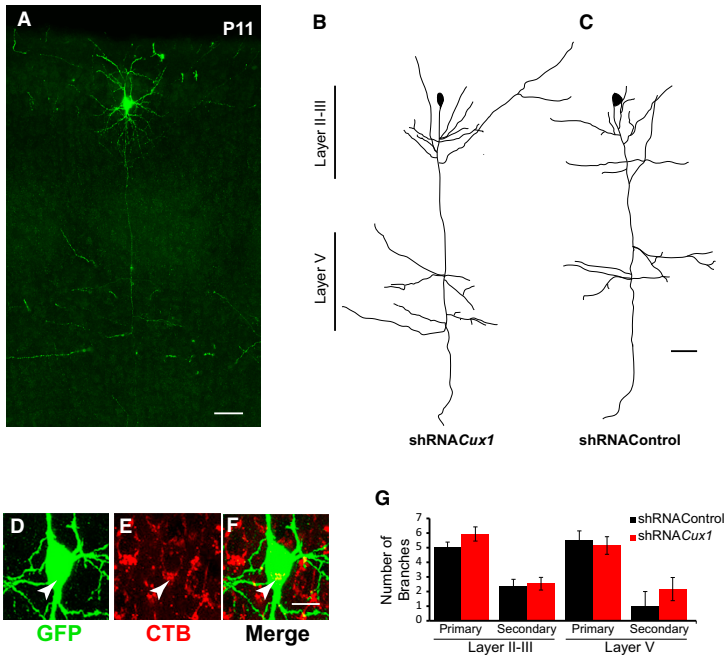

Figure 3. Callosal Cux1-Deficient Neurons Branch Normally in Ipsilateral Territories

(A–G) Callosally projecting neurons were labeled by injection of CTB at the midline at P5. Axonal branches in the ipsilateral hemisphere were reconstructed at P11.

(A) Tile scan image of a CTB$^+$ P11 neuron electroporated at E15.5 with shRNA*Cux1*. Scale bar, 50 μm.

(B) Reconstruction of axonal branches from (A).

(C) Axonal branching morphology of a CTB$^+$ control electroporated neuron.

(D–F) CTB labeling in the soma of the neuron shown in (A). Scale bar, 10 μm.

(G) Quantification of the number of layer II/III or V axonal branches per neuron, divided into primary or secondary branches, obtained after reconstructions of individual CTB$^+$/GFP$^+$ neurons in control and shRNA*Cux1* electroporated brains. No significant differences were found (Student's t test).

branches in layers II/III and V showed that ipsilateral arbors from all *Cux1*-deficient CTB$^+$ callosal neurons were indistinguishable from controls (Figure 3 and Movie S1). Importantly, this demonstrates that *Cux1*-deficient axons branch and develop normally in ipsilateral territories. Altogether, our data demonstrate that loss of *Cux1* does not generally alter the capacity of callosal neurons to establish synapses or axonal branches but specifically disrupts the development of contralateral callosal connectivity.

Cux1 Regulation of Contralateral Callosal Connectivity Is Dependent on Electrical Activity

Activity has a role in regulating CC axonal development (Mizuno et al., 2010; Suárez et al., 2014; Wang et al., 2007). In order to ascertain a possible role for neuronal activity in *Cux1*-mediated CC contralateral patterning, we perturbed electrical activity by utilizing the inwardly rectifying K$^+$ channel Kir2.1. Overexpression of Kir2.1 in WT brains eliminated many of the branches of the primary SS areas (60% innervation compared to controls) and altered the normal CC contralateral layer-specific branching pattern (Figures 4A, 4C, and 4E), coinciding with previously reported data (Mizuno et al., 2010; Suárez et al., 2014; Wang et al., 2007). Strikingly, in contrast to these purely negative effects of Kir2.1 overexpression in WT, coelectroporation of CAG-*Kir2.1* with shRNA*Cux1* partially, but significantly, rescued shRNA*Cux1*-mediated loss of contralateral innervation (Figures 4B, 4D, and 4E). This partial rescue suggests that the loss of contralateral CC axons observed in *Cux1*-deficient neurons depends on electrical activity.

Cux1 Expression Determines the Excitability and Firing Modes of Layer II/III Neurons

Our data pointed to the possibility that *Cux1* deficiency alters certain aspects of the neurons' firing response that in turn affects CC innervation. Differentiation of layer II/III neurons leads to a gradual increase in firing rates and to dynamic changes in intrinsic excitability and firing modes (Maravall et al., 2004). We thus set out to investigate these developmental processes in *Cux1*-deficient neurons. We studied the electrical differentiation of control and shRNA*Cux1*-electroporated neurons by current-clamp recordings on GFP-positive cells in acute slices of IUE brains at various stages of development (P8, P10–P12, and P16).

Recordings were analyzed for passive cell membrane properties (resting membrane potential, input resistance, and capacitance) and parameters to describe the firing mode. As a general descriptor of excitability we calculated firing rates (the average number of APs over time) in response to a given input current. Typically, pyramidal neurons progressively increase the number of APs in response to increasing currents until they reach their maximum firing rates. The fraction of neurons that reach their maximum response for each injected current describes this adapting behavior. We also calculated the spike ratio as a measurement of spike frequency adaptation (inverse ratio of the number of spikes fired during the first 100 ms to the number of spikes fired during the subsequent 100 ms) (Maravall et al., 2004). The spiking ratios reach values close to 1 in mature pyramidal neurons, according to their almost periodic firing (Maravall et al., 2004). As an additional descriptor of the spiking pattern, we measured the first interspike interval (ISI) frequency, as well as the local variation of ISIs (L_V), which measures the degree of intrinsic spiking randomness (Shinomoto et al., 2003).

At P8, shRNA*Cux1* neurons exhibited a slight reduction in AP firing rates (excitability) compared to controls (Figure S4A) and showed similar firing patterns and adaptation to controls

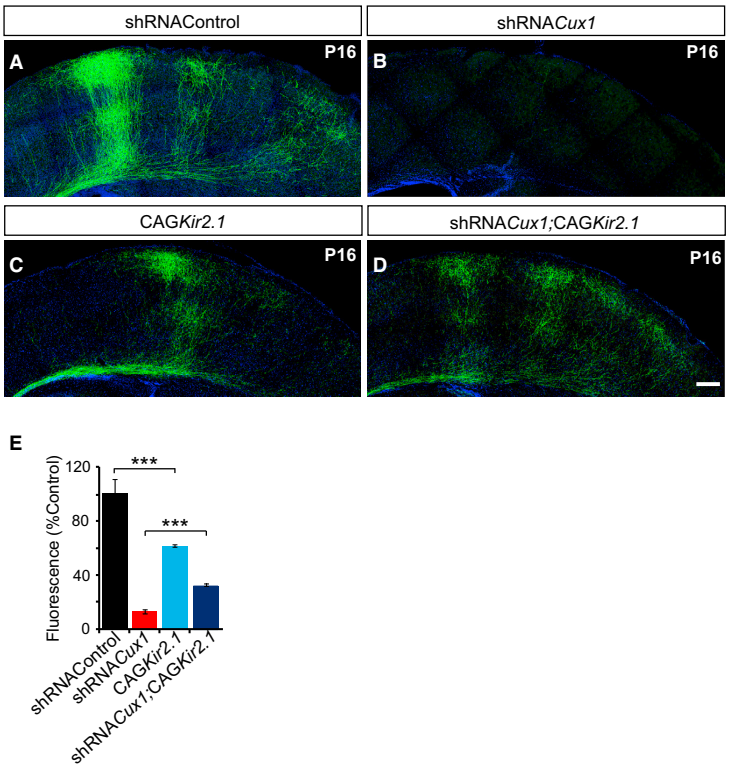

Figure 4. *Cux1* Regulation of Contralateral Callosal Connectivity Is Dependent on Electrical Activity

(A) Contralateral section of a P16 control brain electroporated at E15.5 with CAG-GFP.

(B) Loss of contralateral innervation in brains electroporated with shRNA*Cux1*.

(C) Overexpression of Kir2.1 alters the contralateral pattern of connectivity observed in P16 brains.

(D) *Kir2.1* partially rescues the shRNA*Cux1* phenotype. shRNA*Cux1;CAGKir2.1* neurons were able to develop some projections in the contralateral hemisphere. These axonal projections showed a modified branching pattern.

(E) Quantification of contralateral innervation. Mean ± SEM. Scale bar, 250 μm. Student's t test p value *** ≤ 0.01.

(not shown). However, by P10–P12, layer II/III *Cux1*-deficient neurons exhibited firing responses that were remarkably different from controls: excitability curves showed that their firing rates were higher for most input currents (Figure 5A); the maximum response curve also showed a significant shift toward higher input currents, demonstrative of a weaker adapting response (Figure 5D); and the spike trains exhibited a regular pattern of AP resulting in higher spike-ratio values, also indicative of weak adaptation (Figures 5B and 5C). We also observed slightly decreased resting membrane potential and input resistance (Figure S4B). Thus, P10–P12 *Cux1*-deficient neurons show abnormal firing responses characterized by higher firing rates associated with a weak adapting behavior.

By P16, control neurons increased their firing rates and evolved to weaker-adapting responses compared to P10–P12, as expected (Locke and Nerbonne, 1997; Maravall et al., 2004), while P16 *Cux1*-deficient neurons maintained the weak-adapting phenotypes observed at P10–P12 and experienced a minor increase in firing rates. Overall, P16 shRNA*Cux1* neurons showed moderate decreases in excitability (Figure 5E), resting membrane potential, and input resistance, when compared to control neurons (Figure S4B). They showed no differences in the maximum firing responses, and spiking ratios were also indistinguishable and close to the maximum value of 1 (not shown). These data indicate that shRNA*Cux1* neurons do not eventually acquire the transient strong-adapting phenotype observed during the differentiation of WT layer II/III neurons. Furthermore, we also observed abnormalities in the spiking pattern of P16 shRNA*Cux1*: the first two spikes were abnormally close, resulting in high frequencies of the first ISI (Figures 5F, 5G, and S4C), and subsequent spikes deviated from the predictable pattern of regular spiking, resulting in increased randomness and significantly higher L_V values (Figure 5H). Altogether, our results demonstrate that *Cux1* deficiency alters the normal electrical differentiation of layer II/III neurons during development. Importantly, the time of appearance of acute electrical defects in *Cux1*-deficient neurons (high firing rates and failure to acquire the stronger adapting response at P10–P12) coincides with the observed onset of their axonal loss in the contralateral cortical plate.

Restoring *Kv1* Expression Recues *Cux1*-Associated Defects in Callosal Connectivity, and Knocking Down *Kv1* Mimics the Loss of Callosal Contralateral Axons

Because intrinsic excitability and firing modes depend on the specific ion-channel compositions of neurons, our results indicated that *Cux1* contributes to the dynamic regulation of the expression of one or more ion channels during differentiation. The weak adapting responses observed at P10–P12 in *Cux1*-deficient neurons and the higher frequency of the first ISI at P16 were suggestive of reduced Kv1 currents (Guan et al., 2011; Locke and Nerbonne, 1997; Shu et al., 2007).

To investigate the possible transcriptional regulation of *Kv1* mediated by Cux1, we set out to analyze the expression and function of *Kcna/Kv1* genes in the context of cortical neuronal development. qPCR analysis of P2–P16 total WT cortical cDNA showed a developmental increase in the levels of *Kcna1/Kv1.1* and *Kcna2/Kv1.2* transcripts, with a "switch-on" of *Kv1* total levels after P8. *Kcna3/Kv1.3* transcript levels were similar at all

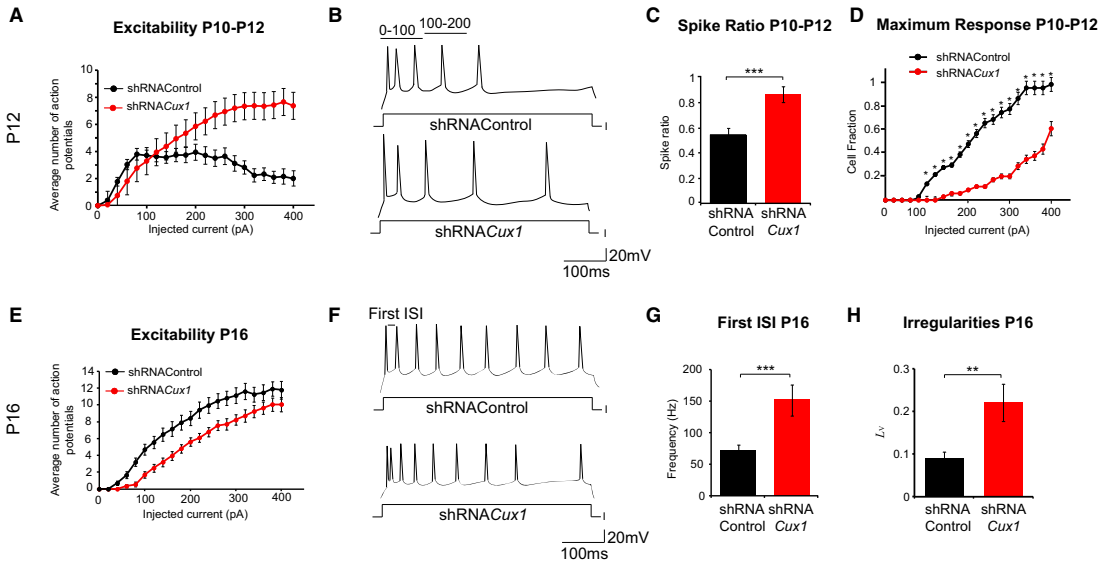

Figure 5. Firing Responses of *Cux1*-Deficient Neurons

(A and E) Firing rates of GFP$^+$ electroporated neurons in acute slices recorded at P10–P12 (A) and P16 (E). Plots show the number of APs elicited by increasing input currents. Mean ± SEM. Results for P10–P12 were as follows: shRNA*Cux1* (n = 31) is significantly different from Control (n = 33); F(1,62) = 23.87; $p \leq 0.0001$. Results for P16 were as follows: shRNA*Cux1* (n = 20) versus Control (n = 20); F(1,753) = 74.03; $p \leq 0.0001$.

(B and F) Representative firing patterns.

(C) Spike ratio calculated using the periods of time indicated in (B). Mean ± SEM. Student's t test p value *** ≤ 0.001.

(D) Fraction of P10–P12 neurons firing at their maximum response. Student's t test p value * ≤ 0.01.

(G) First ISI frequency (Hz) in bursts of nine APs. shRNA*Cux1* neurons generate a higher frequency of the first two APs. Mean ± SEM. Student's t test p value *** ≤ 0.001.

(H) Local variation of ISI (L_V) in bursts of eight APs (shRNA*Cux1* n = 15 versus Control n = 20). Data show mean ± SEM. Welch's two-sample unpaired t test ** ≤ 0.03 compared to control neurons.

of these stages (Figure 6A). Thus, these increases in the total levels of Kv1 expression coincide with the developmental change in firing modes of control layer II/III neurons.

We then analyzed a potential link between *Cux1* and the regulation of *Kv1* transcripts. Due to the low levels of *Kv1* mRNA expression, we were not able to reliably analyze the expression of *Kv1* transcripts in FACS-isolated, GFP-electroporated neurons. We therefore investigated *Kcna*/*Kv1* transcript levels in in vitro-cultured neurons obtained from embryonic *Cux1*$^{-/-}$ and control cortices. Compared to control neurons, *Cux1*$^{-/-}$ neurons showed an increase in AP width and rise and half-decay times (Figures S5A and S5B), indicative of defective Kv1 currents. qPCR showed reduced *Kcna1*/*Kv1.1* and *Kcna3*/*Kv1.3* expression in these *Cux1*$^{-/-}$ cells, whereas there was no change in *Kv.1.2*, *Scn8a*/*Nav1.6*, or *Cacna1c*/*Cav1.2* channels (Figure 6B). We then found evidence to support this possible Cux1 transcriptional regulation of *Kv1*/*KCNA* genes in a study that linked an allelic variant of the human *KCNA3*/*Kv1.3* gene and its Cux1 binding site to diabetes (Tschritter et al., 2006). Our analysis of mouse *Kv1* genes indicated that the mouse *Kv1.3* gene conserves this reported Cux1 binding site and predicted another Cux1 binding site in the same region of the *Kv1.1* gene, suggesting sequence divergence, but functional conservation (Figure 6C). We were not able to identify this conserved sequence in *Kv1.2*, although it contains other unrelated in silico-predicted Cux1 binding sites (not shown). Luciferase reporter assays demonstrated that Cux1 protein activates the promoter fragments containing the Cux1 binding sites of the mouse *Kv1.1* and *Kv1.3* genes (Figure 6D). These data strongly suggest that Cux1 is a direct transcriptional regulator of *Kv1.1* and *Kv1.3* genes and thus contributes to determine the levels of total Kv1 expression in layer II/III neurons.

In order to test whether defective Kv1 expression in *Cux1*-deficient neurons was a contributing cause of axonal loss, we restored Kv1 currents. Overexpression of Kv1 channels in WT layer II/III neurons did not majorly affect CC innervation (Figures S5C and S6E). Overexpression of Kv1 proteins in shRNA*Cux1* neurons recovered the intensity and innervation pattern of contralateral axons in P16 mice (Figures 6F, 6H, and 6I). This rescue could be equally achieved with either Kv1.3 or Kv1.2, suggesting that restoring innervation depends on total Kv1 currents, not on the specific effects of distinct subunits (Figures 6I and S5D).

We next tested whether the function of Kv1 channels is necessary for CC formation. Knocking down *Kv1.3* resulted in a massive loss of contralateral innervation (Figures 6G and 6I),

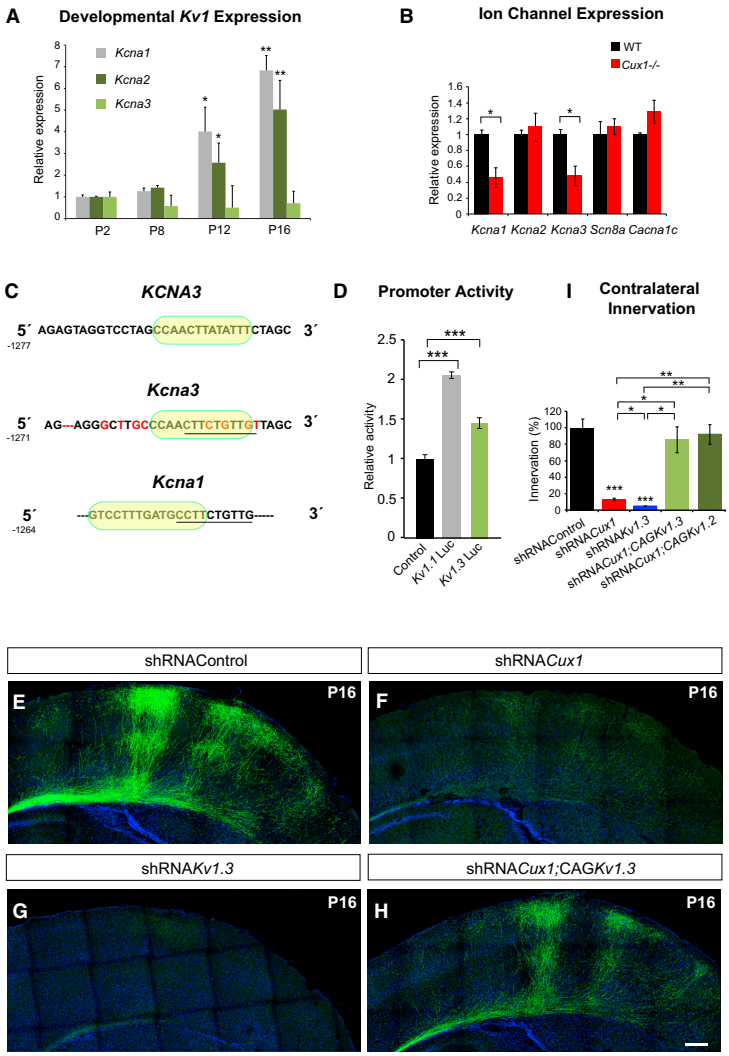

Figure 6. *Cux1* TF Regulates the Transcription of *Kcna1/Kv1.1* and *Kcna3/Kv1.3* Genes, and Overexpression of Kv1 Channels in *Cux1*-Deficient Neurons Rescues Contralateral Connectivity

(A) qPCR analysis of cDNA obtained from total cortices at the indicated postnatal ages. Results are normalized to the expression at P2. Student's t test p value * ≤ 0.05; ** ≤ 0.01.

(B) qPCR analysis of cDNA from ten DIV neurons obtained from WT and *Cux1*$^{-/-}$ animals. Results are normalized to WT. Mean ± SEM. Student's t test p value * ≤ 0.05.

(C) Allelic variant of human *KCNA3* presenting a CCAAC site reported to bind Cux1 protein with high affinity. The mouse *Kcna3/Kv1.3* conserves this genomic sequence and binding site. In the mouse *Kv1.1* gene, which is highly dissimilar to *Kv1.3*, in silico analysis predicted a Cux1 binding site adjacent to the sequence that is conserved with *Kv1.3*, indicating sequence divergence but functional conservation. Underlined sequence denotes sequence conservation between mouse *Kv1.1* and *Kv1.3* genes. Shaded area indicates TRANSFAC-predicted *Cux1* binding sites. Mismatches are shown in red.

(D) Luciferase reporter activity of mouse *Kv1* channel genomic sequences containing *Cux1* binding sites in CAG*Cux1*-transfected neurons. Mean ± SEM. Student's t test p value *** ≤ 0.001.

(E–H) Contralateral innervations of P16 neurons electroporated with Control (E), shRNA*Cux1* (F), shRNA*Kv1.3* (G), and shRNA*Cux1* with CAG*Kv1.3* (H). Scale bar, 250 μm.

(I) Quantification of contralateral innervation normalized to control. Mean ± SEM. Student's t test p value: * ≤ 0.05; ** ≤ 0.03; *** ≤ 0.005 compared to shRNAControl.

while ipsilateral projections were preserved (not shown), as observed in *Cux1* loss of function. This demonstrates the essential and specific role of *Kv1*-dependent functions in CC formation. Together, these data demonstrate that transcriptional regulation of *Kv1* by Cux1 is critical for development of layer II/III callosal projections.

Rescue of the Kv1-Dependent Adapting Response Correlates with Rescue of Callosal Projections

Our results suggest that Kv1-dependent firing critically contributes to activity-dependent CC innervation and demonstrate that axonal loss in *Cux1*-deficient neurons is due to their defective Kv1 expression. We therefore analyzed electrophysiological recordings of shRNA*Cux1*;CAG-*Kv1.3*-targeted neurons in acute slices to determine the aspects of the firing response that underlie rescue of innervation. Overexpression of the Kv1.3 channel had a profound effect on the aberrant firing response observed in P10–P12 shRNA-*Cux1* neurons: it did not normalize excitability curves but changed them by increasing firing rates at low-input currents and decreasing them at high currents (Figure 7A); it rescued spike-frequency adaptation and diminished the high spike-ratio values observed in shRNA*Cux1* neurons at P10–P12 (Figures 7B and 7C); and the maximum firing-response curves shifted closer to control values (Figure 7D), also demonstrating a stronger adapting capacity. At P16, *Kv1.3* overexpression in shRNA*Cux1* neurons fully restored firing-pattern parameters (first ISI and L_V), indicating that rescue of the P10–P12 firing response progresses to normal differentiation (Figure S6A–S6C). CAG-*Kv1.3* overexpression also reversed the minor reductions in resting membrane potential of both P10–P12 and P16 *Cux1*-deficient neurons (Figure S4B). Thus, Kv1-mediated rescue of contralateral innervation in *Cux1*-deficient

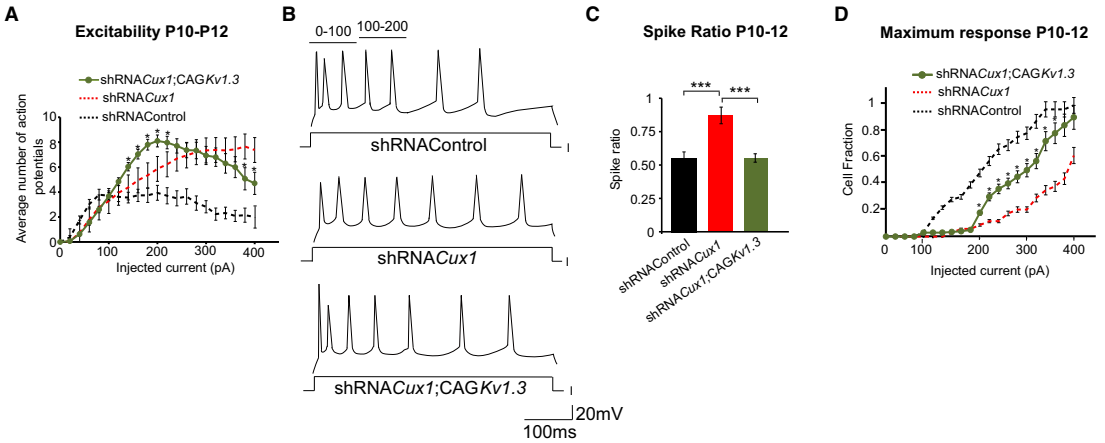

Figure 7. Rescue of Innervation by *Kv1.3* in *Cux1*-Deficient Layer II/III Neurons Correlates with Modification of the Firing Responses and Increasing Adaptation

(A) Firing rates of P10–P12 GFP neurons electroporated as indicated. Curves with dashed lines are taken from Figure 5A for comparison. shRNA*Cux1* (n = 35) is significantly different from Control (n = 33) and shRNA*Cux1*;CAG*Kv1.3* (n = 31), ANOVA $F(2,108) = 10$; $p \leq 0.0001$. Control versus shRNA*Cux1*;CAG*Kv1.3*, $F(1,61) = 26.4$; $p \leq 0.0001$. shRNA*Cux1* versus shRNA*Cux1*;CAG*Kv1.3*, $F(1,61) = 26.4$; $p \leq 0.9$; Student's t test p value for single-input currents * ≤ 0.05 compared to shRNA*Cux1*.

(B) Representative firing patterns.

(C) Spike-ratio values are rescued in shRNA*Cux1* neurons overexpressing *Kv1.3*. Mean ± SEM. Student's t test p value *** ≤ 0.001.

(D) Fraction of neurons firing at their maximum response. Curves with dashed lines are taken from Figure 5D for comparison. Student's t test p value * ≤ 0.01 compared to control or shRNA*Cux1*.

neurons correlates with a shift to a stronger adapting firing response at P10–P12.

Kv1 rescue and loss-of-function experiments demonstrated the necessity of Kv1 currents for CC innervation. Our analysis was not able to parse the individual contributions of each electrical quality modulated by Kv1 channels to axonal loss or rescue but revealed the importance of Kv1-dependent firing as a whole. To further investigate the contribution of firing modes to the development of callosal connectivity, we overexpressed the ankyrinG-binding loop (NavII-III) of the intracellular tail of the Nav channel in layer II/III neurons, a condition that altered firing modes but not firing rates. Expression of the Nav ankyrinG-binding loop caused a significant reduction in contralateral innervation and a change in the columnar patterns (Figures S6D–S6J), supporting an important role of firing modes and the lesser impact of changes in absolute firing rates per se. This supports the conclusion that specific firing modes determine the selection of neuronal connections and the pattern of CC connectivity. Altogether, our data highlight the importance of Kv1 to modulate the firing response required for CC axonal development.

Cux1 Expression after Postnatal Day 8 Mediates the Kv1-Dependent Aspects of Firing Response and CC Contralateral Innervation

Our data demonstrated that regulation of *Kv1* transcripts by Cux1 is a mechanism determining successful callosal innervation and suggested a critical role for the Kv1 modulation switch of the firing response at P10–P12. These predicted that *Cux1*-mediated functions in this developmental process would be essential only past P8. To test this hypothesis, we restored the expression of *Cux1* after P8 in shRNA*Cux1*-electroporated layer II/III neurons using tamoxifen-inducible constructs of the shRNA-resistant form of *Cux1*. Vectors CALNL-*Cux1*, shRNA-*Cux1*, and CAG-GFP were coelectroporated with CAG-ERT2-Cre-ERT2, which drives expression of Cre recombinase upon 4-hydroxytamoxifen (4-OHT) activation (Matsuda and Cepko, 2007). Treatment with 4-OHT rescued Cux1 expression as early as 2 days postinjection (Figures 8F–8K). Postnatal reactivation of *Cux1* expression after 4-OHT injection at P8 was able to restore most CC contralateral innervation (70% compared to controls) (Figures 8A–8C and 8E). Induction at P10 rescued innervation to a lesser degree, but still significantly (Figures 8D and 8E). No significant recovery of innervation was observed when pups were injected with 4-OHT at P12 (not shown), demarcating the limit of *Cux1*-mediated axonal rescue. These experiments indicate that *Cux1*-regulated mechanisms are necessary for proper CC development only after P8, coinciding with the onset of changes in firing modes of the CC-projecting layer II/III neurons.

We next evaluated the firing responses of P11 neurons after induction of *Cux1* re-expression at P8 and compared them to those of neurons at P10–P12 in control, shRNA*Cux1*, and shRNA*Cux1*;CAG*Kv1.3*. Rescue of innervation correlated with rescue of spike ratio and a change in the firing response consistent with a stronger adapting capacity. Strikingly, the firing-rate

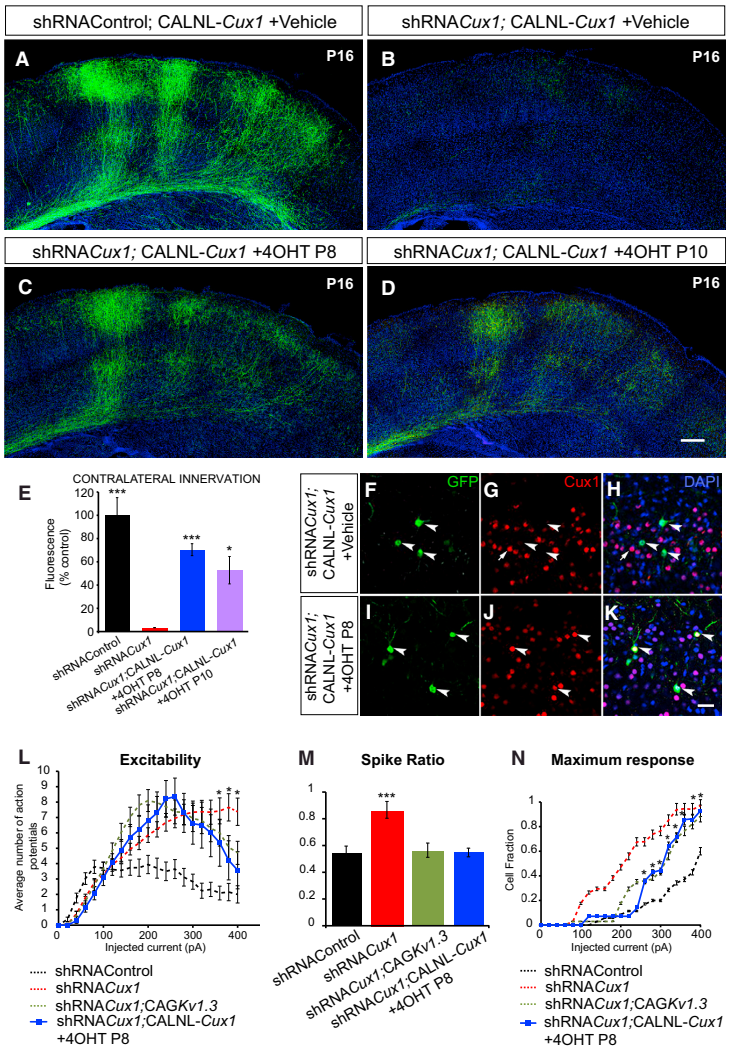

Figure 8. *Cux1* Re-expression in *Cux1*-Deficient Neurons after P8 Is Sufficient for CC Contralateral Innervation and Rescues Kv1-Dependent Firing Properties

(A) Contralateral side of P16 mice electroporated with shRNAControl;CALNL-*Cux1*;ERT2-CRE-ERT2; CAG-GFP and injected with vehicle at P8.

(B–D) Contralateral side of P16 mice electroporated with shRNA*Cux1*;CALNL-Cux1;ERT2-CRE-ERT2;CAG-GFP and injected with vehicle at P8 (B), 4OHT at P8 (C), or 4OHT at P10 (D). Medial is left; scale bar, 250 μm.

(E) Graph shows quantification of contralateral innervation normalized to shRNAControl. Mean ± SEM. Student's t test p value * ≤ 0.05; *** ≤ 0.001 comparing to shRNA*Cux1*.

(F–H) In the absence of 4OHT injection, shRNA-*Cux1*-electroporated GFP-positive neurons do not express Cux1 (arrowheads). Arrows (G and H) point to a nonelectroporated neuron expressing Cux1.

(I–K) After 4OHT injection at P8, P10 GFP-positive neurons show Cux1 expression (arrowheads).

(L) Firing rates calculated from patch-clamp recordings obtained from GFP electroporated neurons. Mean ± SEM. ANOVA comparison of all conditions shRNAControl (n = 33); shRNA*Cux1* (n = 31); shRNA*Cux1*;CAG*Kv1.3* (n = 30); shRNA-*Cux1*;CALNL-*Cux1* + 4OHT (n = 18); F(3,108) = 10; p ≤ 0.0001. shRNA*Cux1*;CALNL-*Cux1* + 4OHT versus shRNAControl F(1,49) = 8.60; p ≤ 0.005; Student's t test p value for single input currents * ≤ 0.05 compared to shRNA*Cux1*. Curves with dashed lines are taken from Figures 5A and 7A for comparison.

(M) Spike-ratio values are rescued in shRNA*Cux1* neurons overexpressing *Cux1* after P8. Student's t test p value *** ≤ 0.001.

(N) Fraction of the neurons firing at their maximum response. Curves with dashed lines are taken from Figures 5D and 7D for comparison. Student's t test p value * ≤ 0.01 comparing shRNACux1;CALNL-Cux1 + 4OHT to control or shRNA*Cux1*. No significance was observed when compared to shRNA*Cux1*;CAG*Kv1.3*.

curves, spike-ratio values, and maximum responses were very similar to those of *Cux1*-deficient neurons overexpressing Kv1 channels (Figures 8L–8N). Of note, firing-rate curves were not normalized to WT values, supporting again that these parameters are not critical for contralateral innervation. This indicates that restoring *Cux1* activity in differentiating neurons after P8 rescues the strong adapting capacity and the Kv1-dependent aspects of the firing response. Taken together, our studies provide strong evidence demonstrating that postnatal *Cux1*-mediated functions that regulate the acquisition of the Kv1-dependent response in callosal layer II/III neurons form part of the developmental mechanisms that determine the formation of the CC.

DISCUSSION

We describe a *Cux1*-dependent developmental mechanism that specifies axon connectivity by modulating the firing response of callosal layer II/III neurons. *Cux1* is essential for the developmental modulation of intrinsic excitability and the switch to a Kv1-dependent firing mode necessary for interhemispheric innervation. In its absence, contralateral axons abrogate their normal development after P9, resulting in virtually complete loss of contralateral innervation at later stages. Ipsilateral axons of *Cux1*-deficient callosal neurons branch normally and are not eliminated, demonstrating the selective dependency of CC axons on Cux1 expression.

Our two major findings are that the switch to a Kv1-dependent firing mode determines successful contralateral innervation and that the regulation of this intrinsic process is a developmental mechanism that couples the callosal neurons' firing responses with their connectivity and subtype molecular identity. Thus, subtype-specific transcriptional programs regulate the acquisition of intrinsic firing responses to define neuronal connectivity. This establishes a mechanistic link between the molecular diversity of neurons, defined by the expression of subtype-specific TFs, and their activity-dependent wiring. Our data add to growing evidence showing the importance of activity-mediated mechanisms in the earliest stages of circuit formation (Ackman and Crair, 2014; Dehorter et al., 2015; Kano and Hashimoto, 2009; Kirkby et al., 2013) and have implications for the understanding of brain mapping and neurological disease.

Two main questions arise from our results. First, how do firing modes encode information? And second, which activity-dependent mechanisms translate this information into patterns of innervation? These two questions are intimately related and can be discussed in the context of this and previous studies.

With regard to the encoding of information, our analysis indicated the importance of the acquisition of a strong-adapting Kv1-dependent firing mode in layer II/III neurons for callosal development. It led us to conclude that, when defining those electrical parameters that correlate with innervation, it is important to analyze the firing responses as a whole, rather than to focus on a single parameter. For example, we found that changes in resting membrane potential do not correlate with the degree of innervation: P10–P12 shRNA*Cux1*-targeted neurons presented minor decreases in resting membrane potential and complete absence of contralateral axons (Figure S4B), whereas Kir2.1 overexpression induces a drastic decrease in resting membrane potential but produces lesser and topologically distinct effects in CC innervation (Figures 4A and 4C; Mizuno et al., 2010; Suárez et al., 2014; Wang et al., 2007). Our data indicated that spike count and resting membrane potential parameters per se are poor predictors of contralateral innervation, in agreement with the conclusions of Suárez et al. (2014). Hence, while our results do not rule out a contribution of firing rates to CC development, they do not support mechanisms solely based on spike count; rather, it appears that information is also encoded in other parameters such as the spike pattern (Doron et al., 2014; Stanley, 2013).

Mechanistically, there are several possibilities to explain how neurons could translate the Kv1-dependent response of P10–P12 layer II/III callosal neurons into patterned innervation. For example, their strong adapting capacity may facilitate spike-dependent plasticity depending on previous activity, or their stronger phasic spiking could more efficiently generate calcium bursts (Kwan and Dan, 2012). Correlated spontaneous patterned activity also mediates axonal refinement (Kirkby et al., 2013; Pietrasanta et al., 2012; Suárez et al., 2014) and should be considered, since *Cux1* regulation of firing modes could influence patterned activity.

Upon *Cux1* knockdown, we observe a normal initial invasion of the cortical plate at P8, followed by a subsequent dramatic decrease in axonal density in the cortical plate and WM. In this context, a possible interpretation of our results is that *Cux1*-deficient phenotypes result from the elimination of axons that, while dynamically emerging from the WM and initiating their invasion of the cortical plate, are only able to sustain further development in the presence of *Cux1*. When evaluating mechanisms of axonal elimination, it is relevant to consider Hebbian or non-Hebbian mechanisms of competition, since in our experiments *Cux1*-deficient neurons elaborate their axons in the presence of normal CC projections. However, there is conflicting evidence regarding mechanisms of axonal refinement, and competition does not necessarily result in the withdrawal of withering axons in all paradigms, making conclusions difficult (Benjumeda et al., 2013; Kerschensteiner et al., 2009; Kirkby et al., 2013; Koch et al., 2011; Morgan et al., 2011; Plazas et al., 2013; Rebsam et al., 2009). Hence, further investigations are required before any stronger conclusions regarding axonal elimination can be made.

Cux1-mediated, *Kv1*-dependent mechanisms regulating axonal innervation are selective to the contralateral territories. We have ruled out general deficits in branching or synapse formation as the cause of axonal loss because Cux1-deficient neurons preserve axonal branches and establish presynaptic structures ipsilaterally, as well as at contralateral territories until P8. Hence, *Cux1*-dependent mechanisms do not appear to control terminal branching intrinsically, as occurs in LKB1 (liver kinase B1)-mediated mechanisms (Courchet et al., 2013). In regard to the formation of layer II/III ipsilateral axons, our results do not rule out the possibility that it depends on the correct firing response, but we do demonstrate its independence from Cux1 and Kv1 expression. We found this to be in agreement with the distinct temporal development of callosal and ipsilateral axons: axons of layer II/III neurons initiate their branching in ipsilateral territories at P4, and they are profusely elaborated by P9 (Srivatsa et al., 2015; Figure S2C), before the onset of the Kv1-mediated switch in the firing response associated with contralateral branching.

Finally, our data also indicate that malfunctions in the mechanisms regulating firing modes are potential causes of the etiology and pathology of mental disorders of developmental origin. Perhaps the most direct ramifications of our findings might be in the context of autism spectrum disorders (ASDs), which are tightly linked to CC dysgenesis and plasticity defects (Ebert and Greenberg, 2013; Pescosolido et al., 2012). Although thus far *CUX1* polymorphisms are only indirectly linked to ASD (Choi et al., 2012), the mechanisms described herein can contribute to our understanding of ASD, other disorders affecting plasticity, and even those involving loss of information transfer in the axon. In addition, modulation of the neurons' excitability could be a therapeutic target for the treatment of developmental diseases showing aberrant connectivity. Our experiments demonstrate that there is a window of postnatal plasticity during which restoring the correct neurons' firing response can rescue innervation. Future investigations are needed to determine whether this plasticity can be boosted and expanded for therapeutic purposes.

EXPERIMENTAL PROCEDURES

Mice

Cux1$^{+/-}$ mice were obtained from A.J. van Wijnen (University of Massachusetts Medical School, Worcester; Luong et al., 2002), and *Cux2*$^{-/-}$ were

previously described (Cubelos et al., 2008). All mice were in a C57BL/6 background. The morning of the day of the appearance of a vaginal plug was defined as embryonic day (E) 0.5. All animal procedures were approved by the Centro Nacional de Biotecnología Animal Care and Use Committee, in compliance with national and European legislation (no. 11001 and PROEX 118-14).

Confocal Imaging and Quantification

Confocal microscopy was performed as described in Supplemental Experimental Procedures. Quantification of innervation was as follows: electroporated, ipsilateral layer V, WM, and contralateral GFP areas were outlined manually (Figure S1A), threshold above noise was set, and quantification was performed essentially as described (Plas et al., 2004) using Fiji. The signal of the innervated area was calculated relative to the value of the ipsilateral electroporated area in layers II/III. Results (mean ± SEM) were normalized to shRNAControl. Axonal reconstruction of ipsilateral branches of CTB^+ neurons and of individual contralateral axons was performed in tile scan images of z sections using Fiji (see Movie S1).

In Utero Electroporation, Plasmids, shRNA-Specific Control, and Immunohistochemistry

These are described in Supplemental Experimental Procedures.

Electrophysiology

Whole cell current-clamp recordings were obtained from layer II/III pyramidal cell neurons identified visually by GFP expression and from in vitro-cultured cells. Acute slices were prepared from GFP-electroporated mouse brains. For intracellular patch pipette solution and artificial cerebrospinal fluid (ACSF), see Supplemental Experimental Procedures. Current-clamp whole cell recordings were obtained with a Multiclamp 700A amplifier (Axon Instruments). All properties were analyzed using pCLAMP Clampfit10.3 (Molecular Devices). Excitability was quantified as the number of APs evoked by a series of depolarizing current steps (0–400 pA, 500 ms). Spike ratio was calculated as described (Maravall et al., 2004). Local variation of interspike intervals was calculated as described (Supplemental Experimental Procedures).

qPCR Analysis

cDNA was obtained from total RNA (1 μg) extracted from cortex, and PCR reactions using SYBR Green (Applied Biosystems) were performed as described (Rodríguez-Tornos et al., 2013). Primers and Taqman probes are described in Supplemental Experimental Procedures. Results were normalized to β-actin.

Primary Neuron Culture and Luciferase Reporter Assays

Neurons from embryonic cortex were cultured on poly-D-Lys-coated coverslips in 24-well plates as described (Rodríguez-Tornos et al., 2013). Cux1 binding sites were identified using TRANSFAC (BIOBASE Corporation). Mouse genomic sequences containing Cux1 binding sites for the *Kcna1* and *Kcna3* genes were cloned into the pGL4.23 luciferase vector (Promega; Supplemental Experimental Procedures). Eight DIV cells from E14 animals were co-transfected with CAG*Cux1*, firefly luciferase, and Renilla luciferase plasmids (1:5:1) using Lipofectamine 2000 (Invitrogen). Luciferase and Renilla activity were measured using the Dual-Luciferase Reporter Assay System (Promega), and promoter activity was normalized to control.

Statistical Analysis

Results are expressed as the mean ± SEM. qPCR results, spike ratio, maximal response, first ISI frequency, and active and passive membrane properties were analyzed by the Student's two-sample unpaired t test; p values are indicated in tables or figure legends. Input-output curve of excitability of different datasets was fit with regression and compared by an F test. For L_V, different conditions were compared using Welch's two-sample unpaired t test applied to L_V calculated using equal number of spikes. Statistical tests were performed using Prism 5 software (GraphPad software) and R (http://www.R-project.org/). An α level of 0.05 was considered significant. Before parametric comparisons were performed, data were tested for normality of distribution (D'Agostino-Pearson test).

SUPPLEMENTAL INFORMATION

Supplemental Information includes Supplemental Experimental Procedures, six figures, and one movie and can be found with this article online at http://dx.doi.org/10.1016/j.neuron.2015.12.020.

AUTHOR CONTRIBUTIONS

Conceptualization, F.M.R.-T., C.G.B., L.A.W., A.S.-S., and M. Nieto; Methodology, F.M.R.-T., C.G.B., L.A.W., M.G., M. Nieto, and J.A.E.; Formal Analysis, F.M.R.-T., C.G.B., L.A.W., A.S.-S., S.A., J.A.E., and M. Nieto; Investigation, F.M.R.-T., C.G.B., A.S.-S., L.A.W., M.G., L.F., and M. Navarrete; Writing – Original Draft, F.M.R.-T., C.G.B., L.A.W., and M. Nieto; Writing – Review & Editing, F.M.R.-T., C.G.B., L.A.W., J.A.E., D.J., and M. Nieto; Visualization, F.M.R.-T., C.G.B., L.A.W., and M. Nieto; Funding Acquisition, J.A.E. and M. Nieto; Supervision, M. Nieto.

ACKNOWLEDGMENTS

We are grateful to A. Fernández, R. Gutiérrez, A. Morales, and members of J.A.E. lab for excellent technical assistance; J.D. Macklis for invaluable technical help and discussion; C.O. Sorzano for statistical advice; C. Mark for editorial assistance; and G. Perea and P. Bovolenta for critical reading. F.M.R.-T. was supported by a fellowship from La Caixa Foundation. C.G.B. and L.A.W. are funded by the Spanish Ministerio de Ciencia e Innovación (MICINN), FPI-BES-2012-056011 to C.G.B. and JCI-2012-14147 to L.A.W.; S.A. holds a J.A.E.-Doc contract (JAEDOC014, 2010 call) from the CSIC program "Junta para la Ampliación de Estudios" cofunded by the European Social Fund. This work was funded by grant PHYSDEV (FIS2012-32349) to S.A., a grant from BBVA Foundation to M. Navarrete, grants CSD2010-00045 and SAF2011-24730 (from MICINN) to J.A.E., and a grant from Ramón Areces Foundation and grants SAF2011-23735 and BFU2014-55738-REDT (from MICINN) to M.Nieto.

Received: February 14, 2015
Revised: April 23, 2015
Accepted: December 1, 2015
Published: January 21, 2016

REFERENCES

Ackman, J.B., and Crair, M.C. (2014). Role of emergent neural activity in visual map development. Curr. Opin. Neurobiol. *24*, 166–175.

Benjumeda, I., Escalante, A., Law, C., Morales, D., Chauvin, G., Muça, G., Coca, Y., Márquez, J., López-Bendito, G., Kania, A., et al. (2013). Uncoupling of EphA/ephrinA signaling and spontaneous activity in neural circuit wiring. J. Neurosci. *33*, 18208–18218.

Britanova, O., de Juan Romero, C., Cheung, A., Kwan, K.Y., Schwark, M., Gyorgy, A., Vogel, T., Akopov, S., Mitkovski, M., Agoston, D., et al. (2008). Satb2 is a postmitotic determinant for upper-layer neuron specification in the neocortex. Neuron *57*, 378–392.

Choi, J., Ababon, M.R., Matteson, P.G., and Millonig, J.H. (2012). Cut-like homeobox 1 and nuclear factor I/B mediate ENGRAILED2 autism spectrum disorder-associated haplotype function. Hum. Mol. Genet. *21*, 1566–1580.

Courchet, J., Lewis, T.L., Jr., Lee, S., Courchet, V., Liou, D.Y., Aizawa, S., and Polleux, F. (2013). Terminal axon branching is regulated by the LKB1-NUAK1 kinase pathway via presynaptic mitochondrial capture. Cell *153*, 1510–1525.

Cubelos, B., Sebastián-Serrano, A., Kim, S., Moreno-Ortiz, C., Redondo, J.M., Walsh, C.A., and Nieto, M. (2008). Cux-2 controls the proliferation of neuronal intermediate precursors of the cortical subventricular zone. Cereb. Cortex *18*, 1758–1770.

Cubelos, B., Sebastián-Serrano, A., Beccari, L., Calcagnotto, M.E., Cisneros, E., Kim, S., Dopazo, A., Alvarez-Dolado, M., Redondo, J.M., Bovolenta, P., et al. (2010). Cux1 and Cux2 regulate dendritic branching, spine morphology, and synapses of the upper layer neurons of the cortex. Neuron *66*, 523–535.

De la Rossa, A., Bellone, C., Golding, B., Vitali, I., Moss, J., Toni, N., Lüscher, C., and Jabaudon, D. (2013). In vivo reprogramming of circuit connectivity in postmitotic neocortical neurons. Nat. Neurosci. *16*, 193–200.

Dehorter, N., Ciceri, G., Bartolini, G., Lim, L., del Pino, I., and Marín, O. (2015). Tuning of fast-spiking interneuron properties by an activity-dependent transcriptional switch. Science *349*, 1216–1220.

Doron, G., von Heimendahl, M., Schlattmann, P., Houweling, A.R., and Brecht, M. (2014). Spiking irregularity and frequency modulate the behavioral report of single-neuron stimulation. Neuron *81*, 653–663.

Ebert, D.H., and Greenberg, M.E. (2013). Activity-dependent neuronal signalling and autism spectrum disorder. Nature *493*, 327–337.

Fame, R.M., MacDonald, J.L., and Macklis, J.D. (2011). Development, specification, and diversity of callosal projection neurons. Trends Neurosci. *34*, 41–50.

García-Frigola, C., and Herrera, E. (2010). Zic2 regulates the expression of Sert to modulate eye-specific refinement at the visual targets. EMBO J. *29*, 3170–3183.

Goldberg, E.M., Clark, B.D., Zagha, E., Nahmani, M., Erisir, A., and Rudy, B. (2008). K+ channels at the axon initial segment dampen near-threshold excitability of neocortical fast-spiking GABAergic interneurons. Neuron *58*, 387–400.

Guan, D., Horton, L.R., Armstrong, W.E., and Foehring, R.C. (2011). Postnatal development of A-type and Kv1- and Kv2-mediated potassium channel currents in neocortical pyramidal neurons. J. Neurophysiol. *105*, 2976–2988.

Kano, M., and Hashimoto, K. (2009). Synapse elimination in the central nervous system. Curr. Opin. Neurobiol. *19*, 154–161.

Kerschensteiner, D., Morgan, J.L., Parker, E.D., Lewis, R.M., and Wong, R.O. (2009). Neurotransmission selectively regulates synapse formation in parallel circuits in vivo. Nature *460*, 1016–1020.

Kirkby, L.A., Sack, G.S., Firl, A., and Feller, M.B. (2013). A role for correlated spontaneous activity in the assembly of neural circuits. Neuron *80*, 1129–1144.

Koch, S.M., Dela Cruz, C.G., Hnasko, T.S., Edwards, R.H., Huberman, A.D., and Ullian, E.M. (2011). Pathway-specific genetic attenuation of glutamate release alters select features of competition-based visual circuit refinement. Neuron *71*, 235–242.

Kole, M.H., and Stuart, G.J. (2012). Signal processing in the axon initial segment. Neuron *73*, 235–247.

Kwan, A.C., and Dan, Y. (2012). Dissection of cortical microcircuits by single-neuron stimulation in vivo. Curr. Biol. *22*, 1459–1467.

Lefort, S., Tomm, C., Floyd Sarria, J.C., and Petersen, C.C. (2009). The excitatory neuronal network of the C2 barrel column in mouse primary somatosensory cortex. Neuron *61*, 301–316.

Locke, R.E., and Nerbonne, J.M. (1997). Role of voltage-gated K+ currents in mediating the regular-spiking phenotype of callosal-projecting rat visual cortical neurons. J. Neurophysiol. *78*, 2321–2335.

Lodato, S., Shetty, A.S., and Arlotta, P. (2015). Cerebral cortex assembly: generating and reprogramming projection neuron diversity. Trends Neurosci. *38*, 117–125.

Luong, M.X., van der Meijden, C.M., Xing, D., Hesselton, R., Monuki, E.S., Jones, S.N., Lian, J.B., Stein, J.L., Stein, G.S., Neufeld, E.J., and van Wijnen, A.J. (2002). Genetic ablation of the CDP/Cux protein C terminus results in hair cycle defects and reduced male fertility. Mol. Cell. Biol. *22*, 1424–1437.

Maravall, M., Stern, E.A., and Svoboda, K. (2004). Development of intrinsic properties and excitability of layer 2/3 pyramidal neurons during a critical period for sensory maps in rat barrel cortex. J. Neurophysiol. *92*, 144–156.

Matsuda, T., and Cepko, C.L. (2007). Controlled expression of transgenes introduced by in vivo electroporation. Proc. Natl. Acad. Sci. USA *104*, 1027–1032.

Mitchell, B.D., and Macklis, J.D. (2005). Large-scale maintenance of dual projections by callosal and frontal cortical projection neurons in adult mice. J. Comp. Neurol. *482*, 17–32.

Mizuno, H., Hirano, T., and Tagawa, Y. (2010). Pre-synaptic and post-synaptic neuronal activity supports the axon development of callosal projection neurons during different post-natal periods in the mouse cerebral cortex. Eur. J. Neurosci. *31*, 410–424.

Morgan, J.L., Soto, F., Wong, R.O., and Kerschensteiner, D. (2011). Development of cell type-specific connectivity patterns of converging excitatory axons in the retina. Neuron *71*, 1014–1021.

Nieto, M., Monuki, E.S., Tang, H., Imitola, J., Haubst, N., Khoury, S.J., Cunningham, J., Gotz, M., and Walsh, C.A. (2004). Expression of Cux-1 and Cux-2 in the subventricular zone and upper layers II-IV of the cerebral cortex. J. Comp. Neurol. *479*, 168–180.

Otsuka, T., and Kawaguchi, Y. (2011). Cell diversity and connection specificity between callosal projection neurons in the frontal cortex. J. Neurosci. *31*, 3862–3870.

Pescosolido, M.F., Yang, U., Sabbagh, M., and Morrow, E.M. (2012). Lighting a path: genetic studies pinpoint neurodevelopmental mechanisms in autism and related disorders. Dialogues Clin. Neurosci. *14*, 239–252.

Petreanu, L., Huber, D., Sobczyk, A., and Svoboda, K. (2007). Channelrhodopsin-2-assisted circuit mapping of long-range callosal projections. Nat. Neurosci. *10*, 663–668.

Pietrasanta, M., Restani, L., and Caleo, M. (2012). The corpus callosum and the visual cortex: plasticity is a game for two. Neural Plast. *2012*, 838672.

Plas, D.T., Visel, A., Gonzalez, E., She, W.C., and Crair, M.C. (2004). Adenylate Cyclase 1 dependent refinement of retinotopic maps in the mouse. Vision Res. *44*, 3357–3364.

Plazas, P.V., Nicol, X., and Spitzer, N.C. (2013). Activity-dependent competition regulates motor neuron axon pathfinding via PlexinA3. Proc. Natl. Acad. Sci. USA *110*, 1524–1529.

Rebsam, A., Petros, T.J., and Mason, C.A. (2009). Switching retinogeniculate axon laterality leads to normal targeting but abnormal eye-specific segregation that is activity dependent. J. Neurosci. *29*, 14855–14863.

Rodríguez-Tornos, F.M., San Aniceto, I., Cubelos, B., and Nieto, M. (2013). Enrichment of conserved synaptic activity-responsive element in neuronal genes predicts a coordinated response of MEF2, CREB and SRF. PLoS ONE *8*, e53848.

Shinomoto, S., Shima, K., and Tanji, J. (2003). Differences in spiking patterns among cortical neurons. Neural Comput. *15*, 2823–2842.

Shu, Y., Yu, Y., Yang, J., and McCormick, D.A. (2007). Selective control of cortical axonal spikes by a slowly inactivating K+ current. Proc. Natl. Acad. Sci. USA *104*, 11453–11458.

Srivatsa, S., Parthasarathy, S., Molnár, Z., and Tarabykin, V. (2015). Sip1 downstream Effector ninein controls neocortical axonal growth, ipsilateral branching, and microtubule growth and stability. Neuron *85*, 998–1012.

Stanley, G.B. (2013). Reading and writing the neural code. Nat. Neurosci. *16*, 259–263.

Suárez, R., Fenlon, L.R., Marek, R., Avitan, L., Sah, P., Goodhill, G.J., and Richards, L.J. (2014). Balanced interhemispheric cortical activity is required for correct targeting of the corpus callosum. Neuron *82*, 1289–1298.

Tschritter, O., Machicao, F., Stefan, N., Schäfer, S., Weigert, C., Staiger, H., Spieth, C., Häring, H.U., and Fritsche, A. (2006). A new variant in the human Kv1.3 gene is associated with low insulin sensitivity and impaired glucose tolerance. J. Clin. Endocrinol. Metab. *91*, 654–658.

Wang, C.L., Zhang, L., Zhou, Y., Zhou, J., Yang, X.J., Duan, S.M., Xiong, Z.Q., and Ding, Y.Q. (2007). Activity-dependent development of callosal projections in the somatosensory cortex. J. Neurosci. *27*, 11334–11342.

Neuron

Supplemental Information

Cux1 Enables Interhemispheric Connections of Layer II/III Neurons by Regulating Kv1-Dependent Firing

Fernanda M. Rodríguez-Tornos, Carlos G. Briz, Linnea A. Weiss, Alvaro Sebastián-Serrano, Saúl Ares, Marta Navarrete, Laura Frangeul, Maria Galazo, Denis Jabaudon, José A. Esteban, and Marta Nieto

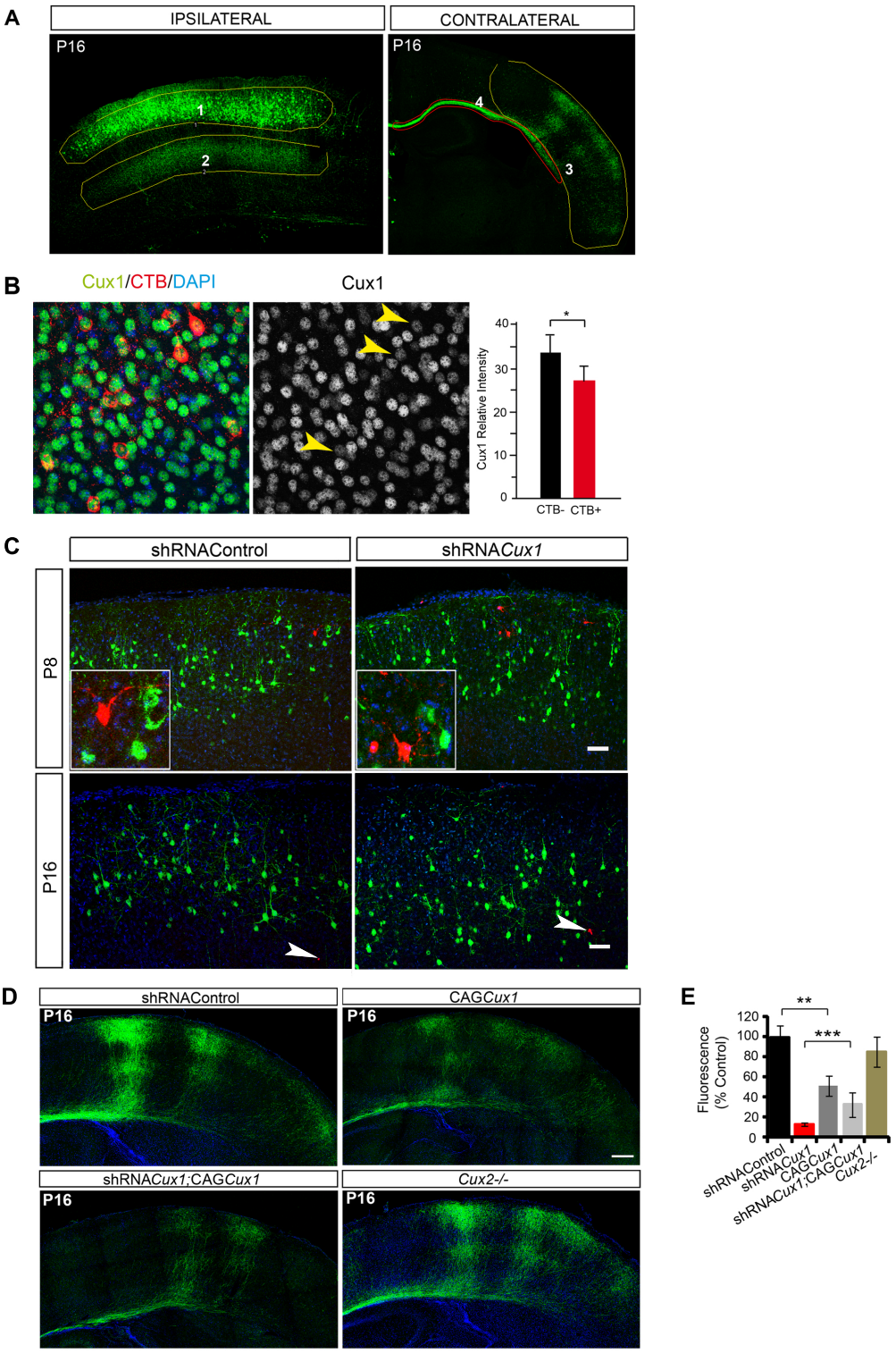
A
IPSILATERAL
CONTRALATERAL
P16
P16
1
2
4
3
B
Cux1/CTB/DAPI
Cux1
Cux1 Relative Intensity
40
30
20
10
0
*
CTB-
CTB+
C
shRNAControl
shRNACux1
P8
P16
D
shRNAControl
CAGCux1
shRNACux1;CAGCux1
Cux2-/-
P16
P16
P16
P16
E
Fluorescence (% Control)
120
100
80
60
40
20
0
**
***
shRNAControl
shRNACux1
CAGCux1
shRNACux1;CAGCux1
Cux2-/-

Figure S1

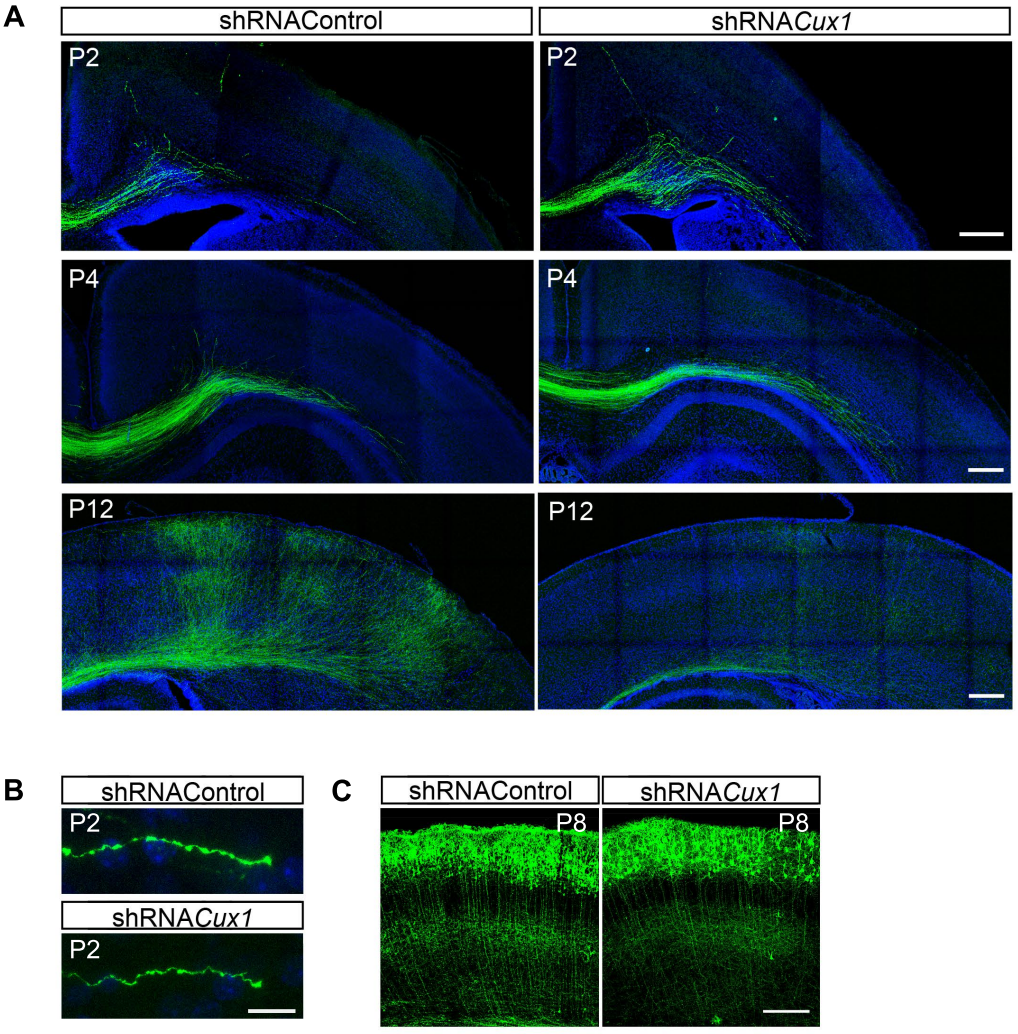
A
shRNAControl
shRNACux1
P2
P2
P4
P4
P12
P12
B
shRNAControl
P2
shRNACux1
P2
C
shRNAControl
shRNACux1
P8
P8

Figure S2

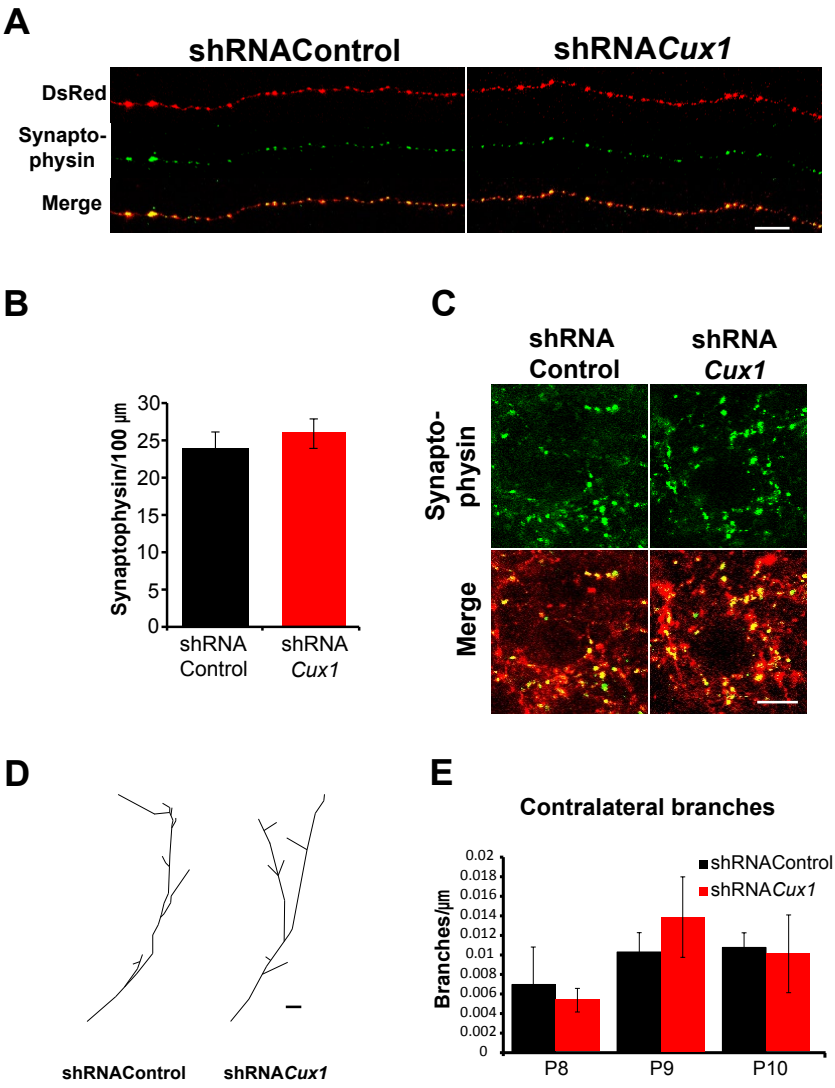
A
shRNAControl
shRNACux1
DsRed
Synapto-physin
Merge
B
Synaptophysin/100 µm
30
25
20
15
10
5
0
shRNA Control
shRNA Cux1
C
shRNA Control
shRNA Cux1
Synapto-physin
Merge
D
shRNAControl
shRNACux1
E
Contralateral branches
Branches/µm
0.02
0.018
0.016
0.014
0.012
0.01
0.008
0.006
0.004
0.002
0
shRNAControl
shRNACux1
P8
P9
P10

Figure S3

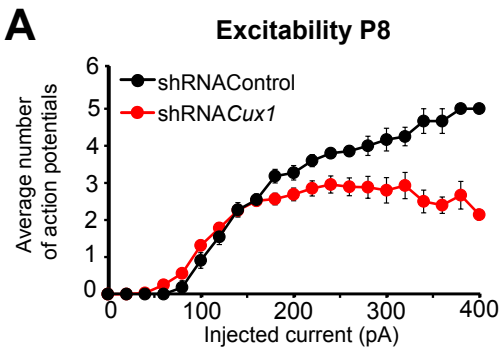

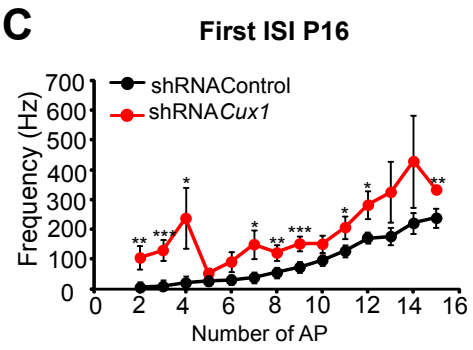

B

P12	shRNAControl	shRNA*Cux 1*	shRNA*Cux1*-CAG*Kv1.3*	shRNA*Cux1*-CAG*Kir2.1*	CAG*Kir2.1*	SynNavII-III	p-value
Resting membrane potential (mV)	-68 ± 1	-71 ± 1	-66 ± 0	-68 ± 1	-85 ± 5	-57 ± 1	0.04
Input resistance (MΩ)	669 ± 34	563 ± 28	422 ± 31	470 ± 30	490 ± 17	330 ± 30	0.02
Capacitance (pF)	88 ± 5	107 ± 5	95 ± 5	90 ± 9	87 ± 8	117 ± 5	0.01
P16	shRNAControl	shRNA*Cux 1*	shRNACux1-CAG*Kv1.3*	shRNA*Cux1*-CAG*Kir2.1*	CAG*Kir2.1*	SynNavII-III	p-value
Resting membrane potential (mV)	-70 ± 1	-78 ± 1	-74 ± 1	-68 ± 1	-90 ± 2	-68 ± 2	0.0013
Input resistance (MΩ)	521 ± 36	298 ± 16	227 ± 28	205 ± 20	209 ± 19	320 ± 19	$5.61*10^{-6}$
Capacitance (pF)	100 ± 6	87 ± 5	84 ± 6	92 ± 10	90 ± 9	78 ± 9	0.0998

Figure S4

A

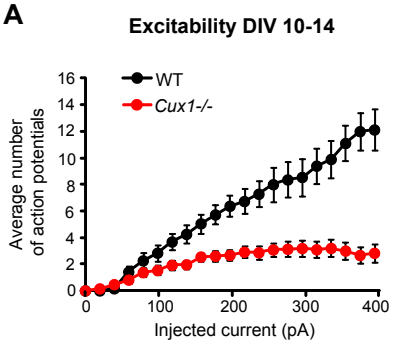

B

DIV10-14	*Cux 1 -/-*	WT	p-value
Rise time (ms)	1.8 ± 0.1	1.4 ± 0.1	0.0288
Half decay time (ms)	2.1 ± 0.1	1.6 ± 0.1	0.0361
Action potential width (ms)	3.1 ± 0.2	2.5 ± 0.2	0.0419

C

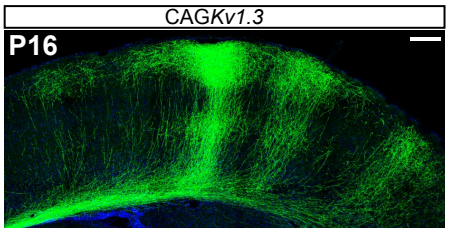

D

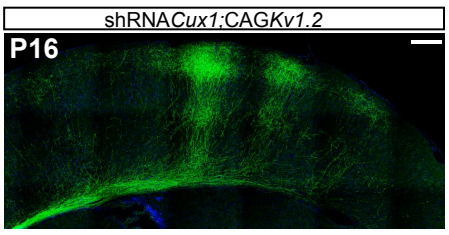

Figure S5

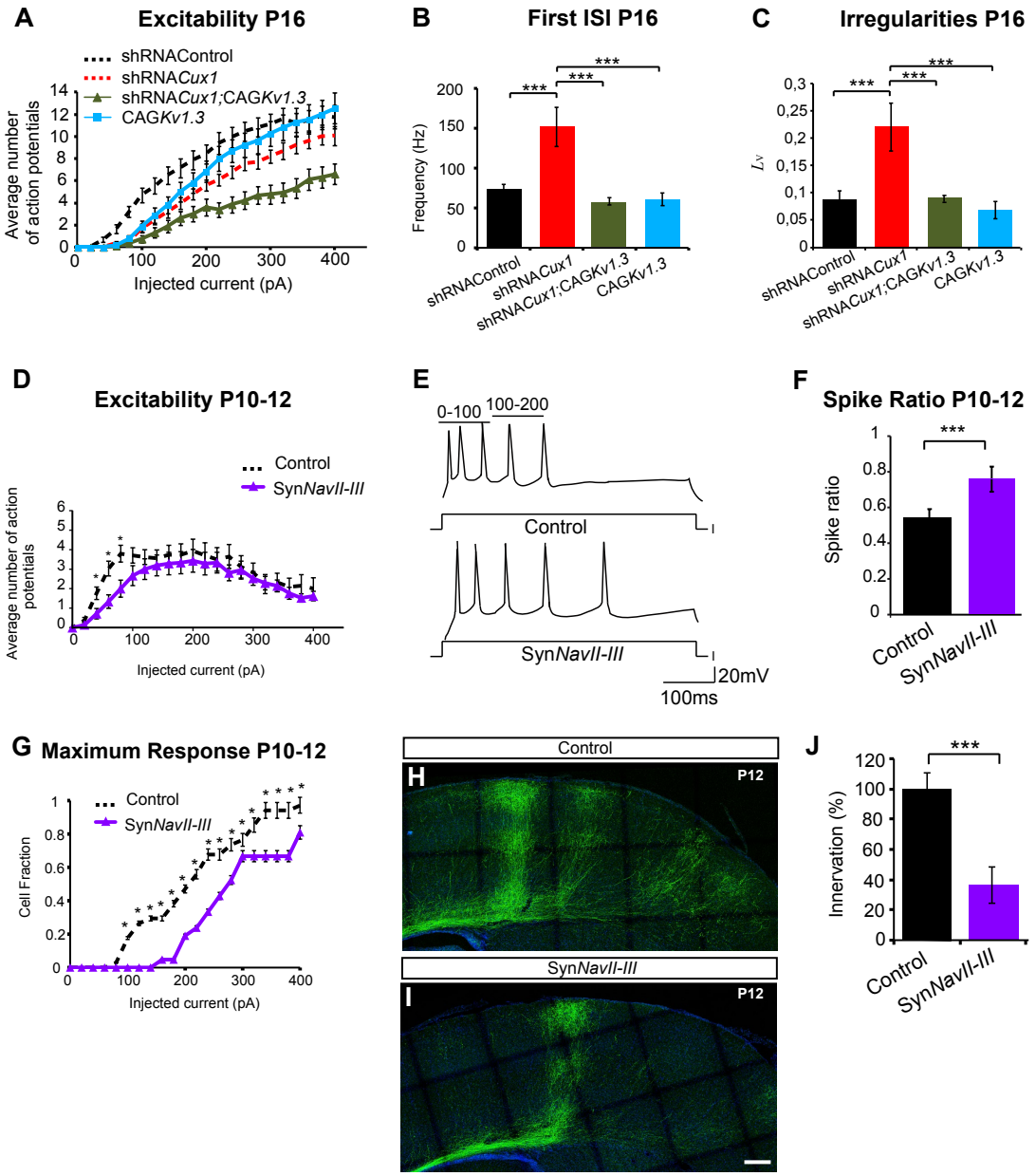
A
Excitability P16
shRNAControl
shRNACux1
shRNACux1;CAGKv1.3
CAGKv1.3
Average number of action potentials
Injected current (pA)
B
First ISI P16
Frequency (Hz)
***
shRNAControl
shRNACux1
shRNACux1;CAGKv1.3
CAGKv1.3
C
Irregularities P16
Lv
D
Excitability P10-12
Control
SynNavII-III
Average number of action potentials
Injected current (pA)
E
0-100
100-200
Control
SynNavII-III
20mV
100ms
F
Spike Ratio P10-12
Spike ratio
G
Maximum Response P10-12
Cell Fraction
H
Control
P12
I
SynNavII-III
J
Innervation (%)

Figure S6

Supplemental Figure Legends

Figure S1 related to Figure 1. Distinct effects of *Cux1* and *Cux2* TF on CC contralateral connectivity. A) Tile scan assembly showing the method used for quantification of tract density, contralateral and ipsilateral innervations. Each of the areas of interest (electroporated neurons, 1; ipsilateral layer V innervations, 2; contralateral layers II/III and V innervations, 3; and tract, 4) was outlined manually and GFP signal above threshold was measured. Each of the areas analyzed was normalized to the GFP signal from ipsilateral electroporated neurons. **B)** Axonal retro-tracing labeling of contralateral projections with CTB followed by immunohistochemistry with *Cux1* antibody determined that callosal layer II/III neurons express intermediate levels of *Cux1*. Arrowheads indicate neurons that are positive for CTB (CTB^{+}). Student's t test p-value * ≤ 0.05 **C)** *Cux1* down-modulation by *in utero* electroporation does not induce pyramidal layer II/III neuronal death. Images show cleaved caspase-3 (CC3) staining of electroporated neurons at P8 and P16. Bar = 75 μm. No CC3 and GFP double-positive neurons were found. Insets and arrowheads show CC3 positive neurons that are not GFP positive. GFP staining, green; nucleus, blue; CC3 staining, red. **D)** Tile scan assembly showing the contralateral innervations in layers II/III and V of P16 neurons electroporated with the indicated plasmids or $Cux2^{-/-}$ mice electroporated with shRNAControl. GFP staining, green; nucleus, blue. Medial, left; lateral, right. The shRNA*Cux1* phenotype was rescued (lower-left panel) by co-electroporation with a mutant form of *Cux1* resistant to shRNA (shRNA*Cux1;*CAG*Cux1*). *Cux1* over-expression reduces axon number, but does not eliminate them, and alters the normal innervation pattern (upper-right panel). Lack of *Cux2* TF does not impede contralateral innervations (lower-right panel). Bar = 250 μm. **E)** Graph

shows quantification of contralateral layer II/III and V innervation normalized to shRNAControl. Student's t test p-value ** ≤0.03; *** ≤0.01.

Figure S2 related to Figure 2. *Cux1* down-modulation eliminates contralateral innervations but not midline crossing or CC axonal pathfinding. A) Tile scan assembly showing the development of the axonal tract at the contralateral hemisphere of P2 and P4 mice, and the contralateral innervations in layers II/III and V of P12 mice electroporated with the indicated plasmids. GFP staining, green; nucleus, blue. Medial, left; lateral, right. Bar= 250 μm. *Cux1* down-modulation does not affect midline crossing or CC axonal pathfinding, but it impedes axonal development at the contralateral cortical plate during the exuberant innervation and refinement period. **B)** Axonal growth cones of control and shRNA*Cux1* targeted P2 neurons. Bar = 10 μm. **C)** Ipsilateral branches in layer V are already observed at P8 in control and shRNA*Cux1* targeted brains. Bar= 250 μm.

Figure S3 related to Figure 3. Synaptophysin clusters in control and Cux1-deficient axons and analysis of contralateral branches. A) No difference in the number of presynaptic synaptophysin puncta was observed in those axons found in the contralateral hemisphere of P8 brains electroporated with shRNA*Cux1* or shRNAcontrol. Brains were co-electroporated with CAG-DsRed-Express, a synaptophysin-turquoise fusion construct, and shRNAs. Sections were stained with anti-GFP to visualize synaptophysin. Bar = 10 μm. **B)** Quantification of the number of synaptophysin puncta per axonal length. **C)** Synaptophysin staining and DsRed signal in the ipsilateral layer V of P8 brains. Bar = 10 μm. **D)** Reconstruction of individual contralateral axons in control shRNA and shRNA*Cux1* P10 brains (see Methods). Bar = 50 μm. **E)** Quantification of the number of

branches per length of the main axonal projection in control and shRNA*Cux1* conditions. No significant differences were found (Student's t test).

Figure S4 related to Figure 5. Electrophysiological properties of *Cux1*$^{-/-}$ neurons in P8, P10-12 and P16 acute slices. A) Plot of the number of AP elicited by increasing input currents in P8 neurons of control or shRNA*Cux1* electroporated mice. Data obtained from patch clamp recordings in P8 acute slices. shRNA*Cux1*-targeted neurons show slightly decreased excitability compared to controls at higher currents. shRNA*Cux1*, n= 32; Control, n= 11; $F(2,691) = 27.8;\ p \leq 0.0001$. **B)** Passive membrane properties of P10-P12 and P16 neurons electroporated as indicated. Control and shRNA*Cux1* neurons were compared using a two-tailed unpaired Student's *t*-test. There is no correlation between active or passive membrane properties and the degree of altered contralateral innervation. **C)** First ISI frequency (Hz) related to the number of AP in a 500 ms train. Down-modulation of *Cux1* generates higher frequency of the first two AP. Student's t test p-value * ≤0.05; ** ≤0.03; *** ≤0.01 compared to control neurons.

Figure S5 related to Figure 6. Electrophysiological properties of *Cux1*$^{-/-}$ neurons *in vitro* and effects of Kv1 modulation on contralateral innervation. A) Plot of the number of AP elicited by increasing input currents (10-14 DIV neurons). Compared to controls, *Cux1*$^{-/-}$ neurons show a lower response to injected currents of all magnitudes. WT, $n = 19$; *Cux1*$^{-/-}$, $n = 32$; $F(2,836) = 275.5;\ p \leq 0.0001$. **B)** Active membrane properties of cultured WT and *Cux1*$^{-/-}$ neurons. Data obtained from patch clamp recordings. **C, D)** Tile scan assembly showing the contralateral innervations of P16 layer II/III neurons electroporated with CAG*Kv1.3* (C), or shRNA*Cux1* and *CAGKv1.2* (D). GFP staining, green; nucleus, blue. Medial, left; lateral, right. Bar = 250 μm.

Figure S6 related to Figure 7. Altering firing modes reduces layer II/III CC contralateral innervation. A) Firing rates and patterns at P16. Plot of the number of AP elicited by increasing input currents of neurons electroporated with the indicated plasmids. Data obtained from patch clamp recordings in P16 acute slices. shRNA*Cux1* (n= 20) *versus* Control (n= 20); $F(2,753) = 74.03$; $p \leq 0.0001$. shRNA*Cux1* (n= 20) *versus* shRNA*Cux1;*CAG*Kv1.3* (n=26) $F(2,938) = 77.81$; $p \leq 0.0001$. **B)** First ISI frequency (Hz) in bursts of 9 AP over a 500 ms period. *Kv1.3* over-expression in WT neurons does not alter first ISI frequency. Data shows mean ± SEM. Student's t test p-value *** ≤0.01. **C)** Local variation of ISI in spike trains of 8 AP. *Kv1.3* over-expression in WT neurons does not alter the L_v. Control, n= 20; shRNA*Cux1*, n= 15; CAG*Kv1.3*, n=20. Data shows mean ± SEM. Student's t test p-value *** ≤0.01. Data for control and shRNA*Cux1* are from Figure 5 and included for comparison. **D-G)** The overexpression of the ankyrinG-binding loop (NavII-III) of the intracellular tail of the Nav channel via IUE decreases the number of available channels by competing with endogenous native Nav proteins, altering firing modes. **D)** Plot of the number of AP elicited by increasing input currents recorded in GFP electroporated neurons at P10-P12. shRNAControl curve is from Figure 5A and included for comparison. shRNAControl (n= 20) versus Syn*NavII-III* (n=20); $F(1,812) = 282.8$; $p \leq 0.0001$. **E)** Representative firing patterns. Overexpression of NavII-III in WT layer II-III neurons reduced spike frequency adaptation (increasing spike ratio) **F)** Spike ratios. Mean ± SEM. Student's t test p-value ***≤ 0.001. **G)** Fraction of neurons firing at their maximum response at the indicated current. The maximum response curves are modified similarly to shRNA*Cux1*. shRNAControl curve is from Figure 5D and included for comparison. Student's t test p-value * ≤ 0.01 **H-I)** This aberrant firing mode correlated with a significant reduction in CC contralateral axons and a disrupted pattern of axonal distribution. P12

contralateral CC axons of layer II-III control neurons **(**H**)** and neurons over-expressing the NavII-III domain **(I)**. Bar = 250 μm. **J)** Quantification of contralateral innervation normalized to control. Student's t test p-value ***$\leq$*0.005*.

Supplemental Movie 1 related to Figure 3. Cux1-deficient neurons preserve their ipsilateral axonal branches. Reconstructions of ipsilateral branches in layers II/III and V in individual GFP+ callosal neurons were performed using Fiji on tilescan images of confocal 0.5 μm serial optical sections**.**

Supplemental Methods

In utero electroporation, plasmid constructs and shRNA specific control

In utero electroporation, *Cux1* lentiviral shRNA, CAG*Cux1* mutated resistant forms were previously described (Cubelos et al., 2010). shRNA for Kv1.3 were from Sigma-Aldrich. The hairpin sequences targeting *Kv1.3* were TCTGAGTAAGTCGGAGTATATCTCGAGATATACTCCGACTTACTCAGA*;* GCATTGCCAGTTCCTGTGATTCTCGAGAATCACAGGAACTGGCAATGC; CTGGCTGAACGACAAGGTAACTCGAGTTACCTTGTCGTTCAGCCAG. Injection solution contained shRNA plasmids mixed with pCAG-GFP (1 μg/μl each). Diminished contralateral axonal innervation was observed using three distinct shRNA sequences targeting *Cux1* (not shown), ruling out off-target effects. *Kir2.1* construct was provided by Y. Tagawa (Kyoto University, Japan) (Mizuno et al., 2010); *Kv1.3* was from M.T. Pérez-García (Universidad de Valladolid, Spain) (Cidad et al., 2012); *Kv1.2* construct was a gift from Chen Gu (The Ohio State University, USA) (Gu and Gu, 2011); ChR2-YFP-NavII-III was a gift from Matthew Grubb (Addgene plasmid #26057); and pCALNL-GFP , pCALNL-*DsRed* and pCAG-ERT2CreERT2 were gifts from Connie Cepko (Addgene plasmids #13770, #13769 and #13777). CAG-Synaptophysin-turquoise plasmid was a gift from Ann Marie Craig. The *Cux1* shRNA resistant form was subcloned from CAG*Cux1* into the CALNL-*DsRed* plasmid (CALNL-*Cux1*). 4-hydroxytamoxifen (4-OHT) (Sigma) was dissolved in 95% ethanol at 20 mg/ml. For intraperitoneal injections, this was diluted with nine volumes of corn oil and 200μl were injected.

Confocal imaging and quantification

Confocal microscopy was performed with a TCS-SP5 (Leica) Laser Scanning System on a Zeiss Axiovert 200 microscope. 50 μm sections were obtained by taking 0.5 μm serial optical sections with Lasaf v1.8 software (Leica) and Tilescan images with Leica Las AF software. Images of synaptophysin were acquired using a 1024x1024 scan format with a 63x objective and puncta were identified as covering at least three pixels above background in compressed z sections using Fiji.

Immunohistochemistry and axonal tracing

Brains were processed as described (Cubelos et al., 2008). Antibodies used were rabbit anti-GFP (A11122, Life Technologies); rabbit anti-Cleaved Caspase-3 antibody (#9661, Cell Signaling); rabbit anti-Cux1 (M-222X, Santa Cruz Biotechnology); mouse anti-GFP (#11814460001, Roche); and goat anti-rabbit-Alexa488, goat anti-rabbit-Alexa594 and goat anti-mouse-Alexa488 (Life Technologies). Nuclei were stained with DAPI (Sigma) or TO-PRO-3 Iodide (Life Technologies). Retrograde labeling from the corpus callosum was performed at P5 using ultrasound guided back-scatter microscopy and injection guidance system (Vevo 770, VisualSonics, Toronto). Alexa Fluor 647 conjugated cholera toxin subunit B (CTB) was injected into the corpus callosum at three subsequent antero-posterior levels at the midline (230 nl per injection site). Reconstructions and quantifications of the number of branches in layer II/III and in V were performed in CTB+ callosal neurons using Fiji. For retrograde labeling from the S1, biotin conjugated CTB was injected at P9 into S1 (400 nl). Biotin-conjugated Post hoc Alexa Fluor 405-conjugated streptavidin (1:250) detected CTB.

Luciferase reporter assays

The mouse genomic sequences containing Cux1 binding sites for the *Kcna1* and *Kcna3* genes and that were cloned into the pGL4.23 luciferase vector (Promega) were the following:

Kcna1:

CTCCCCATTAAAGACAACCATTTTATGTTGATGCATGTCCTTTGATGCCTTCCTG

TTGCCCTCTTCCTCCCAGCCTAAGGGGTCCCATGGTCCACCTGCCATGACCTTC

CTTGTTATTTCTTCCTGTTCACAATGACCTTTTGGTTGCGTT and *Kcna3*:

CAGAAATAAATACAAAGCATCACTTGTTGCAGAATTCAGTACAACAAACAAAT

GCTGAGATCCCAGGATTTCCAAGTTGCTAACAACAGAAGTTGGGCAAGCCCTC

TTTATCATAGTTTAGTAGTTGGGAGAGGGGGTAAGAAAAACATG.

Electrophysiology

Intracellular patch pipette (4-7MΩ) solution for whole cell current-clamp recordings contained 115 mM K-gluconate, 20 mM KCl, 2 mM $MgCl_2$, 10 mM HEPES, 4 mM Na_2ATP and 0.3 mM Na_3GTP, adjusted to pH 7.2 with KOH and to 290 mOsm with KCl. During recording each slice was perfused with artificial cerebrospinal fluid (ACSF) containing 119 mM NaCl, 2.5 mM KCl, 1 mM NaH_2PO_4, 11 mM glucose, 26 mM $NaHCO_3$, 1.25 mM $MgCl_2$ and 2.5 mM $CaCl_2$.

Measure of local variation of inter-spike intervals

Quantitative assessment of the regularity of an AP train was performed using the local variation defined as (Shinomoto et al., 2003):

$$L_V = \frac{1}{n-1}\sum_{i=1}^{n-1}\frac{3(T_i - T_{i+1})^2}{(T_i + T_{i+1})^2},$$

where T_i is the duration of the ith ISI and n is the number of ISIs involved in the calculation (8). We calculated L_V for 9-20 individual cells with equal numbers of spikes for each condition.

Q-PCR

Primers were: *Kcna1/Kv1.1* (forward 5'AGGCTCAGTTGCTCCATGTT3'; reverse 5'TCAGCTGTGGTGCAGTTACC3'); *Scn8a/Nav1.6* (forward 5'CACCATCCTGACCAACTGTG3'; reverse 5'TAACCAGTTCCACGGGTCTC3'); *Cacna1c/Cav1.2* (forward 5'ACATCTTCGTGGGTTTCGTC3'; reverse 5'TGTTGAGCAGGATGAGAACG3'); *β-actin* (forward 5'GGCTGTATTCCCCTCCATCG3'; reverse 5'CCAGTTGGTAACAATGCCATGT5'). PCR reactions using Taqman probes (Applied Biosystems, Foster City, CA) were performed for *Kcna2/Kv1.2* (Mm00434584_s1) and *Kcna3/Kv1.3* (Mm00434599_s1) following TaqMan Gene Expression Assays Protocol.

Supplemental References

Cidad, P., Jimenez-Perez, L., Garcia-Arribas, D., Miguel-Velado, E., Tajada, S., Ruiz-McDavitt, C., Lopez-Lopez, J.R., and Perez-Garcia, M.T. (2012). Kv1.3 channels can modulate cell proliferation during phenotypic switch by an ion-flux independent mechanism. Arterioscler Thromb Vasc Biol *32*, 1299-1307.

Cubelos, B., Sebastian-Serrano, A., Beccari, L., Calcagnotto, M.E., Cisneros, E., Kim, S., Dopazo, A., Alvarez-Dolado, M., Redondo, J.M., Bovolenta, P.*, et al.* (2010). Cux1 and Cux2 regulate dendritic branching, spine morphology, and synapses of the upper layer neurons of the cortex. Neuron *66*, 523-535.

Cubelos, B., Sebastian-Serrano, A., Kim, S., Redondo, J.M., Walsh, C., and Nieto, M. (2008). Cux-1 and Cux-2 control the development of Reelin expressing cortical interneurons. Developmental neurobiology *68*, 917-925.

Gu, C., and Gu, Y. (2011). Clustering and activity tuning of Kv1 channels in myelinated hippocampal axons. J Biol Chem *286*, 25835-25847.

Mizuno, H., Hirano, T., and Tagawa, Y. (2010). Pre-synaptic and post-synaptic neuronal activity supports the axon development of callosal projection neurons during different post-natal periods in the mouse cerebral cortex. Eur J Neurosci *31*, 410-424.

Shinomoto, S., Shima, K., and Tanji, J. (2003). Differences in spiking patterns among cortical neurons. Neural Comput *15*, 2823-2842.

POSTMITOTIC EXPRESSION OF LHX2 IN LAYER 4 INITIATES THE ASSEMBLY OF SOMATOSENSORY CIRCUIT IN BARREL CORTEX

Las neuronas de la lámina IV desarrollan su polaridad y extienden las dendritas asimétricamente hacia el barril gracias a la información talámica que reciben en la primera semana postnatal (Erzurumlu and Gaspar 2012; Li and Crair 2011; Wu et al. 2011). El ensamblaje del circuito de la corteza de barriles requiere una gran coordinación entre las neuronas corticales y talámicas; para que sea correcto es necesario que existan sinapsis entre ellas y que estas transmitan correctamente la actividad originada en los bigotes. Sin embargo, los mecanismos por los que las neuronas de la lámina IV adquieren la capacidad para responder a los axones talamocorticales son desconocidos a día de hoy.

Lhx2 es un FT del tipo homeodominio LIM que es necesario para la especificación de diversos tipos celulares (Shirasaki and Pfaff 2002) y que se expresa en altos niveles en las neuronas corticales de las láminas superficiales y en sus progenitores desde el embrión (Bulchand et al. 2003; Nakagawa et al. 1999). Mediante la eliminación de Lhx2 en los progenitores corticales (utilizando la línea Emx1-Cre), Shetty y colaboradores demostraron que Lhx2 es necesario para la formación de barriles (Shetty et al. 2013). Sin embargo, los defectos dramáticos observados en la neurogénesis de estos ratones (Chou et al. 2009; Chou and O'Leary 2013; Hsu et al. 2015; Shetty et al. 2013) hacían difícil discernir qué alteraciones de la corteza de barriles se debían a éstos defectos y cuáles a una función postmitótica de Lhx2. En el artículo aquí presentado, colaboramos en un estudio del papel específico de Lhx2 en neuronas postmitóticas mediante la línea transgénica Nex-Cre (Goebbels et al. 2006). Gracias a esta estrategia, demostramos que Lhx2 es necesario para la inducción de la expresión de genes regulados por actividad que permiten a las neuronas de la lámina IV de S1 responder a los axones talamocorticales de forma que desarrollan su característica asimetría dendrítica y forman los barriles.

Este artículo es fruto de una colaboración con el laboratorio de Shen-Ju Chou, motivada por mi interés sobre el sistema de barriles y por mis estudios, aún en desarrollo, sobre el papel de la actividad sensorial en el mapa calloso. Mi principal aportación fue en el análisis de los defectos topográficos de la conectividad del ratón cKO (sin Lhx2 en las neuronas corticales). En concreto, diseñé y realicé el análisis de la distribución de las neuronas de cFos en la corteza de barriles con el objeto de identificar desviaciones de la distribución normal. También participé muy activamente en la discusión crítica de la interpretación de los resultados, en la redacción del manuscrito y la elaboración de todas las figuras.

Report

Cell Reports

Lhx2 Expression in Postmitotic Cortical Neurons Initiates Assembly of the Thalamocortical Somatosensory Circuit

Graphical Abstract

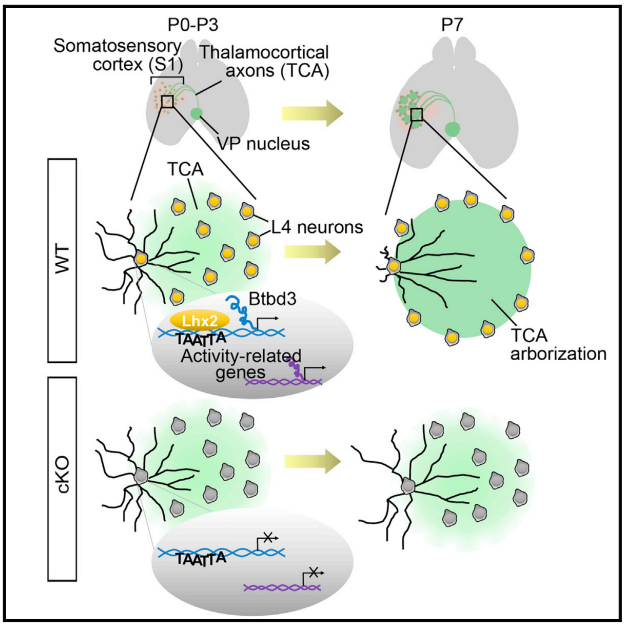

Highlights

- Lhx2 in postmitotic cortical neurons is critical for barrel cortex development
- Deletion of Lhx2 in postmitotic neurons leads to somatosensory functional deficits
- The expression of activity-regulated genes during S1 development requires Lhx2
- Lhx2 directly induces Btbd3 to regulate layer 4 neuron dendritic development

Authors

Chia-Fang Wang, Hsiang-Wei Hsing, Zi-Hui Zhuang, ..., Marta Nieto, Bai Chuang Shyu, Shen-Ju Chou

Correspondence

schou@gate.sinica.edu.tw

In Brief

Wang et al. find that the transcription factor Lhx2 functions in postmitotic cortical neurons to initiate barrel cortex formation. Lhx2 induces the expression of activity-regulated genes that enable layer 4 neurons in the somatosensory cortex to respond to thalamocortical inputs, develop dendritic asymmetry, and form cellular barrels.

Accession Numbers

GSE92372

Wang et al., 2017, Cell Reports *18*, 849–856
January 24, 2017
http://dx.doi.org/10.1016/j.celrep.2017.01.001

Cell Reports
Report

Lhx2 Expression in Postmitotic Cortical Neurons Initiates Assembly of the Thalamocortical Somatosensory Circuit

Chia-Fang Wang,[1] Hsiang-Wei Hsing,[1] Zi-Hui Zhuang,[1] Meng-Hsuan Wen,[1] Wei-Jen Chang,[2] Carlos G. Briz,[3] Marta Nieto,[3] Bai Chuang Shyu,[2] and Shen-Ju Chou[1,4,*]
[1]Institute of Cellular and Organismic Biology, Academia Sinica, Taipei 11529, Taiwan
[2]Institute of Biomedical Sciences, Academia Sinica, Taipei 11529, Taiwan
[3]Centro Nacional de Biotecnología, CNB-CSIC, Darwin 3, Campus de Cantoblanco, Madrid 28049, Spain
[4]Lead Contact
*Correspondence: schou@gate.sinica.edu.tw
http://dx.doi.org/10.1016/j.celrep.2017.01.001

SUMMARY

Cortical neurons must be specified and make the correct connections during development. Here, we examine a mechanism initiating neuronal circuit formation in the barrel cortex, a circuit comprising thalamocortical axons (TCAs) and layer 4 (L4) neurons. When *Lhx2* is selectively deleted in postmitotic cortical neurons using conditional knockout (cKO) mice, L4 neurons in the barrel cortex are initially specified but fail to form cellular barrels or develop polarized dendrites. In *Lhx2* cKO mice, TCAs from the thalamic ventral posterior nucleus reach the barrel cortex but fail to further arborize to form barrels. Several activity-regulated genes and genes involved in regulating barrel formation are downregulated in the *Lhx2* cKO somatosensory cortex. Among them, *Btbd3*, an activity-regulated gene controlling dendritic development, is a direct downstream target of Lhx2. We find that Lhx2 confers neuronal competency for activity-dependent dendritic development in L4 neurons by inducing the expression of Btbd3.

INTRODUCTION

The barrel cortex, a major part of the primary somatosensory cortex (S1), receives and processes inputs from major facial whiskers in a topographic fashion. The barrels are located in cortical layer 4 (L4) and consist of L4 spiny stellate neurons forming cell-dense rings or "cellular barrels" and thalamocortical axons (TCAs) that occupy the barrel hollow. L4 neurons develop polarity and extend dendrites asymmetrically to the hollow upon receiving TCA inputs in the first postnatal week (Erzurumlu and Gaspar, 2012; Li and Crair, 2011; Wu et al., 2011). Assembly of the barrel cortex circuit is critical for somatosensation in rodents, and it requires finely tuned coordination between cortical and thalamic neurons.

Previous studies of genetically modified mice demonstrated that the establishment of neuronal connections and the transmission of neuronal activity from whiskers to the L4 neurons in S1 are required for barrel formation. Deletion of factors functioning in glutamatergic or serotonergic neurotransmission perturbs the formation of patterned TCA inputs and/or the aggregation of L4 neurons (Erzurumlu and Gaspar, 2012; Li and Crair, 2011; Vitali and Jabaudon, 2014; Wu et al., 2011). Furthermore, several activity-dependent transcription factors, such as Lmo4, NeuroD2, and Btbd3, were reportedly involved in the formation of cellular barrels or the development of polarized dendritic patterns (Ince-Dunn et al., 2006; Kashani et al., 2006; Matsui et al., 2013). In spite of these studies, the molecular mechanisms initiating barrel cortex development remain largely unknown. For example, it remains to be determined how L4 neurons acquire the capacity to respond to TCA inputs, and reciprocally, how cortical neurons instruct thalamic axons during barrel cortex formation.

Lhx2, a LIM homeodomain transcription factor that functions to specify multiple cell types (Shirasaki and Pfaff, 2002), is highly expressed in cortical neurons located in the superficial layers embryonically and in the first postnatal weeks (Bulchand et al., 2003; Nakagawa et al., 1999). A previous report showed that conditional *Lhx2* deletion in cortical progenitors using a late-onset *Emx1*-Cre perturbs barrel formation (Shetty et al., 2013), implying that cortical expression of Lhx2 regulates barrel cortex development. However, dramatic defects in neurogenesis, cortical layer formation, and cortical patterning were reported when Lhx2 was deleted in the cortical progenitors (Chou and O'Leary, 2013; Chou et al., 2009; Hsu et al., 2015; Shetty et al., 2013), making it difficult to delineate the postmitotic function of Lhx2 in barrel development. Here, by deleting *Lhx2* specifically in postmitotic cortical neurons with *Nex*-Cre (Goebbels et al., 2006), we find that Lhx2 is required for L4 neurons to form cellular barrels and for the TCAs to extensively arborize in the barrel cortex. Further, Lhx2 induces the expression of several activity-regulated genes and enables cortical neurons to respond to TCA inputs. These findings indicate that Lhx2 acts as a molecular switch in cortical neurons to initiate somatosensory circuit assembly.

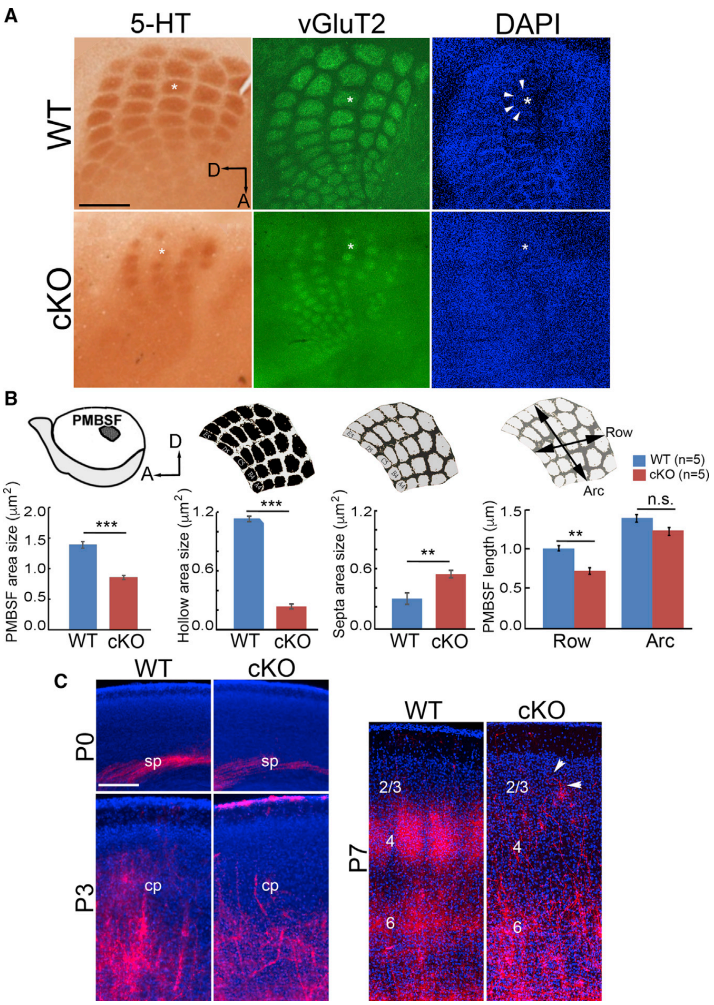

Figure 1. *Lhx2* cKO Mice Show Defects in Barrel Formation

(A) Immunostaining for 5HT and vGluT2 and DAPI nuclear staining on tangential sections of flattened cortex of WT (wild-type) and cKO (*Lhx2*$^{f/f}$;*Nex*-Cre) mice at P7. The 5HT- and vGluT2-positive TCA inputs filled the barrel hollow (for example, C2, marked with an asterisk [*]). Cellular barrels (arrowheads) were apparent in WT but were not detected in the cKO samples. D, dorsal; A, anterior.

(B) Comparison of WT and cKO S1. The size of PMBSF was significantly decreased in cKO S1 ($p < 0.001$), with decreased area size of hollow ($p < 0.001$) and increased area size of septa ($p < 0.01$). The length of PMBSF along rows was decreased ($p < 0.01$), while no significant difference was found in the length of PMBSF along the arc (n.s., not significant, $p > 0.05$).

(C) TCA projections are labeled by DiI (red) injected into VP of the thalamus in WT and cKO brains. Coronal sections were counterstained with DAPI. In WT and cKO mice, VP neuronal axons can reach the subplate (sp) and cortical plate (cp) in S1 at P0 and P3, respectively. At P7, while VP TCAs in WT arborize in layer 4 (4) to fill the barrel hollow, VP TCAs in cKO mice fail to arborize in L4, and some axonal terminals (arrowheads) remain in layers 2/3 (2/3). Scale bars, 200 μm. See also Figures S1 and S2.

RESULTS

The Absence of Lhx2 in Postmitotic Neurons Leads to Anatomical Defects in Barrel Cortex Development

Lhx2 is highly expressed in neurons located in layers 2/3 (L2/3) and L4 (Bulchand et al., 2003; Nakagawa et al., 1999), but its precise functions in these postmitotic neurons have not been fully addressed. In mice, once cellular barrels become apparent at postnatal day 7 (P7), Lhx2 expression in L4 of the somatosensory cortex becomes more concentrated in the barrel wall (Figure S1A), suggesting that it functions in L4 neurons regulating barrel formation. We thus investigated barrel cortex development in the *Lhx2* cKO (*Lhx2*$^{f/f}$; *Nex*-Cre) brains, where *Lhx2* is selectively deleted in postmitotic neurons by *Nex*-Cre (Goebbels et al., 2006).

The location of TCAs targeting the primary sensory areas was determined by immunostaining with antibodies against 5HT and vGluT2 on tangential sections of flattened cortices (Figures 1A and S1B). In contrast to the nearly complete loss of TCA inputs in the cortices where *Lhx2* was deleted by late-onset *Emx1*-Cre (Shetty et al., 2013), the conditional knockout (cKO) mice had detectable 5HT- and vGluT2-positive primary sensory areas, including S1, A1 (primary auditory area), and V1 (primary visual area) (Figure S1B; Zembrzycki et al., 2015). Among the primary sensory areas, the size of S1 in cKO mice was the most dramatically diminished. This change was not due to changes in cortical size, as no major differences were found in the cortical size between cKO and wild-type (WT) mice (including *Lhx2*$^{f/f}$, *Lhx2*$^{f/+}$, *Lhx2*$^{f/+}$;*Nex*-Cre, and *Lhx2*$^{+/+}$;*Nex*-Cre) (Figure S1C; Chou et al., 2009; Zembrzycki et al., 2015). We found that the size of the posterior medial barrel subfield (PMBSF), the major component of the S1, was significantly decreased in cKO mice (Figures 1A and 1B). Within the cKO PMBSF, barrels were disproportionally decreased in size: the area of the vGluT2-positive hollow was significantly decreased, and the vGluT2-negative septal area was significantly increased (Figure 1B). Further, we observed enlarged spacing between barrel rows in cKO PMBSF, where adjacent barrels in two rows were further apart than adjacent barrels within the same row (Figure 1A). This led to significantly decreased length of PMBSF along rows, while the length

along arc remained similar in cKO and WT mice (Figure 1B). This result suggests that Lhx2 in the postmitotic neurons patterns the distribution of TCAs in S1.

To further examine the development of TCAs in cKO mice, we inserted DiI (1,1-dioctadecyl-3,3,3',3'-tetramethyl-indocarbocyanine perchlorate) crystals into the thalamic ventral posterior nucleus (VP) to track VP axonal projections at various time points in the first postnatal week. In both WT and cKO brains, VP TCAs reached the subplate underneath S1 at P0 and extended to superficial layers in the cortical plate at P3 (Figure 1C). At P7, however, while VP TCAs arborized extensively in WT L4 to occupy barrel hollows, they were more sparsely branched in cKO L4 with an increase of branches and terminal endings in L2/3 (Figures 1C and S1D). Thus, *Lhx2* deletion in postmitotic cortical neurons did not impede VP TCAs entering S1; instead, it led to their arborization defects.

We then asked whether the cKO L4 neurons form cellular barrels, the cell-dense rings enclosing TCA patches. We observed cellular barrels by P7 in WT mice, but not in cKO mice (Figure 1A). We measured the cell density across the C2 barrel by DAPI staining on tangential sections of P7 WT and cKO cortices (Figure S1E). We observed higher L4 cell density in septa (with weaker vGluT2 staining) than in hollows (with stronger vGluT2 staining) in WT mice, while L4 cells distributed evenly across barrels in cKO mice (Figures S1F and S1G). Further, we found cellular barrels remained undetectable at P20 (Figure S1H), confirming that barrel formation was not simply delayed in cKO mice. Thus, we concluded that the loss of Lhx2 in postmitotic neurons leads to defects in cellular barrel formation.

To verify that the loss of cellular barrels in cKO mice was not due to the failure of L4 neurons to migrate to their correct layer, we first examined the migration of L4 neurons in WT and cKO brains. We found in both WT and cKO brains, most of the neurons generated on embryonic day 14.5 (E14.5) located in L4 at P7 (Figure S2A). Further, we performed in utero electroporation at E14.5 to deliver CAG-Cre and CAG-mCherry plasmids into L4 neurons in $Lhx2^{f/+}$ and $Lhx2^{f/-}$ cortices. In this system, the expression of Cre recombinase generates WT (*Lhx2* heterozygous) and *Lhx2* mutant cells in $Lhx2^{f/+}$ and $Lhx2^{f/-}$ cortices, respectively, and mCherry expression labels transfected cells. We confirmed the absence of Lhx2 expression in the transfected cells in $Lhx2^{f/-}$ cortices (Figure S2B) and that the majority of mCherry-expressing cells are located in L4 in both $Lhx2^{f/+}$ and $Lhx2^{f/-}$ cortices at P7 (Figures S2C and S2D), indicating that *Lhx2* loss did not lead to L4 neuron migration defects.

Barrel Cortex Showed Functional Deficits in *Lhx2* cKO Mice

As proper connection from whiskers to S1 is required for cellular barrel formation (Ding et al., 2003; Erzurumlu and Kind, 2001; Rebsam et al., 2005), we used CO (cytochrome oxidase) staining to examine the somatosensory pathway in the cKO mice. We observed no detectable difference in size or organization of barreloids and barrelettes, respective somatosensory nuclei in the dorsal thalamus and brainstem, between *Lhx2* cKO and WT brains (Figure S2E). Thus, the anatomical defects we observed in cKO brains were the result of the defective cortical or thalamocortical somatosensory circuit.

Previous studies suggested that defective barrel cortex development is associated with aberrant sensory responsiveness (Petersen, 2007). To test the selective functionality of barrels, we shaved all but the C2 whisker on one side of the head and let the mice explore an enriched environment for 1 hr. We then analyzed the distribution of c-Fos-positive neurons (i.e., the activated neurons) in S1 L4. Although most c-Fos-positive cells were concentrated at the location of the C2 barrel in both WT and cKO mice (Figure 2A), we found a higher proportion of c-Fos-positive neurons located outside the C2 barrel in cKO mice when compared with WT littermates (Figure 2B). This suggested that the cKO S1 failed to receive precisely mapped activity from the whiskers.

We further assessed the function of the whisker-to-S1 pathway in cKO mice with a multichannel probe at S1 to record field potential in multiple cortical layers simultaneously upon whisker stimulations. We compared the current source densities (CSDs) evoked by whisker electric stimulation in WT and cKO mice (Chen et al., 2008; Yang et al., 2006). The CSD profiles across the depth of S1 following whisker stimulation showed that sink currents were first detected in the L4 in both WT and cKO mice (Figures 2C and 2D). However, significantly decreased amplitude and increased latency of the whisker-evoked prominent sink currents in L4 were found in cKO mice than in WT mice (Figure 2E). This demonstrated that cKO shows functional deficits in responding to whisker sensory stimuli. Thus, we concluded that in cortical neurons, Lhx2 plays critical roles assembling the functional somatosensory circuitry.

Lhx2 Regulates Crucial Genetic Pathways in L4 Neurons to Enable Barrel Formation

We next investigated the molecular mechanisms underlying Lhx2 regulation of barrel formation. We performed microarray analyses with RNA collected from P7 WT and cKO S1. We found 2,765 transcripts showing altered expression levels in WT and cKO mice (unpaired t test, $p < 0.05$, $n = 3$), with 1,416 upregulated and 1,349 downregulated. Among them, 2,069 genes were annotated, and 314 of them were shown to be involved in the nervous system development (GO: 0007399) by PANTHER gene ontology (GO) analysis (Mi et al., 2013). Within this category, the top GO terms were pallium development (GO: 0021543), telencephalon development (GO: 0021537), and regulation of dendritic development (GO: 0050773).

Interestingly, among the genes showed changed expression levels in cKO S1, many of them were reportedly regulated by neuronal activity (as shown in Table S1; Pouchelon et al., 2014; Rodríguez-Tornos et al., 2013). For example, we found that *RORb* expression was significantly downregulated in cKO mice at P7 (Figures S2F and S2G). The expression of *RORb* increases in the S1 L4 during barrel cortex development and decreases when TCA inputs are eliminated (Jabaudon et al., 2012; Pouchelon et al., 2014). Using in situ hybridization and qRT-PCR, we found the *RORb* expression level was comparable in WT and cKO mice at P0 (Figures S2F and S2G), suggesting that L4 neurons were initially specified in cKO mice. However, without Lhx2, *RORb* could not be fully induced in cKO S1 at P7.

The misregulation of these activity-regulated genes in cKO was likely associated with barrel formation defects. Thus, we

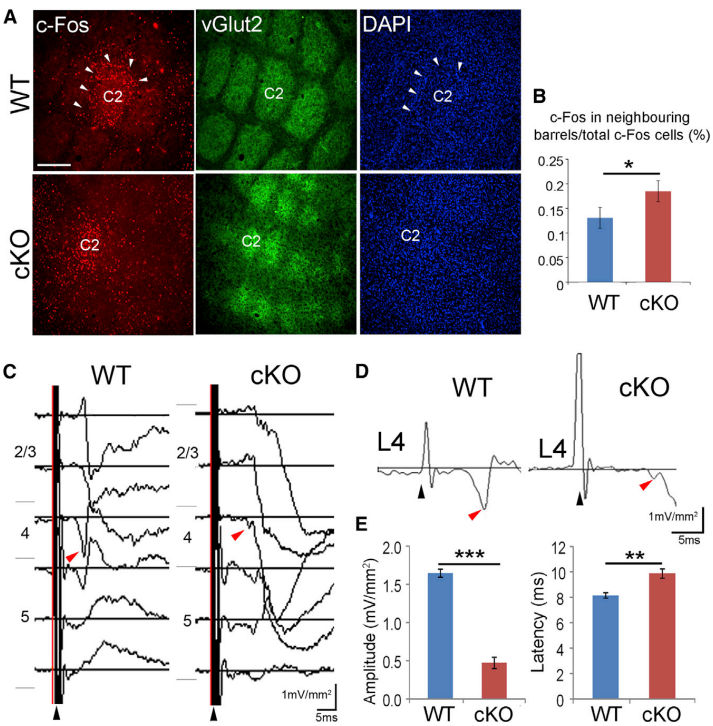

Figure 2. *Lhx2* cKO Mice Show Functional Deficits in Somatosensory Cortex

(A) Immunostaining for c-Fos and vGluT2 on tangential sections of flatten cortices from mice with only C2 whisker. DAPI counterstaining indicates barrel wall (arrowheads) are present in WT cortices, but not in cKO cortices. In both WT and cKO mice, the majority of c-Fos-positive cells are located in the C2 barrel.

(B) More c-Fos-positive neurons were located outside of the C2 barrel in cKO mice when compared with WT ($p < 0.05$, $n = 3$).

(C) Current source density (CSD) sweeps across the cortical layers in WT (left) and cKO (right) S1 upon electrical whisker stimulation. Black and red arrowheads indicate the stimulation and the first follow-up sink current response in layer 4, respectively.

(D) Cortical layer 4 (L4) sink current response in WT (left) and cKO (right) mice.

(E) The amplitude of the L4 sink current response was significantly decreased ($p < 0.001$, $n = 3$) and the latency was significantly higher ($p < 0.01$, $n = 3$) in cKO mice than in their WT littermates.

Scale bar, 100 μm. See also Figure S2.

compared the expression levels of genes reportedly regulating barrel formation in WT and cKO S1. We found that *Adcy1*, *Btbd3*, *Efna5*, and *Lmo4* were significantly downregulated in cKO S1 (Table S2; reviewed by Wu et al., 2011). qRT-PCR confirmed the downregulation of *Lhx2*, as well as *Adcy1*, *Btbd3*, *Efna5*, and *Lmo4* in cKO samples (Figure 3A). We also extended this analysis to confirm that the deletion of *Lhx2* in postmitotic neurons did not affect the expression of other genes involved in barrel development, including *mGluR5*, *NR1*, and *NeuroD2* (Figure S3A). These experiments suggest that Lhx2 regulates a specific set of key factors for barrel formation.

Lhx2 Is Required for Btbd3 Expression in the S1 through Direct Transcriptional Regulation

We then analyzed whether Lhx2 can directly regulate the expression of *Efna5*, *Adcy1*, *Lmo4*, and *Btbd3* genes. We identified multiple consensus Lhx2 binding sites (TAATTA, as described in Roberson et al., 1994) within 1 kb of the *Btbd3* upstream regulatory sequences and in the 4-kb upstream regulatory sequences of the *Efna5*, *Adcy1*, and *Lmo4* genes (Figures 3B and S3B). We tested the ability of Lhx2 to bind to these predicted sites by chromatin immunoprecipitation (ChIP) and found that in the P7 S1, Lhx2 showed significant binding to the most proximal Lhx2 binding site (BS3) in the *Btbd3* promoter region (Figure 3B), but not to the putative binding sites in the *Adcy1*, *Efna5*, or *Lmo4* promoter regions we tested (Figures S3B and S3C). As a control, we confirmed that in S1 at P7, Lhx2 does not bind to the *Pax6* enhancer (Hou et al., 2013), and this agrees with the fact that *Pax6* is not expressed in most postmitotic cortical neurons (Figures S3B and S3C). Without excluding the possibility for Lhx2 to regulate other genes directly through additional binding sites, here we focused on Lhx2 regulation of *Btbd3*. To confirm direct regulation of *Btbd3* by Lhx2, we showed that Lhx2 induced *Btbd3* promoter activity ~3-fold in N2a cells through the most proximal Lhx2 binding site (BS3). When this site is mutated (in m3, m13, m23, and m123), Lhx2 can no longer induce *Btbd3* promoter activity (Figure 3C). We next performed in situ hybridization to determine the expression pattern of *Btbd3* in P7 WT and cKO cortices. Utilizing *RORb* expression to mark L4 in WT and cKO S1, we found *Btbd3* was expressed in the WT S1 L4 at P7 but was not detectable in cKO S1 (Figure 3D), suggesting that Lhx2 is required for *Btbd3* expression in S1.

Lhx2 Regulation of Btbd3 Is Required for Proper Development of L4 Neuronal Dendritic Morphology

To confirm that Lhx2 is an upstream regulator for *Btbd3*, we next examined if the deletion of *Lhx2* in L4 neurons leads to defects in L4 neuronal dendritic polarity, similar to the result of knocking down *Btbd3* (Matsui et al., 2013). To target L4 neurons, we electroporated CAG-mCherry, CAG-Cre, and US2-LNL-GFP plasmids into $Lhx2^{f/+}$ and $Lhx2^{f/-}$ dorsal telencephalon at E14.5. CAG-Cre was electroporated at a low level to sparsely label cells. We used US2-LNL-GFP as a reporter, as Cre expression removes the neomycin gene and stop cassette between two *loxP* sites and allows GFP expression. We selected those neurons with cell bodies located on barrel walls and examined

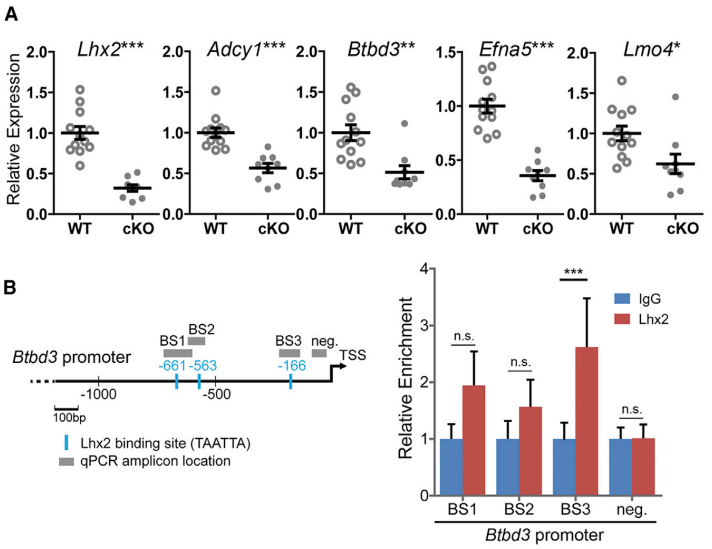

Figure 3. Lhx2 Regulates the Expression of Genes Functioning in Barrel Formation

(A) qRT-PCR analyses performed with RNA collected from S1 of WT and cKO cortices at P7. *Lhx2*, *Adcy1*, *Btbd3*, *Efna5*, and *Lmo4* expression was significantly decreased in cKO samples. Each dot represents one individual sample.

(B) Three consensus Lhx2 binding sites (BS1–3, blue boxes) were identified in the 1.3-kb *Btbd3* promoter. With ChIP analysis, anti-Lhx2 antibody showed a 2.6-fold enriched binding to BS3 when compared with IgG control ($p < 0.001$, $n = 8$).

(C) Lhx2 significantly increases *Btbd3* promoter activity ($p < 0.001$, $n = 4$) in N2a cells. The induction of *Btbd3* promoter activity by Lhx2 is lost only when the proximal Lhx2 binding site (BS3) is mutated.

(D) In situ hybridization for *RORb* and *Btbd3* on coronal sections of P7 WT and cKO cortices. *RORb* expression marks L4 in S1 (arrowheads) in both WT and cKO. *Btbd3* expression is detectable in WT S1 L4 (arrowheads), but not in cKO samples. Scale bar, 200 μm. See also Figures S3 and S4.

their dendritic morphology on tangential sections of flattened cortices. We found total dendritic length was similar in WT and mutant cells (Figures 4A and 4B). However, most dendrites of WT L4 cells projected to the hollow, the barrel center (Figures 4A and 4C), while the mutant cells showed significantly increased dendritic projections toward the septa and significantly decreased projections toward the hollow (Figures 4A and 4C). We further compared the polarity of WT and mutant cells with orientation bias index (OBI), which is the ratio of the length of hollow-projecting dendrites to the total dendrite length. The OBI of WT L4 neurons was close to 1, reflecting the fact that WT neurons are polarized, with most of their dendrites extending toward the hollow. Mutant L4 cells showed a significantly decreased OBI value (Figure 4D). As VP neurons in the thalamus were not affected in either $Lhx2^{f/+}$ or $Lhx2^{f/-}$ electroporated brains, our result indicated that *Lhx2* is required cell autonomously for the development of dendritic asymmetry in S1 L4 neurons.

We next asked whether Btbd3 expression was sufficient to rescue dendritic defects seen in *Lhx2* mutant L4 neurons. We generated a US-myc-Btbd3 expression construct and confirmed it directed Btbd3 overexpression when transfected in cell lines and in electroporated brains (Figures S4A–S4B′). Using a strategy similar to that described above, we electroporated CAG-mCherry, CAG-Cre, US2-LNL-GFP, and US2-myc-Btbd3 and found that total dendritic length was similar in WT and *Lhx2* mutant cells (Figures 4E and 4F). Btbd3 overexpression did not alter dendritic polarity in WT cells but re-established dendritic asymmetry in mutant cells (compare Figures 4E and 4G with Figures 4A and 4C). The OBI value was similar in *Btbd3* expressing WT and mutant cells (Figure 4H), indicating that lack of dendritic asymmetry in *Lhx2* mutant cells was mainly due to the lack of *Btbd3* expression. Taken together, we concluded that Lhx2 regulates the S1 L4 neuronal polarity by inducing *Btbd3* expression.

Lhx2 Regulates the Function of Btbd3 prior to the Activity-Regulated Events of Barrel Development

To further place the *Lhx2-Btbd3* genetic pathway in barrel cortex development, we examined the expression of *Btbd3* in several mutant mice with defects in activity-dependent barrel development, such as *Lmo4* and *mGluR5* cortex-specific knockouts (Ballester-Rosado et al., 2010; Kashani et al., 2006). Lmo4 was of interest, because its expression was downregulated in *Lhx2* cKO S1 (Figure 3A) and it can potentially interact with Lhx2 through the LIM domain (Rétaux and Bachy, 2002). However, qRT-PCR analysis did not detect changes in the expression

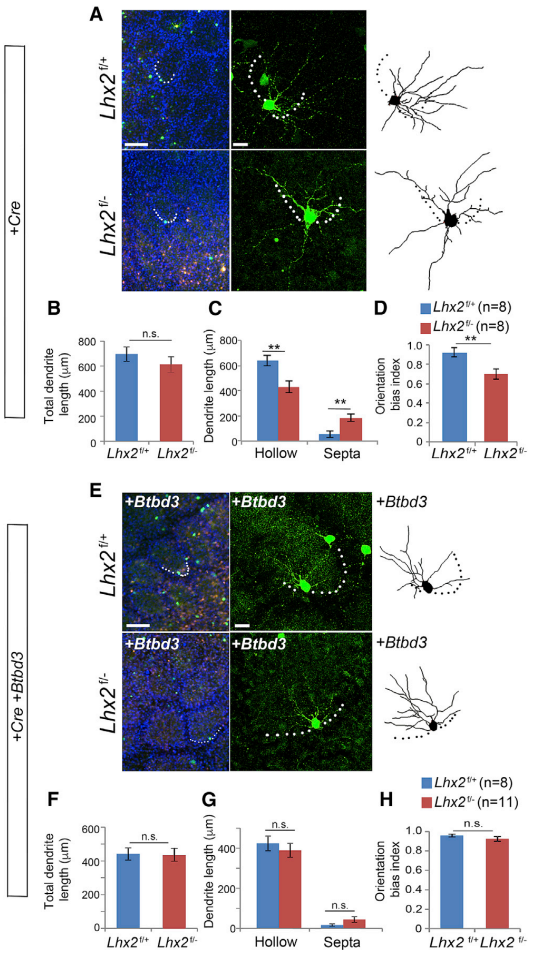

Figure 4. Lhx2 Regulates Dendritic Asymmetry of L4 Neurons via Btbd3

(A) CAG-Cre, CAG-mCherry, and the US-LNL-GFP reporter construct were co-electroporated into $Lhx2^{f/+}$ and $Lhx2^{f/-}$ embryonic cortices at E14.5 to generate WT (in $Lhx2^{f/+}$ cortices) and mutant (in $Lhx2^{f/-}$ cortices) L4 neurons. Immunostaining for GFP on tangential sections of flattened cortices reveals the morphology of WT and mutant L4 spiny stellate neurons, whose cell bodies were located in the barrel wall (dotted line) in P7 $Lhx2^{f/+}$ and $Lhx2^{f/-}$ cortices. Trace of GFP-positive cell morphology is shown on the right.

(B) Total dendritic length was comparable in WT and mutant cells.

(C) WT cells were polarized, with almost all dendrites projecting toward the barrel hollow; *Lhx2* mutant cells showed significantly decreased hollow-projecting dendritic length and significantly increased septa-projecting dendritic length ($p < 0.01$, $n = 8$).

(D) Orientation bias index (OBI), the ratio of the hollow projecting dendritic length to total dendritic length, was close to 1 in WT cells and was significantly decreased in mutant cells ($p < 0.01$, $n = 8$).

(E) A DNA mixture (as described in A) plus US2-myc-Btbd3 were electroporated into $Lhx2^{f/+}$ and $Lhx2^{f/-}$ embryonic cortices at E14.5. The electroporated L4 neuronal morphology was visualized as in (A).

(F) Total dendritic length is comparable in WT and Lhx2 mutant cells.

(G) Both WT and mutant cells show strong polarity, with almost all dendrites projecting toward to the hollow.

(H) Orientation bias index (OBI) was close to 1 in both WT and mutant cells. Scale bars, 100 μm for left panels and 20 μm for right panels in (A) and (E). See also Figure S4.

of *Lhx2*, *Adcy1*, *Btbd3*, or *EfnA5* in *Lmo4* cortical mutant ($Lmo4^{f/f}$:*Nex*-Cre) S1 (Figure S4C). Unaffected expression of *Btbd3* in *Lmo4* cortical mutant S1 was further confirmed by in situ hybridization (Figure S4D). We also found unaffected *Btbd3* expression in *mGluR5* cortical mutant ($mGluR5^{f/f}$:*Nex*-Cre) S1 (Figure S4E). The maintained *Btbd3* expression in these mutants indicates that Lhx2 transcriptional regulation of *Btbd3* is independent of the function of Lmo4 or mGluR5, and it further suggests that the *Lhx2-Btbd3* genetic pathway is likely to function prior to the activity-dependent events of barrel development.

DISCUSSION

Due to its unique cytoarchitecture, the barrel cortex is widely used as a system to delineate the basics of circuit formation. Signaling pathways transmitting neuronal activities from TCA to L4 neurons promote TCA arborization in L4, L4 neuron aggregation to form barrel walls, and the development of L4 neuronal dendrites toward the barrel hollow (Li and Crair, 2011). Here, we uncover a mechanism whereby the transcription factor Lhx2, whose function was previously shown to be activity independent (Kashani et al., 2006), regulates the initiation of barrel cortex formation. In *Lhx2* cKO mice, we did not detect defects in the initial specification of L4 neurons or the initial VP TCAs entering the cortical plate. However, L4 neurons and TCAs did not develop further when *Lhx2* was selectively deleted in postmitotic cortical neurons, leading to a failure of barrel formation. This is likely due to the altered expression of several activity-regulated genes involved in regulating barrel formation in cKO mice. Thus, our findings place Lhx2 at the top of a genetic hierarchy for barrel development.

In this study, we provide evidence that Lhx2 regulates the development of L4 neuron dendritic asymmetry by directly inducing *Btbd3* expression in S1 L4. Knocking down *Btbd3* expression leads to a failure of L4 neurons to develop dendritic asymmetry (Matsui et al., 2013), similar to what we observed when deleting Lhx2. Intriguingly, *Btbd3* expression in S1 was downregulated in *Lhx2* cKO mice, similar to when VP TCA inputs were eliminated (Pouchelon et al., 2014). However, its expression remained in the S1 in cortex-specific knockouts of *NR1*, *mGluR5*, or *Lmo4* (Matsui et al., 2013; Figure S4), despite their defects in barrel formation (Ballester-Rosado et al., 2010; Kashani et al., 2006). As NR1, mGluR5, and Lmo4 were shown to mediate activity-dependent barrel development, based on our findings, we propose that Lhx2 functions in L4 neurons prior to activity-regulated events. Further, by inducing the expression of *Btbd3* and other activity-regulated genes, Lhx2 provides L4 neuronal competency to respond to TCA activities.

Further, our findings suggest that Lhx2 in postsynaptic L4 neurons is required for presynaptic TCAs to arborize in the barrel

hollow. The downregulation of *EphrinA5* and *Adcy1* in cKO S1 could possibly lead to TCA development defects, as EphrinA5 was proposed to induce TCA axonal arborization in S1 (Uziel et al., 2008) and *Adcy1* mutation reportedly led to changes in thalamocortical synaptic activity and TCA projection patterns (Abdel-Majid et al., 1998; Lu et al., 2003; Welker et al., 1996). Nevertheless, we found defects in patterning of barrel rows within cKO S1. It is likely that in L4 neurons, Lhx2 regulates the expression of key factors involved in patterning barrel cortex. In additional to its function in postmitotic neurons, Lhx2 is likely to play additional roles in cortical progenitors to regulate TCA development, as a previous study reported that the deletion of *Lhx2* in cortical progenitors via *Emx1*-Cre leads to an almost complete loss of TCAs in the cortex (Shetty et al., 2013). The fact that *Lhx2* deletion in cortical progenitors altered the timing of neurogenesis and led to a significantly decreased number of superficial layer neurons (Chou and O'Leary, 2013; Hsu et al., 2015) could contribute to the loss of TCAs in the cortex.

In conclusion, our study contributes to the understanding of the initial steps of barrel cortex circuit formation taken by L4 neurons to perceive TCA inputs. Lhx2 serves as a key regulator for the L4 neurons to form cellular barrels, develop dendritic asymmetry, and further induce TCA arborization.

EXPERIMENTAL PROCEDURES

Detailed experimental materials and methods and the different mouse lines used in this study, along with their sources, are described in Supplemental Experimental Procedures. All experiments were conducted in accordance with guidelines of the Academia Sinica Institutional Animal Care and Use Committee.

Immunohistochemistry, Immunostaining, and In Situ Hybridization

CO staining, immunostaining, and in situ hybridization using digoxigenin (DIG)-labeled riboprobes were performed as described previously (Chou et al., 2009; Zembrzycki et al., 2013).

Whisker Trimming and Enriched Environment Stimulation

Mice were anesthetized with Avertin (1.6 mg/mL, intraperitoneally [i.p.], 200 μL/10g body weight [b.w.]), and vibrissae on one side of the whisker pad were cut to fur level (<1 mm), except for C2. 1 day after recovery, mice were sacrificed after explored in enriched environment for 1 hr. The c-Fos distribution was measured by values of integrated density for the intensity of the fluorescence signals.

Chromatin Immunoprecipitation Assay

ChIP assays were performed as described previously (Carey et al., 2009). Dissociated cells from P7 WT S1 were fixed in 1% formaldehyde and then resuspended in lysis buffer (50 mM Tris [pH 8.0], 10 mM EDTA, 1% SDS, and 1× protease inhibitor). Chromatin was sonicated to an average size of 150–500 bp. 2μg antibodies (goat anti-Lhx2 antibody sc-19344 [Santa Cruz Biotechnology] or normal goat immunoglobulin G [IgG]) were used for immunoprecipitation. See Supplemental Experimental Procedures for primer sequences.

In Utero Electroporation

A DNA mixture containing US2-LNL (*loxP*-neomycin-Stop-*loxP*)-GFP (1.0 μg/μL), CAG-mCherry (0.2 μg/μL), and CAG-Cre (0.5 μg/μL) with or without US2-myc-Btbd3 (0.2 μg/μL) was electroporated into mouse dorsal telencephalon at E14.5 with paddle-type electrodes (CUY21 Electroporator) in a series of five square-wave current pulses (35 V, 100 ms × 5). Electroporated brains were collected at P7 for further analyses.

Statistical Analysis

Statistical analysis was performed using GraphPad Prism 5 software. Student's t test or ANOVA were used throughout the study. All data are expressed as mean ± SEM.

ACCESSION NUMBERS

The accession number for the microarray data reported in this paper is NCBI GEO: GSE92372.

SUPPLEMENTAL INFORMATION

Supplemental Information includes Supplemental Experimental Procedures, four figures, and two tables and can be found with this article online at http://dx.doi.org/10.1016/j.celrep.2017.01.001.

AUTHOR CONTRIBUTIONS

C.-F.W. and S.-J.C. designed the research and C.-F.W., H.-W.H., Z.-H.C., M.-H.W., W.-J.C., C.G.B., M.N., B.C.S., and S.-J.C. performed the research and analyzed data. S.-J.C. wrote the paper.

ACKNOWLEDGMENTS

We thank Dr. Dennis O'Leary for providing *Lhx2* floxed mice, Dr. Klaus-Armin Nave for *Nex*-Cre, Drs. Sam Pfaff and Soo-Kyung Lee for *Lmo4* floxed mice, and Dr. Hui-Chen Lu for *mGluR5* mutant brain tissues. We also thank Drs. Hwai-Jong Cheng and Hui-Chen Lu for critical reading and valuable comments and members of the Chou laboratory for their input and technical assistance. This work was supported by the Taiwan Ministry of Science and Technology (grants 104-2321-B-001-062 and 105-2321-B-001-042) (S.-J.C.) and the Institute of Cellular and Organismic Biology, Academia Sinica. M.N. is supported by the Ramón Areces Foundation, the Spanish Ministerio de Economía y Competetividad (MINECO; grants SAF2014-52119-R and BFU2014-55738-REDT). C.G.B. is supported by the Spanish Ministerio de Ciencia e Innovación (MICINN; fellowship FPI-BES-2012-056011).

Received: August 22, 2016
Revised: December 3, 2016
Accepted: December 29, 2016
Published: January 24, 2017

REFERENCES

Abdel-Majid, R.M., Leong, W.L., Schalkwyk, L.C., Smallman, D.S., Wong, S.T., Storm, D.R., Fine, A., Dobson, M.J., Guernsey, D.L., and Neumann, P.E. (1998). Loss of adenylyl cyclase I activity disrupts patterning of mouse somatosensory cortex. Nat. Genet. *19*, 289–291.

Ballester-Rosado, C.J., Albright, M.J., Wu, C.S., Liao, C.C., Zhu, J., Xu, J., Lee, L.J., and Lu, H.C. (2010). mGluR5 in cortical excitatory neurons exerts both cell-autonomous and -nonautonomous influences on cortical somatosensory circuit formation. J. Neurosci. *30*, 16896–16909.

Bulchand, S., Subramanian, L., and Tole, S. (2003). Dynamic spatiotemporal expression of LIM genes and cofactors in the embryonic and postnatal cerebral cortex. Dev. Dyn. *226*, 460–469.

Carey, M.F., Peterson, C.L., and Smale, S.T. (2009). Chromatin immunoprecipitation (ChIP). Cold Spring Harb. Protoc. *2009*, pdb prot5279.

Chen, T.C., Cheng, Y.Y., Sun, W.Z., and Shyu, B.C. (2008). Differential regulation of morphine antinociceptive effects by endogenous enkephalinergic system in the forebrain of mice. Mol. Pain *4*, 41.

Chou, S.J., and O'Leary, D.D. (2013). Role for Lhx2 in corticogenesis through regulation of progenitor differentiation. Mol. Cell. Neurosci. *56*, 1–9.

Chou, S.J., Perez-Garcia, C.G., Kroll, T.T., and O'Leary, D.D. (2009). Lhx2 specifies regional fate in Emx1 lineage of telencephalic progenitors generating cerebral cortex. Nat. Neurosci. *12*, 1381–1389.

Ding, Y.Q., Yin, J., Xu, H.M., Jacquin, M.F., and Chen, Z.F. (2003). Formation of whisker-related principal sensory nucleus-based lemniscal pathway requires a paired homeodomain transcription factor, Drg11. J. Neurosci. *23*, 7246–7254.

Erzurumlu, R.S., and Gaspar, P. (2012). Development and critical period plasticity of the barrel cortex. Eur. J. Neurosci. *35*, 1540–1553.

Erzurumlu, R.S., and Kind, P.C. (2001). Neural activity: sculptor of 'barrels' in the neocortex. Trends Neurosci. *24*, 589–595.

Goebbels, S., Bormuth, I., Bode, U., Hermanson, O., Schwab, M.H., and Nave, K.A. (2006). Genetic targeting of principal neurons in neocortex and hippocampus of NEX-Cre mice. Genesis *44*, 611–621.

Hou, P.S., Chuang, C.Y., Kao, C.F., Chou, S.J., Stone, L., Ho, H.N., Chien, C.L., and Kuo, H.C. (2013). LHX2 regulates the neural differentiation of human embryonic stem cells via transcriptional modulation of PAX6 and CER1. Nucleic Acids Res. *41*, 7753–7770.

Hsu, L.C., Nam, S., Cui, Y., Chang, C.P., Wang, C.F., Kuo, H.C., Touboul, J.D., and Chou, S.J. (2015). Lhx2 regulates the timing of β-catenin-dependent cortical neurogenesis. Proc. Natl. Acad. Sci. USA *112*, 12199–12204.

Ince-Dunn, G., Hall, B.J., Hu, S.C., Ripley, B., Huganir, R.L., Olson, J.M., Tapscott, S.J., and Ghosh, A. (2006). Regulation of thalamocortical patterning and synaptic maturation by NeuroD2. Neuron *49*, 683–695.

Jabaudon, D., Shnider, S.J., Tischfield, D.J., Galazo, M.J., and Macklis, J.D. (2012). RORβ induces barrel-like neuronal clusters in the developing neocortex. Cereb. Cortex *22*, 996–1006.

Kashani, A.H., Qiu, Z., Jurata, L., Lee, S.K., Pfaff, S., Goebbels, S., Nave, K.A., and Ghosh, A. (2006). Calcium activation of the LMO4 transcription complex and its role in the patterning of thalamocortical connections. J. Neurosci. *26*, 8398–8408.

Li, H., and Crair, M.C. (2011). How do barrels form in somatosensory cortex? Ann. N Y Acad. Sci. *1225*, 119–129.

Lu, H.C., She, W.C., Plas, D.T., Neumann, P.E., Janz, R., and Crair, M.C. (2003). Adenylyl cyclase I regulates AMPA receptor trafficking during mouse cortical 'barrel' map development. Nat. Neurosci. *6*, 939–947.

Matsui, A., Tran, M., Yoshida, A.C., Kikuchi, S.S., U, M., Ogawa, M., and Shimogori, T. (2013). BTBD3 controls dendrite orientation toward active axons in mammalian neocortex. Science *342*, 1114–1118.

Mi, H., Muruganujan, A., Casagrande, J.T., and Thomas, P.D. (2013). Large-scale gene function analysis with the PANTHER classification system. Nat. Protoc. *8*, 1551–1566.

Nakagawa, Y., Johnson, J.E., and O'Leary, D.D. (1999). Graded and areal expression patterns of regulatory genes and cadherins in embryonic neocortex independent of thalamocortical input. J. Neurosci. *19*, 10877–10885.

Petersen, C.C. (2007). The functional organization of the barrel cortex. Neuron *56*, 339–355.

Pouchelon, G., Gambino, F., Bellone, C., Telley, L., Vitali, I., Lüscher, C., Holtmaat, A., and Jabaudon, D. (2014). Modality-specific thalamocortical inputs instruct the identity of postsynaptic L4 neurons. Nature *511*, 471–474.

Rebsam, A., Seif, I., and Gaspar, P. (2005). Dissociating barrel development and lesion-induced plasticity in the mouse somatosensory cortex. J. Neurosci. *25*, 706–710.

Rétaux, S., and Bachy, I. (2002). A short history of LIM domains (1993-2002): from protein interaction to degradation. Mol. Neurobiol. *26*, 269–281.

Roberson, M.S., Schoderbek, W.E., Tremml, G., and Maurer, R.A. (1994). Activation of the glycoprotein hormone alpha-subunit promoter by a LIM-homeodomain transcription factor. Mol. Cell. Biol. *14*, 2985–2993.

Rodríguez-Tornos, F.M., San Aniceto, I., Cubelos, B., and Nieto, M. (2013). Enrichment of conserved synaptic activity-responsive element in neuronal genes predicts a coordinated response of MEF2, CREB and SRF. PLoS ONE *8*, e53848.

Shetty, A.S., Godbole, G., Maheshwari, U., Padmanabhan, H., Chaudhary, R., Muralidharan, B., Hou, P.S., Monuki, E.S., Kuo, H.C., Rema, V., and Tole, S. (2013). Lhx2 regulates a cortex-specific mechanism for barrel formation. Proc. Natl. Acad. Sci. USA *110*, E4913–E4921.

Shirasaki, R., and Pfaff, S.L. (2002). Transcriptional codes and the control of neuronal identity. Annu. Rev. Neurosci. *25*, 251–281.

Uziel, D., Mühlfriedel, S., and Bolz, J. (2008). Ephrin-A5 promotes the formation of terminal thalamocortical arbors. Neuroreport *19*, 877–881.

Vitali, I., and Jabaudon, D. (2014). Synaptic biology of barrel cortex circuit assembly. Semin. Cell Dev. Biol. *35*, 156–164.

Welker, E., Armstrong-James, M., Bronchti, G., Ourednik, W., Gheorghita-Baechler, F., Dubois, R., Guernsey, D.L., Van der Loos, H., and Neumann, P.E. (1996). Altered sensory processing in the somatosensory cortex of the mouse mutant barrelless. Science *271*, 1864–1867.

Wu, C.S., Ballester Rosado, C.J., and Lu, H.C. (2011). What can we get from 'barrels': the rodent barrel cortex as a model for studying the establishment of neural circuits. Eur. J. Neurosci. *34*, 1663–1676.

Yang, J.W., Shih, H.C., and Shyu, B.C. (2006). Intracortical circuits in rat anterior cingulate cortex are activated by nociceptive inputs mediated by medial thalamus. J. Neurophysiol. *96*, 3409–3422.

Zembrzycki, A., Chou, S.J., Ashery-Padan, R., Stoykova, A., and O'Leary, D.D. (2013). Sensory cortex limits cortical maps and drives top-down plasticity in thalamocortical circuits. Nat Neurosci. *16*, 1060–1067.

Zembrzycki, A., Perez-Garcia, C.G., Wang, C.F., Chou, S.J., and O'Leary, D.D. (2015). Postmitotic regulation of sensory area patterning in the mammalian neocortex by Lhx2. Proc. Natl. Acad. Sci. USA *112*, 6736–6741.

Cell Reports, Volume *18*

Supplemental Information

Lhx2 Expression in Postmitotic Cortical Neurons Initiates Assembly of the Thalamocortical Somatosensory Circuit

Chia-Fang Wang, Hsiang-Wei Hsing, Zi-Hui Zhuang, Meng-Hsuan Wen, Wei-Jen Chang, Carlos G. Briz, Marta Nieto, Bai Chuang Shyu, and Shen-Ju Chou

Supplemental Experimental Procedures:

Mouse lines
Lhx2, *Lmo4* floxed and *Nex*-Cre mice were generated as described (Chou et al., 2009; Goebbels et al., 2006; Kashani et al., 2006). All lines were maintained on a C57BL/6 background. Mouse colonies were maintained following guidelines of the Academia Sinica Institutional Animal Care and Use Committee.

Immunohistochemistry and immunostaining
Primary and secondary antibodies used were rabbit anti-5HT (ImmunoStar, cat. 20080), rabbit anti-Ctip2 (Novus, cat. NB100-2600), rabbit anti-c-fos (Cell Signaling, cat. 2250), chick anti-GFP (Abcam, cat. Ab13970), goat anti-Lhx2 (Santa Cruz, cat. sc-19344), mouse anti-myc (Sigma, cat. 05419), mouse anti-Satb2 (Abcam, cat. ab51502), guinea pig anti-vGluT2 (Millipore, cat. AB2251), EdU (Click-iT EdU Imaging kit, Molecular Probes, cat. C10637) and biotinylated or Alexa-conjugated secondary antibodies (Jackson ImmunoResearch).

In situ hybridization
Brains were fixed with 4% paraformaldehyde in PBS, cryoprotected with 30% sucrose in 0.1 M PBS, embedded in Tissue Tek OCT compound (Sakura Finetek) and cut in 20 μm sections on a cryostat. *In situ* hybridization using digoxigenin (DIG)-labeled riboprobes was undertaken as described (Chou et al., 2009; Zembrzycki et al., 2013).

Characterization of the barrel cortex
The size and length of the PMBSF area was measured according to the vGluT2 immunostained tangential section of P7 cortices using ImageJ. The PMBSF area including barrels α, β, γ, δ, A1-A4, B1-B4, C1-C5, D1-D5, and E1-E5 was outlined. The hollow area was defined by the vGluT2-positive patches in the PMBSF. The PMBSF area minus the hollow was defined as septa area. The distance between barrels A2 and E2 was defined as the PMBSF length along the arc; the distance from barrel β across the center of C1 to C5 was defined as the length along the row. To measure cell density, a 200 pixels (129.4μm) wide and 620 pixels (400μm) long box was drawn across the C2 barrel. The fluorescence intensity of DAPI and vGluT2 staining was quantified by imageJ. These numerical data were calculated by GraphPad prism 5.

Recording evoked field potentials in S1
Recording method was followed by procedures described in previous paper (Chen et al., 2008). Extracellular field potentials were evoked by electrical pulses (3 mA, 0.5 ms duration, AM systems isolated pulse stimulator modal 2100). Silver ball was placed on S1 surface to search the location with maximal positive field potential responses (~3 mm posterior and 4 mm lateral to bregma, Axoclamp 900A) and designate it as the insertion point for the multichannel electrode (NeuroNexus, 16 contact points, 100μm interval spacing). The multichannel electrode was inserted vertically to record 16 channels of extracellular field potentials simultaneously in the S1. An Ag-AgCl reference electrode was placed in the nasal cavity. The sampling rate of recorded analog signals was 6 kHz and data were processed using a multichannel data acquisition system (TDT Inc., USA). At the end of the experiment, a small lesion was made by passing an anodal current (30mA, 5s) to the deepest electrode of the multichannel electrode. Another lesion was made at the same lead after the multichannel electrode was withdrawn by 500μm. The brains were then fixed with 4% paraformaldehyde and sliced in 40μm-thick coronal sections. The sections were stained with cresyl violet (Sigma) to visualize the electrode tracks and lesion markers in the S1 regions. The positions of recording points were estimated by determining their distance from lesion site.

Current source densities method
A five-point formula (Yang et al., 2006) was adopted for the time span and sampling variations in each recording session in order to smooth the spatial sampling variability. The extracellular current, I_m was derived from the second spatial derivations of the extracellular field potentials, φ, and was calculated with the finite difference formula:

$$I_m = -\left(\frac{1}{kh^2}\right)\sum_{m=-n}^{n} a_m \emptyset(x+mh),$$

where h is the distance between successive measuring points (100μm in the present investigation), and x is the coordinate perpendicular to the cortical layer. The remaining constants are as follows: n = 2, k = 4, a0 = -2, a±1 = 0 and a± 2 = 1.

Chromatin immunoprecipitation (ChIP) assay

The precipitated DNA was purified with QIAquick PCR purification kit (Qiagen, cat. 28106) and quantified by qPCR using LightCycler® 480 SYBR Green I Master (Roche, cat. 04887352001). The primer sequences were provided below. Enrichment of binding (% Input) was determined as immunoprecipitated-DNA/ input-DNA. The level of Lhx2 specific binding on the region of interest was quantified by comparing the normalized enrichment of anti-Lhx2 to the enrichment of IgG, which was set as one for data presentation. Each experiment was repeated at least three times, with each replicate producing a similar pattern. The statistic significance between Lhx2 verse IgG binding was computed by matched two-way ANOVA with Bonferroni post-test, using GraphPad Prism® software.
Primers used for ChIP assays:
Primers for amplifying the *Btbd3* promoters containing putative Lhx2 binding sites are: binding site 1 (BS1) (F: TCCTGAGCAGTGCCCTATCT, R: ACTCAAGCATAAGGCAGACTGT); binding site 2 (BS2) (F: CTGCCTTATGCTTGAGTACAGC, R: CCCAGGTCACAAAACACAGTT); binding site 3 (BS3) (F: AACCCCTCCCTTCCTGTTTG, R: AGGAGCAGCAGTTACATTCTCT).
Primers amplifying the *Btbd3* promoter without Lhx2 binding site (neg.) was used as a negative control (F: AATCCTGATTGGT GGCTTCA, R: CCCTGCAGACGGAGTCAG).
Primers on *Pax6* enhancer (Pax6E) were designed as previous reported (Shetty et al., 2013) (F: CCCCAGCGTGTGATTTGAG, R: CGCTGCTAGGAACCCGTT).
Primers amplifying the region with putative Lhx2 binding sites on *Adcy1* promoter are (F: ATTCCCGTGACCCACACATC, R: AAGCTGATGCCTGCTATGGG);
Primers amplifying the region with putative Lhx2 binding sites on *Efna5* promoter are (F: CAGTTGGTCAGTCATGCAGTC, R: GGGCGTTACTGGACGTGAT).
Primers amplifying the region with putative Lhx2 binding sites on *Lmo4* promoter are (F: CACCAACATGGGGGAAAAGG, R: CAGGGAAGGTGGGAAAGGTG).

Microarray

RNA samples extracted from primary somatosensory cortex (S1) of P7 mice using TriPure Isolation Reagent (Roche, cat. 11667165001). For microarray analysis, the RNA quality of was analyzed by 2100 BioAnalyzer (Agilent Technologies). Total RNA was amplified by a Low Input Quick-Amp Labeling kit (Agilent Technologies, USA), labeled with Cy3 (CyDye, Agilent Technologies, USA), fragmented and hybridized to Agilent SurePrint G3 Mouse GE 8×60K Microarray (Agilent Technologies, USA). Fold change (FC) is the normalized log2 ratio of the expression level of a probe. The data discussed in this publication have been deposited in NCBI's Gene Expression Omnibus (Edgar *et al*., 2002) and are accessible through GEO Series accession number GSE92372.

Quantitative RT-PCR

RNA isolated from P7 somatosensory cortex using TriPure Isolation Reagent (Roche), and genomic DNA was eliminated by DNaseI (Promega, cat. 9PIM610) digestion. First-strand cDNAs were synthesized from 1 μg total RNA using Transcriptor First Strand cDNA Synthesis Kit (Roche, cat. 48970300001), and 0.2 μl of cDNA mixture was used for each quantitative PCR reaction. Real time RT-PCR was undertaken using LightCycler® 480 SYBR Green I Master mix (Roche). Gene expression was normalized to GAPDH and data were analyzed by two-tailed, unpaired *t*-test with Welch's correction. *, $p<0.05$; **, $p<0.01$; ***, $p<0.001$.
Primers used for qPCR:
Adcy1 (F: CCTTTTGGTCACCTTCGTGT, R: GCTGTGACCAGTAAGTGCGA);
Btbd3 (F: GATGAAATCCGAATCCCAGA, R: TGTGTCTGCAGCCAAGTCA);
EphrinA5 (F: GCCAGGCCGAGAGTATTT C, R: CAGGACCTTCTTCCGTTGTC);
GAPDH (F: GGCAAATTCAACGGCAC AG, R: CGGAGATGATGACCCTTTTGG);
Lhx2 (F: GCATCTACTGCAAAGAAGACTACTACA, R: CGCATCACCATCTCTGAGG);
Lmo4 (F: TTGCAATATAGGGGAGAAGCA, R: TCCATGGCATAGAGCAGAAA);
mGluR5 (F: ATCTGCCTGGGTTACTTGTG, R: GCAATACGGTTGGTCTTCG);
NeuroD2 (F: GCTGTCCAAGATCGAGACCC, R: GCACGTAGGACACCAGATCC);
NR1 (F: CCATATCATCCTGCTGGTCA, R: CACCTTCTCTGCCTTGGACT);
RORb (F: TCTGAGGGTGAAGATAGCAACC, R: AAGCGCCAGTTTCACCAG).

Cell culture
Neuro2A (N2a) mouse neuroblastoma cells were cultured in Dulbecco's modified Eagle's medium (Gibco, cat. 12100) supplemented with 10% heat-inactivated fetal bovine serum (GE) under humidified air containing 5% CO_2 at 37 °C. Media for N2a cells was supplemented with 1% mM sodium pyruvate (Gibco, cat. 11360070). Transfections were performed using Lipofectamine2000 (Invitrogen, cat. 11668019) and 3μg of plasmids, including a luciferase (Luc) reporter, CAG-Lhx2 or CAG empty vectors and TK-renilla luciferase. Luciferase assays were performed by using Dual-Glo® Luciferase Assay System (Promega, cat. E2940), and transfection efficiency was normalized to renilla luciferase activity. Cortical neurons isolated from embryonic day 17.5 mouse brains were seeded on poly-L-lysine-coated 12mm coverslip and cultured in neurobasal medium (Invitrogen, cat. 21103049) with 0.5mM Glutamine (Invitrogen, cat. 25030081), 1x Antibiotic-Antimycotic (Invitrogen, cat. 15240062), and 1x B27 supplement (Invitrogen, cat. 17504044)(Huang et al., 2007). US2-myc-Btbd3 (0.8μg was used for transfection) transfected cells were lysed 24 hrs after transfection with Laemmli sample buffer for western blot analysis (Wang and Huang, 2013).

Construction of Btbd3-Luc reporters
The WT reporter contains the 1.3 kb genomic DNA sequence upstream to the *Btbd3* transcription start site in pGL3-basic vector containing firefly luciferase. For the *Btbd3* promoter mutant reporter constructs (m1, m2, m3, m12, m13, m23 and m123), relevant putative Lhx2 binding sites (TAATTA) were mutated to GTCGAG by PCR. For luciferase assays, reads for pGL3-basic and WT (co-transfected with CAG empty vectors) were set to 0 and 1, respectively.

In utero electroporation and cellular morphology analyses
For rescue experiments, we generated the US2-myc-Btbd3 construct, consisting of the Btbd3 coding sequence (FANTOM clone, D430043L03) with a myc tag at the N-terminus under the control of US2 promoter. The electroporation domain was determined by mCherry expression. The cortices with mCherry expression in the S1 were flattened and their tangential sections were stained for GFP and vGluT2. We have noted that the total dendritic length was decreased in the cells co-electroporated with 4 plasmids (CAG-Cre, CAG-mCherry, US2-LNL-GFP and US2-Btbd3) than with 3 constructs (CAG-Cre, CAG-mCherry and US2-LNL-GFP).

Imaging
Images were acquired using a TCS-SP5 confocal microscope (Leica) and analyzed using IMARIS software. Cell counts were made on coronal section images at matching rostral-caudal and medial-lateral levels. Statistical comparisons of cell counts in mutant and control mice were made using a paired t-test.

Supplemental Figures:

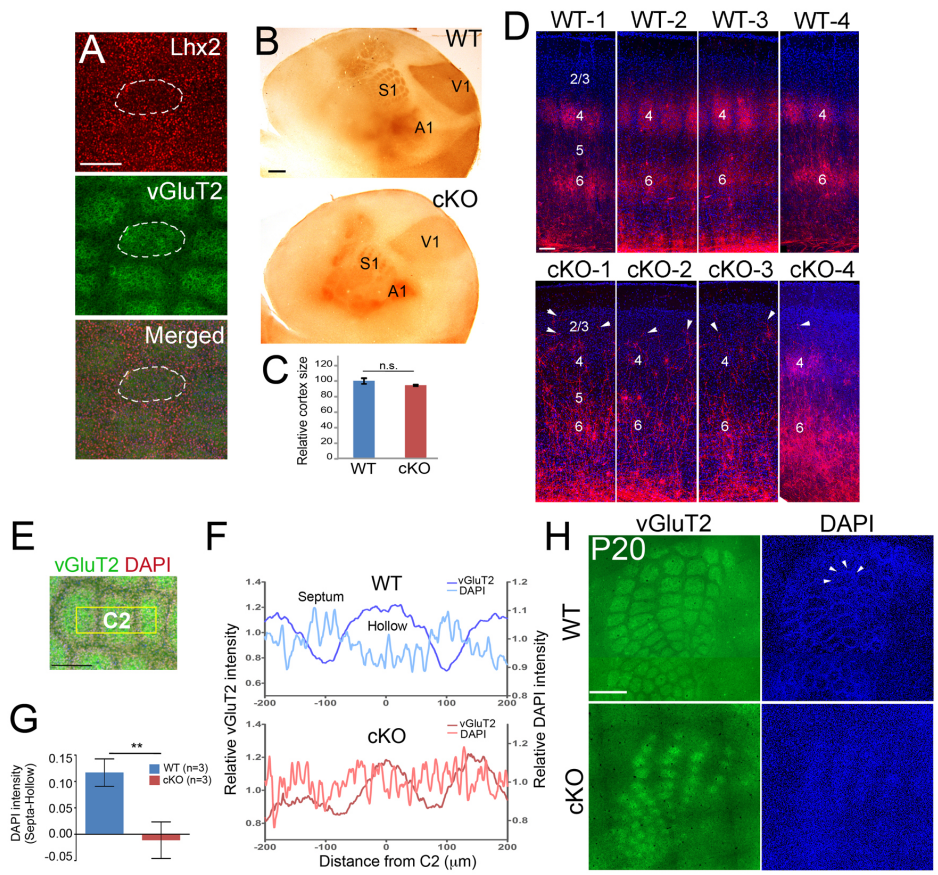

Figure S1 Characterization of *Lhx2* cKO cortex (related to Figure 1)
(A) Immunostaining of tangential sections through layer 4 of P7 flattened cortices with anti-Lhx2 antibody (red). Thalamocortical axons were marked by vGluT2 staining (green). Lhx2 positive neurons are enriched outside the barrel hollow region (circled). (B) Immunostaining for 5HT on tangential sections through layer 4 of P7 flattened cortices to determine the location of primary sensory areas. The primary sensory areas, including visual cortex (V1), somatosensory cortex (S1) and auditory cortex (A1), were present in WT and cKO. However, the location of these primary sensory areas showed a rostral shift in the cKO. (C)The cortex size is similar in P7 WT and cKO mice. (D). TCA projections were labeled by DiI injected into VP of the thalamus in multiple pairs of P7 WT and Lhx2 cKO brains. Coronal sections were counterstained with DAPI. While VP neuronal axons in WT arborize in layer 4 (4) to fill the barrel hollow, VP neuronal axons in cKO mice fail to arborize at L4, and some axonal terminals (arrowheads) remain in layers 2/3. (E) A representative image illustrating the measured area across C2 barrel in WT, TCAs were labeled by vGluT2 (green) and L4 neurons were labeled by DAPI (red). (F) In WT (top), DAPI intensity was higher in septa where vGluT2 intensity was lower, while no difference was detected between hollow and septa in cKO (bottom). (G) The difference of cell densities was demonstrated by subtracting DAPI signal intensity in septa to that in hollow, which was significantly decreased in cKO when compared with WT littermates (p<0.01, n=3). (H) Immunostaining against vGluT2 on tangential sections of P20 WT and cKO cortices reveals the location of thalamocortical inputs in the S1. DAPI staining reveals the cellular barrels surrounding the TCA inputs in WT (arrowheads) but not in the cKO. Scale bars, 200μm (A, E), 500μm (B, H) and 100μm (D).

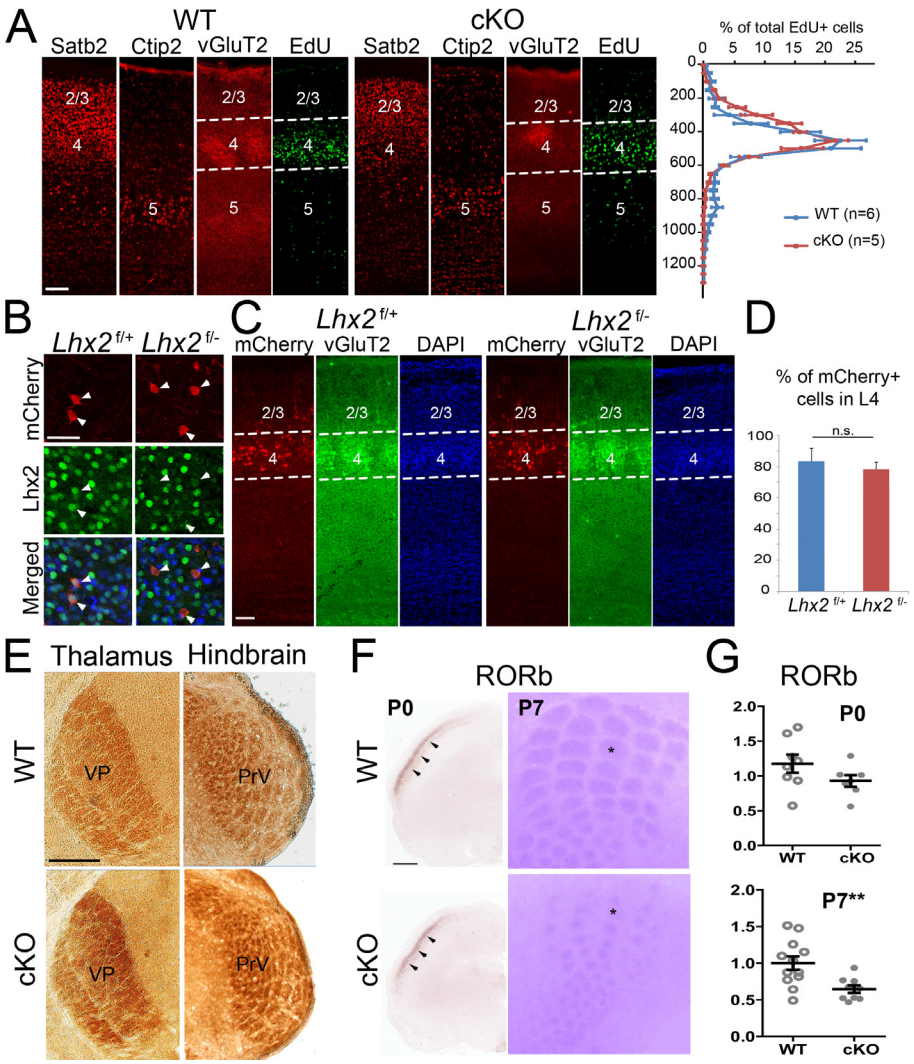

Figure S2 The loss of *Lhx2* in postmitotic neurons did not affect cortical layer formation, L4 neuronal migration, whisker sensory pathway, or the initial L4 neuronal specification (related to Figure 1 and 2)

(A) No significant defects in layer formation were detected in Lhx2 cKO at P7. In WT and cKO cortices at P7, the majority of neurons born on E14.5 (labeled by EdU) were similarly distributed in L4 (between the dotted lines, as labeled by vGluT2) (p=0.3667, by two-way ANOVA; n=4). (B-D) CAG-Cre and CAG-mCherry were electroporated into $Lhx2^{f/+}$ and $Lhx2^{f/-}$ embryonic cortices at E14.5. (B) Lhx2 expression (green) is detected in mCherry-positive (red) electroporated neurons (arrowheads) in $Lhx2^{f/+}$ cortex, but not in $Lhx2^{f/-}$ cortex. (C-D) Approximately 80% mCherry-positive electroporated neurons (red) are located in L4 [between the dotted lines, marked by vGluT2 staining (green)] in both $Lhx2^{f/+}$ and $Lhx2^{f/-}$ cortices at P7 (p=0.4914, n=4). (E) Cytochrome oxidase (CO) staining on coronal sections of P10 WT and cKO brains revealed the similar location and size of ventral posterior (VP) nucleus in the thalamus and PrV in the brain stem in WT and cKO. (F) *In situ* hybridization for RORb (arrowheads), a layer 4 marker, on coronal sections of P0 cortices and on tangential sections of P7 cortices. Similar RORb expression was detected in WT and cKO at P0. RORb is expressed in 5HT and vGluT2 positive barrels (as shown in Figure 1) in both WT and cKO at P7, although the barrels are smaller in cKO. * marked the C2 barrel. (G) Demonstrated by qPCR, the expression level of RORb in S1 showed no significant difference between WT and cKO cortices at P0, but was significantly down-regulated in cKO at P7. Scale bars, 200μm (A, C, E, F), 50μm (B).

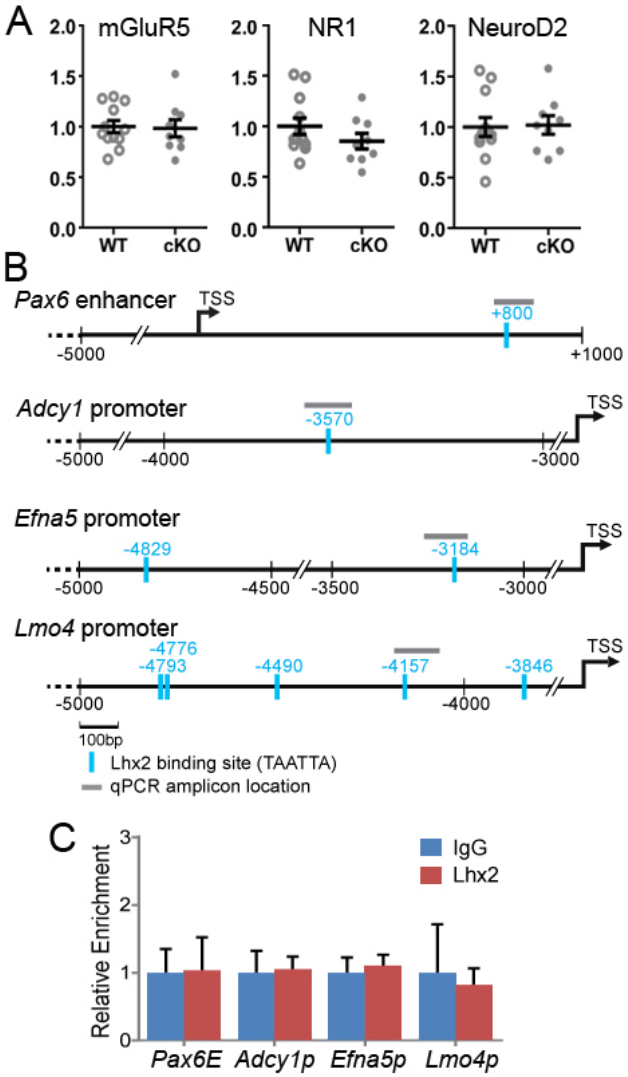

Figure S3 In P7 S1, Lhx2 does not regulate the expression of *mGluR5*, *NR1* or *NeuroD2*, nor directly bind to the enhancer region of *Pax6*, or the promoter regions of the *Adcy1*, *Efna5* and *Lmo4* genes (related to Figure 3)

(A) The expression levels of *mGluR5*, *NR1* and *NeuroD2* were similar between WT and cKO at P7. (B) Schemes illustrating the putative Lhx2 binding sites and the regions of designed PCR amplicon on the *Pax6* enhancer and promoters of *Adcy1*, *Efna5* and *Lmo4*. TSS, transcription start site. (C) Result of ChIP assay by anti-Lhx2 or normal IgG with WT S1 tissues. None of these putative Lhx2 binding sites showed enriched Lhx2 binding (n= 3~8, pair-matched two-way ANOVA with Bonferroni post-test). Additional putative Lhx2 binding sites in the Lmo4 promoter were also tested with corresponding primer sets. However, these primers fail to generate prominent PCR products.

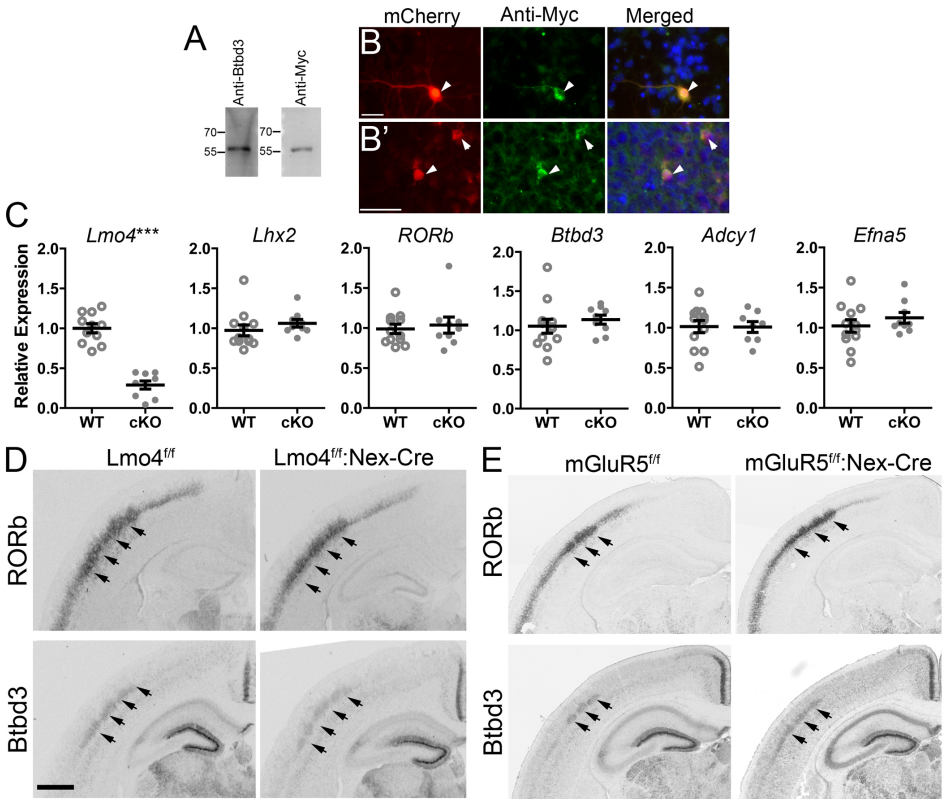

Figure S4 Btbd3 overexpression with the US2-myc-Btbd3 construct and maintained Btbd3 expression in the *Lmo4* and *mGluR5* mutant cortices (related to Figure 3 and 4)

(A) Btbd3 expression was detected in US2-myc-Btbd3 transfected N2A cells by western blotting with anti-Btbd3 and anti-myc antibodies. (B, B') US2-myc-Btbd3 and CAG-mCherry were electroporated into dorsal telencephalon at E14.5. (B) Myc-Btbd3 expression was detected by immunostaining with anti-myc antibody in the mCherry expressing cortical neurons collected from the electroporated cortex at E17.5 and cultured until DIV5. (B') Immunostaining with anti-myc antibody confirmed the expression of myc-Btbd3 in the mCherry expressing cortical neurons on coronal sections of P7 electroporated cortices. (C) Quantitative RT-PCR analyses were performed with RNA collected from S1 of WT and *Lmo4* cKO cortices at P7. *Lmo4* expression is significantly decreased in *Lmo4* cKO samples, while the expression levels of *Lhx2*, *RORb*, *Btbd3, Adcy1* and *Efna5* remained similar in WT and *Lmo4* cKO. Results are shown as the mean ± SEM. Gene expression levels were normalized to *GAPDH*, and data were analyzed by a two-tailed, unpaired *t*-test with Welch's correction. (n=8; ***, $p < 0.001$). (D) No detectable difference in the expression of *RORb* and *Btbd3* in the S1 L4 in WT (*Lmo4*$^{f/f}$) and *Lmo4* cKO (*Lmo4*$^{f/f}$; *Nex*-Cre) cortices. (E) No detectable difference in the expression of *RORb* and *Btbd3* in the S1 L4 in WT (*mGluR5*$^{f/f}$) and *mGluR5* cKO (*mGluR5*$^{f/f}$; *Nex*-Cre) cortices. Scale bars, 20μm (B), 50μm (B') and 200μm (D).

Supplemental Tables:

Table S1. Summary of changes in the expression level of activity-regulated genes in *Lhx2* cKO S1. (related to Figure 3)

Mouse Gene Symbol	Gene ID	Microarray results of Lhx2 cKO vs WT	
		FC	*p*-value
Ventrobasalis ablation-affected genes (Pouchelon 2014)			
Frzb	20378	-2.6452	0.0130
Pcdh20	219257	-1.8997	0.0027
Robo3	19649	-1.6427	0.0323
EphA8	13842	-1.6193	0.0412
Slc18a2	214084	-1.4279	0.0293
Tbata	65971	-1.4010	0.0010
Rorb	225998	-1.3779	0.0481
Btbd3	228662	-1.3655	0.0469
Lmo4	16911	-1.2809	0.0041
Fat3	270120	-1.2447	0.0152
PlxnD1	67784	-1.0882	0.0375
Camk1g	215303	1.2327	0.0044
Flrt3	71436	2.0292	0.0019
Bicucullin stimulation-dependent, SARE containing genes (Rodigues-Tornos, 2013;Upadhya, 2011; Benito, 2011; Liu, 2012)			
Cux1	13047	-2.1555	0.0137
Rasgef1b	320292	-1.5608	0.0010
Odz1 (Tenm3)	23965	-1.4871	0.0087
Atf3	11910	-1.3694	0.0348
Clic4	29876	-1.2880	0.0049
Fbxo33	70611	-1.2746	0.0418
Plxna4	243743	-1.2085	0.0477
Eif1	20918	-1.0934	0.0019
Scn3a	20269	1.2062	0.0075
Ncam1	17967	1.2071	0.0047
Rapgef2	76089	1.2160	0.0112
Hdac9	79221	1.2631	0.0490
Rapgef6	192786	1.3280	0.0101
Rabgap1l	29809	1.3379	0.0020
Nkain2	432450	1.3954	0.0144
Robo1	19876	1.7138	0.0158
Plxnc1	54712	1.7754	0.0405

Table S2. Summary of changes in the expression levels of barrel related genes in *Lhx2* cKO S1. (related to Figure 3)

Barrel Related Genes (Symbol)	Literature Summary				Expression level in *Lhx2* cKO S1 cortex		
	Condition	Barrel Pattern Phenotypes		Reference	Microarray Result (*Lhx2* cKO v.s. WT)		qPCR validation
		TCA patches in PMBSF	L4 Cellular Barrel		Fold change	p-value	
EphrinA5 (Efna5)	global KO	Normal (reduced axonal arbor)	n.d.	Uziel, D. *et.al.* (2008)	-2.122	8.17E-03	down***
		n.d.	+	Yabuta, N.H. *et.al.* (2000)			
Btbd3	EP-KD	n.d.	n.d.	Matsui, A. *et.al.* (2013)	-1.366	4.69E-02	down**
Lmo4	Nex-Cre cKO	Small patches	-	Kashani, A.H. *et.al.* (2006)	-1.281	4.13E-03	down*
AC1 (Adcy1)	global KO	No pattern	-	Iwasato, T. *et.al.* (2008); Abdel-Majid, R.M. *et.al.* (1998)	-1.207	6.62E-03	down***
	Emx1-Cre (KΔN) cKO	Normal	+ (reduced dendritic asymmetry)	Iwasato, T. *et.al.* (2008)			
	Emx1-Cre (KWN) cKO	Obscured patches	-	Suzuki, A. *et.al.* (2015)			
	5HTT-Cre cKO	Obscured patches or no pattern	-	Arakawa, H. et.al. (2014); Suzuki, A. et.al. (2015)			
	Emx1-Cre/ 5HTT-Cre double cKO	No pattern	-	Suzuki, A. *et.al.* (2015)			
NR1 (Grin1)	global KO	No pattern	n.d.	Li, Y. *et.al.* (1994)	±	n.s.	±
	Emx1-Cre cKO	Small patches	-	Iwasato, T. *et.al.* (2000); Datwani, A. *et.al.* (2002); Lee, L.J. *et.al.* (2005)			
	5HTT-Cre cKO	No pattern	-	Arakawa, H. et.al. (2014)			
	Low-level transgene in global KO	No pattern	-	Iwasato, T. *et.al.* (1997)			
mGluR5 (Grm5)	global KO	Normal	-	Wijetunge, L.S. *et.al.* (2008)	±	n.s.	±
		Normal row segregation, but no individual barrel patch	-	Hannan, A.J. *et.al.* (2001)			
	Nex-Cre cKO	Obscured patches	-	Ballester-Rosado, C.J. *et.al.* (2010)			
NeuroD2	global KO	No pattern	-	Ince-Dunn, G. *et.al.* (2006)	±	n.s.	±

KO, knockout; EP-KD, knockdown by electroporation; +, normal; -, absent; n.d., not determined; n.s., no significance ($p>0.05$); ±, not changed; *, $p<0.05$; **, $p<0.01$; ***, $p<0.001$

Supplemental references:

Abdel-Majid, R.M., Leong, W.L., Schalkwyk, L.C., Smallman, D.S., Wong, S.T., Storm, D.R., Fine, A., Dobson, M.J., Guernsey, D.L., and Neumann, P.E. (1998). Loss of adenylyl cyclase I activity disrupts patterning of mouse somatosensory cortex. Nat Genet *19*, 289-291.

Arakawa, H., Akkentli, F., and Erzurumlu, R.S. (2014a). Region-Specific Disruption of Adenylate Cyclase Type 1 Gene Differentially Affects Somatosensorimotor Behaviors in Mice(1,2,3). eNeuro *1*.

Arakawa, H., Suzuki, A., Zhao, S., Tsytsarev, V., Lo, F.S., Hayashi, Y., Itohara, S., Iwasato, T., and Erzurumlu, R.S. (2014b). Thalamic NMDA receptor function is necessary for patterning of the thalamocortical somatosensory map and for sensorimotor behaviors. J Neurosci *34*, 12001-12014.

Benito, E., Valor, L.M., Jimenez-Minchan, M., Huber, W., and Barco, A. (2011). cAMP response element-binding protein is a primary hub of activity-driven neuronal gene expression. J Neurosci *31*, 18237-18250.

Datwani, A., Iwasato, T., Itohara, S., and Erzurumlu, R.S. (2002). NMDA receptor-dependent pattern transfer from afferents to postsynaptic cells and dendritic differentiation in the barrel cortex. Mol Cell Neurosci *21*, 477-492.

Edgar, R., Domrachev, M., Lash, A.E. (2002). Gene Expression Omnibus: NCBI gene expression and hybridization array data repository. Nucleic Acids Res. *30*, 207-210.

Hannan, A.J., Blakemore, C., Katsnelson, A., Vitalis, T., Huber, K.M., Bear, M., Roder, J., Kim, D., Shin, H.S., and Kind, P.C. (2001). PLC-beta1, activated via mGluRs, mediates activity-dependent differentiation in cerebral cortex. Nat Neurosci *4*, 282-288.

Huang Y.S., and Richter J.D. (2007) Analysis of mRNA translation in cultured hippocampal neurons. Methods Enzymol *431*, 143-62.

Iwasato, T., Datwani, A., Wolf, A.M., Nishiyama, H., Taguchi, Y., Tonegawa, S., Knopfel, T., Erzurumlu, R.S., and Itohara, S. (2000). Cortex-restricted disruption of NMDAR1 impairs neuronal patterns in the barrel cortex. Nature *406*, 726-731.

Iwasato, T., Erzurumlu, R.S., Huerta, P.T., Chen, D.F., Sasaoka, T., Ulupinar, E., and Tonegawa, S. (1997). NMDA receptor-dependent refinement of somatotopic maps. Neuron *19*, 1201-1210.

Iwasato, T., Inan, M., Kanki, H., Erzurumlu, R.S., Itohara, S., and Crair, M.C. (2008). Cortical adenylyl cyclase 1 is required for thalamocortical synapse maturation and aspects of layer IV barrel development. J Neurosci *28*, 5931-5943.

Lee, L.J., Iwasato, T., Itohara, S., and Erzurumlu, R.S. (2005). Exuberant thalamocortical axon arborization in cortex-specific NMDAR1 knockout mice. J Comp Neurol *485*, 280-292.

Li, Y., Erzurumlu, R.S., Chen, C., Jhaveri, S., and Tonegawa, S. (1994). Whisker-related neuronal patterns fail to develop in the trigeminal brainstem nuclei of NMDAR1 knockout mice. Cell *76*, 427-437.

Liu, X., Somel, M., Tang, L., Yan, Z., Jiang, X., Guo, S., Yuan, Y., He, L., Oleksiak, A., Zhang, Y.*, et al.* (2012). Extension of cortical synaptic development distinguishes humans from chimpanzees and macaques. Genome Res *22*, 611-622.

Suzuki, A., Lee, L.J., Hayashi, Y., Muglia, L., Itohara, S., Erzurumlu, R.S., and Iwasato, T. (2015). Thalamic adenylyl cyclase 1 is required for barrel formation in the somatosensory cortex. Neuroscience *290*, 518-529.

Upadhya, S.C., Smith, T.K., Brennan, P.A., Mychaleckyj, J.C., and Hegde, A.N. (2011). Expression profiling reveals differential gene induction underlying specific and non-specific memory for pheromones in mice. Neurochem Int *59*, 787-803.

Wang, C.F., and Huang Y.S. (2012) Calpain 2 Activated through N-methyl-D-aspartic acid receptor signaling cleaves CPEB3 and abrogates CPEB3 repressed translation in neurons. Mol Cell Biol 32,3321-32.

Wijetunge, L.S., Till, S.M., Gillingwater, T.H., Ingham, C.A., and Kind, P.C. (2008). mGluR5 regulates glutamate-dependent development of the mouse somatosensory cortex. J Neurosci *28*, 13028-13037.

Yabuta, N.H., Butler, A.K., and Callaway, E.M. (2000). Laminar specificity of local circuits in barrel cortex of ephrin-A5 knockout mice. J Neurosci *20*, RC88.

DISCUSIÓN

"La pregunta que quizá sea más enigmática de todas
es si el cerebro es suficientemente poderoso como
para resolver el problema de su propia creación."
(Gregor Eichele)

DISCUSIÓN

LOS FACTORES DE TRANSCRIPCIÓN, CLAVE DE LA COMPLEJIDAD DEL SISTEMA NERVIOSO Y DE LA IDENTIDAD NEURONAL.

En esta tesis he tratado de diseccionar principalmente la función de los FT Cux1 y Cux2 en la formación de circuitos de la corteza cerebral y, en menor medida, la de Lhx2. Los FT son proteínas con la capacidad de regular la expresión del genoma a través de diferentes mecanismos (Maston et al. 2006). Pueden actuar como activadores o represores e incluso regular el mismo gen de forma distinta en función del momento espacio-temporal en el que actúen (Bansal et al. 2014; de Thonel et al. 2012; Ishihama 2012; Vaquerizas et al. 2009; Wilczynski et al. 2012). La regulación de la expresión génica por FT permite la producción de una gran diversidad de células en un mismo organismo a partir de unos recursos limitados. Comprender el funcionamiento de los FT y las dinámicas de regulación sobre sus dianas es por tanto fundamental para entender la diversidad celular y, en el caso particular del cerebro, es además una de las claves para entender la conectividad.

En las últimas décadas ha habido un interés creciente en identificar aquellos FT cuya expresión, única o combinada, determina la generación y diferenciación de las distintas subpoblaciones neuronales. Las subpoblaciones más semejantes van a compartir un repertorio de FT más similar que las más alejadas (Arlotta et al. 2005; Molyneaux et al. 2005; Shoemaker and Arlotta 2010). Mediante la regulación de la expresión de estos repertorios de FT, el sistema nervioso genera de forma coordinada una infinidad de poblaciones y subpoblaciones neuronales muy similares pero distintas todas ellas. Por ejemplo, todas las neuronas excitatorias de la corteza cerebral van a expresar unos FT concretos (como Lmo4 - Lim domain-only 4- (Molyneaux et al. 2007)). A su vez, dentro de cada lámina, las neuronas tendrán otro grupo adicional de FT que determinará su función (por ejemplo, Cux1, Cux2 y Lhx2) y así sucesivamente se definirá la identidad de cada neurona (Greig et al. 2013; Leone et al. 2008; McConnell 1990; Srinivasan et al. 2012).

Los FT neuronales regulan, entre otras cosas, diversos aspectos de la conectividad a muy diversos niveles. Pueden determinar, por ejemplo, el número y la direccionalidad de las ramificaciones del axón o la dendrita y hacerlo en sentido distinto en las diferentes pobla-

ciones. Estos aspectos no son fácilmente detectables en análisis macroscópicos o poblacionales, pero su importancia para una verdadera comprensión del cerebro requiere desarrollar herramientas como la electroporación in utero (IUE) en neuronas individuales descrita en esta tesis. Esta técnica nos permite marcar neuronas durante el desarrollo para analizar su conectividad y su excitabilidad en el estadío deseado. Su resolución va a ser bastante superior a la IUE convencional, permitiéndonos identificar alteraciones enmascaradas en estudios poblacionales y visualizar aspectos clave de la conectividad, como el número de axones de ramas colaterales por neurona, su topografía precisa y su localización anatómica. Un ejemplo de las posibilidades de esta técnica se proporciona en esta misma tesis, ya que gracias a ella pudimos analizar la conectividad de las neuronas de la lámina II-III del S1 en las que el FT Cux1 había sido eliminado (artículo 3, Figura 3). Además, mediante la alteración de la posición de los electrodos o modificando el día de gestación en el que se lleva a cabo, permite afectar a otras poblaciones neuronales y llevar a cabo experimentos similares marcando neuronas individuales o poblaciones más amplias, dependiendo de la estrategia utilizada. Aunque la estrategia experimental de la dilución del plásmido y la recombinasa CRE ya había sido descrita anteriormente (Woodworth et al. 2016), en este protocolo se unifican criterios, se innova en cuanto a su aplicación para la descripción detallada del axón, y se describe el método de análisis de imagen y cuantificación basado en el software científico gratuito Fiji. Por otra parte, en este artículo se describe en mayor detalle otra de las herramientas utilizadas para el estudio del papel de Cux1 en la corteza: el uso de la IUE combinado con la electrofisiología, con la intención de facilitar su incorporación en otros laboratorios que, por lo general, manejan solo una de las dos técnicas.

RELEVANCIA DE LOS FACTORES DE TRANSCRIPCIÓN CUX1 Y CUX2 EN LA CONTRIBUCIÓN DIFERENCIAL A LOS COMPARTIMENTOS DENDRÍTICOS

La identidad molecular de las neuronas de la lámina II-III está determinada por la expresión combinada de Cux1 y Cux2. A pesar de que este solapamiento y sus similitudes estructurales y funcionales sugerían funciones redundantes, en estudios funcionales previos a esta tesis se determinó que sus funciones en el desarrollo normal de las dendritas son no-redundantes y aparentemente equivalentes (Cubelos et al. 2010). En el trabajo aquí presentado, ahondamos en el estudio de esa posible equivalencia funcional y demostramos que, sorprendentemente, estos FT regulan el desarrollo de los dos compartimentos dendríticos de forma distinta. Más adelante, y apoyando una cierta divergencia funcional, también pudimos constatar que Cux1 y Cux2 tienen efectos diferentes en el desarrollo del axón de las neuronas de la lámina II-III, aspecto que se tratará en el siguiente apartado.

Respecto a su regulación del árbol dendrítico de las neuronas de las lámina II-III, los resultados de nuestros experimentos indican que, pese a que el nivel de expresión de ambos genes afecta a los dos compartimentos dendríticos, los cambios en Cux1 causan un efecto más marcado en el basal mientras que los cambios en Cux2 afectan con más intensidad al apical. Estos efectos diferenciales contribuyen a aclarar la relevancia de la coexpresión y funciones de Cux1 y Cux2 en las neuronas de las láminas II-III, y la forma en la que van a determinar la complejidad final del árbol dendrítico (Cubelos et al. 2010).

La combinación de la expresión de Cux1 y Cux2 permite la diferenciación de las neuronas de las láminas II-III en subpoblaciones especializadas y podría contribuir a la formación y función de subredes intracorticales (Yassin et al. 2010; Yoshimura et al. 2005; Yoshi-

mura and Callaway 2005): la topografía de las dendritas va a ser fundamental a la hora de determinar la función de una neurona, ya que va a restringir el número y tipo de axones con los que potencialmente puede establecer sinapsis. Los propios axones son capaces de discriminar entre los dominios apical y basal de la misma neurona, probablemente a través del reconocimiento de señales polarizadas (Jia et al. 2010; Mainen and Sejnowski 1996; Petreanu et al. 2007). La modulación de las morfologías apical y basal también influye en la computación de la señal de entrada y regula la excitabilidad y plasticidad neuronales, puesto que la propagación de las señales eléctricas difiere entre los distintos volúmenes de los compartimentos dendríticos (Bian et al. 2015; Branco and Hausser 2011; Jia et al. 2010). Las dendritas basales, por ejemplo, son las que reciben mayoritariamente las aferentes de la lámina IV (Petersen 2007) y van a cambiar dinámicamente sus espinas en función de la información sensorial recibida, modulando así la actividad del circuito (Bian et al. 2015). Por otra parte, la combinación de Cux1 y Cux2 podría explicar también la mayor o menor complejidad de las dendritas basales en las neuronas de la lámina II-III en cada una de las diferentes áreas funcionales de la corteza. Estas diferencias entre áreas han sido descritas tanto en las cortezas murina como en la humana (Ballesteros-Yanez et al. 2006; Elston 2003).

A nivel de circuito, la plasticidad específica de los diferentes compartimentos dendríticos podría suponer un nivel añadido de almacenamiento y procesamiento de información por parte de las neuronas (Kastellakis et al. 2015). La regulación de la complejidad dendrítica en combinación con la habilidad para generar disparos locales podría permitir que las neuronas piramidales computaran ciertas señales en partes localizadas de los compartimentos dendríticos (Branco and Hausser 2010; Polsky et al. 2004; Sandler et al. 2016). El tamaño y la orientación de las dendritas apicales y basales va a cambiar de forma dinámica en función de las sinapsis que formen (Branco and Hausser 2010; Major et al. 2013) tanto a lo largo del desarrollo como durante el aprendizaje (Cichon and Gan 2015; Fu et al. 2012). Esto apoya específicamente la posibilidad de que las ramificaciones dendríticas tengan un papel clave en el almacenamiento de información (Chklovskii et al. 2004; Poirazi and Mel 2001).

Se sabe muy poco sobre las dianas transcripcionales de los genes *Cux* en la corteza. Ambos homólogos de *Cut* se unen a las mismas secuencias (muchas de ellas con CCAAT), pero Cux1 como activador o represor (Hulea and Nepveu 2012) y Cux2 únicamente como represor (Gingras et al. 2005). Además, mientras que para *Cux1* se han descrito 6 variantes de splicing alternativo y dos isoformas, en el caso de *Cux2* se ha hallado sólo una forma de splicing y una isoforma. Tampoco se conocen apenas los mecanismos regulados por otros FT que dirigen la diferenciación dendrítica específica de subclase (Cline and Haas 2008; Fame et al. 2011; Grueber et al. 2005; Parrish et al. 2007), aunque probablemente estén ligados a una o varias proteínas del citoesqueleto, receptores de membrana y proteínas de señalización ya implicadas en la diferenciación dendrítica (Kuijpers and Hoogenraad 2011; Kulkarni and Firestein 2012). BDNF y neurotrofina-3 (NT3), por ejemplo, potencian la elongación de las dendritas basales de neuronas piramidales de la lámina II-III en la corteza somatosensorial de rata, pero no afectan a los procesos apicales (Baker et al. 1998; Niblock et al. 2000). La señalización de Sema3A a través de su receptor Nrp1/PlexinaA4 controla la ramificación de las dendritas basales en las neuronas corticales de la lámina V, proporcionando otro ejemplo de vías que estimulan el crecimiento polarizado (Fenstermaker et al. 2004; Tran et al. 2009). TAOK2 (thousand-and-one-amino acid 2 kinasa) interactúa con Neuropilina1, mediando ese efecto y permitiendo restaurar las dendritas basales en ratones que expresan una variante de Nrp1 incapaz de unir Sema3A (de Anda et al. 2012).

Es interesante resaltar que TAOK2 está codificada por el gen de susceptibilidad al trastorno del espectro autista *TAOK2*, lo que pone en relieve la relación entre los fallos del desarrollo en los compartimentos celulares basales y apicales y el autismo. Precisamente, en esta línea, encontramos otras proteínas como la ubiquitina ligasa E3A (Ube3a) y Epac2 (exchange protein directly activated by cAMP 2), implicada en el síndrome del Angelman, y que promueve el crecimiento dendrítico apical (Miao et al. 2013). Por su parte, en esta relación con la enfermedad, cabe mencionar que algunos pacientes diagnosticados con autismo presentan variantes raras de Epac2. La expresión ectópica de estas variantes afecta negativamente a las dendritas basales de las neuronas de la lámina II-III de la misma forma que el silenciamiento de Epac2 endógeno (Srivastava et al. 2012). A la vista de estos estudios, la relación entre la regulación de los compartimentos dendríticos por Cux1 y Cux2 y el autismo parecía probable y así se discutió en este artículo. Estudios recientes han confirmado estas hipótesis y demostrado que CUX1 está implicado en trastornos del espectro autista en humanos (Choi et al. 2012; Doan et al. 2016), lo que se tratará con más detalle en el siguiente apartado.

RELEVANCIA DE CUX1 EN LA FORMACIÓN DEL CUERPO CALLOSO

Puesto que Cux1 y Cux2 se expresan principalmente en las láminas II-III y IV de la corteza cerebral (Nieto et al. 2004) y el 80% del CC está formado por neuronas de la lámina II-III(Fame et al. 2011), decidimos investigar el posible papel de estos dos FT en la formación de esta estructura. En humanos, los defectos en la formación del CC se han asociado con multitud de enfermedades con origen en el desarrollo que afectan al cerebro (Belmonte et al. 2004; Booth et al. 2011; Paul et al. 2007). Aunque el desarrollo del CC cuenta con numerosas etapas y sistemas de control descritos (Alcamo et al. 2008; Baranek et al. 2012; Choe et al. 2012; Mizuno et al. 2007; Rash and Richards 2001; Ren et al. 2007; Richards et al. 2004), en esta tesis doctoral describimos un novedoso mecanismo del desarrollo dependiente de Cux1 que especifica la conectividad axonal de las neuronas callosas de las láminas II-III por medio de la modulación de su excitabilidad y disparo. Nuestros experimentos en ratón demuestran que Cux1 es esencial para la modulación de la excitabilidad intrínseca y para el cambio a un modo de disparo dependiente de Kv1 necesario para la inervación interhemisférica. En ausencia de Cux1 y después de P9, los axones callosos que hasta entonces se extendían con normalidad no se desarrollan en la placa cortical contralateral, lo que supone una pérdida de la inervación contralateral casi absoluta en estadíos tardíos. Todo ello correlaciona con un defecto en la expresión del transcrito y proteína de Kv1.1 y Kv1.3, cuyos promotores son activados por Cux1 y cuya expresión modula la repuesta de disparo. El hecho de que los axones ipsilaterales de estas mismas neuronas puedan ramificar normalmente y no sean eliminados demuestra la dependencia selectiva de Cux1 de los axones del CC. Teniendo en cuenta los resultados en su conjunto, nos decantamos por valorar esta selectividad como dependiente del contexto temporal, y no regional o específica de territorio, porque los axones ipsilaterales y contralaterales se desarrollan en hemisferios simétricos pero en distintos estadios de desarrollo.

Las funciones de Cux1 en la regulación axonal a través del control de la excitabilidad constituyen uno de los primeros ejemplos ilustrativos de cómo los programas transcripcionales específicos de un subtipo neuronal van a regular la adquisición de las respuestas intrínsecas de disparo para definir la conectividad neuronal. Esto establece un enlace mecanístico entre la diversidad molecular de neuronas, definida por la expresión de FT específicos de subtipo, y el establecimiento de su conectividad de forma dependiente de la actividad. Este enlace es, posiblemente, muy relevante para entender el ensamblaje coordinado de los circuitos funcionales

del individuo y sugiere que los fallos en cada uno de los distintos aspectos del desarrollo han de ser considerados como posibles causas de enfermedades del sistema nervioso. En conclusión, nuestros datos aportan evidencias que muestran la importancia de los mecanismos mediados por actividad en las etapas iniciales de la formación del circuito (Ackman and Crair 2014; Dehorter et al. 2015; Kano and Hashimoto 2009; Kirkby et al. 2013) y tienen implicaciones para entender los mapas cerebrales y las enfermedades neurológicas.

Como se ha mencionado anteriormente, una vez más encontramos diferencias en cuanto a la función de Cux1 y Cux2 en el desarrollo neuronal, en este caso en la regulación del desarrollo del CC. Mientras que Cux1 es esencial para el establecimiento de conexiones contralaterales vía el CC, nuestros experimentos demuestran que Cux2 no juega el mismo papel esencial. Al eliminar o disminuir la expresión de Cux2 mediante ratones KO o shRNA por IUE, la inervación del hemisferio contralateral no se ve eliminada y, en todo caso, podría presentar un cierto cambio de patrón que necesitaría ser caracterizado en más detalle. Mediante el análisis de la expresión de proteínas hemos podido corroborar esta posible función antagónica, ya que la eliminación de la expresión de Cux2 provoca, a diferencia de la de Cux1, un aumento en los niveles de proteína Kv1.1 (no mostrado). Esto sugiere una función transcripcional represora sobre el promotor de los Kv1 en lugar de activadora. Aunque estos resultados han de ser analizados en mayor profundidad, indican que la regulación de la conectividad contralateral es una característica exclusiva de Cux1. Por otra parte, como se ha comentado en el apartado relativo a la dendrita y en otros artículos previos del laboratorio (Cubelos et al. 2010), las neuronas deficientes en Cux1 presentan una complejidad reducida de sus ramificaciones dendríticas que no podemos descartar por completo como relacionada con los fenotipos axonales, ya que no hemos analizado el efecto de los Kv1 en estos compartimentos neuronales. Sin embargo, el hecho de que la deficiencia en Cux2 provoque una reducción en la complejidad dendrítica total similar a la de Cux1 (Cubelos et al. 2010), pero no afecte al desarrollo del CC, sugiere que el menor volumen dendrítico en sí mismo no condiciona el desarrollo axonal.

Nuestros análisis han puesto en relieve la importancia de la adquisición de un modo de disparo fuertemente adaptativo dependiente de Kv1 en las neuronas de las láminas II-III para la formación del CC. Por tanto, cabe preguntarse cómo codifican la información los distintos modos de disparo y si hay algún parámetro del disparo que prediga la capacidad de inervar el hemisferio contralateral. En este sentido, los resultados sugieren que para poder definir los parámetros eléctricos que determinan el tipo de disparo que correlaciona con la inervación contralateral es más adecuado analizar las respuestas de disparo y los parámetros que las describen como un todo, en vez de centrarse en un único aspecto del disparo. Al inicio de esta tesis, sin embargo, la frecuencia de disparo (firing rate) era el parámetro considerado clave para el establecimiento de la inervación contralateral (Mizuno et al. 2007; Wang et al. 2007). Debido a estos antecendentes realizamos los experimentos con Kir2.1, cuya sobreexpresión disminuye artificialmente el potencial de membrana en reposo y se opone al disparo por lo que se utiliza para disminuir la actividad espontánea y la inducida. En ratones control, Kir2.1 produjo un descenso del potencial de membrana en reposo mucho mayor que el observado tras la eliminación de Cux1, pero unos defectos menores (y distintos) en la inervación del CC (Mizuno et al. 2007; Suarez et al. 2014; Wang et al. 2007). Por otro lado, la co-electroporación de shCux1 con Kv1.3 o la forma resistente inducible de Cux1, fue capaz de rescatar la inervación contralateral, pero no de normalizar las curvas de frecuencia de disparo. Esto nos llevó a concluir que la frecuencia de disparo en sí misma es un mal predictor de la capacidad para

inervar contralateralmente. En los experimentos en los que rescatamos la inervación tampoco observamos una normalización total de los patrones de disparo, aunque sí de la distancia entre los dos potenciales de acción iniciales, si bien este último parámetro es un descriptor limitado de la variedad de disparos neuronales. Por tanto, consideramos que ningún parámetro electrofisiológico de los analizados puede ser utilizado en exclusiva para predecir cambios en la inervación. Esto no quiere decir que descartemos totalmente una contribución de, por ejemplo, la frecuencia de disparo en el desarrollo del CC, sino que interpretamos que nuestros resultados indican que la información está codificada de forma compleja y se describiría por la combinación de varios parámetros (Doron et al. 2014; Rodriguez-Moreno et al. 2013; Stanley 2013; Suarez et al. 2014).

¿Qué mecanismos dependientes de actividad se utilizan para traducir esta información a patrones de inervación? En realidad no tenemos una respuesta definitiva a esta pregunta y la discusión de todas las posibilidades sería muy extensa. En la literatura encontramos diferentes mecanismos que podrían explicar cómo la modulación del disparo por Kv1 se traduce en la capacidad para elaborar, mantener o eliminar un axón calloso. Estos mecanismos son, en general, los relacionados con la plasticidad axonal y sináptica neuronal y, más en particular, aquellos que actúan durante el desarrollo. Por ejemplo, la neurona con fuerte capacidad de adaptación podría facilitar formas de plasticidad Hebbianas dependientes de la actividad previa, o el disparo fásico mediado por Kv1, que genera con más eficiencia ráfagas de calcio (Kwan and Dan 2012), podría ser indispensable para la estabilización de las sinapsis contralaterales. Sugiriendo otras alternativas muy relacionadas con el patrón de disparo, durante la realización de esta tesis se publicó un estudio que demostraba que, durante el desarrollo, una neurona presináptica es capaz de inducir depresión a largo plazo (LTD) gracias a un patrón de disparo que depende únicamente de sí misma (Rodriguez-Moreno et al. 2013). Un mecanismo no Hebbiano como éste también podría explicar la incapacidad para inervar de las neuronas deficientes en Cux1.

Los mecanismos que implican a las ondas de calcio y a la actividad del circuito están directamente relacionados con la eliminación de axones, por lo que son algunos de los posibles responsables de nuestros fenotipos. Por ejemplo, en el sistema visual, la actividad espontánea está implicada en procesos como la extensión axonal y formación de axones colaterales (Catalano and Shatz 1998; Kirkby et al. 2013; Yamamoto and Lopez-Bendito 2012). Nuestra caracterización de la excitabilidad intrínseca inducida por corriente sugiere que, en ausencia de Cux1, la excitabilidad de las neuronas de la lámina II-III está alterada durante el desarrollo temprano, lo que se podría traducir en cambios en la transmisión de la actividad del circuito que podrían causar una modificación en las ondas de Ca2+ (Kwan and Dan 2012). A lo largo de esta tesis llevé a cabo una serie de experimentos piloto para determinar in vivo si estas ondas estaban alteradas en neuronas en las que la expresión de Cux1 había sido eliminada. Estudiamos dos tipos de eventos previamente caracterizados en las neuronas del área visual (Siegel et al. 2012), y relacionados con los cambios de actividad que se dan en el desarrollo postnatal temprano: los de alta sincronicidad, en los que más del 80% de neuronas disparan a la vez y son característicos de la etapa previa a la entrada de la actividad extrínseca, y los de baja sincronicidad, en los que menos del 80% de neuronas disparan a la vez y están relacionados con la actividad sensorial. No pudimos detectar diferencias significativas en la participación en estos eventos de las neuronas deficientes en Cux1 y sus vecinas WT (**Figura 7**), lo que no excluye que Cux1 pueda alterar otros parámetros relacionados con las ondas de calcio. Además, es necesario reseñar que estos experimentos se realizaron en el V1 asumiendo que las neuronas de esa área sufren la maduración en el disparo dependiente de Kv1 en una ventana temporal cercana a las de S1.

Por tanto, no podemos descartar que las posibles diferencias en el desarrollo postnatal temprano entre estas áreas, no tenidas en cuenta en el diseño experimental, enmascaren posibles defectos en la producción de estos eventos mediados por calcio causados por la falta de Cux1. En cualquier caso, tampoco tenemos evidencias que apoyen cambios en la transmisión de las ondas de calcio ante la modulación por Cux1.

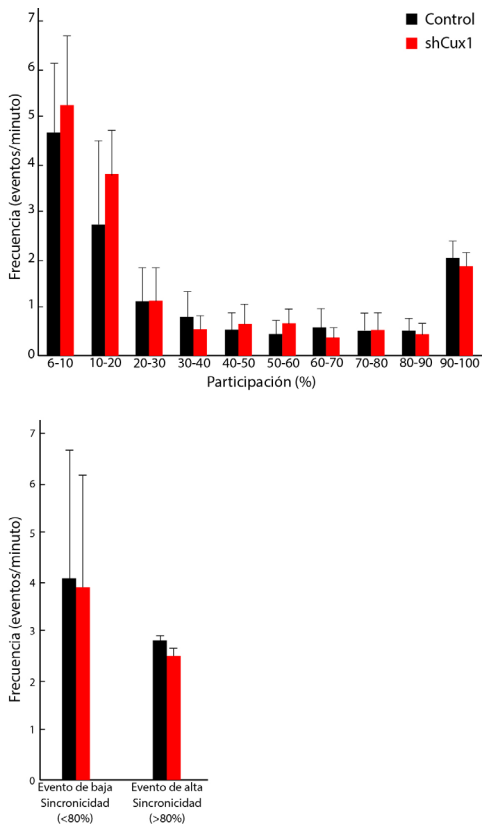

Figura 7. Las neuronas deficientes en Cux1 no presentan alteraciones en la participación enlos eventos de alta y baja sincronicidad.

En este mismo contexto, cabe preguntarse si los patrones de actividad circuital endógena existentes en la corteza cerebral durante el desarrollo temprano pudieran estar modificados debido a una expresión disminuida de Cux1 (Blankenship and Feller ; Khazipov and Luhmann 2006; Kirkby et al. 2013; Siegel et al. 2012). Por ejemplo, las ráfagas fusiformes y las oscilaciones gamma están sincronizadas entre ambos hemisferios antes de que el CC se haya formado (Marcano-Reik and Blumberg 2008), pero los mecanismos responsables de su producción no se conocen más allá de su dependencia de la transmisión glutamatérgica talámica (Dupont et al. 2006; Hanganu et al. 2009). Dado que la expresión de Cux1 en la corteza también depende, al menos parcialmente, de la transmisión glutamatergica talámica (Li et al. 2013) y de que modifica la excitibilidad intrínseca de las neuronas corticales, podría ser un buen candidato para regular estos patrones de actividad circuital endógena implicados en una gran variedad de procesos del desarrollo (J. W. Yang et al. 2016a).

Respecto a los posibles mecanismos de eliminación axonal, es importante mencionar que en el CC no encontramos una situación similar a la retina, el paradigma de la eliminación axonal, en la que tenemos un antes (ramificación axonal exuberante) y un después (pérdida axonal dramática) que define claramente el proceso de eliminación (Kirkby et al. 2013). Nuestros experimentos con neuronas deficientes en Cux1 revelan una invasión inicial de la placa cortical normal a P8 (que va a representar una fracción minoritaria de la señal axonal final en el WT), seguida de un estadío - P10 - caracterizado por el incremento del número de axones contralaterales en el ratón control y una ausencia casi total de señal tanto en la placa cortical como en la materia blanca en el caso de la deficiencia de Cux1. Por tanto, y en base a la idea de que los axones callosos invaden y eliminan la placa cortical de forma continuada y no sincrónica, resulta estrictamente imposible afirmar que estamos ante un proceso de eliminación. No obstante, el hecho de que el momento temporal en el que detectamos la ausencia de axones (a partir de P10) coincida con la entrada de la actividad sensorial del bigote en las láminas II-III de la corteza somatosensorial (Erzurumlu and Gaspar 2012; Maravall et al. 2004), sí apoya mecanismos de eliminación axonal dependientes de actividad sensorial.

A la hora de estudiar mecanismos de eliminación, es necesario considerar los mecanismos de competición Hebbianos y no Hebbianos, ya que en nuestros experimentos, las neuronas deficientes en Cux1 elaboran sus axones en presencia axones provenientes de neuronas normales. Un modelo clásico de competición Hebbiana predeciría que los axones deficientes en Cux1 perderían territorio frente a los normales que están junto a ellos y pueden estabilizarse. Sin embargo, la competición no supone necesariamente la retracción de los axones en todas las situaciones (Benjumeda et al. 2013; Kerschensteiner et al. 2009; Kirkby et al. 2013; Koch et al. 2011; Morgan et al. 2011; Plazas et al. 2013; Rebsam et al. 2009). Por ejemplo, Koch y colaboradores demostraron que durante el refinamiento del circuito visual, la alteración en los niveles de actividad sináptica produce una disminución en la capacidad de competición de los axones afectados que, sin embargo, pueden consolidar y mantener su territorio incluso en presencia de axones con la capacidad de competición intacta (Koch et al. 2011). Por tanto, es necesario realizar experimentos adicionales para sacar una conclusión más fuerte respecto a la causa de la eliminación axonal. Por otro lado, dado que la alteración en la excitabilidad de la neurona deficiente en Cux1 coincide con la pérdida axonal, otra interpretación posible de nuestros resultados es que los fenotipos eléctricos son la consecuencia y no la causa de la incapacidad de los axones para inervar las dianas contralaterales, lo cual no invalida las conclusiones relativas a la necesidad de Kv1 para inervar, pero hace más difícil el análisis del disparo.

Independientemente de los mecanismos de plasticidad implicados en la estabilización o eliminación del axón calloso, una observación muy clara y relevante de nuestros experimentos es que los axones contralaterales son los únicos eliminados ante la pérdida de Cux1 o Kv1, ya que no se observan diferencias en los del hemisferio ipsilateral. Por consiguiente, parece que el disparo dependiente de Kv1 es sólo necesario para la inervación del territorio contralateral. Respecto a la formación de los axones ipsilaterales de las láminas II-III, nuestros resultados no descartan la posibilidad de que también dependan de una respuesta de disparo adecuada, pero ésta sería independiente de la expresión de Cux1 y Kv1. La conservación de los axones ipsilaterales en las neuronas electroporadas con shRNACux1 descarta también que una incapacidad general para establecer ramificaciones o sinapsis sea la causa de la perdida de los axones callosos en estas neuronas. Esto nos lleva a concluir que los mecanismos dependientes de Cux1 no controlan intrínsecamente el proceso de ramificación axonal, como por ejemplo ocurre en los mecanismos mediados por LKB1 (Liver Kinase B1), cuyos defectos afectan a la inervación de ambos hemisferios (Courchet et al. 2013).

Nuestros resultados indican que existe capacidad para discriminar entre los axones que se van a formar en el hemisferio ipsilateral y en el contralateral gracias a la utilización de mecanismos distintos, dependientes o independientes de Cux1. En principio, esta selectividad podría tener una base territorial o temporal, pero puesto que los dos hemisferios son iguales, perfectamente simétricos, y el axón establece patrones de inervación especulares en ambos hemisferios, no apoyamos una selectividad territorial. Sin embargo, aunque el axón inerve las mismas láminas en ambos hemisferios, las conexiones en uno y otro territorio se realizan en momentos totalmente distintos, lo que indica una dependencia temporal en cuanto a la formación axonal mediada por Cux1. Esto cobra sentido teniendo en cuenta el diferente desarrollo temporal de los axones ipsilaterales y callosos: a P4 comienza la ramificación de los axones ipsilaterales y a P9 ya son abundantes, antes de que el cambio en el disparo mediado por Kv1 asociado con las ramificaciones contralaterales haya tenido lugar (Srivatsa et al. 2015). Los axones contralaterales, por el contrario, inician su ramificación en la placa cortical alrededor de P8-P9, correlacionando

con cambios en la excitabilidad y los niveles de los canales Kv1. La implicación de mecanismos diferentes en la formación de mapas topográficos en los que poblaciones axonales generan patrones de inervación idénticos o muy similares no es inédita en el sistema nervioso (Kuwajima et al. 2017). En retina de ratón, por ejemplo, la eliminación de los axones contralaterales del núcleo dorsal lateral geniculado sigue reglas basadas en la competición Hebbiana y requiere la activación de la célula postsináptica. Por el contrario, el refinamiento y la estabilización de los axones ipsilaterales depende principalmente de la actividad de la célula presináptica, apuntando quizás a una regla no Hebbiana (Kirkby et al. 2013; Koch et al. 2011; Rebsam et al. 2009).

Otra implicación importante de nuestro trabajo es que infiere que los problemas en los mecanismos que regulan los modos de disparo (causados por deficiencias en Kv1 u otros canales, elementos del citoesqueleto, FT o cualquier otro gen cuya función afecte al disparo) por sutiles que sean, son causas potenciales de conectividades aberrantes y desbalanceadas, por lo que posiblemente estén relacionados con enfermedades como los trastornos del espectro autista y la esquizofrenia, entre otras (Spooren et al. 2012). Por tanto, nuestros estudios contribuyen a proponer nuevos elementos en la comprensión de la etiología y patología de las enfermedades mentales con origen en el desarrollo y, sobre todo, a apoyar las posturas más recientes que proponen que el autismo está causado por un fallo de la plasticidad homeostática neuronal (Ebert and Greenberg 2013; Ramocki and Zoghbi 2008; Tien et al. 2017). De hecho, los trastornos del espectro autista son las patologías más estrechamente asociadas a la agénesis del CC y a defectos en plasticidad (Ebert and Greenberg 2013; Pescosolido et al. 2012). Más aún, las neuronas deficientes en Cux1 muestran una conectividad a larga distancia alterada pero sin defectos aparentes en los circuitos locales, de manera similar a lo que algunos autores proponen que ocurre en ciertos individuos que presentan trastornos del espectro autista (Belmonte et al. 2004; Just et al. 2004; Khan et al. 2013; Minshew and Williams 2007). En un estudio publicado el año pasado, se identificó precisamente una mutación en la secuencia reguladora de CUX1 asociada a pacientes con trastornos del espectro autista (Doan et al. 2016). Este mismo estudio pone de relevancia también la importancia de CUX1 para la evolución humana, ya que la mutación se encuentra en una región HARS (del inglés, Human accelerated region) (Doan et al. 2016). Las regiones HARS son regiones reguladoras conservadas que, durante la evolución, demuestran una frecuencia de mutaciones acelerada específicamente en humanos en comparación con otras especies. Por consiguiente, se piensa que contribuyen a la aparición de los rasgos humanos y más específicamente a la evolución de la corteza.

En conclusión, los mecanismos dependientes de Cux1 van a ser de gran importancia para la correcta formación del circuito somatosensorial, y los defectos en estas vías pueden influir de manera crítica en la integración cortical de la actividad derivada de la experiencia. Al igual que se señaló en el apartado relativo a la dendrita, los mecanismos aquí descritos pueden contribuir a nuestro entendimiento de las enfermedades del espectro autista y de otras enfermedades que, de manera similar, afectan a estos mecanismos de plasticidad o a otros relacionados con ellos. Nuestros resultados también contribuyen a aumentar la comprensión de lo que ocurre en aquellas situaciones relacionadas con la perdida de transferencia de información en el axón.

Por último, es relevante señalar que una de las puertas que abre nuestra investigación es proponer que la modulación de la excitabilidad de las neuronas podría ser una nueva diana terapéutica para el tratamiento de las enfermedades del desarrollo que muestran una conectividad aberrante. Nuestros experimentos

demuestran que hay una ventana de plasticidad postnatal en la que la restauración del disparo correcto de las neuronas puede rescatar la inervación. Aunque es necesario seguir investigando en esta línea para determinar si esta plasticidad puede ser mejorada y expandida con fines terapéuticos, el año pasado se publicaron trabajos muy esperanzadores relacionados con estas ventanas de plasticidad. Yang y colaboradores llevaron a cabo un trasplante de interneuronas inmaduras en la amígdala, consiguiendo que ésta reactivara su plasticidad juvenil (W. Z. Yang et al. 2016b) probablemente gracias a la desinhibición del circuito (Kuhlman et al. 2013). Por otro lado, el grupo de Magdalena Götz demostró de una forma muy elegante que neuronas embrionarias trasplantadas en tejido dañado pueden madurar funcionalmente e integrarse en circuitos totalmente establecidos. Estas neuronas trasplantadas fueron capaces de conectar adecuadamente, incluso con dianas contralaterales, y de recibir las mismas aferentes que las neuronas que se encontraban allí, a pesar de que el circuito en el que se integraron era adulto (Falkner et al. 2016). Por tanto, ahora más que nunca, entender los mecanismos de formación de estructuras como el CC nos puede ayudar a tratar patologías en las que estas conexiones están implicadas.

LA IMPORTANCIA DE LHX2 EN EL DIÁLOGO ENTRE EL TÁLAMO Y LA CORTEZA

Junto a Cux1 y Cux2, otro de los FT más conocido por expresarse selectivamente en las láminas II-III y IV de la corteza somatosensorial es Lhx2. El artículo presentado en esta tesis, en el que fui colaborador, estudia el papel de Lhx2 en las neuronas de la lámina IV, que es la que integra las señales que vienen del tálamo y contacta con las láminas II-III. Los barriles de S1 están formados por las neuronas de la lámina IV, con sus dendritas orientadas de forma asimétrica hacia el centro del barril, y por los axones talamocorticales, que inervan de manera selectiva y preferente cada una de estas estructuras. Para formar este mapa tienen que converger diferentes procesos, y hasta el momento se ha profundizado sobre todo en aquellos mecanismos dependientes sólo del tálamo, o sólo de las neuronas corticales (Li and Crair 2011). Sin embargo, se conoce menos sobre aquellos mecanismos coordinados que establecen el diálogo necesario entre la lámina IV y los axones talámicos que les permite formar el barril. Estos son los aspectos sobre los que incide este trabajo.

Los experimentos demostraron que Lhx2 es una suerte de interruptor molecular que permite a la neurona iniciar la formación de barriles mediante la regulación de la expresión de programas ligados a la actividad. Si bien la expresión de Lhx2 no es dependiente de la actividad, se observó que este FT induce la expresión de genes implicados en la formación del barril, muchos de los cuales ya estaba descrito que o bien están regulados por actividad o bien que participan en procesos en los que media la actividad, y que permiten que las neuronas de la lámina IV de S1 respondan efectivamente a la entrada talamocortical, remodelen sus conexiones, desarrollen asimetría dendrítica a través de Btbd3, y se agrupen formando los barriles. Por tanto, Lhx2 confiere a las neuronas de la lámina IV competencia para para responder a la actividad del circuito del bigote y para formar de acuerdo a ella, el mapa funcional.

¿Cómo instruyen las neuronas de la lámina IV a los axones talamocorticales para que inerven el barril? Para responder a esta pregunta, se estudió el papel de Lhx2 en la lámina IV por medio de su eliminación selectiva en neuronas postmitóticas mediante una mutación condicional (cKO). Si bien se observó que los axones talamocorticales de los ratones cKO se desarrollan correctamente hasta P3, se encontraron terminales axonales inervando de forma aberrante la lámina II-III a P7, una vez que el periodo crítico de plasticidad estructural del barril se ha cerrado (Erzurumlu and Gaspar 2012; Rebsam et al. 2005). Por tanto, determinamos

que la expresión de Lhx2 en las neuronas postmitóticas corticales no es necesaria para la entrada de los axones talámicos a la corteza, pero sí para que estos axones se ramifiquen correctamente una vez están en ella. Para encontrar potenciales candidatos responsables de estos defectos en la conectividad talamocortical se realizaron estudios de transcriptómica comparando las cortezas del ratón WT y del cKO. Dentro de la lista de genes diferencialmente expresados, aparecen varios que han sido previamente descritos como necesarios para la correcta formación de los barriles. Uno de los más interesantes es Lmo4, un FT dependiente de actividad, cuya eliminación en neuronas postmitóticas corticales produce fenotipos en los axones talamocorticales que recuerdan a los del ratón cKO (Kashani et al. 2006), y cuya expresión aparece reducida en nuestro modelo, pudiendo explicar el porqué de los defectos axonales que observamos. Otro tránscrito destacado de la lista que podría contribuir a entender los fallos axonales es el de la EfrinaA5, un regulador de la formación de ramificaciones talamocorticales (Uziel et al. 2008), cuya expresión también está reducida en el cKO. No se encontraron evidencias de la regulación directa de estos genes por Lhx2, por lo que la determinación del mecanismo concreto responsable de estos fenotipos requeriría experimentos adicionales.

Para que se establezca un verdadero diálogo entre el tálamo y la corteza, es necesario que las neuronas de la lámina IV adquieran la capacidad para responder a los axones talamocorticales. Estudios previos llevados a cabo en neuronas en cultivo determinaron que, a diferencia de otros FT de la misma familia como Lmo4, la actividad transcripcional de Lhx2 es independiente de actividad neuronal (Kashani et al. 2006). Sin embargo, en la publicación presentada en esta tesis, hemos descrito que este FT es responsable de inducir la expresión de muchos genes cuya función sí va a depender de actividad y que van a permitir que la neurona pueda responder adecuadamente a los axones talamocorticales. Uno de estos genes es Btbd3, que anteriormente había sido descrito como un factor necesario para controlar la orientación de la dendrita hacia los axones activos en la neocorteza de mamíferos (Matsui et al. 2013), y cuya expresión está directamente regulada por Lhx2. La expresión ectópica de Btbd3 en las neuronas de la lámina IV de los ratones cKO fue suficiente para que las dendritas recuperaran su asimetría, lo que demostraba la implicación de este gen en los defectos observados en las neuronas deficientes en Lhx2. Los estudios previos apuntan a dos vías principales de señalización, que pueden relacionarse entre sí, implicadas en la transmisión de la actividad neuronal de los axones talamocorticales a la lámina IV: NMDA/AC1/5HT/cAMP y mGluR5/PLC1/MAPK/Lmo4 (Li and Crair 2011). A pesar de que los defectos en los distintos elementos de estas vías provocan que los barriles no se formen adecuadamente, la expresión de Btbd3 sí que fue detectada en la lámina IV del S1 de los ratones con los genes NR1 (Matsui et al. 2013), mGluR5 o Lmo4 específicamente eliminados de la corteza (Ballester-Rosado et al. 2010; Kashani et al. 2006). Dado que en estas neuronas no se ha podido disparar la respuesta a la actividad, nosotros proponemos que el papel de Lhx2 en el proceso de formación del barril precede a la activación de los eventos dependientes de actividad.

Los defectos estructurales observados en el cKO de Lhx2 podrían causar defectos funcionales a nivel de circuito. Los experimentos llevados a cabo para analizar la respuesta cortical ante el estímulo de un bigote concreto (el C2) demostraron que el ratón cKO presenta un número significativamente mayor de neuronas activadas en los barriles adyacentes al estimulado, lo que indica que hay una pérdida de la precisión topográfica en la transmisión de la actividad desde los bigotes a la corteza. Esto podría ser debido a que las dendritas de los barriles vecinos invadan el C2 y los axones talamocorticales correctamente localizados las activen, o porque Lhx2 sea necesario a nivel post-sináptico para

mediar los mecanismos de plasticidad que promueven el refinamiento del axón talamocortical (Schlaggar et al. 1993). En cualquier caso, estos experimentos, junto a las medidas de potenciales evocados, aportan evidencias adicionales para demostrar que Lhx2 es necesario para la correcta formación del mapa somatosensorial.

Puesto que las neuronas de la lámina IV van a ser las encargadas de recibir la señal sensorial, las implicaciones de tener un mapa topográficamente aberrante son notables, y se extienden a todo el circuito. Volviendo a la lámina II-III, por ejemplo, va a determinar qué señales reciben sus neuronas y su conectividad. En modelos de deprivación sensorial, la reducción en la eficacia de la sinapsis de la lámina IV a la lámina II-III (aumento de LTD) provoca la depresión del procesamiento sensorial de las neuronas de la lámina II-III, tanto en S1 (Allen et al. 2003; Rodriguez-Moreno et al. 2013; Shepherd et al. 2003) como en V1 (Heynen et al. 2003). Es decir, es esperable que los defectos en la conectividad de la lámina IV observados en el ratón cKO, resulten en una conectividad aberrante al circuito II-III y posiblemente al resto del mapa cortical. Debido a que Lhx2 es necesario para que otros FT relacionados con la actividad puedan cumplir su función correctamente y se expresa en las mismas láminas que Cux1, sería interesante valorar una posible participación de este último FT en los fenotipos aquí descritos.

El conjunto de los estudios presentados en esta tesis contribuye a la comprensión de los mecanismos moleculares y relacionados con la actividad implicados en la formación de los circuitos corticales complejos en los que participan las neuronas de las láminas II-III y IV. Aunque todavía queda mucho por investigar, este trabajo ha pretendido subrayar cómo la especificación molecular de poblaciones restringidas y los mecanismos que modifican la forma de transmitir y responder a actividad de la neurona, son necesarios para el ensamblaje coordinado de circuitos y territorios. Los defectos en estos mecanismos pueden ser la causa de grandes alteraciones en el circuito y, posiblemente, de enfermedades mentales (Marin 2016). Entender los mecanismos implicados en la formación de este circuito es, sin duda, una de las claves para poder tratar numerosas patologías.

CONCLUSIONES

"Presiento que este es el comienzo
de una hermosa amistad."
(Rick Blaine, "Casablanca")

CONCLUSIONES

1. En el desarrollo de la dendrita, los cambios en los niveles de expresión de Cux1 provocan cambios más acusados en el compartimento basal, mientras que la modulación de Cux2 tiene una influencia mayor en el compartimento apical.

2. El factor de transcripción Cux1 es necesario para el desarrollo postnatal de las proyecciones callosas de las neuronas de la láminas II-III.

3. Las neuronas deficientes en Cux1 no eliminan sus conexiones ipsilaterales.

4. Cux1 regula a nivel transcripcional los niveles de expresión de los canales Kv1 y los modos de disparo de las neuronas de las láminas II/III.

5. Cux1 acopla la identidad neuronal y la conectividad a través de la modulación de la excitabilidad y los modos de disparo.

6. Los modos de disparo determinan el establecimiento de las proyecciones callosas durante el desarrollo.

7. Lhx2 induce, en las neuronas postmitóticas de la lámina IV de la corteza somatonsensorial, la expresión de genes que permiten responder a los aferentes talámicos, desarrollar asimetría dendrítica y formar el mapa de barriles.

CONCLUSIONS

1. In the development of the dendrite, changes in Cux1 expression levels result in a marked effect on the development of the basal compartment whereas modulation of Cux2 has a stronger influence on the apical compartment.

2. Cux1 transcription factor is necessary for the postnatal development of the callosal projections of layer II-III neurons.

3. Cux1 deficient neurons do not eliminate their ipsilateral connections.

4. Cux1 regulates transcriptionally the expression levels of Kv1 channels and the firing modes of layer II/III neurons.

5. Cux1 couples neuronal identity and wiring through modulation of excitability and firing modes.

6. Firing modes determine axonal connectivity during development.

7. Lhx2 induces the expression of genes that enable layer 4 neurons in the somatosensory cortex to respond to thalamocortical inputs, develop dendritic asymmetry, and form the barrel map.

REFERENCIAS

"Si he logrado ver más lejos,
es porque he subido a hombros de gigantes."
(Isaac Newton)

Abdel-Majid, R. M., et al. (1998), 'Loss of adenylyl cyclase I activity disrupts patterning of mouse somatosensory cortex', Nat Genet, 19 (3), 289-91.

Ackman, J. B. and Crair, M. C. (2014), 'Role of emergent neural activity in visual map development', Curr Opin Neurobiol, 24 (1), 166-75.

Adelsberger, H., Garaschuk, O., and Konnerth, A. (2005), 'Cortical calcium waves in resting newborn mice', Nat Neurosci, 8 (8), 988-90.

Alcamo, E. A., et al. (2008), 'Satb2 regulates callosal projection neuron identity in the developing cerebral cortex', Neuron, 57 (3), 364-77.

Alfano, C. and Studer, M. (2013), 'Neocortical arealization: evolution, mechanisms, and open questions', Dev Neurobiol, 73 (6), 411-47.

Allen, C. B., Celikel, T., and Feldman, D. E. (2003), 'Long-term depression induced by sensory deprivation during cortical map plasticity in vivo', Nat Neurosci, 6 (3), 291-9.

AllenDevelopingMouseBrainAtlas (2008), '2008 Allen Institute for Brain Science. Allen Developing Mouse Brain Atla. Available from: http://developingmouse.brain-map.org/'.

Allendoerfer, K. L. and Shatz, C. J. (1994), 'The subplate, a transient neocortical structure: its role in the development of connections between thalamus and cortex', Annu Rev Neurosci, 17, 185-218.

Anderson, S. A., et al. (2001), 'Distinct cortical migrations from the medial and lateral ganglionic eminences', Development, 128 (3), 353-63.

Anderson, S. A., et al. (2002), 'Distinct origins of neocortical projection neurons and interneurons in vivo', Cereb Cortex, 12 (7), 702-9.

Angevine, J. B., Jr. and Sidman, R. L. (1961), 'Autoradiographic study of cell migration during histogenesis of cerebral cortex in the mouse', Nature, 192, 766-8.

Antonini, A. and Stryker, M. P. (1993), 'Rapid remodeling of axonal arbors in the visual cortex', Science, 260 (5115), 1819-21.

Arion, D., et al. (2007), 'Molecular markers distinguishing supragranular and infragranular layers in the human prefrontal cortex', Eur J Neurosci, 25 (6), 1843-54.

Arlotta, P., et al. (2005), 'Neuronal subtype-specific genes that control corticospinal motor neuron development in vivo', Neuron, 45 (2), 207-21.

Bagri, A., et al. (2002), 'Slit proteins prevent midline crossing and determine the dorsoventral position of major axonal pathways in the mammalian forebrain', Neuron, 33 (2), 233-48.

Baker, R. E., et al. (1998), 'Growth of pyramidal, but not non-pyramidal, dendrites in long-term organotypic explants of neonatal rat neocortex chronically exposed to neurotrophin-3', Eur J Neurosci, 10 (3), 1037-44.

Ballester-Rosado, C. J., et al. (2010), 'mGluR5 in cortical excitatory neurons exerts both cell-autonomous and -nonautonomous influences on cortical somatosensory circuit formation', J Neurosci, 30 (50), 16896-909.

Ballesteros-Yanez, I., et al. (2006), 'Density and morphology of dendritic spines in mouse neocortex', Neuroscience, 138 (2), 403-9.

Bansal, M., Kumar, A., and Yella, V. R. (2014), 'Role of DNA sequence based structural features of promoters in transcription initiation and gene expression', Curr Opin Struct Biol, 25, 77-85.

Baranek, C., et al. (2012), 'Protooncogene Ski cooperates with the chromatin-remodeling factor Satb2 in specifying callosal neurons', Proc Natl Acad Sci U S A, 109 (9), 3546-51.

Belford, G. R. and Killackey, H. P. (1980), 'The sensitive period in the development of the trigeminal system of the neonatal rat', J Comp Neurol, 193 (2), 335-50.

Belmonte, M. K., et al. (2004), 'Autism and abnormal development of brain connectivity', J Neurosci, 24 (42), 9228-31.

Bender, K. J. and Trussell, L. O. (2012), 'The physiology of the axon initial segment', Annu Rev Neurosci, 35, 249-65.

Benjumeda, I., et al. (2013), 'Uncoupling of EphA/ephrinA signaling and spontaneous activity in neural circuit wiring', J Neurosci, 33 (46), 18208-18.

Bian, W. J., et al. (2015), 'Coordinated Spine Pruning and Maturation Mediated by Inter-Spine Competition for Cadherin/Catenin Complexes', Cell, 162 (4), 808-22.

Blankenship, A. G. and Feller, M. B. (2010), 'Mechanisms underlying spontaneous patterned activity in developing neural circuits', Nat Rev Neurosci, 11 (1), 18-29.

Booth, R., Wallace, G. L., and Happe, F. (2011), 'Connectivity and the corpus callosum in autism spectrum conditions: insights from comparison of autism and callosal agenesis', Prog Brain Res, 189, 303-17.

Boyd, E. H., Pandya, D. N., and Bignall, K. E. (1971), 'Homotopic and nonhomotopic interhemispheric cortical projections in the squirrel monkey', Exp Neurol, 32 (2), 256-74.

Brager, D. H. and Johnston, D. (2014), 'Channelopathies and dendritic dysfunction in fragile X syndrome', Brain Res Bull, 103, 11-7.

Branco, T. and Hausser, M. (2011), 'Synaptic integration gradients in single cortical pyramidal cell dendrites', Neuron, 69 (5), 885-92.

Bulchand, S., Subramanian, L., and Tole, S. (2003), 'Dynamic spatiotemporal expression of LIM genes and cofactors in the embryonic and postnatal cerebral cortex', Dev Dyn, 226 (3), 460-9.

Butler, A. K., et al. (2001), 'Development of visual cortical axons: layer-specific effects of extrinsic influences and activity blockade', J Comp Neurol, 430 (3), 321-31.

Catalano, S. M. and Shatz, C. J. (1998), 'Activity-dependent cortical target selection by thalamic axons', Science, 281 (5376), 559-62.

Catterall, W. A., et al. (2012), 'The Hodgkin-Huxley heritage: from channels to circuits', J Neurosci, 32 (41), 14064-73.

Caviness, V. S., Jr. (1982), 'Neocortical histogenesis in normal and reeler mice: a developmental study based upon [3H]thymidine autoradiography', Brain Res, 256 (3), 293-302.

Cline, H. and Haas, K. (2008), 'The regulation of dendritic arbor development and plasticity by glutamatergic synaptic input: a review of the synaptotrophic hypothesis', J Physiol, 586 (6), 1509-17.

Cline, H. T. (2001), 'Dendritic arbor development and synaptogenesis', Curr Opin Neurobiol, 11 (1), 118-26.

Cobos, I., et al. (2006), 'Cellular patterns of transcription factor expression in developing cortical interneurons', Cereb Cortex, 16 Suppl 1, i82-8.

Conel, J. L. (1953), 'Contribution of S. Ramon y Cajal to the knowledge of the anatomy of the cerebral cortex', N Engl J Med, 248 (13), 541-3.

Connors, B. W. and Gutnick, M. J. (1990), 'Intrinsic firing patterns of diverse neocortical neurons', Trends Neurosci, 13 (3), 99-104.

Courchet, J., et al. (2013), 'Terminal axon branching is regulated by the LKB1-NUAK1 kinase pathway via presynaptic mitochondrial capture', Cell, 153 (7), 1510-25.

Cubelos, B., et al. (2008), 'Cux-2 controls the proliferation of neuronal intermediate precursors of the cortical subventricular zone', Cereb Cortex, 18 (8), 1758-70.

Cubelos, B., et al. (2010), 'Cux1 and Cux2 regulate dendritic branching, spine morphology, and synapses of the upper layer neurons of the cortex', Neuron, 66 (4), 523-35.

Chen, B., Schaevitz, L. R., and McConnell, S. K. (2005a), 'Fezl regulates the differentiation and axon targeting of layer 5 subcortical projection neurons in cerebral cortex', Proc Natl Acad Sci U S A, 102 (47), 17184-9.

Chen, J. G., et al. (2005b), 'Zfp312 is required for subcortical axonal projections and dendritic morphology of deep-layer pyramidal neurons of the cerebral cortex', Proc Natl Acad Sci U S A, 102 (49), 17792-7.

Chilton, J.K.; and Gordon-Weeks, P.R. (2007), Role of microtubules and MAPs during neuritogenesis. In "Intracellular Mechanisms for Neuritogenesis" (Springer).

Choe, Y., Siegenthaler, J. A., and Pleasure, S. J. (2012), 'A cascade of morphogenic signaling initiated by the meninges controls corpus callosum formation', Neuron, 73 (4), 698-712.

Choi, J., et al. (2012), 'Cut-like homeobox 1 and nuclear factor I/B mediate ENGRAILED2 autism spectrum disorder-associated haplotype function', Hum Mol Genet, 21 (7), 1566-80.

Chou, S. J. and O'Leary, D. D. (2013), 'Role for Lhx2 in corticogenesis through regulation of progenitor differentiation', Mol Cell Neurosci, 56, 1-9.

Chou, S. J., et al. (2009), 'Lhx2 specifies regional fate in Emx1 lineage of telencephalic progenitors generating cerebral cortex', Nat Neurosci, 12 (11), 1381-9.

Dantzker, J. L. and Callaway, E. M. (1998), 'The development of local, layer-specific visual cortical axons in the absence of extrinsic influences and intrinsic activity', J Neurosci, 18 (11), 4145-54.

de Anda, F. C., et al. (2012), 'Autism spectrum disorder susceptibility gene TAOK2 affects basal dendrite formation in the neocortex', Nat Neurosci, 15 (7), 1022-31.

De Juan Romero, C. and Borrell, V. (2015), 'Coevolution of radial glial cells and the cerebral cortex', Glia, 63 (8), 1303-19.

De la Rossa, A., et al. (2013), 'In vivo reprogramming of circuit connectivity in postmitotic neocortical neurons', Nat Neurosci, 16 (2), 193-200.

de la Torre-Ubieta, L. and Bonni, A. (2011), 'Transcriptional regulation of neuronal polarity and morphogenesis in the mammalian brain', Neuron, 72 (1), 22-40.

de Thonel, A., Le Mouel, A., and Mezger, V. (2012), 'Transcriptional regulation of small HSP-HSF1 and beyond', Int J Biochem Cell Biol, 44 (10), 1593-612.

DeFelipe, Javier and Ramon y Cajal, S (1988), Cajal on the cerebral cortex: an annotated translation of the complete writings (Oxford University Press).

Degano, A. L., et al. (2014), 'MeCP2 is required for activity-dependent refinement of olfactory circuits', Mol Cell Neurosci, 59, 63-75.

Dehay, C., et al. (1991), 'The effects of bilateral enucleation in the primate fetus on the parcellation of visual cortex', Brain Res Dev Brain Res, 62 (1), 137-41.

Dehorter, N., et al. (2015), 'Tuning of fast-spiking interneuron properties by an activity-dependent transcriptional switch', Science, 349 (6253), 1216-20.

Doan, R. N., et al. (2016), 'Mutations in Human Accelerated Regions Disrupt Cognition and Social Behavior', Cell, 167 (2), 341-54 e12.

Doron, G., et al. (2014), 'Spiking irregularity and frequency modulate the behavioral report of single-neuron stimulation', Neuron, 81 (3), 653-63.

Douglas, R. J. and Martin, K. A. (2007), 'Mapping the matrix: the ways of neocortex', Neuron, 56 (2), 226-38.

Dupont, E., et al. (2006), 'Rapid developmental switch in the mechanisms driving early cortical columnar networks', Nature, 439 (7072), 79-83.

Durham, D. and Woolsey, T. A. (1984), 'Effects of neonatal whisker lesions on mouse central trigeminal pathways', J Comp Neurol, 223 (3), 424-47.

Ebert, D. H. and Greenberg, M. E. (2013), 'Activity-dependent neuronal signalling and autism spectrum disorder', Nature, 493 (7432), 327-37.

Eckler, M. J., et al. (2015), 'Cux2-positive radial glial cells generate diverse subtypes of neocortical projection neurons and macroglia', Neuron, 86 (4), 1100-8.

Edwards, T. J., et al. (2014), 'Clinical, genetic and imaging findings identify new causes for corpus callosum development syndromes', Brain, 137 (Pt 6), 1579-613.

Elston, G. N. (2003), 'Cortex, cognition and the cell: new insights into the pyramidal neuron and prefrontal function', Cereb Cortex, 13 (11), 1124-38.

Englund, C., et al. (2005), 'Pax6, Tbr2, and Tbr1 are expressed sequentially by radial glia, intermediate progenitor cells, and postmitotic neurons in developing neocortex', J Neurosci, 25 (1), 247-51.

Erzurumlu, R. S. and Gaspar, P. (2012), 'Development and critical period plasticity of the barrel cortex', Eur J Neurosci, 35 (10), 1540-53.

Falkner, S., et al. (2016), 'Transplanted embryonic neurons integrate into adult neocortical circuits', Nature, 539 (7628), 248-53.

Fame, R. M., MacDonald, J. L., and Macklis, J. D. (2011), 'Development, specification, and diversity of callosal projection neurons', Trends Neurosci, 34 (1), 41-50.

Feldmeyer, D. (2012), 'Excitatory neuronal connectivity in the barrel cortex', Front Neuroanat, 6, 24.

Feller, M. B. and Scanziani, M. (2005), 'A precritical period for plasticity in visual cortex', Curr Opin Neurobiol, 15 (1), 94-100.

Fenlon, L. R. and Richards, L. J. (2015), 'Contralateral targeting of the corpus callosum in normal and pathological brain function', Trends Neurosci, 38 (5), 264-72.

Fenstermaker, V., et al. (2004), 'Regulation of dendritic length and branching by semaphorin 3A', J Neurobiol, 58 (3), 403-12.

Ferland, R. J., et al. (2003), 'Characterization of Foxp2 and Foxp1 mRNA and protein in the developing and mature brain', J Comp Neurol, 460 (2), 266-79.

Ferrere, A., et al. (2006), 'Expression of Cux-1 and Cux-2 in the developing somatosensory cortex of normal and barrel-defective mice', Anat Rec A Discov Mol Cell Evol Biol, 288 (2), 158-65.

Finger, J. H., et al. (2002), 'The netrin 1 receptors Unc5h3 and Dcc are necessary at multiple choice points for the guidance of corticospinal tract axons', J Neurosci, 22 (23), 10346-56.

Franco, S. J., et al. (2012), 'Fate-restricted neural progenitors in the mammalian cerebral cortex', Science, 337 (6095), 746-9.

Frangeul, L., et al. (2016), 'A cross-modal genetic framework for the development and plasticity of sensory pathways', Nature, 538 (7623), 96-98.

Frost, D. O. (1982), 'Anomalous visual connections to somatosensory and auditory systems following brain lesions in early life', Brain Res, 255 (4), 627-35.

Garcia-Frigola, C. and Herrera, E. (2010), 'Zic2 regulates the expression of Sert to modulate eye-specific refinement at the visual targets', EMBO J, 29 (18), 3170-83.

Gelman, D. M., et al. (2009), 'The embryonic preoptic area is a novel source of cortical GABAergic interneurons', J Neurosci, 29 (29), 9380-9.

Georgala, P. A., Carr, C. B., and Price, D. J. (2011), 'The role of Pax6 in forebrain development', Dev Neurobiol, 71 (8), 690-709.

Gibson, D. A. and Ma, L. (2011), 'Developmental regulation of axon branching in the vertebrate nervous system', Development, 138 (2), 183-95.

Gil-Sanz, C., et al. (2015), 'Lineage Tracing Using Cux2-Cre and Cux2-CreERT2 Mice', Neuron, 86 (4), 1091-9.

Gilbert, C. D. (1993), 'Circuitry, architecture, and functional dynamics of visual cortex', Cereb Cortex, 3 (5), 373-86.

Gingras, H., et al. (2005), 'Biochemical characterization of the mammalian Cux2 protein', Gene, 344, 273-85.

Goebbels, S., et al. (2006), 'Genetic targeting of principal neurons in neocortex and hippocampus of NEX-Cre mice', Genesis, 44 (12), 611-21.

Goldberg, E. M., et al. (2008), 'K+ channels at the axon initial segment dampen near-threshold excitability of neocortical fast-spiking GABAergic interneurons', Neuron, 58 (3), 387-400.

Gomez, T. M. and Spitzer, N. C. (1999), 'In vivo regulation of axon extension and pathfinding by growth-cone calcium transients', Nature, 397 (6717), 350-5.

Gray, L. T., et al. (2017), 'Layer-specific chromatin accessibility landscapes reveal regulatory networks in adult mouse visual cortex', Elife, 6.

Greig, L. C., et al. (2013), 'Molecular logic of neocortical projection neuron specification, development and diversity', Nat Rev Neurosci, 14 (11), 755-69.

Grueber, W. B., et al. (2005), 'The development of neuronal morphology in insects', Curr Biol, 15 (17), R730-8.

Guillemot, F. (2007), 'Cell fate specification in the mammalian telencephalon', Prog Neurobiol, 83 (1), 37-52.

Gulledge, A. T., Kampa, B. M., and Stuart, G. J. (2005), 'Synaptic integration in dendritic trees', J Neurobiol, 64 (1), 75-90.

Guo, C., et al. (2013), 'Fezf2 expression identifies a multipotent progenitor for neocortical projection neurons, astrocytes, and oligodendrocytes', Neuron, 80 (5), 1167-74.

Gutman, G. A., et al. (2005), 'International Union of Pharmacology. LIII. Nomenclature and molecular relationships of voltage-gated potassium channels', Pharmacol Rev, 57 (4), 473-508.

Hanganu, I. L., et al. (2009), 'Cellular mechanisms of subplate-driven and cholinergic input-dependent network activity in the neonatal rat somatosensory cortex', Cereb Cortex, 19 (1), 89-105.

Haubensak, W., et al. (2004), 'Neurons arise in the basal neuroepithelium of the early mammalian telencephalon: a major site of neurogenesis', Proc Natl Acad Sci U S A, 101 (9), 3196-201.

Hedreen, J. C. and Yin, T. C. (1981), 'Homotopic and heterotopic callosal afferents of caudal inferior parietal lobule in Macaca mulatta', J Comp Neurol, 197 (4), 605-21.

Herculano-Houzel, S. (2009), 'The human brain in numbers: a linearly scaled-up primate brain', Front Hum Neurosci, 3, 31.

Hetts, S. W., et al. (2006), 'Anomalies of the corpus callosum: an MR analysis of the phenotypic spectrum of associated malformations', AJR Am J Roentgenol, 187 (5), 1343-8.

Heusser, K. and Schwappach, B. (2005), 'Trafficking of potassium channels', Curr Opin Neurobiol, 15 (3), 364-9.

Heynen, A. J., et al. (2003), 'Molecular mechanism for loss of visual cortical responsiveness following brief monocular deprivation', Nat Neurosci, 6 (8), 854-62.

Holtmaat, A., Randall, J., and Cane, M. (2013), 'Optical imaging of structural and functional synaptic plasticity in vivo', Eur J Pharmacol, 719 (1-3), 128-36.

Hong, K., et al. (1999), 'A ligand-gated association between cytoplasmic domains of UNC5 and DCC family receptors converts netrin-induced growth cone attraction to repulsion', Cell, 97 (7), 927-41.

Horev, G., et al. (2011), 'Dosage-dependent phenotypes in models of 16p11.2 lesions found in autism', Proc Natl Acad Sci U S A, 108 (41), 17076-81.

Hsu, L. C., et al. (2015), 'Lhx2 regulates the timing of beta-catenin-dependent cortical neurogenesis', Proc Natl Acad Sci U S A, 112 (39), 12199-204.

Hu, Z., et al. (2003), 'Corpus callosum deficiency in transgenic mice expressing a truncated ephrin-A receptor', J Neurosci, 23 (34), 10963-70.

Hua, J. Y., et al. (2005), 'Regulation of axon growth in vivo by activity-based competition', Nature, 434 (7036), 1022-6.

Huang, Y., et al. (2013), 'Sensory input is required for callosal axon targeting in the somatosensory cortex', Mol Brain, 6, 53.

Hubel, D. H. and Wiesel, T. N. (1962), 'Receptive fields, binocular interaction and functional architecture in the cat's visual cortex', J Physiol, 160, 106-54.

--- (1963), 'Shape and arrangement of columns in cat's striate cortex', J Physiol, 165, 559-68.

Hulea, L. and Nepveu, A. (2012), 'CUX1 transcription factors: from biochemical activities and cell-based assays to mouse models and human diseases', Gene, 497 (1), 18-26.

Innocenti, G. M. (2011), 'Development and evolution: two determinants of cortical connectivity', Prog Brain Res, 189, 65-75.

Inoue, K., et al. (2004), 'Fez1 is layer-specifically expressed in the adult mouse neocortex', Eur J Neurosci, 20 (11), 2909-16.

Ishihama, A. (2012), 'Prokaryotic genome regulation: a revolutionary paradigm', Proc Jpn Acad Ser B Phys Biol Sci, 88 (9), 485-508.

Iulianella, A., Vanden Heuvel, G., and Trainor, P. (2003), 'Dynamic expression of murine Cux2 in craniofacial, limb, urogenital and neuronal primordia', Gene Expr Patterns, 3 (5), 571-7.

Iulianella, A., et al. (2009), 'Cux2 functions downstream of Notch signaling to regulate dorsal interneuron formation in the spinal cord', Development, 136 (14), 2329-34.

Jan, L. Y. and Jan, Y. N. (2012), 'Voltage-gated potassium channels and the diversity of electrical signalling', J Physiol, 590 (11), 2591-9.

Jan, Y. N. and Jan, L. Y. (2010), 'Branching out: mechanisms of dendritic arborization', Nat Rev Neurosci, 11 (5), 316-28.

Jia, H., et al. (2010), 'Dendritic organization of sensory input to cortical neurons in vivo', Nature, 464 (7293), 1307-12.

Jiang, X., et al. (2015), 'Principles of connectivity among morphologically defined cell types in adult neocortex', Science, 350 (6264), aac9462.

Jiao, Y., et al. (2011), 'A key mechanism underlying sensory experience-dependent maturation of neocortical GABAergic circuits in vivo', Proc Natl Acad Sci U S A, 108 (29), 12131-6.

Johnston, J., Forsythe, I. D., and Kopp-Scheinpflug, C. (2010), 'Going native: voltage-gated potassium channels controlling neuronal excitability', J Physiol, 588 (Pt 17), 3187-200.

Just, M. A., et al. (2004), 'Cortical activation and synchronization during sentence comprehension in high-functioning autism: evidence of underconnectivity', Brain, 127 (Pt 8), 1811-21.

Kaas, Jon H (2009), Evolutionary neuroscience (Academic Press).

Kandel, E.R., Schwartz, J.H., and Jessell, T.M. (2000), Principles of Neural Science (4th Edition edn.).

Kano, M. and Hashimoto, K. (2009), 'Synapse elimination in the central nervous system', Curr Opin Neurobiol, 19 (2), 154-61.

Kashani, A. H., et al. (2006), 'Calcium activation of the LMO4 transcription complex and its role in the patterning of thalamocortical connections', J Neurosci, 26 (32), 8398-408.

Kato, M. (2015), 'Genotype-phenotype correlation in neuronal migration disorders and cortical dysplasias', Front Neurosci, 9, 181.

Katz, L. C. and Shatz, C. J. (1996), 'Synaptic activity and the construction of cortical circuits', Science, 274 (5290), 1133-8.

Keino-Masu, K., et al. (1996), 'Deleted in Colorectal Cancer (DCC) encodes a netrin receptor', Cell, 87 (2), 175-85.

Kerschensteiner, D., et al. (2009), 'Neurotransmission selectively regulates synapse formation in parallel circuits in vivo', Nature, 460 (7258), 1016-20.

Khan, S., et al. (2013), 'Local and long-range functional connectivity is reduced in concert in autism spectrum disorders', Proc Natl Acad Sci U S A, 110 (8), 3107-12.

Khazipov, R. and Luhmann, H. J. (2006), 'Early patterns of electrical activity in the developing cerebral cortex of humans and rodents', Trends Neurosci, 29 (7), 414-8.

Kier, E. L. and Truwit, C. L. (1996), 'The normal and abnormal genu of the corpus callosum: an evolutionary, embryologic, anatomic, and MR analysis', AJNR Am J Neuroradiol, 17 (9), 1631-41.

Kirkby, L. A., et al. (2013), 'A role for correlated spontaneous activity in the assembly of neural circuits', Neuron, 80 (5), 1129-44.

Koch, S. M., et al. (2011), 'Pathway-specific genetic attenuation of glutamate release alters select features of competition-based visual circuit refinement', Neuron, 71 (2), 235-42.

Koester, S. E. and O'Leary, D. D. (1994), 'Axons of early generated neurons in cingulate cortex pioneer the corpus callosum', J Neurosci, 14 (11 Pt 1), 6608-20.

Kole, M. H. and Stuart, G. J. (2012), 'Signal processing in the axon initial segment', Neuron, 73 (2), 235-47.

Kole, M. H., Letzkus, J. J., and Stuart, G. J. (2007), 'Axon initial segment Kv1 channels control axonal action potential waveform and synaptic efficacy', Neuron, 55 (4), 633-47.

Kollins, KM; and Davenport, RW (2013), Branching Morphogenesis in Vertebrate Neurons. (Madame Curie Bioscience Database [Internet]; Austin (TX): Landes Bioscience).

Krishnan, A. V., et al. (2009), 'Axonal ion channels from bench to bedside: a translational neuroscience perspective', Prog Neurobiol, 89 (3), 288-313.

Kuhlman, S. J., et al. (2013), 'A disinhibitory microcircuit initiates critical-period plasticity in the visual cortex', Nature, 501 (7468), 543-6.

Kuijpers, M. and Hoogenraad, C. C. (2011), 'Centrosomes, microtubules and neuronal development', Mol Cell Neurosci, 48 (4), 349-58.

Kulkarni, V. A. and Firestein, B. L. (2012), 'The dendritic tree and brain disorders', Mol Cell Neurosci, 50 (1), 10-20.

Kwan, A. C. and Dan, Y. (2012), 'Dissection of cortical microcircuits by single-neuron stimulation in vivo', Curr Biol, 22 (16), 1459-67.

Kwon, C. H., et al. (2006), 'Pten regulates neuronal arborization and social interaction in mice', Neuron, 50 (3), 377-88.

Lefort, S., et al. (2009), 'The excitatory neuronal network of the C2 barrel column in mouse primary somatosensory cortex', Neuron, 61 (2), 301-16.

Leid, M., et al. (2004), 'CTIP1 and CTIP2 are differentially expressed during mouse embryogenesis', Gene Expr Patterns, 4 (6), 733-9.

Leighton, A. H. and Lohmann, C. (2016), 'The Wiring of Developing Sensory Circuits-From Patterned Spontaneous Activity to Synaptic Plasticity Mechanisms', Front Neural Circuits, 10, 71.

Lendvai, B., et al. (2000), 'Experience-dependent plasticity of dendritic spines in the developing rat barrel cortex in vivo', Nature, 404 (6780), 876-81.

Leone, D. P., et al. (2008), 'The determination of projection neuron identity in the developing cerebral cortex', Curr Opin Neurobiol, 18 (1), 28-35.

Leone, D. P., et al. (2015), 'Satb2 Regulates the Differentiation of Both Callosal and Subcerebral Projection Neurons in the Developing Cerebral Cortex', Cereb Cortex, 25 (10), 3406-19.

Li, H. and Crair, M. C. (2011), 'How do barrels form in somatosensory cortex?', Ann N Y Acad Sci, 1225, 119-29.

Li, H., et al. (2013), 'Laminar and columnar development of barrel cortex relies on thalamocortical neurotransmission', Neuron, 79 (5), 970-86.

Libersat, F. and Duch, C. (2004), 'Mechanisms of dendritic maturation', Mol Neurobiol, 29 (3), 303-20.

Lickiss, T., et al. (2012), 'Examining the relationship between early axon growth and transcription factor expression in the developing cerebral cortex', J Anat, 220 (3), 201-11.

Lindwall, C., Fothergill, T., and Richards, L. J. (2007), 'Commissure formation in the mammalian forebrain', Curr Opin Neurobiol, 17 (1), 3-14.

Locke, R. E. and Nerbonne, J. M. (1997), 'Three kinetically distinct Ca2+-independent depolarization-activated K+ currents in callosal-projecting rat visual cortical neurons', J Neurophysiol, 78 (5), 2309-20.

Lodato, S., Shetty, A. S., and Arlotta, P. (2015), 'Cerebral cortex assembly: generating and reprogramming projection neuron diversity', Trends Neurosci, 38 (2), 117-25.

Lopez-Bendito, G. and Molnar, Z. (2003), 'Thalamocortical development: how are we going to get there?', Nat Rev Neurosci, 4 (4), 276-89.

Lu, H. C., et al. (2003), 'Adenylyl cyclase I regulates AMPA receptor trafficking during mouse cortical 'barrel' map development', Nat Neurosci, 6 (9), 939-47.

Luskin, M. B., Pearlman, A. L., and Sanes, J. R. (1988), 'Cell lineage in the cerebral cortex of the mouse studied in vivo and in vitro with a recombinant retrovirus', Neuron, 1 (8), 635-47.

Magdaleno, S., et al. (2006), 'BGEM: an in situ hybridization database of gene expression in the embryonic and adult mouse nervous system', PLoS Biol, 4 (4), e86.

Mainen, Z. F. and Sejnowski, T. J. (1996), 'Influence of dendritic structure on firing pattern in model neocortical neurons', Nature, 382 (6589), 363-6.

Malatesta, P., Hartfuss, E., and Gotz, M. (2000), 'Isolation of radial glial cells by fluorescent-activated cell sorting reveals a neuronal lineage', Development, 127 (24), 5253-63.

Malatesta, P., et al. (2003), 'Neuronal or glial progeny: regional differences in radial glia fate', Neuron, 37 (5), 751-64.

Mallamaci, A. and Stoykova, A. (2006), 'Gene networks controlling early cerebral cortex arealization', Eur J Neurosci, 23 (4), 847-56.

Maor-Nof, M., et al. (2013), 'Axonal pruning is actively regulated by the microtubule-destabilizing protein kinesin superfamily protein 2A', Cell Rep, 3 (4), 971-7.

Maravall, M., Stern, E. A., and Svoboda, K. (2004a), 'Development of intrinsic properties and excitability of layer 2/3 pyramidal neurons during a critical period for sensory maps in rat barrel cortex', J Neurophysiol, 92 (1), 144-56.

Maravall, M., et al. (2004b), 'Experience-dependent changes in basal dendritic branching of layer 2/3 pyramidal neurons during a critical period for developmental plasticity in rat barrel cortex', Cereb Cortex, 14 (6), 655-64.

Marcano-Reik, A. J. and Blumberg, M. S. (2008), 'The corpus callosum modulates spindle-burst activity within homotopic regions of somatosensory cortex in newborn rats', Eur J Neurosci, 28 (8), 1457-66.

Marcano-Reik, A. J., et al. (2010), 'An abrupt developmental shift in callosal modulation of sleep-related spindle bursts coincides with the emergence of excitatory-inhibitory balance and a reduction of somatosensory cortical plasticity', Behav Neurosci, 124 (5), 600-11.

Marcos-Mondejar, P., et al. (2012), 'The lhx2 transcription factor controls thalamocortical axonal guidance by specific regulation of robo1 and robo2 receptors', J Neurosci, 32 (13), 4372-85.

Marik, S. A., et al. (2013), 'Death receptor 6 regulates adult experience-dependent cortical plasticity', J Neurosci, 33 (38), 14998-5003.

Marin-Padilla, M. (1998), 'Cajal-Retzius cells and the development of the neocortex', Trends Neurosci, 21 (2), 64-71.

Marin, O. (2016), 'Developmental timing and critical windows for the treatment of psychiatric disorders', Nat Med, 22 (11), 1229-38.

Maston, G. A., Evans, S. K., and Green, M. R. (2006), 'Transcriptional regulatory elements in the human genome', Annu Rev Genomics Hum Genet, 7, 29-59.

Matsui, A., et al. (2013), 'BTBD3 controls dendrite orientation toward active axons in mammalian neocortex', Science, 342 (6162), 1114-8.

Mattson, M. P., Guthrie, P. B., and Kater, S. B. (1988), 'Components of neurite outgrowth that determine neuronal cytoarchitecture: influence of calcium and the growth substrate', J Neurosci Res, 20 (3), 331-45.

McAllister, A. K. (2000), 'Cellular and molecular mechanisms of dendrite growth', Cereb Cortex, 10 (10), 963-73.

McConnell, S. K. (1990), 'The specification of neuronal identity in the mammalian cerebral cortex', Experientia, 46 (9), 922-9.

Mendes, S. W., Henkemeyer, M., and Liebl, D. J. (2006), 'Multiple Eph receptors and B-class ephrins regulate midline crossing of corpus callosum fibers in the developing mouse forebrain', J Neurosci, 26 (3), 882-92.

Merot, Y., Retaux, S., and Heng, J. I. (2009), 'Molecular mechanisms of projection neuron production and maturation in the developing cerebral cortex', Semin Cell Dev Biol, 20 (6), 726-34.

Meyer, M. P. and Smith, S. J. (2006), 'Evidence from in vivo imaging that synaptogenesis guides the growth and branching of axonal arbors by two distinct mechanisms', J Neurosci, 26 (13), 3604-14.

Miao, S., et al. (2013), 'The Angelman syndrome protein Ube3a is required for polarized dendrite morphogenesis in pyramidal neurons', J Neurosci, 33 (1), 327-33.

Mihalas, A. B., et al. (2016), 'Intermediate Progenitor Cohorts Differentially Generate Cortical Layers and Require Tbr2 for Timely Acquisition of Neuronal Subtype Identity', Cell Rep, 16 (1), 92-105.

Ming, G., et al. (2001), 'Electrical activity modulates growth cone guidance by diffusible factors', Neuron, 29 (2), 441-52.

Minshew, N. J. and Williams, D. L. (2007), 'The new neurobiology of autism: cortex, connectivity, and neuronal organization', Arch Neurol, 64 (7), 945-50.

Mitchell, B. D. and Macklis, J. D. (2005), 'Large-scale maintenance of dual projections by callosal and frontal cortical projection neurons in adult mice', J Comp Neurol, 482 (1), 17-32.

Miyata, T., et al. (2004), 'Asymmetric production of surface-dividing and non-surface-dividing cortical progenitor cells', Development, 131 (13), 3133-45.

Mizuno, H., Hirano, T., and Tagawa, Y. (2007), 'Evidence for activity-dependent cortical wiring: formation of interhemispheric connections in neonatal mouse visual cortex requires projection neuron activity', J Neurosci, 27 (25), 6760-70.

Molnar, Z. (2011), 'Evolution of cerebral cortical development', Brain Behav Evol, 78 (1), 94-107.

Molyneaux, B. J., et al. (2007), 'Neuronal subtype specification in the cerebral cortex', Nat Rev Neurosci, 8 (6), 427-37.

Molyneaux, B. J., et al. (2005), 'Fezl is required for the birth and specification of corticospinal motor neurons', Neuron, 47 (6), 817-31.

Monuki, E. S., Porter, F. D., and Walsh, C. A. (2001), 'Patterning of the dorsal telencephalon and cerebral cortex by a roof plate-Lhx2 pathway', Neuron, 32 (4), 591-604.

Morcom, Laura R, Edwards, Timothy J, and Richards, Linda J (2016), 'Cortical architecture, midline guidance, and tractography of 3D white matter tracts'.

Moreno-Juan, V., et al. (2017), 'Prenatal thalamic waves regulate cortical area size prior to sensory processing', Nat Commun, 8, 14172.

Morgan, J. L., et al. (2011), 'Development of cell type-specific connectivity patterns of converging excitatory axons in the retina', Neuron, 71 (6), 1014-21.

Mountcastle, V. B., Davies, P. W., and Berman, A. L. (1957), 'Response properties of neurons of cat's somatic sensory cortex to peripheral stimuli', J Neurophysiol, 20 (4), 374-407.

Muller, F. and O'Rahilly, R. (1988), 'The first appearance of the future cerebral hemispheres in the human embryo at stage 14', Anat Embryol (Berl), 177 (6), 495-511.

Muzio, L. and Mallamaci, A. (2003), 'Emx1, emx2 and pax6 in specification, regionalization and arealization of the cerebral cortex', Cereb Cortex, 13 (6), 641-7.

Nakagawa, Y., Johnson, J. E., and O'Leary, D. D. (1999), 'Graded and areal expression patterns of regulatory genes and cadherins in embryonic neocortex independent of thalamocortical input', J Neurosci, 19 (24), 10877-85.

Niblock, M. M., Brunso-Bechtold, J. K., and Riddle, D. R. (2000), 'Insulin-like growth factor I stimulates dendritic growth in primary somatosensory cortex', J Neurosci, 20 (11), 4165-76.

Nieto, M., et al. (2004), 'Expression of Cux-1 and Cux-2 in the subventricular zone and upper layers II-IV of the cerebral cortex', J Comp Neurol, 479 (2), 168-80.

Niquille, M., et al. (2009), 'Transient neuronal populations are required to guide callosal axons: a role for semaphorin 3C', PLoS Biol, 7 (10), e1000230.

Nishikimi, M., Oishi, K., and Nakajima, K. (2013), 'Axon guidance mechanisms for establishment of callosal connections', Neural Plast, 2013, 149060.

Noctor, S. C., et al. (2004), 'Cortical neurons arise in symmetric and asymmetric division zones and migrate through specific phases', Nat Neurosci, 7 (2), 136-44.

Noctor, S. C., et al. (2001), 'Neurons derived from radial glial cells establish radial units in neocortex', Nature, 409 (6821), 714-20.

O'Leary, D. D. and Sahara, S. (2008), 'Genetic regulation of arealization of the neocortex', Curr Opin Neurobiol, 18 (1), 90-100.

Olavarria, J. F. and Van Sluyters, R. C. (1995), 'Overall pattern of callosal connections in visual cortex of normal and enucleated cats', J Comp Neurol, 363 (2), 161-76.

Otsuka, T. and Kawaguchi, Y. (2011), 'Cell diversity and connection specificity between callosal projection neurons in the frontal cortex', J Neurosci, 31 (10), 3862-70.

Pal, R., et al. (2015), 'CUX2 protein functions as an accessory factor in the repair of oxidative DNA damage', J Biol Chem, 290 (37), 22520-31.

Parrish, J. Z., et al. (2007), 'Mechanisms that regulate establishment, maintenance, and remodeling of dendritic fields', Annu Rev Neurosci, 30, 399-423.

Paul, L. K., et al. (2007), 'Agenesis of the corpus callosum: genetic, developmental and functional aspects of connectivity', Nat Rev Neurosci, 8 (4), 287-99.

Peinado, A., Yuste, R., and Katz, L. C. (1993), 'Extensive dye coupling between rat neocortical neurons during the period of circuit formation', Neuron, 10 (1), 103-14.

Penn, A. A., et al. (1998), 'Competition in retinogeniculate patterning driven by spontaneous activity', Science, 279 (5359), 2108-12.

Pescosolido, M. F., et al. (2012), 'Lighting a path: genetic studies pinpoint neurodevelopmental mechanisms in autism and related disorders', Dialogues Clin Neurosci, 14 (3), 239-52.

Petreanu, L., et al. (2007), 'Channelrhodopsin-2-assisted circuit mapping of long-range callosal projections', Nat Neurosci, 10 (5), 663-8.

Piochon, C., et al. (2012), 'Non-Hebbian spike-timing-dependent plasticity in cerebellar circuits', Front Neural Circuits, 6, 124.

Piper, M., et al. (2009), 'Neuropilin 1-Sema signaling regulates crossing of cingulate pioneering axons during development of the corpus callosum', Cereb Cortex, 19 Suppl 1, i11-21.

Plazas, P. V., Nicol, X., and Spitzer, N. C. (2013), 'Activity-dependent competition regulates motor neuron axon pathfinding via PlexinA3', Proc Natl Acad Sci U S A, 110 (4), 1524-9.

Polleux, F., Morrow, T., and Ghosh, A. (2000), 'Semaphorin 3A is a chemoattractant for cortical apical dendrites', Nature, 404 (6778), 567-73.

Polleux, F., Ghosh, A., and Grueber, W. B. (2016), Molecular determinants of dendrite and spine development. Dendrites, 95-115.

Porter, J. T., Johnson, C. K., and Agmon, A. (2001), 'Diverse types of interneurons generate thalamus-evoked feedforward inhibition in the mouse barrel cortex', J Neurosci, 21 (8), 2699-710.

Pouchelon, G., et al. (2014), 'Modality-specific thalamocortical inputs instruct the identity of postsynaptic L4 neurons', Nature, 511 (7510), 471-4.

Quinn, J. C., et al. (2007), 'Pax6 controls cerebral cortical cell number by regulating exit from the cell cycle and specifies cortical cell identity by a cell autonomous mechanism', Dev Biol, 302 (1), 50-65.

Rakic, P. (1974), 'Neurons in rhesus monkey visual cortex: systematic relation between time of origin and eventual disposition', Science, 183 (4123), 425-7.

--- (1988), 'Specification of cerebral cortical areas', Science, 241 (4862), 170-6.

Rakic, P. and Komuro, H. (1995), 'The role of receptor/channel activity in neuronal cell migration', J Neurobiol, 26 (3), 299-315.

Ramdzan, Z. M. and Nepveu, A. (2014), 'CUX1, a haploinsufficient tumour suppressor gene overexpressed in advanced cancers', Nat Rev Cancer, 14 (10), 673-82.

Ramon y Cajal, S. (1899), Textura del sistema nervioso del hombre y de los vertebrados. (Nicolas Moya: Madrid).

Rash, B. G. and Richards, L. J. (2001), 'A role for cingulate pioneering axons in the development of the corpus callosum', J Comp Neurol, 434 (2), 147-57.

Rash, B. G. and Grove, E. A. (2006), 'Area and layer patterning in the developing cerebral cortex', Curr Opin Neurobiol, 16 (1), 25-34.

Rebsam, A., Seif, I., and Gaspar, P. (2005), 'Dissociating barrel development and lesion-induced plasticity in the mouse somatosensory cortex', J Neurosci, 25 (3), 706-10.

Rebsam, A., Petros, T. J., and Mason, C. A. (2009), 'Switching retinogeniculate axon laterality leads to normal targeting but abnormal eye-specific segregation that is activity dependent', J Neurosci, 29 (47), 14855-63.

Ren, T., et al. (2007), 'Diffusion tensor magnetic resonance imaging and tract-tracing analysis of Probst bundle structure in Netrin1- and DCC-deficient mice', J Neurosci, 27 (39), 10345-9.

Richards, L. J., Plachez, C., and Ren, T. (2004), 'Mechanisms regulating the development of the corpus callosum and its agenesis in mouse and human', Clin Genet, 66 (4), 276-89.

Robertson, B. (1997), 'The real life of voltage-gated K+ channels: more than model behaviour', Trends Pharmacol Sci, 18 (12), 474-83.

Rodriguez-Moreno, A., et al. (2013), 'Presynaptic self-depression at developing neocortical synapses', Neuron, 77 (1), 35-42.

Roe, A. W., et al. (1990), 'A map of visual space induced in primary auditory cortex', Science, 250 (4982), 818-20.

Roe, A. W., et al. (1993), 'Experimentally induced visual projections to the auditory thalamus in ferrets: evidence for a W cell pathway', J Comp Neurol, 334 (2), 263-80.

Rouaux, C. and Arlotta, P. (2013), 'Direct lineage reprogramming of post-mitotic callosal neurons into corticofugal neurons in vivo', Nat Cell Biol, 15 (2), 214-21.

Ruthazer, E. S., Li, J., and Cline, H. T. (2006), 'Stabilization of axon branch dynamics by synaptic maturation', J Neurosci, 26 (13), 3594-603.

Sansregret, L. and Nepveu, A. (2008), 'The multiple roles of CUX1: insights from mouse models and cell-based assays', Gene, 412 (1-2), 84-94.

Schaeren-Wiemers, N., et al. (1997), 'The expression pattern of the orphan nuclear receptor RORbeta in the developing and adult rat nervous system suggests a role in the processing of sensory information and in circadian rhythm', Eur J Neurosci, 9 (12), 2687-701.

Schlaggar, B. L., Fox, K., and O'Leary, D. D. (1993), 'Postsynaptic control of plasticity in developing somatosensory cortex', Nature, 364 (6438), 623-6.

Schmunk, G. and Gargus, J. J. (2013), 'Channelopathy pathogenesis in autism spectrum disorders', Front Genet, 4, 222.

Segraves, M. A. and Rosenquist, A. C. (1982), 'The afferent and efferent callosal connections of retinotopically defined areas in cat cortex', J Neurosci, 2 (8), 1090-107.

Serafini, T., et al. (1996), 'Netrin-1 is required for commissural axon guidance in the developing vertebrate nervous system', Cell, 87 (6), 1001-14.

Sharma, J., Angelucci, A., and Sur, M. (2000), 'Induction of visual orientation modules in auditory cortex', Nature, 404 (6780), 841-7.

Shatz, C. J. and Stryker, M. P. (1978), 'Ocular dominance in layer IV of the cat's visual cortex and the effects of monocular deprivation', J Physiol, 281, 267-83.

--- (1988), 'Prenatal tetrodotoxin infusion blocks segregation of retinogeniculate afferents', Science, 242 (4875), 87-9.

Shen, Q., et al. (2006), 'The timing of cortical neurogenesis is encoded within lineages of individual progenitor cells', Nat Neurosci, 9 (6), 743-51.

Shepherd, G. M., Pologruto, T. A., and Svoboda, K. (2003), 'Circuit analysis of experience-dependent plasticity in the developing rat barrel cortex', Neuron, 38 (2), 277-89.

Shetty, A. S., et al. (2013), 'Lhx2 regulates a cortex-specific mechanism for barrel formation', Proc Natl Acad Sci U S A, 110 (50), E4913-21.

Shirasaki, R. and Pfaff, S. L. (2002), 'Transcriptional codes and the control of neuronal identity', Annu Rev Neurosci, 25, 251-81.

Shoemaker, L. D. and Arlotta, P. (2010), 'Untangling the cortex: Advances in understanding specification and differentiation of corticospinal motor neurons', Bioessays, 32 (3), 197-206.

Shoykhet, M., Land, P. W., and Simons, D. J. (2005), 'Whisker trimming begun at birth or on postnatal day 12 affects excitatory and inhibitory receptive fields of layer IV barrel neurons', J Neurophysiol, 94 (6), 3987-95.

Shu, T. and Richards, L. J. (2001), 'Cortical axon guidance by the glial wedge during the development of the corpus callosum', J Neurosci, 21 (8), 2749-58.

Shu, T., et al. (2003), 'Slit2 guides both precrossing and postcrossing callosal axons at the midline in vivo', J Neurosci, 23 (22), 8176-84.

Shu, Y., et al. (2007), 'Selective control of cortical axonal spikes by a slowly inactivating K+ current', Proc Natl Acad Sci U S A, 104 (27), 11453-8.

Siegel, F., et al. (2012), 'Peripheral and central inputs shape network dynamics in the developing visual cortex in vivo', Curr Biol, 22 (3), 253-8.

Silver, J., Edwards, M. A., and Levitt, P. (1993), 'Immunocytochemical demonstration of early appearing astroglial structures that form boundaries and pathways along axon tracts in the fetal brain', J Comp Neurol, 328 (3), 415-36.

Silver, J., et al. (1982), 'Axonal guidance during development of the great cerebral commissures: descriptive and experimental studies, in vivo, on the role of preformed glial pathways', J Comp Neurol, 210 (1), 10-29.

Smart, I. H. (1973), 'Proliferative characteristics of the ependymal layer during the early development of the mouse neocortex: a pilot study based on recording the number, location and plane of cleavage of mitotic figures', J Anat, 116 (Pt 1), 67-91.

Smith, K. M., et al. (2006), 'Midline radial glia translocation and corpus callosum formation require FGF signaling', Nat Neurosci, 9 (6), 787-97.

Splawski, I., et al. (2004), 'Ca(V)1.2 calcium channel dysfunction causes a multisystem disorder including arrhythmia and autism', Cell, 119 (1), 19-31.

Spooren, Will, et al. (2012), 'Synapse dysfunction in autism: a molecular medicine approach to drug discovery in neurodevelopmental disorders', Trends in pharmacological sciences, 33 (12), 669-84.

Srinivasan, K., et al. (2012), 'A network of genetic repression and derepression specifies projection fates in the developing neocortex', Proc Natl Acad Sci U S A, 109 (47), 19071-8.

Srivastava, D. P., et al. (2012), 'An autism-associated variant of Epac2 reveals a role for Ras/Epac2 signaling in controlling basal dendrite maintenance in mice', PLoS Biol, 10 (6), e1001350.

Srivatsa, S., et al. (2015), 'Sip1 downstream Effector ninein controls neocortical axonal growth, ipsilateral branching, and microtubule growth and stability', Neuron, 85 (5), 998-1012.

Srivatsa, S., et al. (2014), 'Unc5C and DCC act downstream of Ctip2 and Satb2 and contribute to corpus callosum formation', Nat Commun, 5, 3708.

Stanley, G. B. (2013), 'Reading and writing the neural code', Nat Neurosci, 16 (3), 259-63.

Stern, E. A., Maravall, M., and Svoboda, K. (2001), 'Rapid development and plasticity of layer 2/3 maps in rat barrel cortex in vivo', Neuron, 31 (2), 305-15.

Suarez, R., et al. (2014), 'Balanced interhemispheric cortical activity is required for correct targeting of the corpus callosum', Neuron, 82 (6), 1289-98.

Sugitani, Y., et al. (2002), 'Brn-1 and Brn-2 share crucial roles in the production and positioning of mouse neocortical neurons', Genes Dev, 16 (14), 1760-5.

Sur, M. and Leamey, C. A. (2001), 'Development and plasticity of cortical areas and networks', Nat Rev Neurosci, 2 (4), 251-62.

Sur, M. and Rubenstein, J. L. (2005), 'Patterning and plasticity of the cerebral cortex', Science, 310 (5749), 805-10.

Sur, M., Garraghty, P. E., and Roe, A. W. (1988), 'Experimentally induced visual projections into auditory thalamus and cortex', Science, 242 (4884), 1437-41.

Suter, B. A., Migliore, M., and Shepherd, G. M. (2013), 'Intrinsic electrophysiology of mouse corticospinal neurons: a class-specific triad of spike-related properties', Cereb Cortex, 23 (8), 1965-77.

Tang, F., Dent, E. W., and Kalil, K. (2003), 'Spontaneous calcium transients in developing cortical neurons regulate axon outgrowth', J Neurosci, 23 (3), 927-36.

Tarabykin, V., et al. (2001), 'Cortical upper layer neurons derive from the subventricular zone as indicated by Svet1 gene expression', Development, 128 (11), 1983-93.

Tasic, B., et al. (2016), 'Adult mouse cortical cell taxonomy revealed by single cell transcriptomics', Nat Neurosci, 19 (2), 335-46.

Tissir, F. and Goffinet, A. M. (2003), 'Reelin and brain development', Nat Rev Neurosci, 4 (6), 496-505.

Tran, T. S., et al. (2009), 'Secreted semaphorins control spine distribution and morphogenesis in the postnatal CNS', Nature, 462 (7276), 1065-9.

Unni, D. K., et al. (2012), 'Multiple Slits regulate the development of midline glial populations and the corpus callosum', Dev Biol, 365 (1), 36-49.

Unwin, N. (1989), 'The structure of ion channels in membranes of excitable cells', Neuron, 3 (6), 665-76.

Urbanska, M., Blazejczyk, M., and Jaworski, J. (2008), 'Molecular basis of dendritic arborization', Acta Neurobiol Exp (Wars), 68 (2), 264-88.

Uziel, D., Muhlfriedel, S., and Bolz, J. (2008), 'Ephrin-A5 promotes the formation of terminal thalamocortical arbors', Neuroreport, 19 (8), 877-81.

Van der Loos, H. and Woolsey, T. A. (1973), 'Somatosensory cortex: structural alterations following early injury to sense organs', Science, 179 (4071), 395-8.

Vaquerizas, J. M., et al. (2009), 'A census of human transcription factors: function, expression and evolution', Nat Rev Genet, 10 (4), 252-63.

Vucic, S. and Kiernan, M. C. (2006), 'Axonal excitability properties in amyotrophic lateral sclerosis', Clin Neurophysiol, 117 (7), 1458-66.

Wang, C. L., et al. (2007), 'Activity-dependent development of callosal projections in the somatosensory cortex', J Neurosci, 27 (42), 11334-42.

Welker, E., et al. (1996), 'Altered sensory processing in the somatosensory cortex of the mouse mutant barrelless', Science, 271 (5257), 1864-7.

West, A. E. and Greenberg, M. E. (2011), 'Neuronal activity-regulated gene transcription in synapse development and cognitive function', Cold Spring Harb Perspect Biol, 3 (6).

Wiesel, T. N. and Hubel, D. H. (1963), 'Single-Cell Responses in Striate Cortex of Kittens Deprived of Vision in One Eye', J Neurophysiol, 26, 1003-17.

Wilczynski, B., et al. (2012), 'Predicting spatial and temporal gene expression using an integrative model of transcription factor occupancy and chromatin state', PLoS Comput Biol, 8 (12), e1002798.

Wolfram, V., et al. (2012), 'The LIM-homeodomain protein islet dictates motor neuron electrical properties by regulating K(+) channel expression', Neuron, 75 (4), 663-74.

Woodworth, M. B., et al. (2016), 'Ctip1 Regulates the Balance between Specification of Distinct Projection Neuron Subtypes in Deep Cortical Layers', Cell Rep, 15 (5), 999-1012.

Woolsey, T. A. and Van der Loos, H. (1970), 'The structural organization of layer IV in the somatosensory region (SI) of mouse cerebral cortex. The description of a cortical field composed of discrete cytoarchitectonic units', Brain Res, 17 (2), 205-42.

Wu, C. S., Ballester Rosado, C. J., and Lu, H. C. (2011), 'What can we get from 'barrels': the rodent barrel cortex as a model for studying the establishment of neural circuits', Eur J Neurosci, 34 (10), 1663-76.

Yamamoto, N. and Lopez-Bendito, G. (2012), 'Shaping brain connections through spontaneous neural activity', Eur J Neurosci, 35 (10), 1595-604.

Yang, J. W., et al. (2009), 'Three patterns of oscillatory activity differentially synchronize developing neocortical networks in vivo', J Neurosci, 29 (28), 9011-25.

Yang, J. W., et al. (2016a), 'Spindle Bursts in Neonatal Rat Cerebral Cortex', Neural Plast, 2016, 3467832.

Yang, W. Z., et al. (2016b), 'Fear Erasure Facilitated by Immature Inhibitory Neuron Transplantation', Neuron, 92 (6), 1352-67.

Yassin, L., et al. (2010), 'An embedded subnetwork of highly active neurons in the neocortex', Neuron, 68 (6), 1043-50.

Yorke, C. H., Jr. and Caviness, V. S., Jr. (1975), 'Interhemispheric neocortical connections of the corpus callosum in the normal mouse: a study based on anterograde and retrograde methods', J Comp Neurol, 164 (2), 233-45.

Yoshimura, Y. and Callaway, E. M. (2005), 'Fine-scale specificity of cortical networks depends on inhibitory cell type and connectivity', Nat Neurosci, 8 (11), 1552-9.

Yoshimura, Y., Dantzker, J. L., and Callaway, E. M. (2005), 'Excitatory cortical neurons form fine-scale functional networks', Nature, 433 (7028), 868-73.

Yu, C. R., et al. (2004), 'Spontaneous neural activity is required for the establishment and maintenance of the olfactory sensory map', Neuron, 42 (4), 553-66.

Zeisel, A., et al. (2015), 'Brain structure. Cell types in the mouse cortex and hippocampus revealed by single-cell RNA-seq', Science, 347 (6226), 1138-42.

Zhao, H., et al. (2011), 'A molecular mechanism that regulates medially oriented axonal growth of upper layer neurons in the developing neocortex', J Comp Neurol, 519 (5), 834-48.

Zhou, J., et al. (2013), 'Axon position within the corpus callosum determines contralateral cortical projection', Proc Natl Acad Sci U S A, 110 (29), E2714-23.

Zimmer, C., et al. (2004), 'Dynamics of Cux2 expression suggests that an early pool of SVZ precursors is fated to become upper cortical layer neurons', Cereb Cortex, 14 (12), 1408-20.